






Universitat Autònoma de Barcelona

**ADVERTIMENT.** L'accés als continguts d'aquesta tesi queda condicionat a l'acceptació de les condicions d'ús establertes per la següent llicència Creative Commons:  [http://cat.creativecommons.org/?page\\_id=184](http://cat.creativecommons.org/?page_id=184)

**ADVERTENCIA.** El acceso a los contenidos de esta tesis queda condicionado a la aceptación de las condiciones de uso establecidas por la siguiente licencia Creative Commons:  <http://es.creativecommons.org/blog/licencias/>

**WARNING.** The access to the contents of this doctoral thesis it is limited to the acceptance of the use conditions set by the following Creative Commons license:  <https://creativecommons.org/licenses/?lang=en>



**Universitat Autònoma  
de Barcelona**

Escola d'Enginyeria

Departament d'Enginyeria Química, Biològica i Ambiental

**Assessment of sulfate reduction  
process in sulfidogenic biological reactors  
using glycerol as the electron donor**

PhD Thesis

**Xudong Zhou**

PhD program in Environmental Science and Technology

Supervised by:

Dr. David Gabriel Buguña

Dr. Xavier Gamisans Noguera

Dr. Antonio David Dorado Castaño

Bellaterra, Cerdanyola del Vallès, Barcelona

January 2022

Title: Assessment of sulfate reduction process in sulfidogenic biological reactors using glycerol as the electron donor

Presented by: Xudong Zhou

Supervised by: Dr. David Gabriel Buguña, Dr. Xavier Gamisans Noguera, Dr. Antonio David Dorado Castaño

PhD program in Environmental Science and Technology

Departament d'Enginyeria Química, Biològica i Ambiental

Escola d'Enginyeria

Universitat Autònoma de Barcelona. Bellaterra

This work was supported by the Spanish government (projects SONOVA CTQ2015-69802-C2-1-R and ENSURE RTI2018-099362-B-C2). The author acknowledges the fellowship from China Scholarship Council (CSC, 201706300052).

This work was done in Departament d'Enginyeria Química, Biològica i Ambiental, Universitat Autònoma de Barcelona.



**DAVID GABRIEL BUGUÑA**, catedràtic laboral del Departament d'Enginyeria Química, Biològica i Ambiental de la Universitat Autònoma de Barcelona; **XAVIER GAMISANS NOGUERA**, catedràtic d'escola universitària del Departament d'Enginyeria Minera, Industrial i Tic de la Universitat Politècnica de Catalunya; **ANTONIO DAVID DORADO CASTAÑO**, professor agregat del Departament d'Enginyeria Minera, Industrial i Tic de la Universitat Politècnica de Catalunya.

**CERTIFIQUEM:**

Que el Llicenciat en Ciències Ambientals **Xudong Zhou** ha realitzat sota la nostra direcció el treball amb títol "Assessment of sulfate reduction process in sulfidogenic biological reactors using glycerol as the electron donor" que es presenta en aquesta memòria i que constitueix la seva Tesi per optar al Grau de Doctor per la Universitat Autònoma de Barcelona.

I per a què se'n prengui coneixement i consti als afectes oportuns, presentem a l'Escola d'Enginyeria de la Universitat Autònoma de Barcelona l'esmentada Tesi, signant el present certificat a

Dr. David Gabriel Buguña

Dr. Xavier Gamisans Noguera

Dr. Antonio David Dorado Castaño

Gener 2022



## **Acknowledgments**

This is the fourth year since I came to Spain. I would like to thank all my friends who have helped and cared for me. Thank you! First of all, I would like to thank the supervisors of the thesis, David Gabriel Buguña, Xavier Gamisans Noguera, and Antonio David Dorado Castaño. David, Thank you for giving me the opportunity to do experimental research in the Genocov group. I appreciate for sharing your experiences in academia and let me think about scientific issues independently from different perspectives. Thanks to David, Xavier, and Toni's suggestions for my thesis, experiments, and the model that guided me to learn from the ground up. Thank you for your help in my work. It is a pleasure to work with you for these years. I also want to thank the China Scholarship Council (CSC, 201706300052) for funding.

It is really nice to meet all members of the Gases group. Mabel, I am very happy that I just came to Spain and met you in the laboratory. Your outgoing personality quickly integrated me into this research group. Thank you for helping me get familiar with the laboratory at the beginning and teaching me various experimental skills. Eva, it is really nice to work with you in the lab for almost three years. Thank you for teaching me everything you know during the experiment. I remember you encouraged me to dance at a party, even though I was very bad at it. That is a great memory. Hahaha. Dani, I am glad that when I first came to school, we were in the same office. You helped me get familiar with the environment so that I did not feel lonely in a new place. David Cueto, your grace, it is an honor to meet you here. Thank you for your help with the modeling. I remember the good moments when we talked about many topics after lunch during coffee time. Similarly, I would like to thank Luis, Enric Cecilia, Chiara, and Eric. Thank you for your comments and suggestions to me when we have meetings.

I also want to thank my colleagues from Departament d'Enginyeria Química, Biològica i Ambiental of Universitat Autònoma de Barcelona. I cannot forget a lot of happy times together with you. You guys made me join different cultures and let me enjoy the shooting of funny videos. Enjoy the happy moments in “pica-pica” after the defense. And Natalia, my Spanish teacher, it is a pity that I cannot speak Spanish, but I remember all the beautiful words that you taught me. Kaidi, from the acquaintance in Beijing, and finally to accompany each other on the way to and from the school, thank you. You all are very welcome to China, to Xi'an when you are available in the future.

最后我想特别感谢我的家人们。爸爸，妈妈，妹妹，感谢你们对我在科研道路上的鼓励与支持，是你们让我无所顾虑。我还要谢谢我的爱人，谢谢你在大学七年，西班牙三年的陪伴，谢谢你给我带来的可爱小棉袄，我们彼此共勉，共同成长。

# Thesis abstract

Increasing anthropogenic activities, such as combustion of sulfur-containing fossil fuels and mining-smelting industrial process, results in flue gases or wastewaters emissions containing large quantities of sulfur compounds that require treatment before being directly discharged into the atmosphere or hydrosphere. Sulfate is the main component in the effluent after conventional treatments. Sulfate is not toxic, but the uncontrolled discharge of a large amount of sulfate can disturb the balance of the sulfur cycle. Moreover, in an uncontrolled anaerobic environment, sulfate can be reduced by sulfate-reducing bacteria (SRB) to toxic sulfide, thereby affecting the environment and human health. Therefore, an environmentally friendly treatment system is needed to treat these sulfur-containing waste gases and wastewaters.

The most successful reactors widely used in the anaerobic treatment technology of industrial organic wastewater are up-flow anaerobic sludge blanket (UASB) reactors or their derivatives.

The aim of this PhD thesis is to assess the sulfate reduction process in sulfidogenic biological reactors (both UASB reactor and batch systems) using glycerol as the main electron donor, and to understand the complex underlying mechanisms behind the anaerobic and sulfidogenic reactors.

A laboratory-scale UASB reactor was set up and inoculated with granular sludge from a paper recycling industry, which was mainly used for biogas production. The UASB reactor was performed under a constant TOC/S-SO<sub>4</sub><sup>2-</sup> ratio of  $1.5 \pm 0.3$  g C g<sup>-1</sup> S and an OLR of  $7.3 \pm 1.6$  kg C m<sup>-3</sup> d<sup>-1</sup> for a long-term operation. Methanogenic granular sludge quickly adapted to sulfidogenic conditions and maintained a sulfate removal capacity of  $4.5 \pm 0.7$  kg S-SO<sub>4</sub><sup>2-</sup> m<sup>-3</sup> d<sup>-1</sup> in 280 days. The sulfate removal capacity decreased gradually from day 280 to 639. Methanogenic activity was ceased after 200 days, accompanied by a progressive VFAs accumulation (mainly acetate). A filamentous and fluffy flocculant



material, namely slime-like substances (SLS) along this thesis, accumulated in the reactor after the cease of methanogenic activity. Batch activity tests showed that SLS did not affect the mechanisms of glycerol fermentation and sulfate reduction, but it might affect the mass transfer of sulfate to the granular biomass. Moreover, the SLS led to the flotation of sludge, which resulted in a loss of sulfate removal efficiency in the UASB and the failure of its operation.

In order to assess the mechanism of sulfate reduction using glycerol as electron donor and its specific consumption/production rates, a battery of batch activity tests with and without sulfate were performed using a variety of carbon sources, including glycerol, n-butanol, 2,3-butanediol, 1,3-propanediol, ethanol, formate, propionate and acetate. Glycerol was mainly fermented to 1,3-propanediol, ethanol, formate, propionate and acetate by fermentative microorganisms. Except for acetate, other organic intermediates were found to be further used by SRB for sulfate reduction. The sulfate reduction process mainly used 1,3-propanediol and ethanol as electron donors in glycerol-fed tests.

Finally, a mathematical model was established to describe the mechanism of sulfate reduction and anaerobic glycerol fermentation through multiple pathways and multiple intermediate products. The model was able to properly reproduce experimental results of batch activity tests. Biokinetic parameters (maximum specific uptake rates of substrate and Monod half saturation coefficients) were the parameters estimated from experimental data in the calibration step of the model. Model predictions, consistent with data collected during experiments, confirmed that the bioconversion of 1,3-propanediol and ethanol were the main pathways of glycerol fermentation. It was also found that 3-hydroxypropionate might be an additional intermediate product in the fermentation process of glycerol and in the degradation of 1,3-propanediol for sulfate reduction.

# Resumen de la tesis

El aumento de las actividades antropogénicas, como la combustión de combustibles fósiles que contienen azufre o procesos industriales de minería-fundición, da como resultado la emisión de gases de combustión y aguas residuales que contienen grandes cantidades de compuestos de azufre que requieren tratamiento antes de verterlas directamente a la atmósfera o la hidrosfera. El sulfato es generalmente el componente principal del efluente después de los tratamientos convencionales. El sulfato no es tóxico, pero el vertido incontrolado de una gran cantidad de sulfato puede alterar el equilibrio del ciclo del azufre. Además, en un entorno anaeróbico no controlado, las bacterias reductoras de sulfato (SRB) pueden reducir el sulfato a sulfuro de hidrógeno, compuesto tóxico que afecta también al medio ambiente y la salud humana. Por lo tanto, se necesita un sistema de tratamiento respetuoso con el medio ambiente para tratar estos gases y aguas residuales que contienen azufre.

Los reactores más utilizados y con más éxito en la tecnología de tratamiento anaeróbico de aguas residuales industriales son los reactores de tipo UASB o sus variantes.

El objetivo de esta tesis doctoral es evaluar el proceso de reducción de sulfato en reactores biológicos sulfidogénicos (reactor UASB y botellas de suero) utilizando glicerol como principal donador de electrones, y comprender los complejos mecanismos subyacentes detrás de los reactores anaeróbicos sulfidogénicos.

Para ello, se instaló un reactor UASB a escala de laboratorio y se inoculó con lodo granular de una industria de reciclaje de papel, que se utilizaba principalmente para la producción de biogás. El reactor UASB operó bajo una relación  $\text{TOC/S-SO}_4^{2-}$  constante de  $1,5 \pm 0,3 \text{ g C g}^{-1} \text{ S}$  y una carga volumétrica de C de  $7,3 \pm 1,6 \text{ kg C m}^{-3} \text{ d}^{-1}$  durante toda la operación a largo plazo. El lodo granular metanogénico se adaptó rápidamente a las condiciones sulfidogénicas y mantuvo una capacidad de eliminación de sulfato de  $4.5 \pm 0.7 \text{ kg S-SO}_4^{2-} \text{ m}^{-3} \text{ d}^{-1}$  en 280 días. La capacidad de eliminación de sulfato disminuyó

gradualmente entre los días 280 y 639 de operación. La actividad metanogénica cesó a los 200 días, acompañada de una acumulación progresiva de AGV (principalmente acetato). Un material floculante filamentoso y esponjoso, llamada limo o largo de esta tesis, se acumuló en el reactor después del cese de la actividad metanogénica. Las pruebas de actividad en discontinuo mostraron que el limo no afectó los mecanismos de fermentación de glicerol y reducción de sulfato, pero podría afectar la transferencia de masa de sulfato a la biomasa granular. Además, la acumulación de limo provocó la flotación de lodos, lo que resultó en una pérdida de rendimiento en el UASB traducido en una reducción de la eficiencia de eliminación de sulfato y al fracaso de la operación.

Con el fin de evaluar el mecanismo de reducción de sulfato usando glicerol como donador de electrones y sus tasas específicas de consumo / producción, se realizó una batería de pruebas de actividad en discontinuo con y sin sulfato usando una variedad de fuentes de carbono, incluyendo glicerol, n-butanol, 2,3-butanodiol, 1,3-propanodiol, etanol, formiato, propionato y acetato. El glicerol fermentó principalmente a 1,3-propanodiol, etanol, formiato, propionato y acetato por microorganismos fermentativos. Excepto por el acetato, se descubrió que SRB utilizaba otros intermedios orgánicos para la reducción de sulfato en vez de glicerol. El proceso de reducción de sulfato utilizó principalmente 1,3-propanodiol y etanol como donadores de electrones en test alimentados únicamente con glicerol.

Finalmente, se estableció un modelo matemático para describir el mecanismo de reducción de sulfato y fermentación anaeróbica de glicerol a través de múltiples vías y múltiples productos intermedios. El modelo pudo reproducir los resultados experimentales de las pruebas de actividad en discontinuo de una manera muy consistente. El modelo fue calibrado a partir de la estimación de los parámetros biocinéticos (tasas máximas de específicas de consumo de sustrato y coeficientes de semisaturación de Monod). Las predicciones del modelo, consistentes con el comportamiento experimental observado, confirmó que la bioconversión de 1,3-propanodiol y etanol eran las principales vías de fermentación del glicerol. También se encontró que el 3-hidroxipropionato sería otro

producto intermedio en el proceso de fermentación del glicerol y en la degradación del 1,3-propanodiol para la reducción de sulfato.

# Resum de la tesi

L'augment de les activitats antropogèniques, com la combustió de combustibles fòssils que contenen sofre o processos industrials de mineria-foneria, dona com a resultat l'emissió de gasos de combustió i aigües residuals que contenen grans quantitats de compostos de sofre que requereixen tractament abans de vessar-les directament a l'atmosfera o hidrosfera. El sulfat és generalment el component principal de l'efluent després dels tractaments convencionals. El sulfat no és tòxic, però l'abocament incontrolat de gran quantitat de sulfat pot alterar l'equilibri del cicle del sofre. A més, en un entorn anaeròbic no controlat, els bacteris reductors de sulfat (SRB) poden reduir el sulfat a sulfur d'hidrogen, compost tòxic que afecta també el medi ambient. Per tant, cal un sistema de tractament respectuós amb el medi ambient per tractar aquests gasos i aigües residuals que contenen sofre.

Els reactors més utilitzats i amb més èxit a la tecnologia de tractament anaeròbic d'aigües residuals industrials són els reactors de tipus UASB i els seus derivats.

L'objectiu d'aquesta tesi doctoral és avaluar el procés de reducció de sulfat en reactors biològics sulfidogènics (reactor UASB i ampolles de sèrum) utilitzant glicerol com a principal donador d'electrons i comprendre els complexos mecanismes subjacents darrere dels reactors anaeròbics sulfidogènics.

Per fer-ho, es va instal·lar un reactor UASB a escala de laboratori i es va inocular amb fang granular d'una indústria de reciclatge de paper que s'utilitzava principalment per a la producció de biogàs. El reactor UASB va operar sota una relació  $\text{TOC/S-SO}_4^{2-}$  constant d' $1,5 \pm 0,3 \text{ g C g}^{-1} \text{ S}$  i una càrrega volumètrica de C de  $7,3 \pm 1,6 \text{ kg C m}^{-3} \text{ d}^{-1}$  durant tota l'operació a llarg termini. El fang granular metanogènic es va adaptar ràpidament a les condicions sulfidogèniques i va mantenir una capacitat d'eliminació de sulfat de  $4.5 \pm 0.7 \text{ kg S-SO}_4^{2-} \text{ m}^{-3} \text{ d}^{-1}$  en 280 dies. La capacitat d'eliminació de sulfat va disminuir gradualment entre els dies 280 i 639 d'operació. L'activitat metanogènica va cessar al cap de 200 dies, acompanyada d'una acumulació progressiva d'AGV (principalment acetat). Un material

floculant filamentós i esponjós, anomenada llim al llarg d'aquesta tesi, es va acumular al reactor després del cessament de l'activitat metanogènica. Les proves d'activitat en discontinu van mostrar que el llim no va afectar els mecanismes de fermentació de glicerol i reducció de sulfat, però podria afectar la transferència de massa de sulfat a la biomassa granular. A més, l'acumulació de llim va provocar la flotació de llots, cosa que va resultar en una pèrdua de rendiment a l'UASB a causa de la reducció de l'eficiència d'eliminació de sulfat i del fracàs de l'operació.

Per tal d'avaluar el mecanisme de reducció de sulfat usant glicerol com a donador d'electrons i les seves taxes específiques de consum/producció, es va realitzar una bateria de proves d'activitat en discontinu amb i sense sulfat usant una varietat de fonts de carboni, incloent-hi glicerol, n-butanol, 2,3-butanodiol, 1,3-propanodiol, etanol, formiat, propionat i acetat. El glicerol va fermentar principalment a 1,3-propanodiol, etanol, formiat, propionat i acetat per microorganismes fermentatius. Excepte per l'acetat, es va descobrir que SRB utilitzava altres intermedis orgànics per a la reducció de sulfat en comptes del glicerol. El procés de reducció de sulfat va utilitzar principalment 1,3-propanodiol i etanol com a donadors d'electrons en tests alimentats únicament amb glicerol.

Finalment, es va establir un model matemàtic per descriure el mecanisme de reducció de sulfat i fermentació anaeròbica de glicerol a través de múltiples vies i múltiples productes intermedis. El model va poder reproduir els resultats experimentals de les proves d'activitat en discontinu d'una manera molt consistent. La calibració del model es va realitzar a partir de l'estimació dels paràmetres biocinètics (taxes màximes d'específiques de consum de substrat i coeficients de semisaturació de Monod). El model va confirmar que la bioconversió de 1,3-propanodiol i etanol eren les principals vies de fermentació del glicerol. També es va trobar que el 3-hidroxiopropionat seria un producte intermedi en el procés de fermentació del glicerol i en la degradació de l'1,3-propanodiol per a la reducció de sulfat.

## List of main abbreviations

AD	Anaerobic digestion
AMP	Adenosine monophosphate
APS	Adenosine-phosphosulphate
ASRB	Autotrophic sulfate reducing bacteria
ATP	Adenosine triphosphate
BOD	Biochemical oxygen demand
COD	Chemical oxygen demand
CSTR	Continuous stirred tank reactor
EDTA	Ethylenediaminetetraacetic acid
EGSB	Expanded granular sludge bed reactor
EPS	Extracellular polymeric substances
FB	Fermentative bacteria
FIM	Fisher information matrix
GS	Granular sludge
HRT	Hydraulic retention time
HSRB	Heterotrophic sulfate reducing bacteria
LCFAs	Long-chain fatty acids
MCRT	Mean cell residence time
OLR	Organic loading rate
Pi	Inorganic phosphate
PPi	Inorganic pyrophosphate
PSD	Particle size distribution
RC	Removal capacity
RE	Removal efficiency

SAOB	Sulfide antioxidant buffer
SCGS	Slime-covered granular sludge
SLR	Sulfate loading rate
SLS	Slime-like substances
SRB	Sulfate reducing bacteria
SRR	Sulfate reduction rate
TDS	Total dissolved sulfide
TIC	Total inorganic carbon
TOC	Total organic carbon
TOC RE	Total organic carbon removal efficiency
TOC RC	Total organic carbon removal capacity
TSS	Total suspended solids
UASB	Up-flow anaerobic sludge bed
VFAs	Volatile fatty acids
VOCs	Volatile organic compounds
VSCs	Volatile sulfur compounds
VSS	Volatile suspended solids





---

# Table of contents

<b>Thesis abstract.....</b>	<b>I</b>
<b>Resumen de la tesis .....</b>	<b>III</b>
<b>Resum de la tesi.....</b>	<b>VI</b>
<b>List of main abbreviations.....</b>	<b>VIII</b>
<b>Chapter 1</b>	
<b>Motivations, objectives and thesis overview .....</b>	<b>1</b>
1.1 Motivations .....	3
1.2 Objectives .....	4
1.3 Thesis overview .....	4
<b>Chapter 2</b>	
<b>Introduction and literature review .....</b>	<b>7</b>
2.1 Sulfur cycle and sulfur pollution.....	9
2.1.1 Sulfur cycle .....	9
2.1.2 Sulfur pollution in flue gas and wastewater.....	11
2.1.3 Technological alternatives for flue gas treatment .....	13
2.2 Anaerobic digestion and glycerol fermentation .....	14
2.3 Sulfate reduction process .....	17
2.3.1 Sulfate reducing bacteria.....	17
2.3.2 Electron donors for sulfate reduction.....	19
2.3.3 Bioreactors for sulfate reduction.....	22
2.4 Modeling biological sulfate reduction .....	24
2.4.1 Modeling of anaerobic digestion .....	24
2.4.2 Modeling of sulfate reduction in anaerobic digestion.....	27
<b>Chapter 3</b>	
<b>General materials and methods.....</b>	<b>31</b>

---

3.1 Description of reactors .....	33
3.1.1 UASB reactor .....	33
3.1.2 CSTR reactor .....	35
3.2 Batch activity tests in serum bottles.....	36
3.3 Analytical methods.....	37
3.3.1 Sulfur compounds .....	37
3.3.2 Carbon compounds .....	38
3.3.3 Volatile suspended solids (VSS) .....	38
3.3.4 Gas analysis .....	39
3.3.5 Particle size .....	40
3.3.6 Microbial population identification .....	40
3.3.7 Characterization of crude glycerol.....	40

## **Chapter 4**

<b>Anaerobic treatment of sulfate-rich wastewater in a UASB reactor fed with crude glycerol .....</b>	<b>43</b>
Abstract .....	45
4.1 Introduction.....	47
4.2 Materials and methods .....	49
4.2.1 Operating conditions of the UASB reactor .....	49
4.2.2 Assessment of stratification in the UASB reactor.....	49
4.2.3 C and S mass balances assessment .....	50
4.2.4 Volumetric rates along the UASB height.....	50
4.3 Results and discussion .....	51
4.3.1 Performance of the sulfidogenic UASB reactor .....	51
4.3.2 Assessment of stratification in the UASB reactor.....	63
4.4 Conclusions.....	69

## **Chapter 5**

**Specific activity of anaerobic sludge and of slime-like substances in a methanogenic -**

---

<b>sulfidogenic UASB reactor .....</b>	<b>71</b>
Abstract .....	73
5.1 Introduction.....	75
5.2 Materials and methods .....	76
5.2.1 Experimental setup of activity tests .....	76
5.2.2 Analytical methods.....	79
5.3 Results and discussion .....	80
5.3.1 Specific activities of the inoculum sludge of the UASB reactor .....	80
5.3.2 Specific activities through the UASB reactor heights .....	86
5.3.3 Specific activities of granular sludge and slime-like substances .....	96
5.4 Conclusion .....	104
<b>Chapter 6</b>	
<b>Assessing main process mechanism and rates of sulfate reduction by granular biomass fed with glycerol under sulfidogenic conditions .....</b>	<b>105</b>
Abstract .....	107
6.1 Introduction.....	109
6.2 Materials and methods .....	110
6.2.1 Batch activity tests .....	110
6.2.2 Analytical methods.....	111
6.2.3 Illumina sequencing analysis .....	111
6.2.4 Stoichiometric calculation for the sulfate reducing process by glycerol .....	112
6.3 Results and discussion .....	117
6.3.1 Activity tests with glycerol as sole external carbon source .....	117
6.3.2 Sulfate reduction with single organic compounds .....	125
6.3.3 Contribution of different electron donors to sulfate reduction .....	135
6.4 Conclusion .....	139

**Chapter 7**

**Modeling sulfate reduction and glycerol fermentation under sulfidogenic conditions** ..... **141**

Abstract ..... 143

7.1 Introduction ..... 146

7.2 Materials and methods ..... 151

    7.2.1 Experimental data ..... 151

    7.2.2 Model development ..... 151

    7.2.3 Model calibration and validation ..... 156

    7.2.4 Confidence interval determination by Fisher Information Matrix.... 159

7.3 Results and discussion ..... 160

    7.3.1 Parameters estimation and sensitivity analysis ..... 160

    7.3.2 Model calibration of sulfate reduction process with single organic  
compounds ..... 166

    7.3.3 Model calibration with glycerol as carbon source ..... 170

7.4 Conclusion ..... 176

**Chapter 8**

**General conclusions and future work** ..... **177**

    8.1 General conclusions ..... 179

    8.2 Future work ..... 180

**Chapter 9**

**References** ..... **183**

# **Chapter 1**

---

## **Motivations, objectives and thesis overview**



## 1.1 Motivations

This thesis has been carried out in the GENOCOV research group from the Department of Chemical, Biological and Environmental Engineering at Universitat Autònoma de Barcelona. The thesis was supported by the project SONOVA (CTQ2015-69802-C2) and project ENSURE (ref. RTI2018-099362-B-C21) funded by Ministerio de Ciencia, Innovación y Universidades of Spanish government.

Increasing anthropogenic activities lead to large amounts of SO<sub>x</sub> and NO<sub>x</sub> emissions that require treatment before being directly discharged into the atmosphere. Compared to physical-chemical technologies, biological techniques have proven to be more cost-effective and environmentally friendly for removing pollutants from contaminated air. The projects SONOVA and ENSURE aim at providing a new approach based on a multi-stage bioscrubber process to treat gaseous effluents using biological processes in the view of waste gases valorization. In order to understand the sulfidogenic capacity of the granular sludge in an upflow anaerobic sludge blanket (UASB) reactor, a variety of electron donors (organic carbon sources) and a series of operating parameters have been tested, such as the sulfate loading rate, the organic loading rate, the C/S ratio or the upflow velocity, based on the application in the previous project SONOVA. Acetate, pig slurry, cheese whey, vinasses, and crude glycerol were chosen for the sulfate reduction process in the project SONOVA. Results demonstrated that the most appropriate organic carbon source for sulfate reduction was crude glycerol (a by-product of the biodiesel industry), because it provides a higher carbon utilization efficiency for sulfate reduction. In previous works of the research group, the performance of an upflow anaerobic sludge blanket (UASB) reactor was identified under a range of conditions, but the underlying mechanism of the sulfate reduction and glycerol fermentation processes was still unclear due to the complexity of this system.



## 1.2 Objectives

The main objective of this PhD thesis was to assess the sulfate reduction process in sulfidogenic biological reactors using both crude glycerol and pure glycerol as electron donor to understand the underlying complex mechanisms behind sulfidogenic reactors. In order to deepen the knowledge of this complex system, the following specific objectives were proposed:

- To assess the performance of a UASB reactor at constant sulfate and carbon loading rates using crude glycerol as carbon source to evaluate the stability of sulfate and carbon removal efficiencies under long-term operating conditions.
- To gain knowledge about the possible limitations of the operation in the UASB reactor.
- To determine the main mechanisms and process rates involved in the glycerol fermentation and the sulfate reduction under sulfidogenic conditions.
- To setup, calibrate and validate a model to describe the mechanism of the sulfate reduction using glycerol as electron donor.

## 1.3 Thesis overview

The present chapter (Chapter 1) introduces the motivations of this thesis, the general and particular objectives, and the thesis overview. In Chapter 2, the general introduction of relevant topics of the thesis is presented. Chapter 2 reviews the literature for the sulfur cycle, sulfur pollution in flue gas and wastewater, technologies for waste gases treatment, sulfate reducing bacteria, electron donors for sulfate reduction as well as different reactor configurations. A brief overview of the kinetic models related to anaerobic digestion and sulfate reduction is also shown. This information helps to understand the following chapters and outlines the different aspects that will be discussed in the following chapters. In Chapter 3, the general materials and methods required by this thesis are introduced, and the specific methods and materials required in each chapter are described in the

---

corresponding chapters (Chapter 4 to Chapter 7).

In Chapter 4, a UASB reactor was operated at a constant sulfate and carbon loading rate for long-term operation using crude glycerol as carbon source. The performance of the UASB reactor was estimated in terms of the sulfate removal capacity and organic carbon compounds removal capacity. This chapter also discusses the reasons for the progressive decrease in sulfate and organic carbon removal capacities, which may be caused by the accumulation of SLS, which is a filamentous and fluffy flocculant material formed in the reactor after the long-term operation. Moreover, the stratification of the reactor performance was also analyzed.

Chapter 5 analyzes the specific activity through batch experiments in serum bottles of the inoculum sludge of the UASB reactor from a pulp and paper recycling industry and of sludge withdrawn along time and along the reactor height during the UASB operation. This chapter also aims at explaining the decline of sulfate reduction capacity in the UASB reactor based on the analysis of granular sludge and SLS accumulated during the long-term operation of the reactor.

In order to determine the main mechanisms of glycerol fermentation and sulfate reduction under sulfidogenic conditions, Chapter 6 assesses the principal reactions involved using glycerol and its fermentation products as electron donors together with their specific consumption/production rates. In Chapter 6, a battery of batch activity tests with and without sulfate were performed with glycerol and its fermentation by-products (n-butanol, 2,3-butanediol, 1,3-propanediol, ethanol, formate, propionate and acetate) as carbon sources.

Chapter 7 sets up a model that considers the mechanism of the glycerol fermentation processes with sulfate reduction occurring under sulfidogenic conditions. Maximum specific substrate uptake rate of glycerol fermentation and sulfate reduction processes were calibrated. Chapter 7 supplements and revises the mechanism of glycerol degradation proposed in Chapter 6 through the establishment of the model.

Chapter 8 presents the main conclusions and future perspectives of the research. Finally,

Chapter 9 provides the references used in this thesis.

## **Chapter 2**

---

### **Introduction and literature review**



## 2.1 Sulfur cycle and sulfur pollution

### 2.1.1 Sulfur cycle

Sulfur is the fourteenth most abundant element on the surface of the earth, and the sixth most abundant element in microorganisms (Fike et al., 2016; Klotz et al., 2011). As an important constituent of amino acids, proteins, enzymes and vitamins, sulfur is essential for animals and humans (Komarnisky et al., 2003). It is also a minor constituent of fats, body fluids, and skeletal minerals (Lide, 2004). In addition to the above-mentioned organic sulfur, sulfur is widely distributed in atmosphere, lithosphere and hydrosphere, which occurs in a broad range of redox states from -2 to +6. Main forms of inorganic sulfur and its oxidation state are shown in Table 2.1. The sulfur cycle is shown in Figure 2.1. Gypsum ( $\text{CaSO}_4$ ), iron pyrites ( $\text{FeS}_2$ ), galena ( $\text{PbS}$ ), sphalerite ( $\text{ZnS}$ ), cinnabar ( $\text{HgS}$ ) and other minerals are deposited in rocks or buried deep under ocean sediments (Komarnisky et al., 2003). Large amounts of sulfur compounds deposited underground enter the atmosphere via volcanic eruptions, burning of fossil fuels and processing of metals. Then, atmospheric sulfur falls to the earth's surface by wet and dry deposition. Afterwards, sulfur accumulated in the soil by wet and dry deposition is converted into organic sulfur by microorganisms and plants, and then further ingested by animals. Additionally, sulfate converted by microorganisms or produced in industries flow into lakes and rivers, and finally into the ocean that represents the main reservoir for dissolved sulfate (Sievert et al., 2007). Thereafter, assimilatory and dissimilatory sulfate reduction occurs in anaerobic digestion to form organic sulfur compounds or sulfide that is released into the atmosphere or combined with minerals as sediments.

**Table 2.1.** Main forms of inorganic sulfur and its oxidation state.

Compounds	Sulfide $\text{H}_2\text{S}/\text{HS}^-$	Pyrite $\text{FeS}_2$	Thiosulfate $\text{S}_2\text{O}_3^{2-}$	Elemental sulfur $\text{S}^0$	Sulfite $\text{SO}_3^{2-}$	Sulfate $\text{SO}_4^{2-}$
Oxidation state	-2	-1	-1 (+5)	0	+4	+6

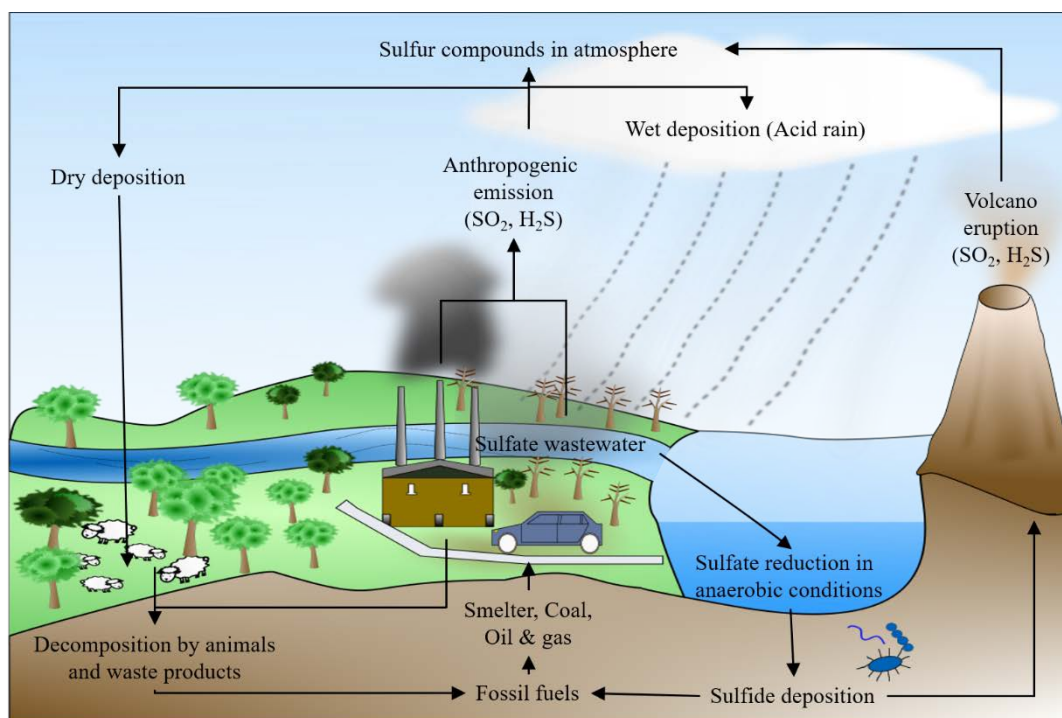


**Figure 2.1.** The sulfur cycle in ecosystem.

Microorganisms play an essential role in sulfur transformations. The microbial activity involved in the biological sulfur cycle is shown in Figure 2.2. Sulfate (final product of complete sulfur oxidation) is the most stable form of sulfur on Earth (Sievert et al., 2007), which serves as an electron acceptor and is converted to sulfide in dissimilatory energy-generating electron transport by a wide range of microorganisms. Moreover, in the assimilatory sulfate reduction pathway, sulfate is used to synthesize organic sulfur compounds by prokaryotes, algae, fungi and plants (Barton et al., 2014). The decaying organic matter releases hydrogen sulfide (H<sub>2</sub>S) to the air (Kellogg et al., 1972). Sulfide (final product of complete sulfur reduction) can be oxidized mainly to S<sup>0</sup>, sulfite, thiosulfate, or sulfate by phototrophic and chemolithotrophic bacteria (Gijs Kuenen, 1975).

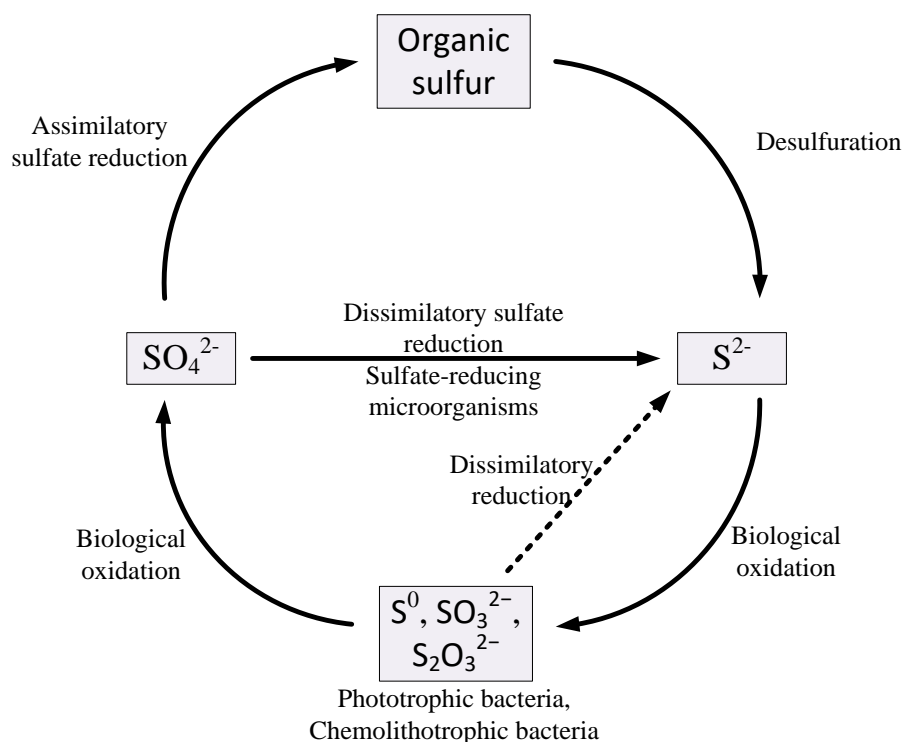


**Figure 2.2.** The biological sulfur cycle (Adapted from Gijs Kuenen 1975).

### 2.1.2 Sulfur pollution in flue gas and wastewater

Increasing anthropogenic activities, such as combustion of sulfur-containing fossil fuels and mining-smelting industrial processes, results in large quantities of sulfur compounds emission to the atmosphere and disturbs the balance of the cyclic conversions of sulfur cycle (Lens and Kuenen, 2001). Sulfur has been ascertained as a main component of air pollution as sulfur oxides ( $\text{SO}_x$ ), hydrogen sulfide ( $\text{H}_2\text{S}$ ) and mercaptans. Among them,  $\text{SO}_2$  contributed the most of gaseous sulfur compounds in anthropogenic emissions (about 95 percent) (Kellogg et al., 1972).  $\text{SO}_2$  is a colorless, odorous, corrosive pollutant, which is not only hazardous to human health, such as respiratory illness, asthma and lung cancer, but also causes environment problems (acid rain). Various emission control strategies have been applied, which have led to an  $\text{SO}_2$  emissions decline since the 1970s. Global contributions of anthropogenic activities and natural sources to  $\text{SO}_2$  emissions from 2005 to 2019 is shown in Figure 2.3. Although global anthropogenic  $\text{SO}_2$  emissions showed a downward trend from 2005 to 2019, anthropogenic  $\text{SO}_2$  emissions still accounted for 69% of total emission in 2019, of which



the combustion of coal accounted for the largest proportion, reaching 36%.

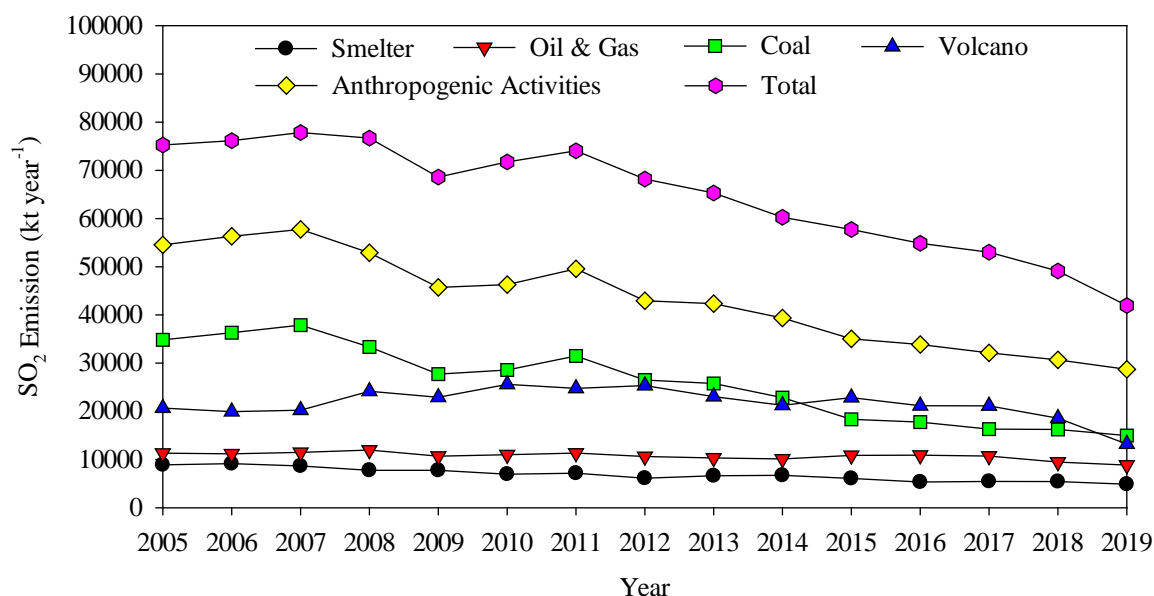


**Figure 2.3.** Global contributions of anthropogenic activities and natural sources to SO<sub>2</sub> emissions from 2005 to 2019 (Data from Dahiya et al. 2020).

Sulfur compounds also cause pollution to aquatic systems by direct discharge of sulfur-containing wastewaters, including sulfate, sulfite, thiosulfate, SO<sub>2</sub>, H<sub>2</sub>S, as well as lignosulfonates (Meyer and Edwards, 2014). Anthropogenic activities include the use of sulfur-containing materials in industrial operations, such as Kraft process and sulfite process in pulp and paper industry, and the use of sulfuric acid in the fermentation industry (Lens et al., 1998). Sulfite process is one of the chemical process in paper and pulp industry that uses sulfurous acid and/or its alkali salts (Na<sup>+</sup>, Ca<sup>2+</sup>, K<sup>+</sup>, Mg<sup>2+</sup>, NH<sub>4</sub><sup>+</sup>) to remove the lignin from cellulose. Sulfate is the most common component of sulfur compounds in pulp and paper industry wastewaters and fermentation industry wastewaters. Compared to H<sub>2</sub>S or SO<sub>2</sub> with high toxicity, sulfate is a fully oxidized compound, thus less toxic for the environment. However, sulfate concentrations above 1100 mg L<sup>-1</sup> have been reported to have a toxic effect on whitefish in the aquatic environment (Karjalainen et al., 2021). Moreover, excessive sulfate discharge can affect the sulfur cycle in the environment. Sulfate can form atmospheric SO<sub>2</sub> and SO<sub>3</sub> by sea salt

aerosols emission, or it can be reduced to sulfide in anaerobic environments. Atmospheric  $\text{SO}_2$  and  $\text{SO}_3$  form acid rain that leads to soil or freshwater acidification that further results in the loss of plant nutrients, the effect of vegetation, and the decrease of species diversity (Komarnisky et al., 2003). Therefore, treatment of sulfur gaseous emissions and wastewaters generated from industries is required.

### 2.1.3 Technological alternatives for flue gas treatment

The emission of volatile sulfur compounds (VSCs) can be treated physicochemically and biologically. Physicochemical technologies include scrubbing, adsorption and incineration (Smet et al., 1998), shown in Table 2.2. Physicochemical technologies are effective for VSCs removal from flue gases, but are expensive and the additional byproducts obtained require further treatments (Lens et al., 1998).

**Table 2.2.** Physicochemical treatment of volatile sulfur compounds.

Treatment	Consumption of reactants	Sulfur conversion	Reference
Alkaline Scrubbing	NaOH	$\text{H}_2\text{S}_{(g)}$ to $\text{H}_2\text{S}_{(l)}$	Mansfield et al., 1992
Oxidative Scrubbing	Hypochlorite	$\text{H}_2\text{S}$ to $\text{S}^0$ , sulfate	Durme et al., 1992
	$\text{H}_2\text{O}_2$ , NaOH	$\text{H}_2\text{S}$ to sulfate	Couvert et al., 2006
		$\text{CH}_3\text{SH}$ to $\text{CH}_3\text{SO}_3\text{H}$	
Catalytic Scrubbing	Chelated iron	$\text{H}_2\text{S}$ to $\text{S}^0$	Mansfield et al., 1992
Adsorption	Adsorbents (activated carbon, zeolites)	-	Ozekmekci et al., 2015; Turk et al., 1989
Incineration	-	$\text{H}_2\text{S}$ to $\text{SO}_2$	Smet et al., 1998

Biological techniques are an alternative for removing pollutants from contaminated air, which are economical and environmentally friendly (Qian et al., 2019; Smet et al., 1998). The main types of bioreactors for removal of  $\text{H}_2\text{S}$  and organic sulfur compounds include biofilters, bioscrubbers and biotrickling filters. Some references for the biological treatment of sulfur-containing gases are summarized in Table 2.3.

**Table 2.3.** Removal of H<sub>2</sub>S and organic sulfur compounds using biofilters, bioscrubbers and biotrickling filters.

Reactor type	Treated pollutants	Removal efficiency	Reference
Biofilters	13.6-68.2 g H <sub>2</sub> S m <sup>-3</sup> h <sup>-1</sup>	90-99%	Omri et al., 2011
	2320-2447 mg m <sup>-2</sup> d <sup>-1</sup> methanethiol	> 98%	Yao et al., 2019
Bioscrubbers	37-100 g S m <sup>-3</sup> h <sup>-1</sup> H <sub>2</sub> S	85-94%	San-Valero et al., 2019
	150 mg m <sup>-3</sup> ethanethiol	90%	Mhemid et al., 2019
Biotrickling filters	3-56.1 g H <sub>2</sub> S m <sup>-3</sup> h <sup>-1</sup>	> 81%	Lafita et al., 2012
	5.9 to 33.9 g S m <sup>-3</sup> h <sup>-1</sup> H <sub>2</sub> S	99%	Ramírez et al., 2011
	2.7 g S m <sup>-3</sup> h <sup>-1</sup> methanethiol	91%	
	2.3 g S m <sup>-3</sup> h <sup>-1</sup> dimethyl sulphide	95%	
	5.7 g S m <sup>-3</sup> h <sup>-1</sup> dimethyl disulphide	93%	

Cost-effective and efficient biological treatment processes consider not only pollutant treatment but also resources recovery. Biogas desulfurization technology has been applied in full-scale installations by Paques company, which developed processes to oxidize sulfide to elemental sulfur as well as to recover valuable metals from metal-sulfides precipitation. A multistage bioscrubber process has been investigated by GENOCOV to develop a two-stage process (sulfate reduction and sulfide oxidation) for biosulfur production to valorize the SO<sub>x</sub> and NO<sub>x</sub> contained in flue gases, named as SONOVA process (Mora et al., 2020a). The process consists of a sequential absorption of SO<sub>x</sub> that oxidizes SO<sub>2</sub> to sulfate. Then, sulfate is firstly reduced to sulfide in an up-flow anaerobic sludge blanket (UASB) reactor. Sulfide produced in the UASB reactor is partially oxidized to elemental sulfur (S<sup>0</sup>) in a continuous stirred tank reactor (CSTR). This thesis is specially focused on the reductive side in dissimilatory sulfate reduction.

## 2.2 Anaerobic digestion and glycerol fermentation

Anaerobic digestion (AD) occurs naturally in lakes and oceanic sediments, marshes, soils and municipal sewers (Van Lier et al., 2008). As a technology, AD for municipal

sewage and industrial wastewaters treatment removes organic pollutants and produces biogas as a renewable and sustainable energy source, which can be used for electricity, heat and biofuel production. Anaerobic treatment of food industrial wastewater was first investigated by Buswell et al. (1932). From 1970s, anaerobic sludge bed reactor technology attracted attention due to its simplicity of system construction, low sludge production and less space requirement. AD have widespread been used for treating various types of organic wastewater including food waste, beverage waste, alcohol distillery waste, pulp and paper industry, agricultural waste and chemical waste nowadays (Van Lier et al., 2015).

AD is a process that breaks down organic matter into simpler molecules that further converts into biogas. Four different stages are often identified: hydrolysis, fermentation or acidogenesis, acetogenesis, methanogenesis (Van Lier et al., 2008). During hydrolysis, fermentative bacteria convert complex particulate organic matter to dissolved compounds, such as proteins to amino acids, polysaccharides to monosaccharides, and lipids to fatty acids. The hydrolytic enzymes involved in the hydrolysis process include lipases, proteases, cellulases and amylases (Molino et al., 2013). In the acidogenesis/fermentation process, dissolved compounds are converted by fermentative bacteria to volatile fatty acids (VFAs), CO<sub>2</sub> and H<sub>2</sub>. In the acetogenesis process, acetogenic bacteria further convert VFAs (propionic acid, butyric acid) produced from acidogenesis process to acetic acid, CO<sub>2</sub> and H<sub>2</sub>. In methanogenesis, methane is produced from acetic acid by acetoclastic methanogens and from the reduction of carbon dioxide with hydrogen by hydrogenotrophic methanogens. In general, 70% of the methane produced is sourced from acetic acid (Van Lier et al., 2008).

Crude glycerol is an inexpensive by-product mainly produced in biodiesel production process. Approximately, 0.1 kg crude glycerol is produced per kg of biodiesel. It is estimated that worldwide glycerol production will reach 4.0 billion liters in 2020 (Nomanbhay et al., 2018). The composition of crude glycerol varies depending on the process, where the concentration of glycerol is about 70% to 98%, and the remaining

impurities include water, long-chain fatty acids, fatty acid methyl esters, salts, methanol, water, soap and ashes (Angeloni et al., 2016; Viana et al., 2012; Vivek et al., 2017). In order to maximize the value of crude glycerol and make it an energy source, glycerol valorization technologies are needed. The purification of crude glycerol can be carried out by distillation, but the technology at industrial scale is usually expensive because of high investment and low glycerol price (Demaman Oro et al., 2019). Direct application of crude glycerol is an alternative way, such as the bioconversion of glycerol to biodiesel (Chen et al., 2018), methane production and hydrogen production in anaerobic digestion (Baba et al., 2013; Mangayil et al., 2012), composting (Fehmberger et al., 2020) and combustion (Muelas et al., 2020).

Metabolic pathways of glycerol fermentation in anaerobic digestion have been clearly described by a combination of reductive and oxidative reactions (Viana et al., 2012). From one side, glycerol is first dehydrated to 3-hydroxypropionaldehyde that is further reduced to 1,3-propanediol by the enzyme 1,3-propanediol dehydrogenase. On the other hand, via an oxidative pathway, glycerol is also converted to phosphoenolpyruvate, which subsequently produces propionate and pyruvate. Pyruvate can further produce other compounds such as n-butanol, 2,3-butanediol, ethanol, lactate, butyrate, formate, acetate, hydrogen and CO<sub>2</sub> depending on the microbial cultures and environmental conditions. In addition to H<sub>2</sub>, most of the abovementioned organic compounds can be used as electron donors by SRB to reduce sulfate to sulfide. Due to the abundance of glycerol generated as a by-product in the biodiesel production process and the requirement for electron donors and energy source in sulfate reduction process, glycerol points to the potential for treating sulfate-rich wastewater. In this sense, this thesis researched the long-term stability and sulfate reduction efficiency in a UASB reactor using crude glycerol as the carbon source, and explored its degradation mechanism.

## 2.3 Sulfate reduction process

### 2.3.1 Sulfate reducing bacteria

Sulfate reducing bacteria (SRB) are a diverse group of prokaryotes microorganisms including bacteria and archaea, that can use sulfate, sulfite, thiosulfate or sulfur as electron acceptors for energy metabolism under anaerobic conditions (Barton and Hamilton, 2007). SRB are widespread in the natural environment and engineered ecosystems, such as marine sediments, wetland, soils, oil reservoirs, acid mine drainage, sewage and industrial wastewater (Leloup et al., 2007; Meyer and Edwards, 2014; Qian et al., 2019; Rabus and Strittmatter, 2007; Wu et al., 2013). Meyer (1864) first discovered that sulfate could be reduced to sulfide in aquatic sediments, and Beijerinck (1895) firstly isolated and characterized a SRB *Spirillum Desulfuricans*. More than 220 species of 60 genera of SRB have been reported (Barton and Fauque, 2009).

According to 16S ribosomal RNA (rRNA) sequence analysis, SRB can be divided into seven phylogenetic lineages, in which five are bacteria and two are archaea (Muyzer and Stams, 2008), as shown in Figure 2.4. Another criterion for SRB classification is the pathway of sulfate reduction through SRB. The reduction of sulfate to sulfide by SRB follows both assimilative and dissimilative metabolisms. Dissimilatory sulfate reduction is the main pathway to produce hydrogen sulfide (Madigan and Martinko, 1997) by SRB using sulfate as the terminal electron acceptor either through autotrophic or heterotrophic metabolisms (Lens and Kuenen, 2001). Heterotrophic SRB include incomplete oxidizers (that partly oxidize organic compounds to acetate), and complete oxidizers (that entirely oxidize organic compounds to CO<sub>2</sub>) (Muyzer and Stams, 2008). Incomplete-oxidizing SRB include *Desulfobulbus*, *Desulfomicrobium*, *Desulfomonas*, *Desulfovibrio*, *Thermodesulfobacterium*, *Desulfohalobium*, *Desulfonatrum* and *Archaeoglobus*. Complete-oxidizing SRB include *Desulfobacter*, *Desulfobacterium*, *Desulfococcus*, *Desulfomonile*, *Desulfonema* and *Desulfosarcina* (Castro et al., 2000).

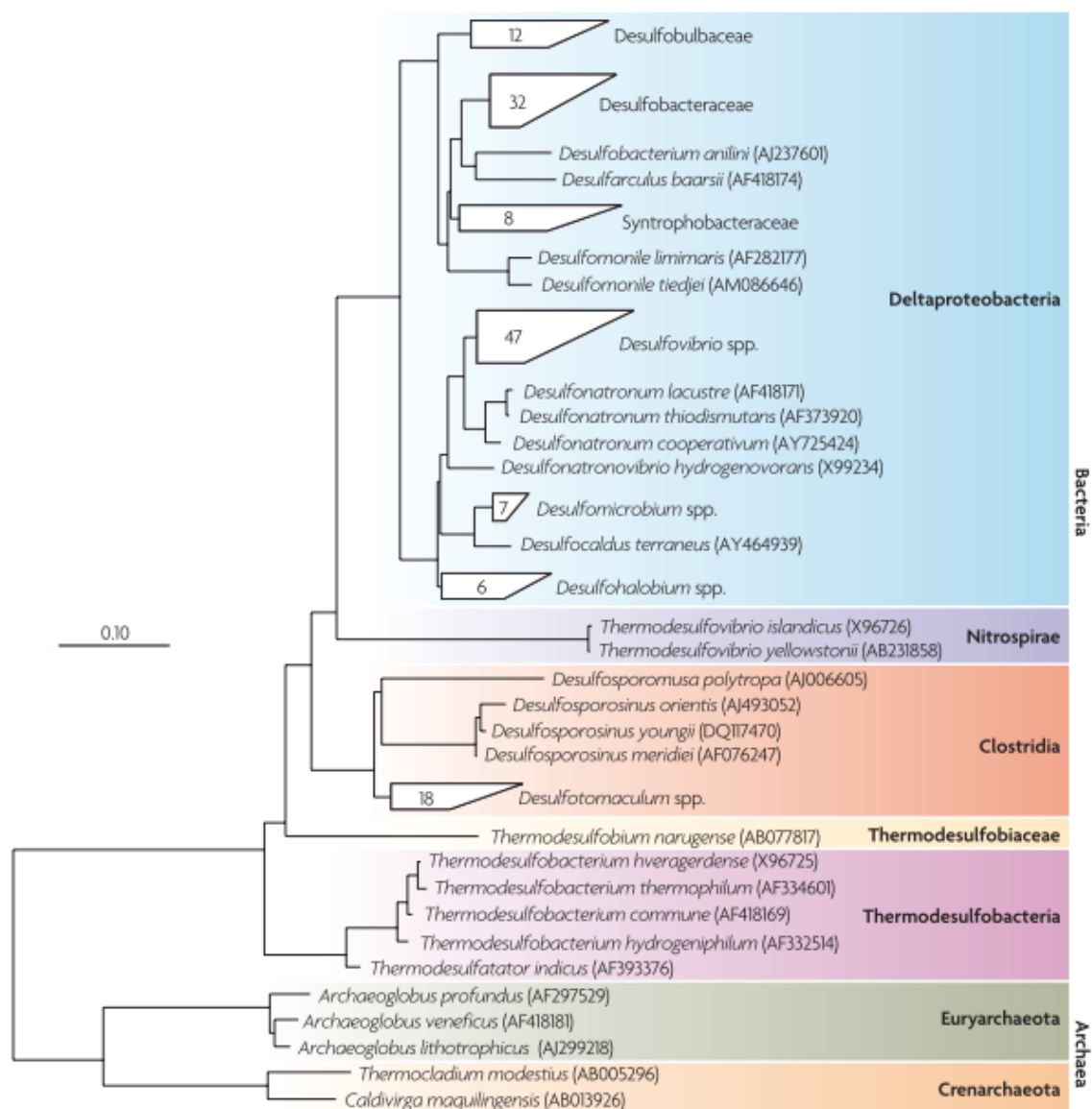


**Figure 2.4.** Phylogenetic tree of sulfate reducing bacteria (SRB) based on 16S ribosomal RNA (rRNA) sequence (Data from Muyzer and Stams, 2008).

Since the sulfate-sulfite redox couple is too negative (-516 mv), it is hard to reduce sulfate directly by the intracellular electron mediators ferredoxin or NADH present in sulfate reducers. Sulfate is first activated with adenosine triphosphate (ATP) to form adenosine-phosphosulphate (APS) and inorganic pyrophosphate (PPi) (Muyzer and Stams, 2008). PPi is further hydrolyzed by pyrophosphatase to inorganic phosphate (Pi) and APS is rapidly reduced by a cytoplasmic iron-sulfur flavoprotein (APS reductase) to sulfite and adenosine monophosphate (AMP). In the dissimilatory pathway, the six-electron

reduction of sulfite to sulfide is catalyzed by dissimilatory sulfite reductase (DSR), a siroheme containing protein. Sulfite can also be reduced to sulfide in assimilatory pathway by assimilatory sulfite reductase (ASR), a NADPH-dependent or a ferredoxin-dependent enzyme (Grein et al., 2013).

### **2.3.2 Electron donors for sulfate reduction**

A wide range of compounds can be utilized as electron donors in the sulfate reduction process, including inorganic and organic compounds. Autotrophic SRB use CO<sub>2</sub>, or CO as carbon source and H<sub>2</sub> as electron donor to reduce sulfate while heterotrophic SRB can use a large variety of organic compounds as electron donor including monocarboxylic acids, dicarboxylic acids, alcohols, sugars and industrial organic wastewaters. Table 2.4 summarizes the possible electron donors for sulfate reduction and their corresponding reactors as well as the dominant SRB species.



**Table 2.4.** Dominant sulfate reducing bacteria (SRB) and electron donors for sulfate reduction under different bioreactors.

Electron donors	Dominant species	Bioreactors	Reference
<b>Inorganic compounds</b>			
H <sub>2</sub> /CO <sub>2</sub>	<i>Desulfovibrio</i>	Gas-lift	Van Houten et al., 1995; Weijma et al., 2002
H <sub>2</sub> /CO	<i>Desulfovibrio</i>	Gas-lift	Van Houten et al., 1995
CH <sub>4</sub>	<i>Desulfosarcina</i>	Biotrickling filter	Cassarini et al., 2019
<b>Organic compounds</b>			
<b>Monocarboxylic acids</b>			
Formate	NA	Membrane	Bijmans et al., 2008
Acetate	<i>Desulfotalea, Desulfobacter</i>	Batch reactor	Van Den Brand et al., 2014
Propionate	<i>Desulfotomaculum</i>	Membrane	Qiao et al., 2016
Butyrate	NA	Anaerobic chemostat reactor	Mizuno et al., 1994
Valerate	<i>Desulfonatronobacter</i>	NA	Wang et al., 2008
Lactate	<i>Desulfomonas,</i> <i>Desulfovibrio</i>	UASB	Bertolino et al., 2012
pyruvate	<i>Desulfovibrio</i>	Serum bottles	Sass et al., 1998
<b>Dicarboxylic acids</b>			
Malate	<i>Desulfovibrio</i>	Serum bottles	Sass et al., 1998
Fumarate	<i>Desulfovibrio</i>	Serum bottles	Sass et al., 1998
Succinate	<i>Desulfovibrio</i>	Serum bottles	Sass et al., 1998
<b>Alcohols</b>			
Methanol	NA	UASB	Vallero et al., 2003
Ethanol	<i>Desulfobulbus,</i> <i>Desulfomicrobium</i>	ASBRs	Zeng et al., 2019
Glycerol	<i>Desulfovibrio</i>	UASB	Mora et al., 2020b
1,3-propanediol	<i>Desulfovibrio</i>	Serum bottles	Qatibi et al., 1991
<b>Others</b>			
Sucrose	NA	UASB	Lopes et al., 2007
Molasses	<i>Desulfovibrio,</i> <i>Desulfobacter</i>	CSTR	Nanqi et al., 2007
Citric acid	<i>Trichococcus,</i> <i>Veillonella</i>	Anaerobic bioreactors	Stams et al., 2009
Woodchips, alfalfa and sawdust	<i>Desulfosporosinus</i>	SRBRs	Drennan et al., 2017

Note: NA: Not available; ASBRs: Anaerobic sequencing batch reactors; CSTR: Continuous stirred tank reactor; SRBRs: Sulfate-reducing bioreactors (SRBRs); UASB: Up-flow anaerobic sludge blanket.

Among these electron donors, SRB are more favorable with the utilization of low molecular weight organic acids and alcohols as electron donors due to their high affinity (Johnson and Sánchez-Andrea, 2019; Reyes-Alvarado et al., 2018). In the sulfate reduction processes at laboratory-scale, hydrogen has also proven to be an effective electron donor (Bijmans et al., 2008), but the production of high-purity hydrogen is expensive. In addition, syngas (a mixture of H<sub>2</sub>, CO<sub>2</sub> and CO) could be a cost-effective alternative. However, the toxicity of CO, which inhibits the growth of some SRB, reduces the sulfate reduction efficiency (Kaksonen and Puhakka, 2007). Moreover, compared with lactate and glycerol as electron donors to reduce sulfate, lactate is more energetically favored by SRB, but glycerol is a cost-effective carbon source. Thus, when processing sulfate-enriched sewage from laboratory-scale to full-scale operation, the selection of electron donors needs to be considered from many aspects. They include the output and local availability of the electron donor, the price and operating cost of the electron donor, the applicability and suitability to treat special sewage (depending on temperature, salinity and composition), undesirable by-products that are subsequently produced after treatment of sewage, and regulations regarding safety and environment (Bijmans et al., 2011). When acetate, cheese whey, pig slurry, crude glycerol and vinasses were selected as carbon sources for sulfate reduction process and several conditions were tested, such as temperature, pH, COD/S-SO<sub>4</sub><sup>2-</sup> ratio, crude glycerol was the most adequate carbon source to reduce sulfate (Mora et al., 2018).

Crude glycerol has been proposed as a potential electron donor for sulfate reduction in industrial applications (Bertolino et al., 2014). Biosulfidogenesis-based technology has been applied for the treatment of metal-rich wastewaters, such as acid mine drainage (AMD), where sulfate is firstly reduced to sulfide using glycerol as carbon source and secondly sulfide contacts metals to form metal sulfide precipitates to achieve the purpose of removing and recovering metals (Santos and Johnson, 2017). Moreover, crude glycerol has been proven to be an electron donor for the valorization of sulfate-rich effluents to recover elemental sulfur in the long-term operation (Fernández-Palacios et al., 2019;

Mora et al., 2020a), where different chemical oxygen demand to sulfate ratios (COD/S-SO<sub>4</sub><sup>2-</sup>) were investigated and assessed in a sulfidogenic UASB. However, the mechanism of crude glycerol degradation and sulfate reduction was still not clear, which is discussed in Chapter 6 of this thesis.

### **2.3.3 Bioreactors for sulfate reduction**

An anaerobic reactor was firstly designed by Karl Imhoff in 1905 (Van Lier et al., 2008). Subsequently, in the last 40 years, anaerobic reactors have been worldwide used in various types of industries to treat wastewater (Van Lier et al., 2008), and the full-scale installations for treating industrial wastewater have gradually increased to 2266 in 2006. It is also estimated that more than 4000 anaerobic high-rate reactors had been established and applied in 2015 (van Lier et al., 2008; 2015). A variety of anaerobic treatment configurations have been reported, including CSTR, anaerobic contact process (ACP), gas lift reactors (GLR), anaerobic filter reactor (AFR), fluidized-bed reactor (FBR), UASB, anaerobic hybrid reactor (AHR), anaerobic baffled reactor (ABR), extractive membrane bioreactor (EMBR) and membrane bioreactor (MBR) (Bijmans et al., 2011; Kaksonen and Puhakka, 2007), as shown in Figure 2.5. These anaerobic bioreactors for organic wastewater treatment can also be applied for biological sulfate reduction, in which organic compounds are degraded by sulfate reduction and fermentation process (Kaksonen and Puhakka, 2007; Lens et al., 1998).

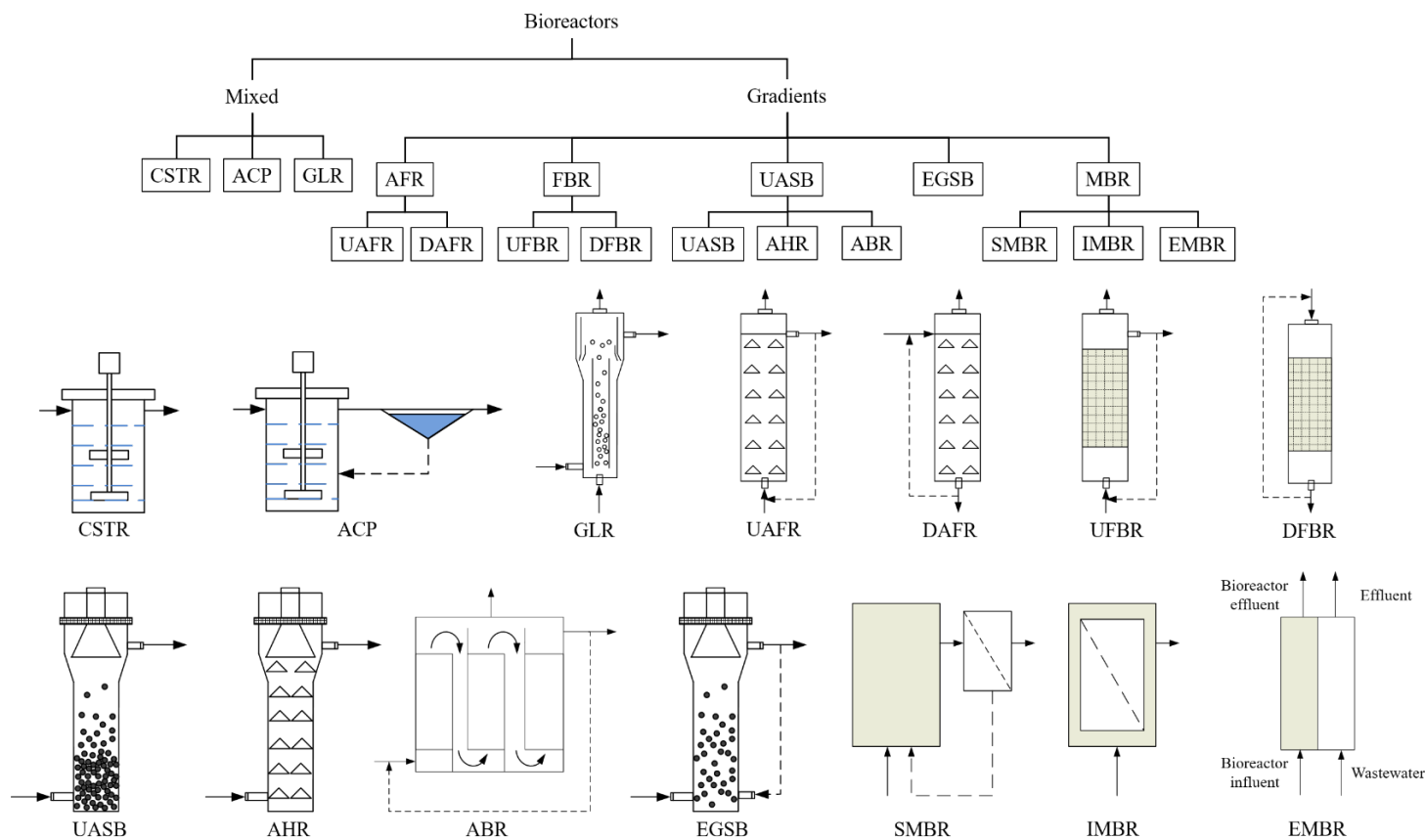


**Figure 2.5.** Various types of reactors in anaerobic wastewater treatment: continuous stirred tank reactors (CSTR), anaerobic contact process (ACP), up-flow anaerobic filter reactor (UAFR), down-flow anaerobic filter reactor (DAFR), up-flow fluidized-bed reactor (UFBR), down-flow fluidized-bed reactor (DFBR), up-flow anaerobic sludge blanket (UASB), anaerobic hybrid reactor (AHR), anaerobic baffled reactor (ABR), expanded granular sludge blanket (EGSB), sidestream membrane bioreactor (SMBR), immersed membrane bioreactor (IMBR), extractive membrane bioreactor (EMBR) (adapted from Bijmans et al., 2011; Kaksonen and Puhakka, 2007).

The most widely and successfully used reactors configuration in the anaerobic treatment technology of industrial wastewater are UASB and EGSB reactors and their derivatives (van Lier et al., 2015). The UASB reactor was invented by Lettinga and coworkers in the 1970s, and its application rapidly extended. The success of UASB application in wastewater treatment benefits from its high concentration of sludge, no channeling of flow, no compacting of sludge, hardly clogging problems, high rates and removal efficiency, simple construction, no requirements for mixing equipment, low operating and maintenance costs, small land occupation and low residual sludge output (Daud et al., 2018; Kaksonen and Puhakka, 2007). The EGSB reactor, a variant of the conventional UASB reactor, operates with high up-flow velocities that is achieved by recirculating liquid from the effluent to the influent. The high up-flow velocities of EGSB reactors improve mass transfer rate, and they can treat wastewaters containing biodegradable toxic or inhibitory compounds, since the dilution of toxicity effects on bacterial activity (Jeison and Chamy, 1999). However, the high up-flow velocities could lead to the washout of biomass resulting in process failures. Therefore, the UASB reactor was investigated in this thesis using crude glycerol as the carbon source.

## **2.4 Modeling biological sulfate reduction**

### **2.4.1 Modeling of anaerobic digestion**

With the increasing interest in applying biotechnologies in a variety of bioreactors, mathematical modelling is a useful tool to study the sensitivity of various operating parameters and to optimize the design of anaerobic digestion systems (Saravanan and Sreekrishnan, 2006). Models can also quantitatively express and validate hypothesis, and predict the system's behavior under other similar circumstances (Donoso-Bravo et al., 2011). The development of a mathematical model generally includes six steps: model selection, parameter selection, data collection, parameter estimation, accuracy estimation and validation (Lauwers et al., 2013). Its schematic overview is shown in Figure 2.6.

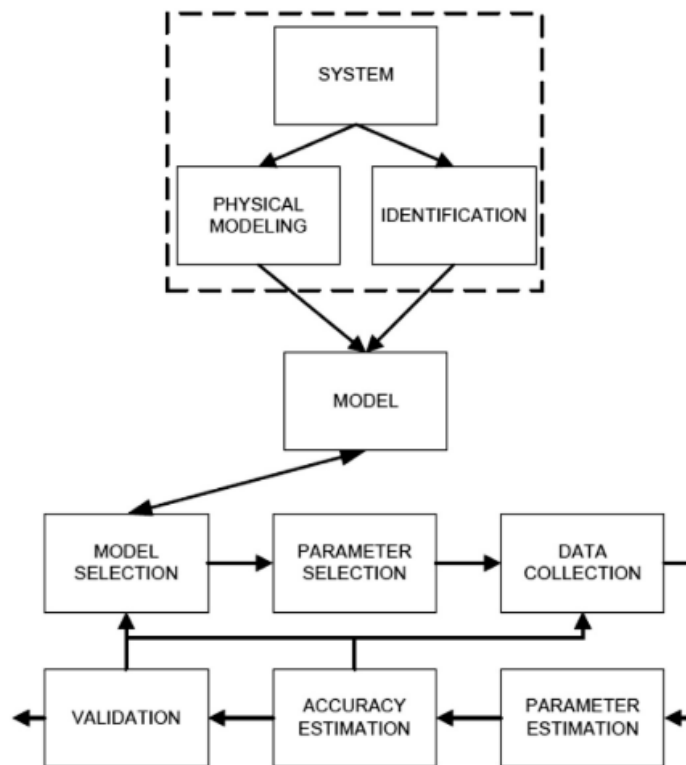


Figure 2.6. Schematic overview of a mathematic model procedure (Lauwers et al., 2013).

Anaerobic digestion is a multi-step process, in which each step involves a variety of microbial activities. In order to effectively describe, design and predict the operation of anaerobic digestion systems, appropriate mathematical models need to be developed. Initially, the first model describing anaerobic digestion process used the rate-limiting step concept, which is the overall rate of a process determined by the rate of the slowest step (Hill and Barth, 1977). The rate-limiting step model is simple and readily usable, but it cannot describe the performance of anaerobic digestion appropriately, especially under transient operating conditions (Lyberatos and Skiadas, 1999). Subsequently, Bryers (1985) and Mosey (1983) developed a model that considered intermediate metabolites (VFAs or hydrogen) as key variables also considering other indicators such as pH and the hydrogen partial pressure. When describing the transformation of substance and their rates in AD, kinetic equation rates also began to consider microbial growth, decay of biomass, acid-base equilibrium, gas-liquid equilibrium, mass diffusion, mass transfer coefficient, as

well as the temperature (Manchala et al., 2017). In AD, hydrolysis of complex organic compounds and biomass decay are usually simplified as first-order rate equations, while fermentation or acidogenesis, acetogenesis, methanogenesis are often modeled by Monod kinetics (Angelidaki et al., 1999; McCarty and Mosey, 1991).

The hydrolysis rate using first-order reaction is represented by Eq.2.1.

$$-r_{\text{hyd}} = k_{\text{hyd}} * X \quad \text{Eq.2.1}$$

Where  $r_{\text{hyd}}$  is the hydrolysis rate of substrate, g COD L<sup>-1</sup> d<sup>-1</sup>;  $k_{\text{hyd}}$  is the hydrolysis rate coefficient, g COD g VSS<sup>-1</sup> d<sup>-1</sup>;  $X$  is the concentration of biomass, g VSS L<sup>-1</sup>.

The decay rate of microorganism is defined by Eq.2.2.

$$-r_d = k_d * X \quad \text{Eq.2.2}$$

Where  $r_d$  is the biomass decay rate, g VSS L<sup>-1</sup> d<sup>-1</sup>;  $k_d$  is the decay coefficient, d<sup>-1</sup>.

The growth rate of microorganism is defined by Eq.2.3.

$$r_g = \mu * X \quad \text{Eq.2.3}$$

Where  $r_g$  is the biomass growth rate, g VSS L<sup>-1</sup> d<sup>-1</sup>;  $\mu$  is the biomass specific growth rate, d<sup>-1</sup>.

Monod equation is shown in Eq.2.4.

$$\mu = \mu_{\text{max}} * \frac{S}{k_s + S} \quad \text{Eq.2.4}$$

Where  $\mu$  is microbial specific growth rate, g L<sup>-1</sup> d<sup>-1</sup>;  $\mu_{\text{max}}$  is maximum specific growth rate, d<sup>-1</sup>;  $S$  is the concentration of substrate, g L<sup>-1</sup>;  $k_s$  is the half-saturation coefficient for substrate  $S$ , g L<sup>-1</sup>. Microbial specific growth rate may be affected by other substrates or potential limitations. Other terms similar to substrates can be added to Eq.2.4, which is not described in detail here.

The substrate consumption rate is correlated to the microbial growth rate divided by a growth yield coefficient ( $Y_{B/S}$ , g VSS/g), expressed as Eq.2.5.

$$-r_s = \frac{r_g}{Y} \quad \text{Eq.2.5}$$

With increasing interest in anaerobic digestion simulation, the IWA Task Group for Mathematical Modeling of Anaerobic Digestion Processes developed the Anaerobic

Digestion Model No.1 (ADM1) as a unified anaerobic model (Batstone et al., 2002). ADM1 is a structured model that describes biochemical and physical-chemical processes, which involved 24 soluble variables, 3 gas variables and 19 biochemical processes. The biochemical processes include (1) disintegration of complex particulate waste and inactive biomass (first-order kinetics); (2) extracellular hydrolysis of carbohydrates, proteins and lipids (first-order kinetics); (3) acidogenesis of sugars, amino acids and long-chain fatty acids (LCFAs) to VFAs (Monod-type kinetics); (4) acetogenesis of VFAs to acetate (Monod-type kinetics); (5) methanogenesis of acetate and hydrogen/CO<sub>2</sub> (Monod-type kinetics). The physical-chemical equations include ion association/dissociation and gas-liquid mass transfer. Several inhibition indicators are also considered in ADM1, of which two empirical equations are used for pH inhibition, and the non-competitive functions are applicable for hydrogen and free ammonia inhibition.

The ADM1 has been applied in a wide variety of organic wastes for anaerobic digestion simulation, such as olive pulp (Kalfas et al., 2006), grass silage (Koch et al., 2010), domestic green and food wastes (Poggio et al., 2016), slaughterhouse wastes (Poggio et al., 2016), municipal solid waste (Fatollahi et al., 2020), brewery waste (Siqueiros et al., 2019), wastewater treatment in pilot-scale, full-scale of sewage sludge digestion (Blumensaat and Keller, 2005; Shang et al., 2005). The ADM1 allows extensions and modifications to expand its application capacity in terms of simulating fermentation to hydrogen, sulfate reduction, description of phosphorous performance and mineral precipitation (Batstone et al., 2006; Lauwers et al., 2013).

### **2.4.2 Modeling of sulfate reduction in anaerobic digestion**

The extension of ADM1 to describe sulfate reduction processes has been also developed. Fedorovich et al. (2003) incorporated sulfate reduction into ADM1 to predict the long-term operation of a VFAs-fed UASB reactor, which was described by multiple reaction stoichiometry, microbial growth kinetics, conventional material balances for ideally mixed reactor, liquid-gas interactions and liquid-phase equilibrium chemistry. This



extension model can predict the competition among three types of microorganisms (acetogenic bacteria, methanogenic archaea and sulfate-reducing bacteria). However, their dynamics and competition were not included. This model was not able to predict H<sub>2</sub>S in the gas phase since H<sub>2</sub>S gas-liquid mass transfer was not considered (Fedorovich et al., 2003). Afterwards, another extension of ADM1 with sulfate reduction for a high-strength and sulfate-rich wastewater treatment was developed to overcome the limitation of prediction of H<sub>2</sub>S in liquid and gas phases, which included propionate and acetate as main VFAs (Barrera et al., 2015). Chen et al. (2019) described a structured mathematical model based on ADM1 to describe the sulfate reduction process, which explored the long-term competitive dynamics of microorganism in 329 days of continuous operation of an ethanol-fed UASB reactor. Moreover, carbon-nitrate-sulfate removal under anaerobic or oxygen-limited conditions was described by a comprehensive model that incorporated Activated Sludge Models Nos. 1, 2 and 3 (ASMs) and extended ADM1 with sulfate reduction, which involved the interactions of SRB, sulfide-oxidizing bacteria (SOB), nitrate-reducing bacteria (NRB), facultative bacteria and methanogens (Xu et al., 2017).

In addition to the extension of ADM1 for sulfate reduction, some studies described the sulfate reduction process based on Monod-type kinetics. Kalyuzhnyi and Fedorovich (1998) described a structured mathematical model for studying competition between SRB and methanogens in anaerobic reactors. Xu et al. (2013) developed a Monod-based model to describe the sulfate reducing and sulfide oxidizing process. The model that used ethanol as carbon source described methane production and sulfate reduction process based on growth kinetics of microorganism, which predicted the stratified distribution of methanogens, SRB and fermentative bacteria (Sun et al., 2016).

The carbon source studied in this thesis is glycerol. There are many intermediate metabolites during the fermentation of glycerol, such as ethanol, 1,3-propanediol, n-butanol, 2,3-butanediol, lactate, butyrate, formate, acetate, propionate and hydrogen (Viana et al., 2012). A kinetic model based on Edward and Andrew's equation has been developed in an anaerobic bioreactor to describe glycerol degradation and sulfate

reduction, but the degradation process of glycerol described in the model is that glycerol was directly oxidized to acetate with sulfate reduction (Dinkel et al., 2010). Few works mentioned alcohols (ethanol and 1,3-propanediol) as intermediate metabolites of complex organic compounds to describe the sulfate reduction process. Although there are models describing the process of sulfate reduction with VFAs (Fedorovich et al., 2003), ethanol (Chen et al., 2019) and glycerol (Dinkel et al., 2010) as carbon sources, the current modelling approach described in literature is not enough to describe the sulfate reduction process when other intermediates (alcohols) are produced during hydrolysis or fermentation of complex organic compounds. Thus, a model that includes the production of various intermediates during the fermentation process with sulfate reduction needs to be established, which is discussed in Chapter 7 of this thesis.



## **Chapter 3**

---

### **General materials and methods**



## 3.1 Description of reactors

### 3.1.1 UASB reactor

A 2.5 L laboratory-scale up-flow anaerobic sludge bed (UASB) reactor was operated in this thesis. The cylindrical reactor was made of glass with 51 mm diameter and 80 mm in height. The liquid inlet is composed of a liquid distributor at the bottom of the UASB. On top of the UASB a gas-liquid-solid separator was used. The liquid outlet of the UASB is connected to a continuous stirred-tank reactor (CSTR). Six sampling ports were set up along the UASB reactor (Figure 3.1 and Figure 3.2). The sampling ports, located at different heights of the UASB reactor (at 7, 20, 30, 45, 54 and 72 cm from the bottom of UASB) are sequentially named UASB1, UASB2, UASB3, UASB4, UASB5 and UASB6. The outer wall of the UASB reactor is covered with a water jacket connected with a thermostated water bath (RP100, Lauda, Germany) to control the temperature at 35 °C. pH and oxidation-reduction potential (ORP) were monitored online by a digital multimeter (multimeter44, Crison, Germany) using probes (pH 5333 and ORP 5350, Crison, Spain). A 3 L tedlar sampling bag (FlexFoil, SKC Inc, USA) is attached to the top of the UASB for collecting gas production.

The UASB reactor was inoculated with 1 L of granular sludge from a full-scale UASB from a pulp and paper recycling industry (UIPSA, Spain), which was mainly used for methane production by the industrial facility. The initial volatile suspended solids (VSS) concentration of granular sludge was 27.1 g VSS L<sup>-1</sup>. In order to maintain the constant conditions, the sulfate inlet concentration was set to 250 mg S-SO<sub>4</sub><sup>2-</sup> L<sup>-1</sup>, while the crude glycerol to sulfate ratio (TOC/sulfate) was steadily maintained at 1.5 ± 0.3 g C g<sup>-1</sup> S. These conditions were selected according to the period of maximum sulfate reduction and organic matter removal efficiencies studied by Fernández-Palacios et al. (2019). The mineral medium (MM) composition of the UASB was (in g L<sup>-1</sup>): NH<sub>4</sub>Cl (0.2), K<sub>2</sub>HPO<sub>4</sub> (3) and Na<sub>2</sub>SO<sub>4</sub> (1.15) dissolved in tap water. Since sulfate reducing bacteria (SRB) with better growth characteristics have an optimum pH higher than methanogens (O'Flaherty et al.,

1998), the pH of MM was adjusted to 8.5-8.8 using 2M NaOH or 2M HCl to achieve sulfidogenic conditions. The flow rate of crude glycerol was 30 mL h<sup>-1</sup> using a peristaltic pump (TR11, Watson, UK). Once mixed with the carbon source (crude glycerol), the medium was pumped (A773, Milton, USA) into the UASB from the bottom of the reactor, as shown in Figure 3.2. The temperature was controlled at 35 °C and the up-flow velocity was set at 0.25 m h<sup>-1</sup>. The temperature and up-flow rate corresponded to those previously also studied by Fernández-Palacios et al. (2019). The hydraulic residence time (HRT) was 2 h, which is the reaction volume (the sludge bed volume) divided by the flow rate. The UASB reactor was operated under constant conditions for 639 days.

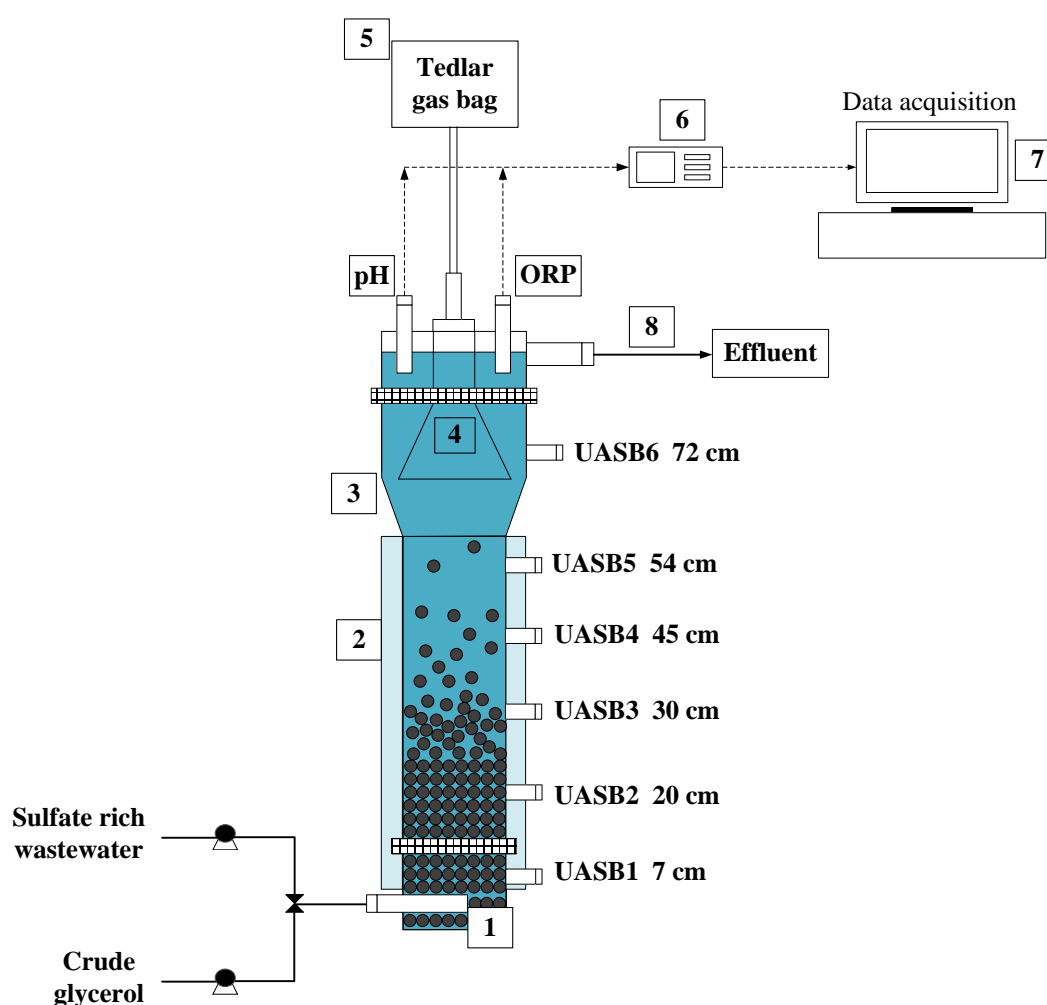


**Figure 3.1.** Schematic diagram of UASB reactor and CSTR. 1, liquid distributor; 2, Thermostat water bath; 3, UASB reactor; 4, Gas-liquid-solid separator; 5, Tedlar gas bag for biogas collecting; 6, Digital multimeter; 7, Data acquisition unit; 8, Effluent of UASB reactor that connected CSTR to partially oxidize sulphide to elemental sulfur.

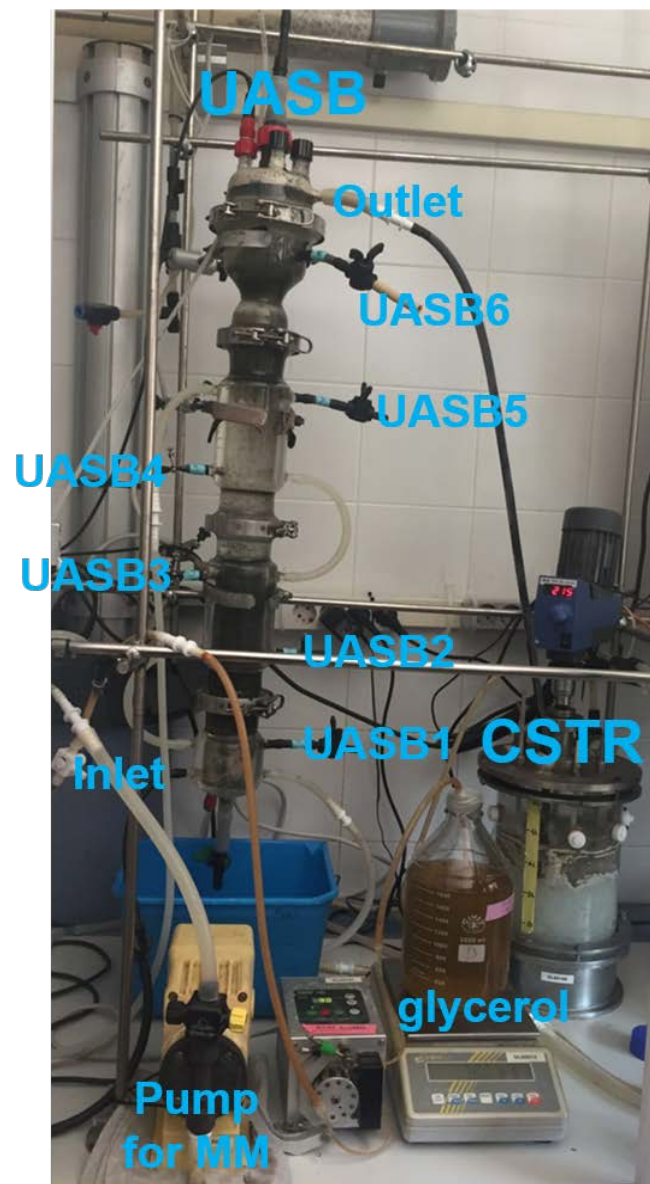


**Figure 3.2.** Overview of UASB reactor and CSTR setup.

### 3.1.2 CSTR reactor

A continuous stirred-tank reactor (CSTR) was used to partially oxidize sulfide (from the effluent of UASB reactor) to elemental sulfur. The sulfide oxidizing biomass used to inoculate the CSTR was obtained from a desulfurizing biotrickling filter. The CSTR is a glass-made container (effective volume of 6 L). The metal container at the bottom of CSTR is a water jacket connected with a thermostat water bath controlled at 35 °C, as shown in

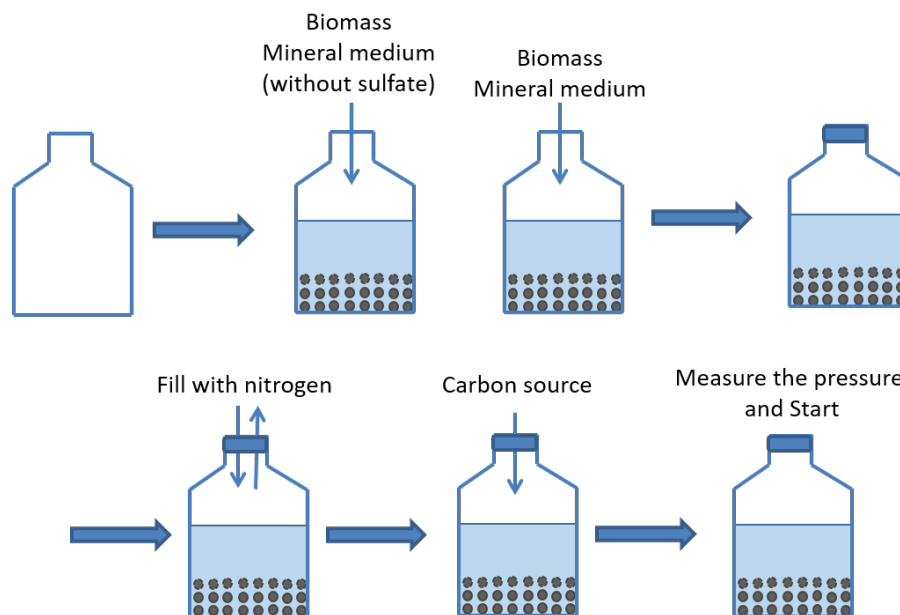


Figure 3.2. The liquid volume was maintained at 5 L when the CSTR was operating. The CSTR was under microaerobic conditions by connecting the agitator (RW20, IKA, Germany) at a speed of 200 rpm to transfer atmospheric oxygen into the liquid. pH and ORP were monitored online by probes (pH 5333 and ORP 5350, Crison, Spain) with a digital multimeter (multimeter44, Crison, Germany). Dissolved oxygen (DO) was monitored by an optical oxygen sensor (VisiFerm DO 120, Hamilton, USA) connected to a multimeter (Oxy 2405, Stratos Eco, Germany).

### **3.2 Batch activity tests in serum bottles**

Batch activity tests were conducted by feeding different carbon sources, in which the sludge was either the inoculum of the UASB or the sludge taken from different heights of the UASB as further detailed in chapters 5 and 6.

Batch tests were conducted using 250 mL serum bottles. The inoculation procedure of the batch tests is shown in Figure 3.3. Sludge samples were firstly rinsed with MM (without sulfate) before inoculating into 250 mL serum bottles, which were afterwards fed with 150 mL of the same MM that was used to feed the UASB. The control group consisted of MM without sulfate supplied with different carbon sources, while sulfate was added in addition to the carbon source in the experimental group. After adding MM and the granular sludge, the pH was adjusted to 8-8.5 by adding either 2M NaOH or 2M HCl. The gas-phase was exchanged with N<sub>2</sub> and bottles were instantly capped with rubber stoppers and aluminum caps. After adding the carbon source, the batch test started. The incubation time was between 96 and 120 h depending on the test. Bottles were cultivated in a shaker (NB-T205, N-Biotek) at a constant temperature of 35 ± 1 °C and a stirring speed of 150 rpm during the culture.



**Figure 3.3.** The inoculation process of the batch tests.

### 3.3 Analytical methods

The inlet and outlet of the UASB reactor were sampled every two or three days to monitor the sulfur compounds, volatile fatty acids (VFAs), volatile suspended solids and total organic carbon. The gas phase was monitored between two to ten days, depending on the gas production. The sampling procedure along the height of the UASB reactor is explained in Chapter 4.

In the batch tests, the analysis of components in the liquid were the same as the analysis of the UASB reactor, in addition to alcohols monitoring. Bottles headspace was monitored for gas analysis. All liquid samples were filtered by 0.22  $\mu\text{m}$  filters (Millipore, USA) before analysis.

#### 3.3.1 Sulfur compounds

Total dissolved sulfide (TDS) was analyzed off-line by a sulfide selective electrode (9616BNWP, Thermo Scientific, USA) connected to a benchtop meter (Symphony, VWR, USA). Before TDS measurements, samples were diluted one-to-two for UASB samples

and one-to-twenty for activity tests samples with a sulfide antioxidant buffer (SAOB) containing ( $\text{g L}^{-1}$ ): ascorbic acid (35), EDTA (67) and NaOH (80). NaOH was added to keep pH above 12, thereby converting  $\text{HS}^-$  and  $\text{H}_2\text{S}_{(\text{aq})}$  to  $\text{S}^{2-}$ . Ascorbic acid is an antioxidant to protect sulfide from oxidation. EDTA (ethylenediaminetetraacetic acid) is a metal chelating agent that can combine with divalent metal ions such as  $\text{Mg}^{2+}$ ,  $\text{Ca}^{2+}$ , etc. (existing in tap water), which can be used to prevent precipitation reactions between sulfide and metal ions.

Sulfate and thiosulfate were analyzed by ion chromatography (ICS-2000 system, Dionex, USA) with a suppressed conductivity detector using an IonPac AS18-HC column (4X250 mm, Dionex, USA). Prior to the analysis of sulfate and thiosulfate, samples were bubbled with nitrogen to avoid chemical oxidation of sulfide, and samples were diluted to one fifth with ultrapure water.

### **3.3.2 Carbon compounds**

Prior to the analysis of carbon compounds, the samples were bubbled with nitrogen. Volatile fatty acids (VFAs) and alcohols (ethanol, 1,3-propanediol, n-butanol, 2,3-butanediol) were measured by high-performance liquid chromatography (HPLC, Ultimate 3000, Dionex, USA) equipped with an ICsep ICE-CPREGEL 87H3 column (7.8 mm  $\times$  150 mm) and a variable wavelength detector at 210 nm with a 6 mM  $\text{H}_2\text{SO}_4$  mobile phase at a flow rate of  $0.5 \text{ mL min}^{-1}$ . Samples for VFAs and alcohols were not diluted.

Total organic carbon (TOC), total inorganic carbon (TIC) and total carbon (TC) were determined in a TOC analyzer (multi N/C 2100S, analytikjena, Germany) equipped with a furnace at the catalytic high-temperature of  $850 \text{ }^\circ\text{C}$ . Samples for TOC analysis were diluted to one third with ultrapure water.

### **3.3.3 Volatile suspended solids (VSS)**

VSS were measured along the UASB reactor to calculate the biomass concentration in the UASB as well as at the outlet of UASB to quantify the loss of biomass. VSS were

also measured in the serum bottles to calculate the biomass growth and specific substrate uptake rates. VSS were analyzed according to Standard Methods (APHA, 2012). First, 0.7  $\mu\text{m}$  glass fiber filters (Merck Millipore Ltd, Ireland) were ignited in the muffle furnace (300 Serie 8B, Hoberal, Spain) at 550 °C for 30 minutes to weight ( $W_1$ ). Then, the liquid sample (A, volume of sample) was filtered by the pre-weighted glass filter and dried at 105 °C until the constant weight and weighted ( $W_2$ ). The filter with the dried sample was retained for subsequent ignition at 550 °C for 1 hour and weighed ( $W_3$ ). TSS and VSS concentrations are calculated as follows:

$$\text{TSS} = (W_2 - W_1)/A \quad \text{Eq.3.1}$$

$$\text{VSS} = (W_2 - W_3)/A \quad \text{Eq.3.2}$$

### 3.3.4 Gas analysis

Biogas collected from the UASB and the headspace of activity test bottles were analyzed for  $\text{CH}_4$ ,  $\text{CO}_2$  and  $\text{H}_2$  determination by gas chromatography (7820A, Agilent Technologies, USA) equipped with a capillary column ( $\text{Al}_2\text{O}_3$  PLOT: 50 m  $\times$  0.53 mm).  $\text{H}_2\text{S}$  was analyzed by gas chromatography (HP 5890A GC, Hewlett Packard, USA) equipped with a thermal conductivity detector and a Porapak Q column. Before measuring the gas composition in the headspace of serum bottles, the pressure was measured by a manometer (SMC ISE30A-01-P, Japan).

The gas production of the UASB reactor was analyzed by the gas bag method (Ambler and Logan, 2011). It can be divided into three steps. Firstly, the initial gas composition in the Tedlar bag was analyzed. Secondly, a gas volume of known concentration (180 mL of pure  $\text{CO}_2$  in this thesis) was added into the Tedlar bag. Finally, the gas composition in the Tedlar bag was measured again after adding  $\text{CO}_2$ . The volume of gas produced in the UASB reactor is calculated by the change of  $\text{CO}_2$  concentration and the quantitative volume added. The volume of gas in the bag divided by the elapsed time results in the gas production flowrate of the UASB reactor.

### **3.3.5 Particle size**

The particle size distribution (PSD) of sludge was evaluated by a laser diffraction testing instrument (Mastersizer 2000, Malvern Panalytical, USA). The sludge samples were taken from different heights of the UASB reactor, and measured in the Mastersizer 2000 in triplicates. Samples for PSD analysis were not diluted.

### **3.3.6 Microbial population identification**

Identification of the microbial populations was performed using Illumina platform of samples collected on day 538 of the long-term operation of the UASB. Genomic DNA was extracted by applying the protocol of PowerSoil™ DNA isolation kit (MoBio Laboratories, USA) following the supplier's instructions. The quantity and quality of the extracted DNA were assessed by using a NanoDrop 1000 Spectrophotometer (Thermo Fisher Scientific, USA). Then, DNA samples were preserved at -20 °C for further analysis. Sequencing analyses were performed by the "Genomic and Bioinformatics service" at the Universitat Autònoma de Barcelona. Amplicon sequencing that targets the V3-V4 hypervariable regions (HVRs) of the 16S rRNA gene on Illumina MiSeq platform were carried out using the universal primers 341F (5' - CCT ACG GGN GGC WGC AG-3') and 805R (5' - GAC TAC HVG GGT ATC TAA TCC -3'). The database used for the classification of organisms is based on the Greengenes database (<http://greengenes.lbl.gov/>).

### **3.3.7 Characterization of crude glycerol**

Crude glycerol was provided by Ecomotion biodiesel S.A. (Spain), and its physical-chemical properties are shown in Table 2.1 according to the supplier data.

**Table 2.1.** Physical-chemical properties of crude glycerol.

<b>Parameters analyzed</b>	<b>Glycerol</b>
Organic Material	67.0%
Water	20.0%
Soluble salts	11.0%
Sulfur content	4.4%
COD	800 mg O <sub>2</sub> L <sup>-1</sup>
BOD <sub>5</sub>	400 mg O <sub>2</sub> L <sup>-1</sup>
Total solids	734 g kg <sup>-1</sup>
Volatile solids	637 g kg <sup>-1</sup>
Kjeldahl nitrogen	7700 mg L <sup>-1</sup>
pH	6.1



## Chapter 4

---

# Anaerobic treatment of sulfate-rich wastewater in a UASB reactor fed with crude glycerol

**Part of this chapter has been published as:**

Fernández-Palacios, E., Zhou, X., Mora, M., Gabriel, D., 2021. Microbial Diversity Dynamics in a Methanogenic-Sulfidogenic UASB Reactor. *Int. J. Environ. Res. Public Health* 18, 1305. <https://doi.org/10.3390/ijerph18031305>





*Anaerobic biotechnology has been successfully applied in treating sulfate-rich wastewaters with a variety of organic carbon compounds. The performance and stability of crude glycerol as a carbon source for reducing sulfate has been investigated in up-flow anaerobic sludge blanket (UASB) reactors under variable organic and sulfate loading rates (Fernández-Palacios et al., 2019; Mora et al., 2020b). However, many questions still need to be answered, such as the stability of removal efficiency during long-term constant operating conditions and the identification of the mechanisms of glycerol biodegradation and sulfate reduction. The motivation of this chapter was to assess the performance and limitations of a UASB reactor at constant sulfate and carbon loading rates for long-term operation using crude glycerol as a carbon source, in terms of conversion capacity and stratification of the reactor.*

## **Abstract**

In this chapter, the performance and stability of sulfate removal were assessed in a UASB reactor using crude glycerol as a carbon source under a constant TOC/S-SO<sub>4</sub><sup>2-</sup> ratio of  $1.5 \pm 0.3 \text{ g C g}^{-1} \text{ S}$  for 639 days of operation. The performance and stratification of the reactor were investigated in terms of sulfate reduction, glycerol fermentation, biogas production and VFAs accumulation. Results showed that glycerol fermentation and sulfate reduction were mainly completed at the bottom part of the UASB reactor. The reactor showed a sulfate removal capacity of  $4.5 \pm 0.7 \text{ kg S-SO}_4^{2-} \text{ m}^{-3} \text{ d}^{-1}$  during 280 days of operation. Particle size distribution analyses showed that granulation was progressively lost from day 149 to day 230. Sulfate removal efficiency decreased after 280 days, accompanied by the accumulation of SLS in the reactor. SLS may cause sludge flotation and lead to biomass washout, which was one of the main reasons for the significant decrease of the sulfate and glycerol removal efficiency in the long-term operation.



## 4.1 Introduction

Anaerobic digestion is a well-known process in wastewater treatment to remove different types of organic pollutants. In terms of anaerobic biotechnology processes for sulfate-rich wastewater treatment, the success of the sulfate reduction process has been proved using a variety of carbon sources, such as methanol, ethanol, butanol, or crude glycerol (Fernández-Palacios et al., 2019; Sarti and Zaiat, 2011; Vallero et al., 2003; Wu et al., 2018). Further partial oxidation of sulfide to elemental sulfur as a value-added product to valorize sulfate-rich effluents has also been reported in Mora et al. (2020a).

In order to further extend the application of valorizing sulfate-rich effluents, it is necessary to improve the robustness of biological processes stabilizing the process, optimizing operating conditions and avoiding inhibitory compounds. Management strategies that are insufficiently evaluated may exacerbate risks, which further results in unexpected process failure and economic losses from their commercial application (Westerholm et al., 2018). Thus, long-term stability is a prerequisite for considering biological technologies as an alternative at industrial scale.

Several problems have been identified in the long-term operation of UASB reactors. For example, fat and oil attached onto the biomass or the high up-flow velocity led to sludge flotation and the washout of biomass, which decreased the COD removal efficiency and failure ensued (Jeganathan et al., 2006; Rizvi et al., 2015). Lu et al. (2015b) also described that the lack of consumption of excess extracellular polymeric substances produced and the biogas generated in a UASB reactor treating starch wastewater resulted in the flotation of sludge that was not able to settle, which eventually led to sludge washout and the clogging of the outlet. The required cleaning procedures due to clogged outlets or reinoculation of biomass due to washout increase operating costs. Furthermore, when treating some specific wastewater (such as methanol-containing wastewater) in UASB reactors, the disintegration of granular sludge increased the washout of sludge, which not only reduced the quality of the outlet but also affected the imbalance of the reactor, thus

increasing the risk of failure (Lu et al., 2015a). Therefore, long-term operation is needed to evaluate the stability performance of reactors for sulfate-rich effluents treatment and/or valorization.

Many studies have already studied several factors affecting the anaerobic treatment of sulfate-rich wastewaters, including carbon source, temperature, pH, sulfate loading rate and carbon to sulfur (C/S) ratio (Lopes et al., 2007b; Mora et al., 2020b; Shin et al., 1996; Marcus V.G. Vallero et al., 2004a). Inoculated sludge is also an indispensable and critical factor for the robust treatment of sulfate-rich wastewater. Anaerobic granular sludge is successfully implemented and well-spread in the anaerobic treatment of industrial effluents in UASB and expanded granular sludge bed reactors (Hao et al., 2014; Hulshoff Pol et al., 2004). Anaerobic methanogenic sludge can be adapted to sulfidogenic conditions in order to achieve the treatment of sulfate-rich wastewaters (Lens et al., 2002). However, it can take a long time for sulfate reducing bacteria (SRB) to outcompete methanogens. Both methanogenesis and sulfidogenesis were suppressed at thermophilic temperatures (55 °C), but the suppressive effect on sulfidogenesis was greater than methanogenesis (Jung et al., 2019). However, Visser et al. (1993) observed that after temperature shocks of 55 °C or 65 °C for 8 h, the sulfidogenesis recovered rapidly and methanogenesis was suppressed when a UASB reactor was set back to mesophilic temperature. Thus, temperature shocks could be a strategy to speed up the process of sulfidogenesis outcompetition over methanogenesis. There are also other alternatives to speed up the start-up of the process such as adding a pure culture of SRB (Omil et al., 1997b) or using SRB enriched to target specific organic compounds (Kaksonen and Puhakka, 2007). Moreover, Fernández-Palacios et al. (2019) investigated different sulfate and organic loading rates in a sulfidogenic UASB reactor, and the highest average sulfate removal capacity was obtained at COD/S-SO<sub>4</sub><sup>2-</sup> ratio of 5.4 g O<sub>2</sub> g<sup>-1</sup> S-SO<sub>4</sub><sup>2-</sup> and an organic loading rate of 15.8 kg O<sub>2</sub> m<sup>-3</sup> d<sup>-1</sup>. These conditions were applied constantly in a long-term UASB treatment of sulfate-rich wastewater in this chapter to evaluate sludge adaptability, the stability and durability of sulfate removal in terms of sulfate removal

capacity, organic carbon compounds removal capacity, and stratification of carbon and sulfur species concentration along the reactor.

## 4.2 Materials and methods

### 4.2.1 Operating conditions of the UASB reactor

The UASB reactor used in this thesis and the experimental setup are explained in Section 3.1.1 of chapter 3. In the experiments reported herein, the reactor was fed with crude glycerol as a carbon source and operated for 639 days with a constant sulfate loading rate (SLR) and organic loading rate (OLR). Average operating conditions and standard deviations obtained from the whole operation are shown in Table 4.1. These conditions were selected according to the period of maximum sulfate reduction and organic removal efficiencies obtained by Fernández-Palacios et al. (2019).

**Table 4.1.** Operating conditions in the UASB reactor under long-term stable performance.

<b>Time (Days)</b>	<b>Sulfate<sub>inlet</sub> (mg S L<sup>-1</sup>)</b>	<b>Glycerol<sub>inlet</sub> (mg C L<sup>-1</sup>)</b>	<b>SLR* (kg S m<sup>-3</sup> d<sup>-1</sup>)</b>	<b>OLR* (kg C m<sup>-3</sup> d<sup>-1</sup>)</b>	<b>TOC<sub>inlet</sub>/S<sub>inlet</sub> (g C g<sup>-1</sup> S)</b>
0-639	251.2 ± 8.1	306.5 ± 73.1	5.0 ± 0.6	7.3 ± 1.6	1.5 ± 0.3

Note: \* SLR and OLR were calculated considering the sludge bed volume.

The analysis of the liquid phase was monitored at the inlet and outlet of the reactor two to three times per week measuring sulfate, thiosulfate, TDS, VFAs, glycerol, TOC, TIC and TC. Reactor gas phase composition was measured every three to five days, depending on biogas production. The analytical methods are presented in Section 3.3.

### 4.2.2 Assessment of stratification in the UASB reactor

The stratification of the UASB reactor was assessed by sampling at different heights after 49, 169, 198, 271, 294 and 575 days of operation. The choice of these days depended on changes in the performance of the reactor. VSS were measured at different heights of the UASB (UASB1, UASB2 and UASB3, as shown in Figure 3.1) to calculate the biomass

concentration in the reactor as well as at the outlet of UASB to quantify the loss of biomass. Accordingly, the mean cell residence time (MCRT, d) of the biomass was calculated based on Eq.4.1.

$$\text{MCRT} = \frac{X_R \times V_R}{X_{\text{OUT}} \times F} \quad \text{Eq.4.1}$$

Where  $X_R$  is the concentration of biomass in the UASB reactor, g VSS  $L^{-1}$ ;  $V_R$  is the volume of biomass in the UASB, L;  $X_{\text{OUT}}$  is the washout biomass concentration, g VSS  $L^{-1}$ ;  $F$  is the total flow rate,  $L d^{-1}$ . The sludge particle size was assessed at different bed heights of the UASB reactor (UASB1, UASB2 and UASB3) on days 50, 149 and 230.

### 4.2.3 C and S mass balances assessment

The carbon balance was calculated according to Eq.4.2.

$$\text{Carbon mass balance (\%)} = \frac{\text{Inlet}_{\text{TC}(\text{liq})} - \text{Outlet}_{\text{TC}(\text{liq})} - \text{Outlet}_{\text{CH}_4\text{CO}_2(\text{gas})} - \text{Outlet}_{\text{biomass}(\text{liq})}}{\text{Inlet}_{\text{TC}(\text{liq})}} \times 100 \quad \text{Eq.4.2}$$

Where  $\text{TC}(\text{liq})$  is the total carbon mass flowrate in the liquid phase,  $\text{mg C } d^{-1}$ ;  $\text{CH}_4$ ,  $\text{CO}_2$  (gas) are the mass flowrates of  $\text{CH}_4$ ,  $\text{CO}_2$  detected in the gas phase,  $\text{mg C } d^{-1}$ ;  $\text{Outlet}_{\text{biomass}(\text{liq})}$  is the mass flowrate of VSS in the effluent flushed from the reactor,  $\text{mg C } d^{-1}$ .  $\text{Inlet}_{\text{TC}(\text{liq})}$  was  $5396 \pm 1023 \text{ mg C } d^{-1}$  during the operation.

The sulfur balance was calculated according to Eq.4.3.

$$\text{Sulfur mass balance} = \frac{\text{Inlet}_{\text{sulfur species}(\text{liq})} - \text{Outlet}_{\text{sulfur species}(\text{liq})} - \text{Outlet}_{\text{H}_2\text{S}(\text{gas})}}{\text{Inlet}_{\text{sulfur species}(\text{liq})}} \times 100\% \quad \text{Eq.4.3}$$

$\text{Sulfur species}(\text{liq})$  is the sum of sulfate, thiosulfate and TDS mass flowrates in the liquid phase,  $\text{mg S } d^{-1}$ ; and  $\text{H}_2\text{S}(\text{gas})$  is the  $\text{H}_2\text{S}$  mass flowrate stripped out to the gas phase,  $\text{mg S } d^{-1}$ .  $\text{Inlet}_{\text{sulfur species}(\text{liq})}$  was  $3410 \pm 177 \text{ mg S } d^{-1}$  during the operation.

### 4.2.4 Volumetric rates along the UASB height

The volumetric rates calculated in each section of the UASB during the stratification sampling events were calculated according to Eq.4.4:

$$R = \frac{(C_{i+1} - C_i) \times F}{V} \quad \text{Eq.4.4}$$

Where  $R$  is the rate between two adjacent sampling ports ( $i$  and  $i+1$ ) of the UASB reactor ( $\text{mg C L}^{-1} \text{ h}^{-1}$ , or  $\text{mg S L}^{-1} \text{ h}^{-1}$ );  $C_{i+1}$  is the substrate concentration at the UASB reactor sampling port UASB $_{i+1}$  ( $\text{mg C L}^{-1}$ , or  $\text{mg S L}^{-1}$ );  $C_i$  is the substrate concentration at UASB $_i$  ( $\text{mg C L}^{-1}$ , or  $\text{mg S L}^{-1}$ );  $V$  is the volume between two adjacent sampling points of the UASB reactor (L); and  $F$  is the total inlet flow rate which was set to  $565 \pm 22 \text{ L h}^{-1}$ .

## 4.3 Results and discussion

### 4.3.1 Performance of the sulfidogenic UASB reactor

#### 4.3.1.1 Chemical parameters monitoring

A long-term experiment was performed under a constant sulfate loading rate of  $5.0 \pm 0.6 \text{ kg S m}^{-3} \text{ d}^{-1}$  and an organic loading rate of  $7.3 \pm 1.6 \text{ kg C m}^{-3} \text{ d}^{-1}$  for 639 days. Figure 4.1 shows the monitoring of sulfur and carbon species, and the biogas flowrate of the UASB reactor. According to the performance of the reactor, the operation was divided into four periods; stage I, from 0 day to 16 day, corresponding to the start-up and granular sludge adaptation period; stage II, from 16 day to 100 day, corresponding to a period with stable sulfate reduction with methane production; stage III, from 100 day to 280 day, under stable sulfate reduction with VFAs accumulation; stage IV, from 280 day to 639 day, when a decline in the sulfate removal efficiency occurred. Table 4.2 shows the average and standard deviation of the glycerol, sulfate and TOC removal efficiency (RE) and TOC and sulfate removal capacity (RC) of the UASB reactor in each one of the four periods.

**Table 4.2.** The removal efficiency and removal capacity of the UASB reactor in the four stages.

Period	Time (days)	Glycerol RE (%)	TOC RE (%)	Sulfate RE (%)	TOC RC ( $\text{kg C m}^{-3} \text{ d}^{-1}$ )	Sulfate RC ( $\text{kg S m}^{-3} \text{ d}^{-1}$ )
I	0-14	$96.5 \pm 9.2$	$86.4 \pm 12.8$	$42.9 \pm 19.0$	$4.2 \pm 1.5$	$1.5 \pm 0.7$
II	14-100	$100.0 \pm 0.0$	$92.6 \pm 4.2$	$83.5 \pm 7.4$	$6.7 \pm 1.3$	$4.6 \pm 0.7$
III	100-280	$98.0 \pm 3.8$	$45.9 \pm 23.8$	$83.7 \pm 9.2$	$3.5 \pm 1.9$	$4.3 \pm 0.7$
IV	280-640	$64.3 \pm 14.0$	$15.8 \pm 10.5$	$38.8 \pm 12.5$	$1.2 \pm 0.8$	$1.8 \pm 0.6$



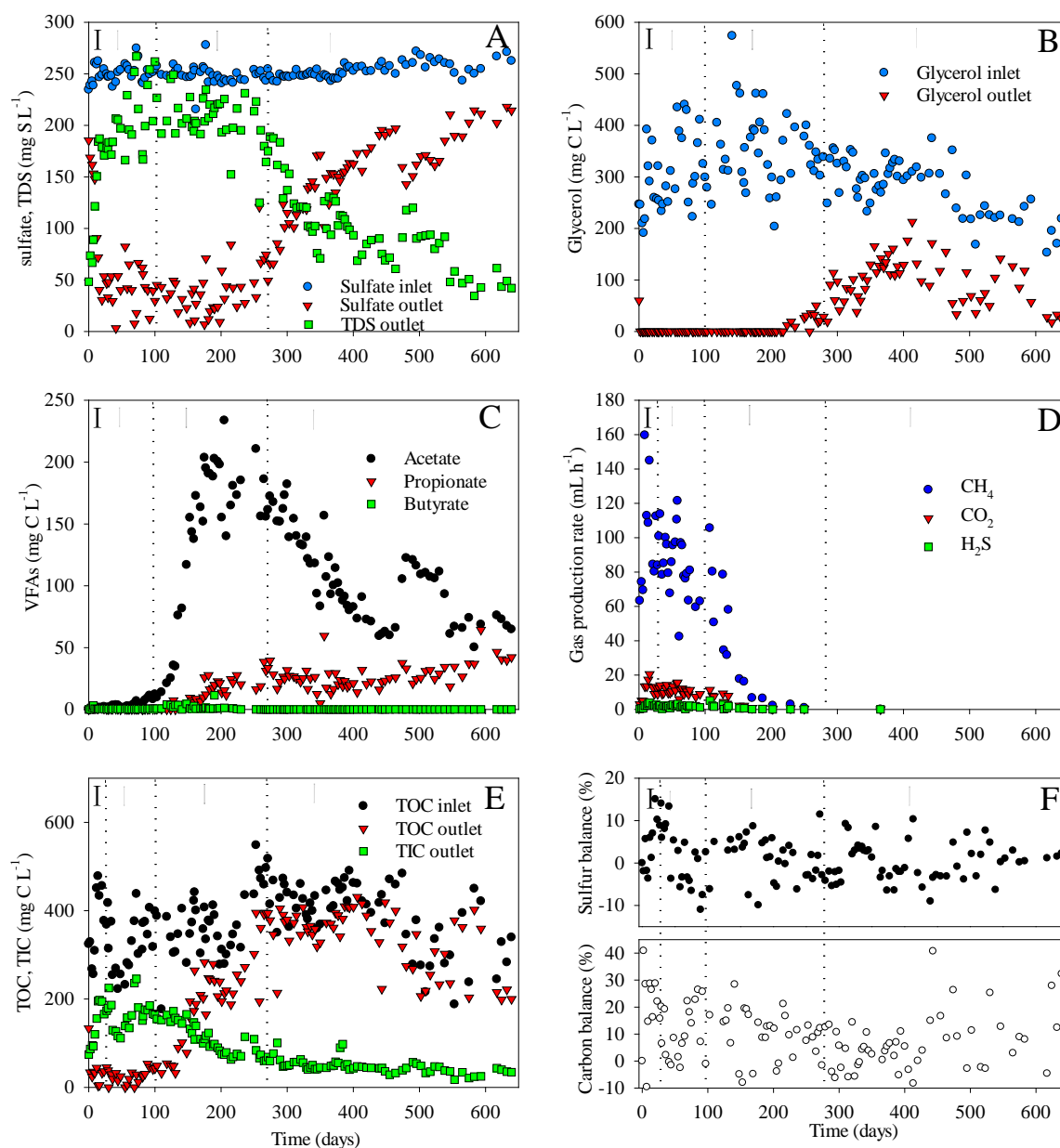


**Figure 4.1.** Performance obtained from the sulfidogenic UASB over 639 days. (A) Sulfur profile; (B) Glycerol concentration in the inlet and outlet; (C) VFAs concentration in the outlet; (D) Biogas production; (E) TOC and TIC concentration; (F) Carbon mass balance.

Since inoculated sludge was taken from an anaerobic digester for methane production, stage I corresponded to the adaptation period of the inoculated sludge for sulfate treatment. As can be observed in Figure 4.1A, after the adaptation period,  $250 \text{ mg S-SO}_4^{2-} \text{ L}^{-1}$  were converted to  $180\text{-}240 \text{ mg S-TDS L}^{-1}$  on stage II and III. After 280 days of continuous operation, the TDS decreased from  $200 \text{ mg S-TDS L}^{-1}$  to  $50 \text{ mg S-TDS L}^{-1}$  along stage IV. As can be observed in Table 4.2, stable sulfate RE higher than 83% was achieved on stage

II and stage III and then, it decreased to 39% on stage IV. In terms of carbon, glycerol was completely degraded on stage I, II and III, while glycerol concentrations between 20 and 200 mg C L<sup>-1</sup> were measured in the effluent on stage IV (Figure 4.1B). Figures 4.1C and 4.1D show the products of glycerol fermentation, including VFAs in the effluent, and CH<sub>4</sub>, CO<sub>2</sub> in the gas phase. CH<sub>4</sub> was produced over 60 mL h<sup>-1</sup>, while no VFAs accumulated on stage I and stage II. A progressive VFAs accumulation (mainly acetate) coincided with a significant decrease of CH<sub>4</sub> production on stage III. However, acetate accumulation decreased on stage IV. Figure 4.1E showed the TOC and TIC concentrations at the inlet and outlet of the UASB. The outlet TOC concentration was below 50 mg C L<sup>-1</sup>, and the outlet TIC concentration was between 110 and 245 mg C L<sup>-1</sup> on stage I and II. The TOC outlet concentration increased on stage III, while the TIC outlet concentration decreased. Comparing the TOC REs in Table 4.2, it can be observed that the TOC RE was positively correlated with gas production. When the gas production rate was higher than 60 mL h<sup>-1</sup>, the TOC RE was higher than 86% on stage I and II. A progressive decrease in the gas production was accompanied by the decrease of TOC RE on stage III and stage IV. In summary, a sulfidogenic UASB reactor was successfully operated using crude glycerol as a carbon source with 4.3 kg S m<sup>-3</sup> d<sup>-1</sup> of sulfate removal capacity for 280 days. However, a decline of the sulfate RC down to 1.8 kg S m<sup>-3</sup> d<sup>-1</sup> and the sulfate RE down to 39% indicated the failure of the sulfate reduction process in stage IV.

After the inoculation of methanogenic granular sludge, and in order to adapt to the sulfate reduction conditions, previous studies have shown that the inoculum of pure culture of SRB and the use of lactate as a carbon source may speed up the start-up of the sulfidogenic process (Kaksonen and Puhakka, 2007; Omil et al., 1997b; Visser et al., 1993). In addition, an optimum COD/S-SO<sub>4</sub><sup>2-</sup> ratio may also accelerate the adaptation period. Several start-ups of sulfidogenic UASB reactors using ethanol or crude glycerol as carbon source are shown in Table 4.3. Comparing the results of these studies, it was found that when ethanol was the carbon source for sulfate reduction, the sulfate RE with a COD/S-SO<sub>4</sub><sup>2-</sup> ratio of 1.0 g O<sub>2</sub> g<sup>-1</sup> S was almost twice than that of 0.67 g O<sub>2</sub> g<sup>-1</sup> S

(Rodriguez et al., 2012; Wu et al., 2018). In terms of crude glycerol as a carbon source, the sulfate RE increased with the increment of COD/S-SO<sub>4</sub><sup>2-</sup> ratio (Mora et al., 2020b). When the COD/S-SO<sub>4</sub><sup>2-</sup> ratio was set as 3.8 g O<sub>2</sub> g<sup>-1</sup> S (Fernández-Palacios et al., 2019) and 5.1 g O<sub>2</sub> g<sup>-1</sup> S (this study) for start-up the UASB operation, the sulfate RE exceeded 80% in both cases. Fernández-Palacios et al. (2019) took 30 days after the inoculation to reach over 80% of sulfate RE, while this work used 16 days (Figure 4.1A). In sum, the sulfate removal rate can exceed 80%, when the COD/S-SO<sub>4</sub><sup>2-</sup> ratio exceeds 1 g O<sub>2</sub> g<sup>-1</sup> S. Theoretically, sulfate reduction required a COD/S-SO<sub>4</sub><sup>2-</sup> ratio of 0.67 assuming that organic carbon was only oxidized for sulfidogenesis. However, organic carbon undergoes the fermentation process during the sulfate reduction process, thus requiring a larger organic carbon loading. Therefore, a COD/S-SO<sub>4</sub><sup>2-</sup> ratio higher than 0.67 is needed for sulfate reduction to reach an appropriate removal efficiency. Comparing the above different COD/S ratios, the adaptation period of sulfate removal herein was the shortest at 5.1 g O<sub>2</sub> g<sup>-1</sup> S of COD/S-SO<sub>4</sub><sup>2-</sup> ratio. In addition, the initial sulfate concentration in the above studies ranged from 220 mg S L<sup>-1</sup> to 250 mg S L<sup>-1</sup> using crude glycerol as electron donor. The adaptation time of the reactor with higher sulfate concentration under different COD/S ratios still needs further investigation.

**Table 4.3.** Start-up conditions of a sulfidogenic UASB reactor.

<b>Carbon source</b>	<b>Sulfate<sub>inlet</sub> (mg S L<sup>-1</sup>)</b>	<b>OLR<sup>A</sup> (kg O<sub>2</sub> m<sup>-3</sup> d<sup>-1</sup>)</b>	<b>COD<sub>inlet</sub>/S<sub>inlet</sub> (g O<sub>2</sub> g<sup>-1</sup> S)</b>	<b>Sulfate RE</b>	<b>Reference</b>
Ethanol	315 ± 42	N.A.	0.67	46 ± 14%	Rodriguez et al., 2012
Ethanol	1000	12	1.0	over 86%	Wu et al., 2018
Crude glycerol	220 ± 17	6.7 ± 1.0	2.5	34%	Mora et al., 2020b
		19.3 ± 3.2	7.0	83%	
Crude glycerol	235 ± 17	12.0 ± 2.1	3.8 ± 0.8	over 80%	Fernández-Palacios et al., 2019
Crude glycerol	251 ± 8	18.3 ± 6.2	5.1 ± 0.8	over 84%	This study

Note: N.A. not applicable. <sup>A</sup> OLR is organic loading rate calculated by the sludge bed volume.

In stage II, over 83% of sulfate RE and 92% of TOC RE were achieved, where no accumulation of VFAs was accompanied by a significant production of biogas and accumulation of inorganic carbon. Results indicated the coexistence of SRB and methanogens. The competition between methanogenic bacteria and sulfidogenic bacteria in anaerobic wastewater treatment has been reported in many previous studies due to the competition of electron donors, such as acetate or hydrogen (Dar et al., 2008; Omil et al., 1998; Zhou and Fang, 1998). However, as reported by Mora et al. (2020b), sulfate reduction was mainly through acetogenic and hydrogenotrophic processes using crude glycerol as a carbon source, while the acetate produced was further consumed by methanogens for biogas production. Thus, despite the competition between methanogens and SRB, they can coexist with an appropriate supply of electron donors. On the other hand, Fernández-Palacios et al. (2019) found that acetotrophic SRB were hardly found in the sulfidogenic UASB reactor, which contradicted the view described by Mora et al. (2020b). Thus, the pathway to reduce sulfate using glycerol as carbon source needs further study as will be discussed in Chapter 6 in this thesis.

In stage III, TOC RE decreased due to the accumulation of VFAs coupled to no biogas production. During the operation, microbial diversity was studied in Fernández-Palacios et al. (2021), proving that methanogens were washed out from the system after 200 days of operation when there was no biogas production. The pH and sulfide concentration play a major role in the competition between SRB and methanogens (O'Flaherty et al., 1998). The latter described that the growth rate of methanogens was higher than that of SRB at  $\text{pH} < 7.0$ , and opposite results were found at  $\text{pH} > 7.5$ . The toxicity of sulfide is caused by undissociated sulfide molecules that permeate the cell membrane (Kaksonen and Puhakka, 2007; Neculita et al., 2007). The inhibitory effect of  $\text{H}_2\text{S}$  on methanogens was greater than that on SRB (Sarti and Zaiat, 2011). However, previous studies indicated that free  $\text{H}_2\text{S}$  caused a 50% inhibition of methanogenic activity at a concentration of  $184 \text{ mg S L}^{-1}$  (Visser et al., 1996) or  $285 \text{ mg S L}^{-1}$  (Kalyuzhnyi and Fedorovich, 1998), respectively. Free  $\text{H}_2\text{S}$

was  $90 \pm 11 \text{ mg S L}^{-1}$  on stage III in this thesis, which indicated that free  $\text{H}_2\text{S}$  might not a key factor in this case. Moreover, affinity for substrate and specific growth rate may be important in the competition between sulfate reducers and methanogens (J.W.H. et al., 1994). Vallero et al. (2004a) reported that hydrogenotrophic SRB have a higher substrate affinity than methanogens and that SRB had a competitive advantage over methanogens in sulfate-containing wastewater treatment. In addition, the methane production by methanogenic archaea can be limited by long-chain fatty acids (LCFAs), specifically palmitic acid (Deaver et al., 2020; Silva et al., 2016). Fernández Palacios (2020) characterized the crude glycerol used in this thesis and found that palmitic acid was the main component among the LCFAs, which might be a potential factor for the inhibition of methanogenic activity.

Sulfur and carbon mass balances in the UASB reactor are shown in Figure 4.1F while mass balance calculations are detailed in section 4.2.3. Considering the  $\text{H}_2\text{S}$  stripping in the UASB, the sulfur imbalance along the operation oscillated between -10% and +20%. The sulfur imbalance was attributed to the production of undetected sulfur species in the reactor. As reported by Mora et al. (2020b), the sulfur imbalance was not caused by the metallic sulfide precipitating but due to the production of organic sulfur compounds as intermediate compounds of the biodegradation. The negative imbalance was attributed to the standard deviation in the measurement of TDS (8%). Considering the  $\text{CH}_4$  and  $\text{CO}_2$  stripping on the gas phase of the UASB, the carbon imbalance was mainly between -5% and 30%, which is in concordance with the sulfur imbalance. The positive imbalance was attributed to the growth of biomass in the reactor (Fernández-Palacios et al., 2019). Anaerobic digestion is widespread in the treatment of organic wastewater because of its low energy requirements and the low production of sludge (Xu et al., 2020), but still, low growth rates have been reported in anaerobic digestion for granulation of sludge (Van Den Brand et al., 2014b).

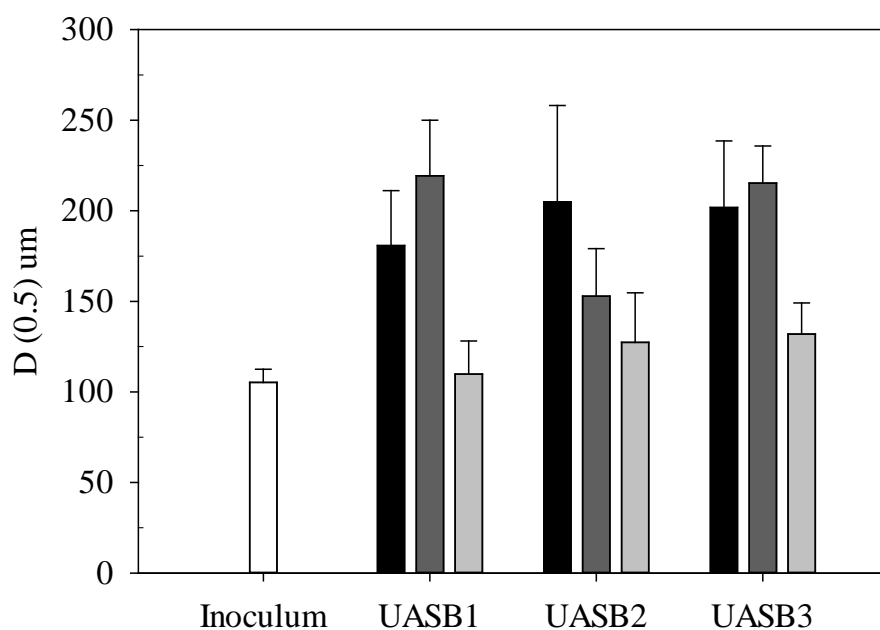
Moreover, organic sulfur compounds are produced by assimilatory sulfate reduction (Barton et al., 2014), and volatile organic sulfur compounds were identified from a municipal sewage water treatment plant treating S-containing organic material. Li et al.

(2020) also described the conversion pathway of volatile sulfur compounds in high-solid sludge anaerobic digestion containing the organic and inorganic sulfur sources. Therefore, the formation of organic sulfur compounds could contribute to the carbon imbalance as well. Moreover, in UASB reactors for the treatment of oily wastewater, fat, oil and grease accumulated onto the biomass which was taken into account on COD mass balance (Jeganathan et al., 2006). The accumulation of extracellular polymeric substances may be another factor for carbon imbalance.

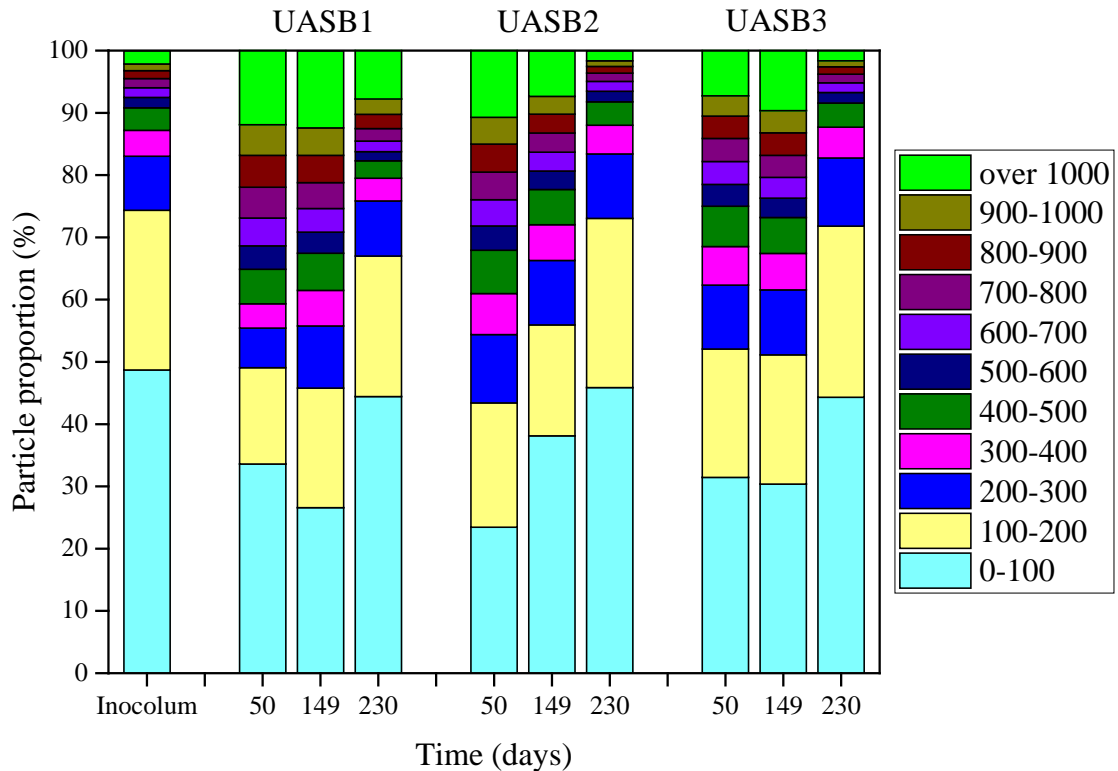
#### 4.3.1.2 Particle size of sludge and biomass monitoring

Figure 4.2 shows the particle size as mass median diameter  $D(0.5)$  of sludge at different heights of the UASB reactor.  $D(0.5)$  is the sample size that half of the sample is smaller and half is larger than this diameter. For most of the literature, there is no clear cutoff value to consider a granule in the case of sludge. Mora et al. (2020b) considered that biomass aggregate as a granule at  $D(0.5)$  of around 200  $\mu\text{m}$ . Results of  $D(0.5)$  revealed that granulation was observed from 50 days to 149 days, since inoculum sludge of  $D(0.5)$  was 105  $\mu\text{m}$ , while sludge of  $D(0.5)$  in UASB1, UASB2 and UASB3 were higher than 150  $\mu\text{m}$  at 50 and 149 days. However, the  $D(0.5)$  of the sludge measured at different heights of the UASB reactor decreased with varying degrees on day 230 of operation. The sludge fraction of particle size distribution over the operation period is shown in Figure 4.3. The particle size of the inoculated sludge below 200  $\mu\text{m}$  accounted for 74%. Compared with inoculated sludge, at day 50 and 149, the proportion of 0-200  $\mu\text{m}$  sludge in UASB1, UASB2 and UASB3 decreased, accounting for  $49.6 \pm 4.5\%$  in average. However, the proportion of particles smaller than 200  $\mu\text{m}$  in UASB1, UASB2 and UASB3 increased to  $70.6 \pm 3.2\%$  on day 230. And the proportion of sludge greater than 1000  $\mu\text{m}$  increased from 2.1% in inoculum sludge to over 7.3% at different heights of the UASB reactor on days 50 and 149. However, on day 230, the proportion of particles larger than 1000  $\mu\text{m}$  reduced to 1.6% (in UASB2) and 1.7% (in UASB3), respectively. The results of  $D(0.5)$  and particle size distribution revealed that the granule size of sludge increased on 50 and 149 days in

UASB1, UASB2 and UASB3, but decreased on day 230 when no biogas was produced (Figure 4.1D). Wu et al. (2016) found that granule size was positively correlated with biogas production rate. Acetotrophic methanogens played a key role in granulation (Hulshoff Pol et al., 2004), and the lack of methane production resulted in poor sludge granulation (Mora et al., 2020b). Previous studies found that the granular strength was reduced upon sulfidogenic operation of anaerobic reactors and the diameter of granular sludge decreased (Kobayashi et al., 2015; Omil et al., 1997a), which might explain the observation of degranulation when methanogenic activity was ceased.



**Figure 4.2.** The median diameter of sludge particles  $D(0.5)$  at different heights of UASB (from dark grey to light grey: 50, 149, 230 days of operation, white column: inoculum sludge).



**Figure 4.3.** The particle size distribution of sludge at different heights of the UASB.

Weijma et al. (2000) found the disintegration of sludge in an expanded granular sludge bed reactor treating methanol during the period of low biogas production, and the sludge particles were gradually covered by fluffy cotton-like material. Similarly, in our study, after no biogas was produced in the UASB reactor, the size of the sludge granules decreased caused by the disintegration and then, SLS accumulated. Figure 4.4 shows the inoculated granular sludge and the gradual change of the sludge in the UASB reactor. When the TOC RE decreased with low biogas production, the granular sludge gradually became sludge surrounded by flocculent loose SLS (Figure 4.4B). During the continuous operation, SLS formed aggregates and became a cover of the granular sludge and attached the reactor wall (Figure 4.4C and 4.4D). SLS was loose and fluffy, which caused severe sludge flotation. As can be observed in Figure 4.4B, part of the sludge floated to the gas-liquid-solid separator and remained suspended on top of the reactor after 316 days of operation and later on (Figure 4.4C and 4.4D).



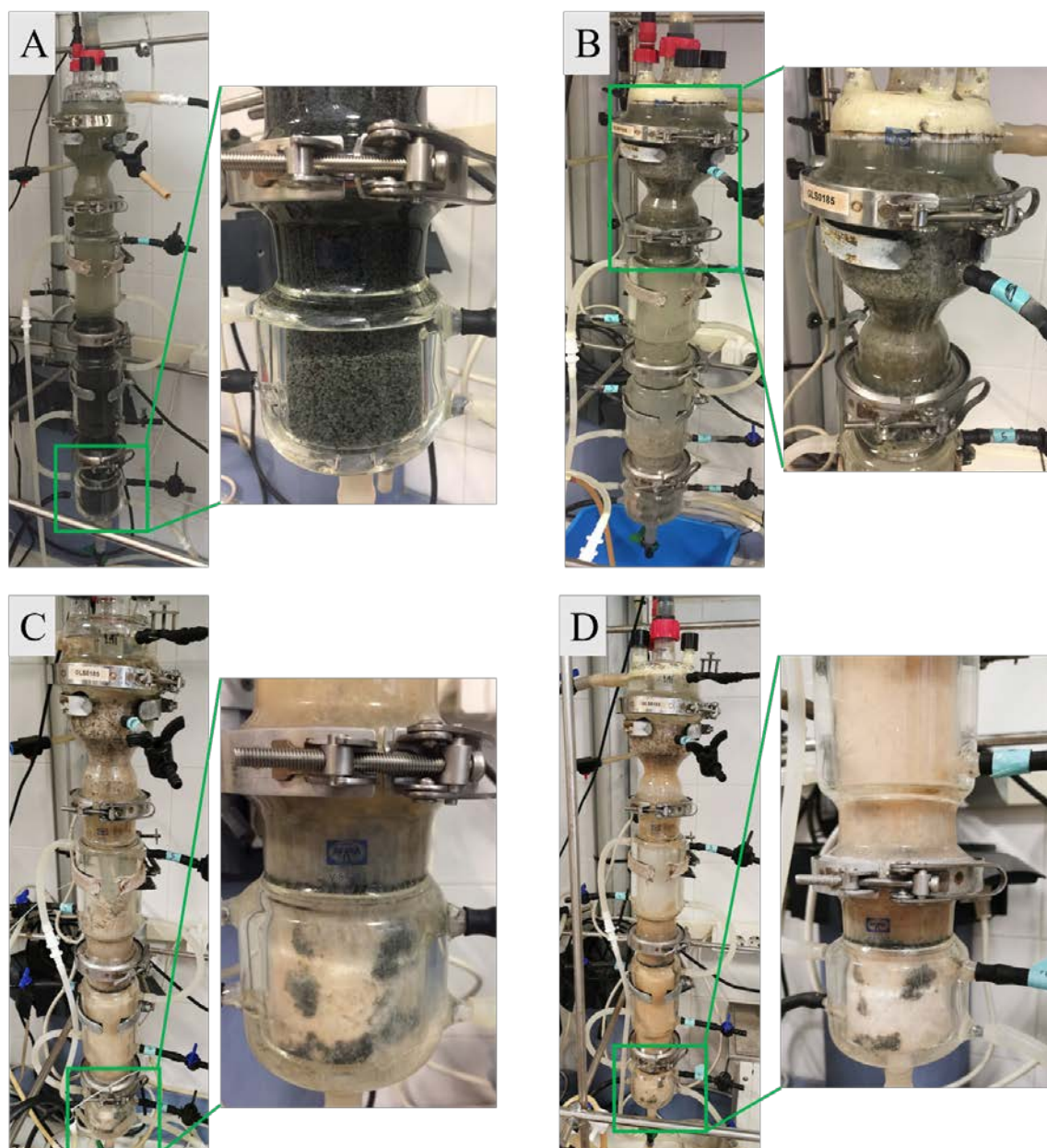


**Figure 4.4.** The UASB reactor under long-term stable operation treating sulfate-rich wastewater. (A) Operating 5 days; (B) Operating 316 days; (C) Operating 420 days; (D) Operating 639 days.

The formation of SLS may be due to the continuous accumulation of other organic carbon substances in crude glycerol that was not completely degraded by granular sludge and encircled the granular sludge. It is mentioned that crude glycerol contains fatty acid methyl esters, free fatty acids, glycerides and LCFAs (Hu et al., 2012; Viana et al., 2012). LCFAs can not only form a layer on the surface of biomass and prevent the substrate from entering the biomass that can affect the diffusion of substrate limitation, but also can attach

the biomass to cause its flotation (Viana et al., 2012). The sludge flotation may cause the washout of biomass.

Biomass concentration in the UASB reactor and washout of biomass are shown in Figure 4.5. As shown in Figure 4.5A, the biomass concentration measured in UASB1 showed a decline from 58.6 g L<sup>-1</sup> on day 78 to 22.1 g L<sup>-1</sup> on day 639. The biomass concentration in UASB3 was between 20 and 30 g L<sup>-1</sup>, but it dropped to 4.3 g L<sup>-1</sup> on day 639. The biomass concentration in UASB6 was 0 g L<sup>-1</sup> before 300 days. Due to flotation, part of the sludge was suspended at UASB6, in which the biomass concentration was 21.6 g L<sup>-1</sup> on day 390 and dropped to 8.7 g L<sup>-1</sup> on day 639 in UASB6. The average biomass concentration in the UASB reactor gradually dropped from 48.5 g L<sup>-1</sup> to 14.9 g L<sup>-1</sup> during 639 days operation. The TSS concentration in the UASB reactor showed the same trend as VSS (data was not shown). The VSS/TSS ratio ranged from 74% to 87% during the whole operation, which shows that there was almost no accumulation of non-volatile suspended solids in the UASB reactor. This proves that the main component of SLS accumulated in the reactor was also volatile suspended solids.

Figure 4.5B shows the washout of biomass from the reactor. The biomass loss fluctuated in the range of 0.04 to 2.4 g L<sup>-1</sup> before day 200. Such fluctuations were supposed to be caused by an excess of biomass provided to the reactor in the inoculation stage coupled to the movement and raising of granules caused by methane bubbles produced, thus resulting in sludge washout. When there was no methane production in the reactor, the bed become a static bed, leading to a reduced sludge loss that remained stable between 0.1 to 0.6 g L<sup>-1</sup> after 260 days. Mean cell residence time (MCRT) is shown in Figure 4.5C. MCRT was below 65 days during the period of methane production, and the sludge remained longer in the reactor during the period of non-methane production between 200 and 300 days. MCRT was maintained around 50 days after 400 days of operation. Figure 4.5D shows that the biomass in the reactor is positively correlated with sulfate RE and sulfate RC.

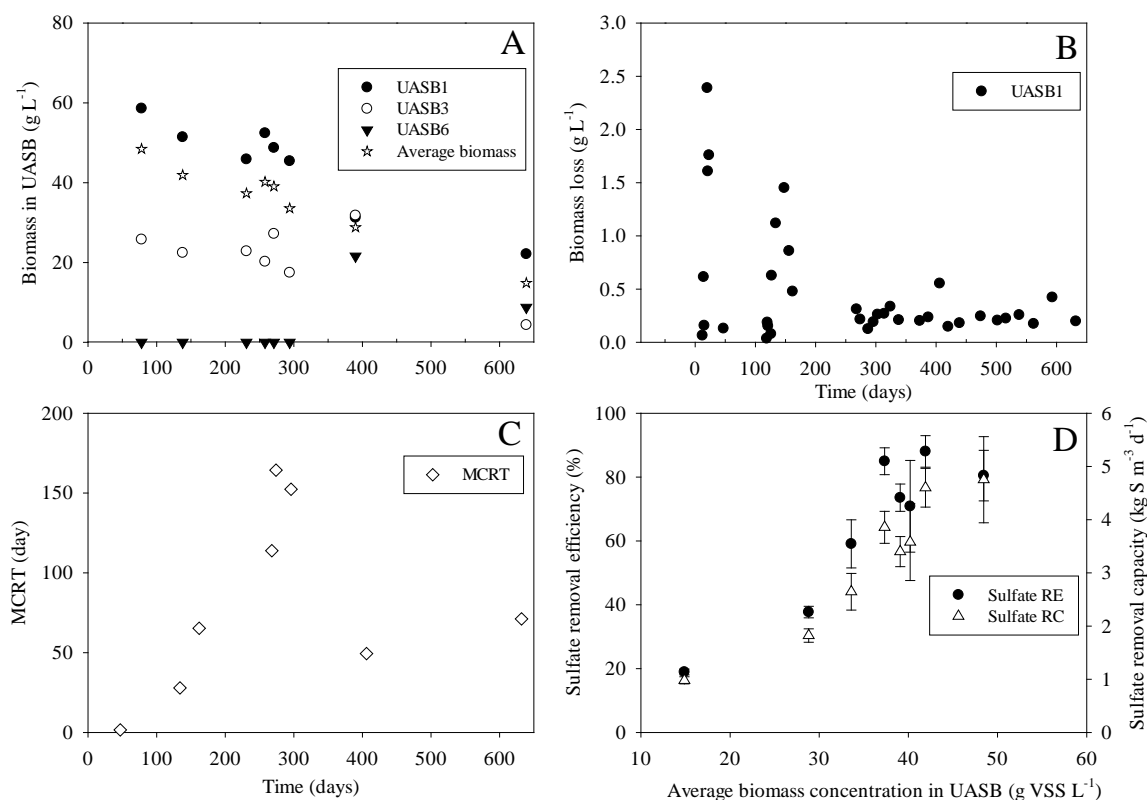


**Figure 4.5.** Variation of biomass in the UASB reactor (A), biomass loss (B), mean cell residence time (C) and biomass concentration in UASB versus sulfate removal efficiency and sulfate removal capacity (D).

As shown in Table 4.2, the overall glycerol RE of the UASB reactor was over 90% with high sulfate RE (over 83%) before day 280. After the accumulation of SLS, both the overall glycerol RE and sulfate RE declined in the stage IV after 280 days of operation. With the accumulation of SLS, sludge flotation was also observed. There is a dynamic balance between flotation and sedimentation, that is, when the flotation granular sludge releases biogas, it can settle back to the bottom of the reactor (Lu et al., 2015b). In this study, compared with granular sludge, SLS is more viscous and fluffy. The accumulated SLS may block the gas channels between granular sludge, and up-flow liquid and a small amount of gas production promoted a part of sludge (granular sludge with SLS) to ascend to the gas-liquid-solid separator and suspend in UASB6. Moreover, sludge floating is also attributed to the accumulation of excess substrate or intermediate metabolites in extracellular polymeric substances, such as fats, oils, greases, or polysaccharides (Jeganathan et al., 2006; Lu et al., 2015b).

The sludge flotation is a limiting factor for anaerobic treatment of wastewater with higher loading rates because the sludge flotation can lead to a severe biomass washout and system performance deterioration (Jeganathan et al., 2006). As can be observed in Figure 4.5D, the concentration of biomass decreased is accompanied by a decrease in sulfate RE and sulfate RC, which indicated that sludge flotation may lead to the washout of biomass and the reactor performance deteriorated. This may explain the gradual decline of sulfate RE and Sulfate RC at the stage IV in the UASB reactor.

Oleszkiewicz and Romanek (1989) described that the direct treatment of wastewater and the addition of calcium and phosphate treatment wastewater showed larger, sticky flocculant sludge presented after running the reactor for 85 days, while granular biomass was formed in the treatment of wastewater supplemented with ferric ions and traces of nickel and cobalt. Although the flocculant sludge had a higher specific activity compared to granular sludge, the reactor with flocculant sludge accumulation was accompanied by a severe washout of the biomass. It suggested that trace of the metallic element can promote granulation and avoid sludge disintegration and washout of biomass in an anaerobic sludge bed reactor for the treatment of waste from the food industry. Compared to SLS, granular biomass are dense with high settling velocities (Guo and Kang, 2018; McSwain et al., 2005). Increasing the shear force in the reactor could be another strategy for preventing granule flotation (Chen et al., 2014). Appropriate shear forces can stimulate the production of polysaccharides that contribute to the self-immobilization of cells, which is essential for the formation of granules (Qin et al., 2004). The change of shearing forces can be achieved by the effluent recycling system to adjust the up-flow velocity. The latter is a potential strategy that needs further investigation.

### **4.3.2 Assessment of stratification in the UASB reactor**

In order to identify the substrate consumption and products accumulation rates along the height of the UASB reactor in each period, stratification of the UASB reactor was investigated during the four different periods established in which the profiles of sulfur

species and carbon species are shown in Figure 4.6 and Figure 4.7, respectively. Figure 4.6 shows that the sulfate RE calculated from inlet to outlet of the reactor was over 80% on days 49, 169, 198 and 271. In contrast, sulfate RE was reduced to 50% on day 294 and 20% on day 575, while sulfate reduction was also mainly occurring in the lower part of the reactor. It is observed that sulfate was not completely reduced to sulfide. Compared with sulfur species in the inlet, the stripping of H<sub>2</sub>S in the gas phase of UASB accounted for  $0.03 \pm 0.02\%$ . Thus, the sulfur imbalance may contribute to undetected sulfur species accumulated in the reactor. As described by Mora et al. (2020b), the organic sulfur compounds may be produced as intermediate products during crude glycerol fermentation, which was the main cause of sulfur imbalance. Moreover, sulfate was mainly reduced in the bottom part of the UASB reactor (UASB inlet to UASB2) and sulfate reduction rate was the highest from UASB inlet to UASB1 during the whole operation, as can be observed in Figure 4.6. Table 4.4 shows the relative contribution of each layer on sulfate reduction compared to the overall sulfate reduction of UASB, which shows the bottom part of the UASB reactor (UASB inlet to UASB2) accounted for the majority of sulfate reduction. This indicated that sulfidogenesis was achieved at the bottom part.

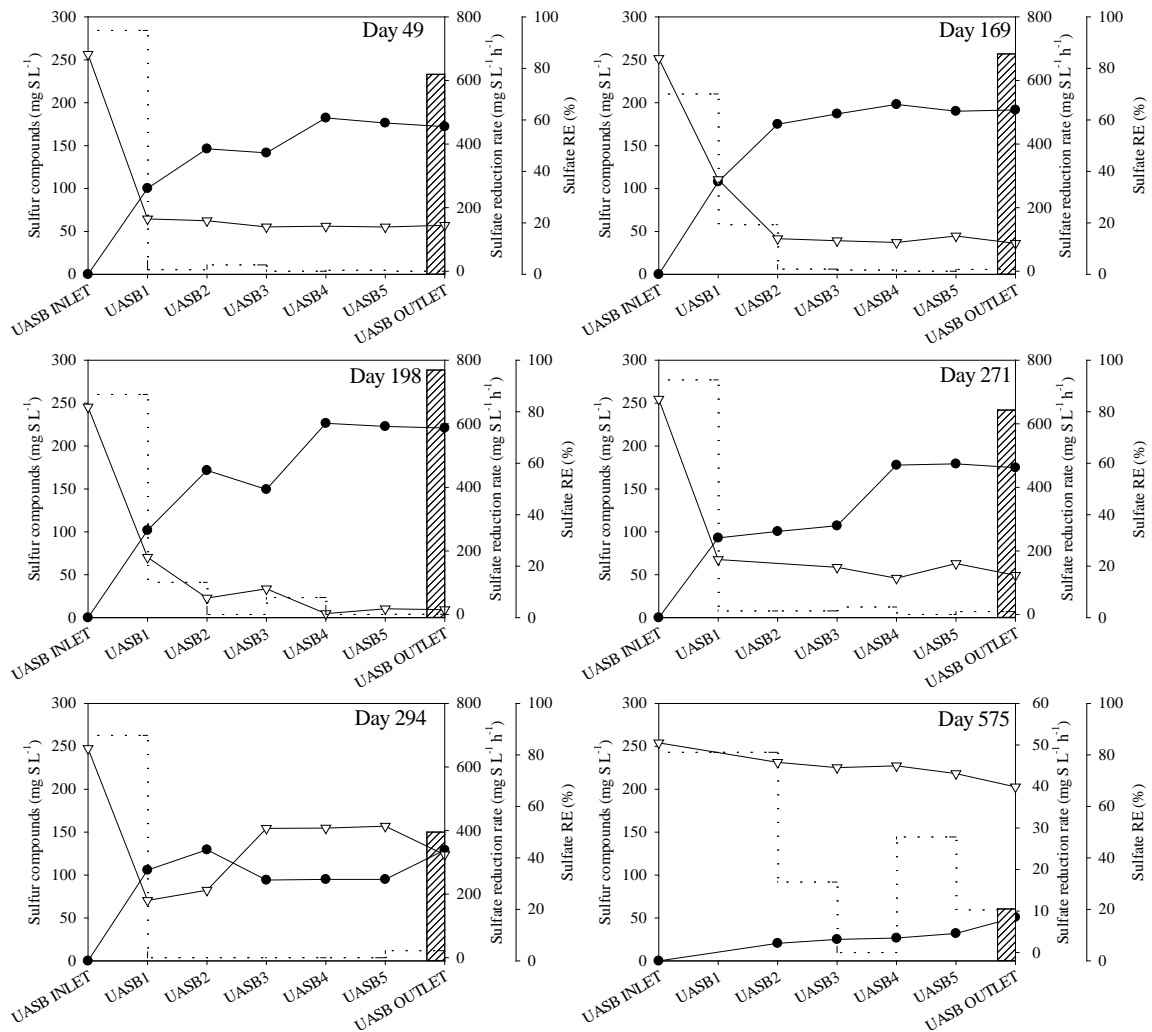


**Figure 4.6.** Sulfur compounds, sulfate reduction rate and sulfate removal efficiency of UASB stratification on 49, 169, 198, 271, 294 and 575 days. Symbols: sulfate (white triangle), TDS (black circle), sulfate reduction rate in each stratification (dotted line) and sulfate removal efficiency (Columnar slash).

It is noticed that the sum of each column in Table 4.4 is not 100%, which may be due to sampling errors or channeling between sludge particles. Some sampling points in the upper sections of the UASB reactor had a lower sulfide concentration than those in the lower sections. For example, on day 198 and 294, sulfide concentration in UASB3 was lower than that in UASB2 (Figure 4.6). Therefore, when calculating the sulfate reduction rate of each layer, an excessive sulfate reduction rate may be calculated, so that the sum of each column is not 100%.

**Table 4.4.** Relative contribution of each stratification on sulfate reduction compared to the overall sulfate reduction in the UASB.

UASB stratification	Relative contribution (%)						
	Sampling days	49	169	198	271	294	575
Inlet to UASB1		96.2	65.5	74.2	91.0	100	22.1
UASB1 to UASB2		1.1	31.9	20.1	2.2	0	22.1
UASB2 to UASB3		3.6	1.1	0	2.2	0	12
UASB3 to UASB4		0	0.9	9.8	6.2	0	0
UASB4 to UASB5		0.5	0	0	0	0	17.7
UASB5 to Outlet		0	4.0	0.4	6.7	0	30.1

Figure 4.7 shows the concentration of glycerol and VFAs of the UASB profile and glycerol consumption rate. When the reactor was in the period with extensive biogas production (day 49), glycerol was completely fermented at a rate of  $884 \text{ mg C L}^{-1} \text{ h}^{-1}$  and converted to acetate in UASB1, while acetate was completely consumed in UASB2. On day 49, UASB reactor was in the stage of high methane production, and acetate was used by methanogens to produce methane. When a decline in biogas production occurred (days 169 and 198), glycerol was still completely fermented in UASB1. However, acetate did not accumulate in UASB1 but in UASB3 on day 169 and UASB4 on day 198. This probably was due to the presence of other intermediate products of glycerol fermentation to VFAs. When no biogas was produced in the reactor (day 271), glycerol was degraded and acetate and propionate accumulated simultaneously in UASB1. When the sulfate RE of the reactor declined (days 294 and 575), the glycerol RE dropped to 68% on day 294 and 60% on day 575. In general, glycerol consumption rate was the highest from UASB inlet to UASB1 comparing the whole stratification of UASB during the entire operation. Table 4.5 shows the relative contribution of each layer on glycerol consumption. It can be seen that the degradation of glycerol was mainly completed from UASB inlet to UASB1 during the entire operation. This indicated that glycerol fermentation was also achieved at the bottom part of the UASB reactor.

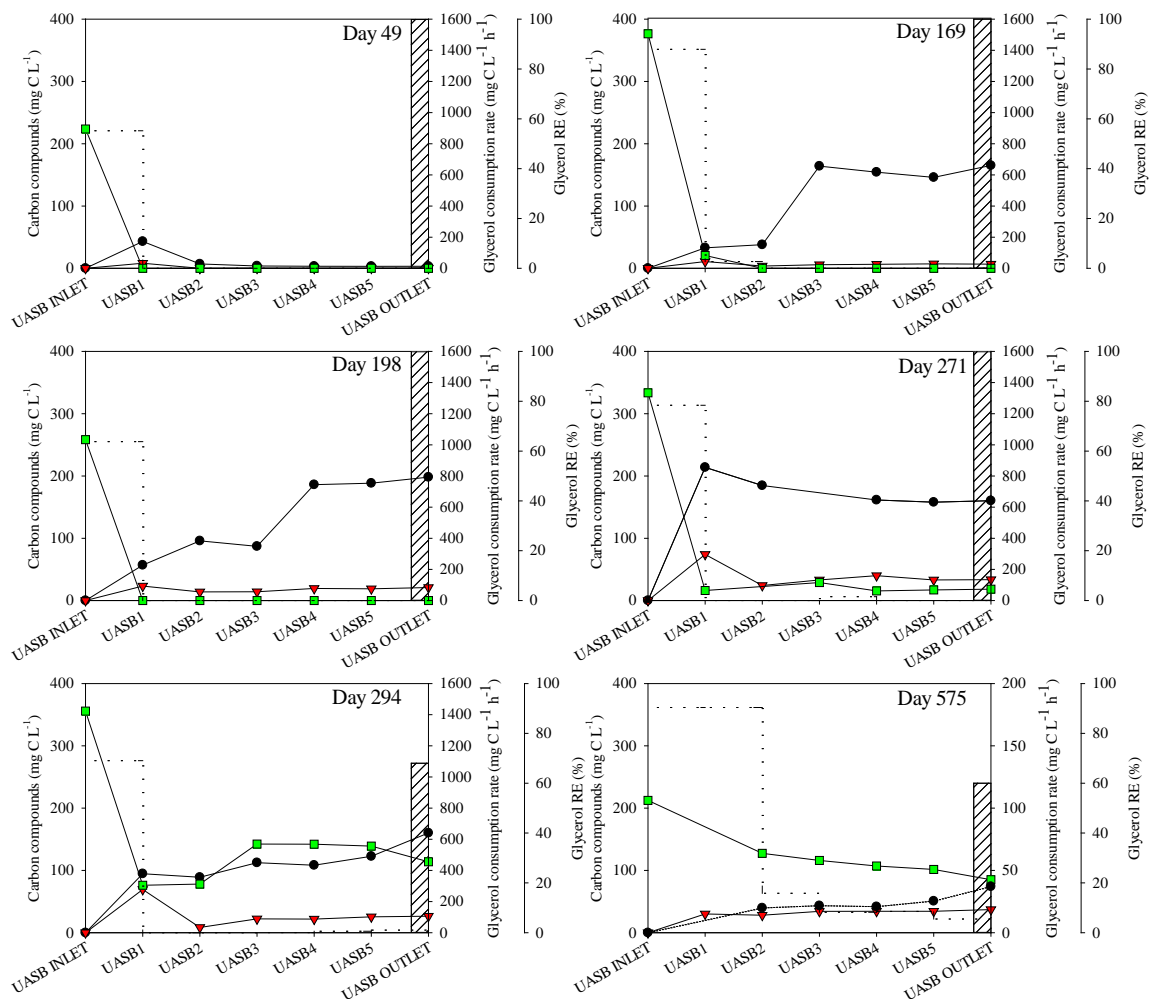


**Figure 4.7.** Carbon compounds, glycerol consumption rate and glycerol removal efficiency of UASB stratification on 49, 169, 198, 271, 294 and 575 days. Symbols: Glycerol (green square), acetate (black circle), propionate (red triangle), glycerol consumption rate in each stratification (dotted line) and glycerol removal efficiency (Columnar slash).

Both sulfate reduction and glycerol degradation were mainly completed in UASB1 on day 294, and neither was completely reduced or degraded (Figures 4.6 and 4.7). At this time, a part of the sludge accumulated on the top of the reactor (UASB6) due to flotation, which indicates that the top sludge did not further degrade glycerol or reduce sulfate. This showed that the flotation caused by SLS led to the inactivation/loss of activity of the biomass accumulating on top of the reactor. On day 575, the sulfate removal capacity and glycerol removal capacity were severely reduced (Figures 4.6 and 4.7), accompanied by a



large amount of SLS accumulated in the reactor (Figure 4.4). Mass transfer limitation could be an important factor affecting the sulfate and glycerol removal capacity. Baillod and Boyle (1970) described that the mass transfer limits the overall rate of substrate removal. Since the granular sludge was completely surrounded by the accumulated SLS in the UASB reactor, SLS may limit the diffusion of the substrate from mineral medium to granular sludge. In order to characterize SLS and its impact on reactor performance, batch tests of this substance were investigated and discussed in Chapter 5.

**Table 4.5.** Relative contribution of each stratification on glycerol consumption compared to the overall glycerol consumption in the UASB.

UASB stratification	Relative contribution (%)					
	49	169	198	271	294	575
Sampling days	49	169	198	271	294	575
Inlet to UASB1	100	94.5	100	95.2	100	33.3
UASB1 to UASB2	0	5.5	0	0	0	33.3
UASB2 to UASB3	0	0	0	0	0	9.0
UASB3 to UASB4	0	0	0	4.0	0	7.0
UASB4 to UASB5	0	0	0	0	1.2	4.4
UASB5 to Outlet	0	0	0	5.1	10.4	12.9

The evaluation of UASB reactor stratification can help to understand the effect of the sludge at different heights on sulfate reduction and degradation of organic compounds. It is observed that sulfate reduction and glycerol degradation were mainly completed at the bottom of the UASB reactor, which may be due to the high biomass concentration at the bottom of the UASB reactor. The biomass at the bottom of the sludge bed accounted for over 70% of the overall sludge of the reactor before the 300 days of UASB operation. The biomass at the bottom of the sludge bed also accounted for 57% and 78% on day 390 and day 639, respectively. The results are consistent with previous studies, which presented that the highest specific methanogenic activity was observed at bottom of the reactor in an UASB-anaerobic membrane bioreactor treating municipal wastewater (Ozgun et al., 2019).

The concentration of VSS increased along with the decreasing height of the sludge bed, and the highest concentration of VSS was observed at the bottom of the sludge bed where the most active sludge was obtained (Mahmoud et al., 2004; Ozgun et al., 2019).

In summary, methanogenic granular sludge progressively switched to sulfidogenic sludge performing high sulfate removal efficiency at a TOC/S-SO<sub>4</sub><sup>2-</sup> ratio of  $1.5 \pm 0.3$ . The sulfate removal capacity was over  $4.3 \text{ kg S m}^{-3} \text{ d}^{-1}$  in 280 days, while methanogenic activity was progressively decreased in the first 200 days of operation. Assessment of the sludge bed stratification showed that glycerol fermentation and sulfate reduction were mainly performed at the bottom of sludge bed. After long-term operation at low up-flow velocity ( $0.25 \text{ m h}^{-1}$ ), unexpected SLS accumulated and formed a biofilm that covered granular sludge, and both the overall glycerol RE and sulfate RE in UASB significantly declined. This formed biofilm cause sludge flotation, which resulted in the deterioration of system performance. Batch tests of SLS are investigated and discussed in Chapter 5 to characterize SLS. The mechanism of sulfate reduction using glycerol as a carbon source is further discussed in Chapter 6.

## 4.4 Conclusions

An UASB reactor was employed to treat sulfate-rich wastewater using crude glycerol as carbon source at a constant TOC/S-SO<sub>4</sub><sup>2-</sup> ratio of  $1.5 \pm 0.3 \text{ g C g}^{-1} \text{ S}$  for 639 days operation. The granular sludge inoculated quickly adapted to perform sulfidogenesis. The sulfate removal efficiency exceeded 84% within 16 days. The reactor processed  $4.3 \text{ kg S m}^{-3} \text{ d}^{-1}$  of sulfate during 280 days of operation. During this period, the VFAs accumulation was accompanied by the decrease of biogas production, resulting in a decline of TOC removal efficiency, which was caused by the washout of methanogens. In all cases, results of UASB reactor stratification revealed that the glycerol fermentation and sulfate reduction processes were mainly achieved at the bottom part of the reactor. Sulfate reduction and glycerol fermentation correlated well with the sludge concentration in the

UASB. During the period of no biogas production, the particle size of the biomass was reduced and the UASB reactor accumulated SLS, which resulted in sludge flotation. The flotation led to the inactivation of the biomass accumulating on top of the reactor and the flotation and degranulation resulted in biomass loss. Both result in a decrease in sulfate removal efficiency and glycerol removal efficiency in the reactor and deteriorated system performance. The failure of the reactor performance may be also affected by the limitation of substrate diffusion caused by the formation of SLS in the UASB.

## Chapter 5

---

# Specific activity of anaerobic sludge and of slime-like substances in a methanogenic - sulfidogenic UASB reactor

**Part of this chapter is in preparation for publication in:**

Zhou, X., Fernández-Palacios, E., Gabriel, D. The effect of slime accumulated in a long-term operating UASB using crude glycerol to treat S-rich wastewater.



*Chapter 4 did not reveal the interaction among carbon and sulfur species. The motivation of this chapter was the limited understanding obtained from the performance analysis of the reactor and the concentration profiles from different heights of the reactor depicted in Chapter 4. This chapter was aimed at assessing the specific activity of the anaerobic sludge, both the inoculum sludge of the reactor from a pulp and paper recycling industry (UIPSA, Spain) and the biomass in the reactor during its operation through well-defined batch activity tests, in terms of sulfate reduction capacity of the sludge using different carbon sources. Moreover, the stratification of microbial diversity dynamics and the rates of both fermentation and sulfate reduction along different heights of UASB reactor was also studied. Moreover, this chapter was devoted to explain the decrease of sulfate reduction capacity in the UASB reactor, according to the analysis of both granular sludge (GS) and SLS appeared, as described in Chapter 4.*

## **Abstract**

In this chapter, batch activity tests were performed with the inoculum sludge of the UASB reactor or the sludge taken from the continuous operation of the UASB reactor. The inoculum sludge was fed with glycerol, acetate, propionate, isobutyrate, butyrate, valerate in absence and presence of sulfate to assess the sulfate reduction capacity. The sludge from different heights of the UASB reactor was taken on days 169 and 198 to characterize stratification of the reactor by its microbial diversity and biological reaction rates. As described in chapter 4, the accumulation of SLS was observed in the long-term operation of the sulfidogenic UASB reactor fed with crude glycerol. GS, slime-covered granular sludge (SCGS) and SLS were investigated on days 315 and 431, with the aim to explain the decrease of sulfate removal efficiency and performance deterioration in the UASB reactor. Results showed that glycerol was not used as direct electron donor for sulfate reduction. The carbon source used for sulfate reduction were other products of

glycerol fermentation such as propionate. Activity tests of sludge sampled at different heights of the UASB showed that the sludge from UASB1 had a higher fermentative rate than the sludge from UASB3. The activity tests performed with GS, SCGS and SLS showed that there was no difference between GS and SLS in the mechanism of glycerol fermentation and sulfate reduction. But the specific sulfate reduction rate of GS was higher than that of SLS, while SLS showed a higher glycerol fermentation rate than that of GS. The different rates in GS and SLS may be caused by higher relative abundances of fermentative microorganisms found in SLS and higher relative abundances of sulfate reducing bacteria (SRB) found in GS. *Desulfovibrio* was the most abundant genus found in the sludge taken from the UASB reactor.

## 5.1 Introduction

The enrichment of GS from methanogenic into non-methanogenic but sulfidogenic one is of interest in order to start up and to establish long-term, stable systems that optimize the consumption of the electron donor towards the production of sulfide. Chapter 4 and previous studies investigated the performance and stability of UASB using crude glycerol as a carbon source under variable organic and sulfate loading rates (Fernández-Palacios et al., 2019; Mora et al., 2020b). During the reactor operation, SRB compete with acetogenic bacteria and methanogens for the fermentation intermediates.

Many factors influence the competition between SRB, fermentative bacteria and methanogens (MPB) by affecting the microbial acclimation of different species that drive the rates of the production/consumption reactions. Sulfidogenesis spontaneously outcompeted methanogenesis when sulfate-rich wastewaters were treated under mesophilic conditions (Wu et al., 2018). It is mentioned that SRB have faster growth kinetics and higher affinity for substrates than methanogens (J.W.H. et al., 1994). Besides, SRB have lower Monod half saturation constants than methanogens, which allowed SRB to operate at low concentrations of substrate where MPB cannot sustain growth (Gupta et al., 1994a). Moreover, preferred carbon substrates for microorganisms could affect competition. Methanogens outcompeted SRB in an acetate-fed anaerobic reactor, but SRB became dominant with propionate as a carbon source (Van Den Brand et al., 2014b). When using methanol as a feedstock, methanogens outcompeted sulfate reducers under mesophilic conditions (30 °C) (Weijma et al., 2003), and it demonstrated opposite behavior under thermophilic conditions (exceeding 65 °C) (Marcus V.G. Vallero et al., 2004a). Since there are many factors affecting methanogenesis and sulfidogenesis, the competition between methanogens and SRB in UASB reactors still needs to be investigated. Moreover, as shown in Chapter 4, there are still unexpected issues in the long-term operation of a sulfidogenic UASB reactor. One of them is the accumulation of the SLS depicted in Chapter 4, so further research is needed to determine the effect of slime on the



performance of the UASB.

The aim of this chapter was to assess the specific activity of anaerobic sludge obtained both from the inoculum sludge of the reactor and sludge of the UASB reactor during its operation through well-defined batch activity tests. The purpose of this chapter was also to explain the decrease of the sulfate reducing capacity in the UASB reactor, according to the analysis of GS and SLS. This was accomplished by assessing the process rates and microbial diversity of sludge in the UASB reactor, characterizing the SLS that was accumulated in the reactor, and exploring its effect on the stability of the UASB performance over long-term periods.

## **5.2 Materials and methods**

### **5.2.1 Experimental setup of activity tests**

Batch activity tests were conducted by feeding different carbon sources, in which the sludge was taken from the inoculum sludge of the UASB reactor from the pulp and paper recycling industry (as described in section 3.1.1 of Chapter 3) or different heights of the UASB reactor in different operating periods. Table 5.1 summarizes the operating conditions of activity tests performed with different carbon sources. VFAs were selected as carbon sources because they are reported as the most common intermediate products of glycerol degradation (Bertolino et al., 2014; Dinkel et al., 2010; Mora et al., 2020b).

**Table 5.1.** Conditions of batch activity tests using glycerol and VFAs as carbon source.

Sample time	Biomass	Tests with sulfate	Tests without sulfate	Carbon Source	TOC (mg C L <sup>-1</sup> )	Sulfate (mg S L <sup>-1</sup> )	TOC/S (g C g <sup>-1</sup> S)	Biomass fed with sulfate (g VSS L <sup>-1</sup> )	Biomass fed carbon source only (g VSS L <sup>-1</sup> )
0	GS <sup>A</sup>	✓	✓	Glycerol	349	247	1.41	1.10 ± 0.01	1.17 ± 0.00
		✓	✓	Acetate	533	249	2.14	2.98 ± 1.13	4.54 ± 0.45
		✓	✓	Propionate	537	249	2.16	5.08 ± 0.64	4.26 ± 2.04
		✓	✓	Isobutyrate	557	255	2.18	5.06 ± 1.96	3.98 ± 1.59
		✓	✓	Butyrate	520	253	2.06	4.06 ± 2.36	6.22 ± 0.37
		✓	✓	Valerate	322	253	1.27	4.01 ± 1.57	8.06 ± 2.38
169	GS <sup>B</sup>	✓	×	Glycerol	400	247	1.62	1.58 ± 0.44	N.A.
198	GS <sup>B</sup>	✓	✓	Glycerol	327	230	1.42	1.07 ± 0.24	1.20 ± 0.48
315	GS and SCGS <sup>C</sup>	✓	×	Acetate	326	248	1.31	0.28 ± 0.08	N.A.
		✓	×	Propionate	328	248	1.32	0.35 ± 0.05	N.A.
431	GS <sup>D</sup>	✓	✓	Glycerol	324	240	1.35	0.38 ± 0.13	0.23 ± 0.10
	SLS <sup>D</sup>							0.38 ± 0.03	0.40 ± 0.02

Note: N.A. The activity tests were not applied. <sup>A</sup> Biomass inoculum from a pulp and paper recycling industry.

<sup>B</sup> Biomass from different heights of the UASB reactor (UASB1, UASB2 and UASB3, showed in Figure 3.1).

<sup>C</sup> Biomass from UASB1.

<sup>D</sup> Biomass from UASB6.

From one side, sludge taken from a pulp and paper recycling industry was used to investigate the mechanism of the glycerol degradation and the sulfate reduction capacity by the methanogenic biomass using glycerol and different VFAs as carbon sources. On the other side, the sludge was also taken from different heights of the UASB reactor (UASB1, UASB2 and UASB3) on days 169 and 198 to perform activity tests to characterize the sludge activity in different layers of the reactor using glycerol as the carbon source. In the former cases, GS was directly fed with MM into serum bottles with no further manipulation, and the culture process and conditions are described in section 3.2 of Chapter 3.

In order to study the effect of the presence of SLS on the sulfate removal efficiency in the UASB reactor, the sludge was taken out from the UASB reactor on days 315 and 431 to perform activity batch tests. Acetate, propionate and glycerol were used as carbon sources to study the sulfate reduction process in batch tests. The sludge collected from UASB1 on day 315 was separated into SCGS and GS. The SCGS was the sludge taken directly from the reactor without any treatment, which contained GS covered with SLS, whereas GS was GS that had been cleaned to remove SLS. The cleaning process was performed as follows: 10 mL of the original sludge from the UASB reactor were collected into a 250 mL serum bottle, then 100-150 mL of MM without sulfate was added, and the bottle was shaken so as to re-suspend all the sludge in the liquid. Since GS is heavier than SLS, GS settled first to the bottom of the bottle. Afterwards, the suspension containing SLS was discarded and then more MM without sulfate was added, and the same process was repeated 5 to 10 times until only GS remained in the bottle. The processed GS and SCGS in serum bottles are shown in Figure 5.1B and 5.1C. 150 mL of MM were fed both to GS and SCGS, and acetate and propionate were added as carbon sources. The initial concentration was set to maintain the same conditions as the TOC/S ratio used along the long-term UASB performance.

The sludge collected from UASB6 on day 431 was divided into GS and SLS. Due to the low concentration of GS at UASB1 where all was almost surrounded by SLS (Figure 4.4C of Chapter 4), the sludge was collected from UASB6 on day 431. The process of cleaning the sludge to get GS was the same as the one described above. SLS was obtained from the

suspension containing SLS during the above-mentioned cleaning process, and the small amount of GS contained in the suspension was removed with plastic pipettes. The GS and SLS were fed with 150 mL of MM and pure glycerol as the carbon source.

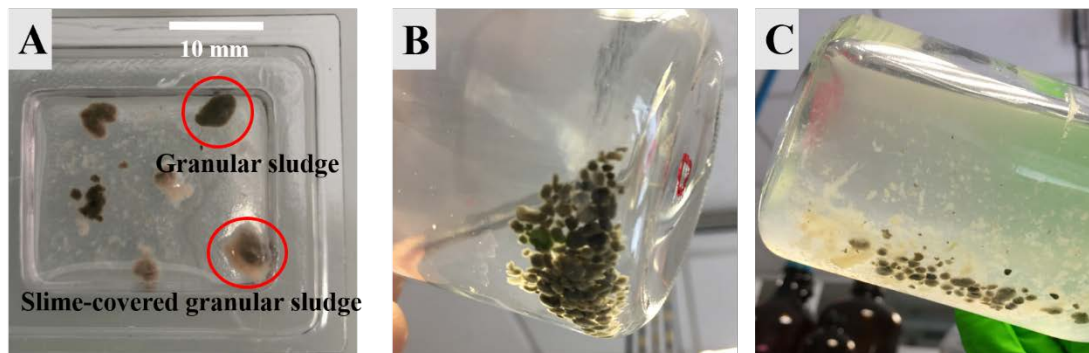


**Figure 5.1.** SCGS and GS obtained from the UASB reactor. A) SCGS and GS; B) GS in batch tests; C) SCGS in batch tests.

### 5.2.2 Analytical methods

The analysis of the liquid and gas phases is described in section 3.3 of Chapter 3.

Volumetric consumption/production observed rates ( $\text{mg C L}^{-1} \text{h}^{-1}$  or  $\text{mg S L}^{-1} \text{h}^{-1}$ ) of the measured species were calculated by the concentration changes between two consecutive sampling times, which is described as follows:

$$\text{Volumetric rate} = \frac{D_{x2} - D_{x1}}{T_{x2} - T_{x1}} \quad \text{Eq.5.1}$$

Where  $D_{x2}$  and  $D_{x1}$  ( $\text{mg C/L}$  or  $\text{mg S/L}$ ) are the concentration of species D under culture time  $T_{x2}$  and  $T_{x1}$  (h), respectively.

The specific rate ( $\text{mg C gVSS}^{-1} \text{h}^{-1}$  or  $\text{mg S g VSS}^{-1} \text{h}^{-1}$ ) was determined as follows:

$$\text{Specific rate} = \frac{\text{Volumetric rate}}{\text{VSS}} \quad \text{Eq.5.2}$$

## 5.3 Results and discussion

### 5.3.1 Specific activities of the inoculum sludge of the UASB reactor

#### 5.3.1.1 Activity tests using glycerol as carbon source

Profiles for carbon and sulfur species using inoculum sludge of the UASB reactor using glycerol as carbon source added with and without sulfate into serum bottles are shown in Figure 5.2. When glycerol was added into serum bottles, glycerol was consumed from 10 h to 72 h at a rate of  $4.5 \pm 2.2 \text{ mg C g VSS}^{-1} \text{ h}^{-1}$ , as shown in Figure 5.2A. Propionate was accumulated and consumed from 58 h to 96 h, while acetate was not accumulated and 191  $\text{mg C L}^{-1}$  of  $\text{CH}_4$  were detected in the gas phase. The anaerobic digestion process includes four main phases: hydrolysis, acidogenesis, acetogenesis and methanogenesis (Van Lier et al., 2008). Through acidogenesis and acetogenesis, glycerol produced intermediate products (VFAs) under anaerobic conditions, such as acetic acid, propionic acid, butyric acid, etc. Acetic acid was further converted into methane by methanogens. When glycerol and sulfate were added, glycerol was consumed from 10 h to 72 h at a rate of  $4.7 \pm 1.8 \text{ mg C g VSS}^{-1} \text{ h}^{-1}$  (Figure 5.2B). During the period of glycerol fermentation, propionate was accumulated and consumed from 58 h to 82 h, while sulfate reduction rate increased from  $0.7 \pm 0.1 \text{ mg C g VSS}^{-1} \text{ h}^{-1}$  (from 10 h to 58 h) to  $1.9 \pm 0.1 \text{ mg C g VSS}^{-1} \text{ h}^{-1}$  (from 58 h to 82 h). Acetate was not accumulated during the culture time, while 151  $\text{mg C L}^{-1}$  of  $\text{CH}_4$  were detected in the gas phase.

Comparing the glycerol consumption rate in the absence and presence of sulfate, the glycerol consumption rate was not affected by the presence of sulfate, which indicates that sulfate reduction was not mediated using glycerol as carbon source. This means that glycerol was first fermented to intermediate products, and the sludge used the intermediate products as electron donors to reduce sulfate. It is also observed that regardless of whether sulfate was added or not, there was little VFAs production accompanied by a large amount of total inorganic carbon (TIC) accumulation. Moreover, sulfate reduction rate increased with the accumulation of propionate from 58 h to 82 h (Figure 5.2). In order to understand the capability of methanogenic sludge to reduce sulfate using VFAs as carbon sources,

acetate, propionate, butyrate, isobutyrate and valerate were selected to further investigate.

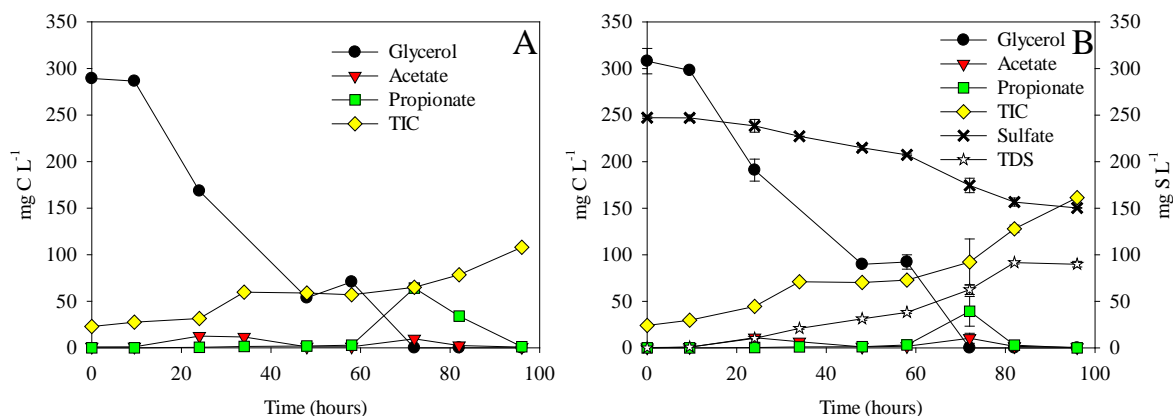


**Figure 5.2.** Activity tests of inoculum sludge of the UASB reactor using glycerol as carbon source. (A) Fed with glycerol only, (B) Fed with glycerol and sulfate. TIC represents total inorganic carbon.

### 5.3.1.2 Activity tests using acetate and propionate as carbon source

Specific activity tests of inoculum sludge of the UASB reactor using acetate and propionate as the carbon source are shown in Figure 5.3. Acetate was consumed in 29 h in absence of sulfate (Figure 5.3A). In the presence of sulfate, acetate was consumed in 34 h after the lag phase (0 to 10 h) using acetate as a carbon source, and sulfate was reduced from 249 mg S L<sup>-1</sup> to 224 mg S L<sup>-1</sup> (Figure 5.3B).

When propionate was used as carbon source, propionate was continued to be consumed throughout the entire culture period in absence of sulfate (Figure 5.3C). There was almost no accumulation of acetate, but 251 mg C L<sup>-1</sup> of CH<sub>4</sub> were detected in the gas phase after 58 h culture in absence of sulfate. The metabolic pathways of propionate degradation in anaerobic digestion are well-described (Li et al., 2017). According to catabolism and anabolism, acetogenic bacteria convert propionate to acetate, which further produce CH<sub>4</sub> by acetoclastic methanogens; and to CO<sub>2</sub> and H<sub>2</sub>, which further produce CH<sub>4</sub> by hydrogenotrophic methanogens. In the presence of sulfate, propionate was completely consumed within 24 h, as shown in Figure 5.3D. 29 mg C L<sup>-1</sup> of acetate were detected after 5 h cultivation, but were completely consumed after 24 h. In the gas phase, 182 mg C L<sup>-1</sup> of CH<sub>4</sub> were detected after 58 h. In presence of sulfate, propionate can be partially oxidized to

acetate and bicarbonate, or it can be completely oxidized to bicarbonate (Luis, 2018). In the activity test fed with propionate, there was no accumulation of acetate, but the production of methane indicated that the consumption rate of acetate by the inoculum sludge was greater than the cumulative rate of acetate production.

The specific rates of acetate and propionate consumption and sulfate reduction are shown in Table 5.2. The acetate consumption rate with sulfate added was 1.3 times than the rate without sulfate, while the sulfate reduction rate was  $0.2 \text{ mg S g VSS}^{-1} \text{ h}^{-1}$  when acetate was the carbon source. This indicated that methanogenic sludge could use acetate as a carbon source to reduce sulfate with low reduction rate, and the main degradation pathway of acetate was methane production. The propionate consumption rate with sulfate added was 2.1 times that rate without sulfate. This indicates that propionate was consumed through acidogenesis and sulfidogenesis. Moreover, from 0 h to 24 h, the sulfate reduction rate of propionate as carbon source was 10.5 times that of acetate, which indicates propionate is a favorable electron donor to reduce sulfate compared to acetate. Similarly, previous studies described that SRB preferred to use propionate rather than acetate in the long-term operation of anaerobic conditions treating sulfate-rich wastewater (Huang et al., 2012; Van Den Brand et al., 2014a).

**Table 5.2.** Specific rates obtained from inoculum GS fed acetate and propionate.

Carbon source	Sulfate	Time (hours)	Substrate consumption rate (mg C g VSS <sup>-1</sup> h <sup>-1</sup> )	Sulfate reduction rate (mg S g VSS <sup>-1</sup> h <sup>-1</sup> )
Acetate	-	5-24	$4.7 \pm 1.6$	
	+	10-34	$6.1 \pm 2.4$	$0.2 \pm 0.1$
Propionate	-	0-24	$2.0 \pm 0.6$	
	+	0-24	$4.4 \pm 1.0$	$2.1 \pm 0.7$

Note: - without sulfate; + with sulfate.

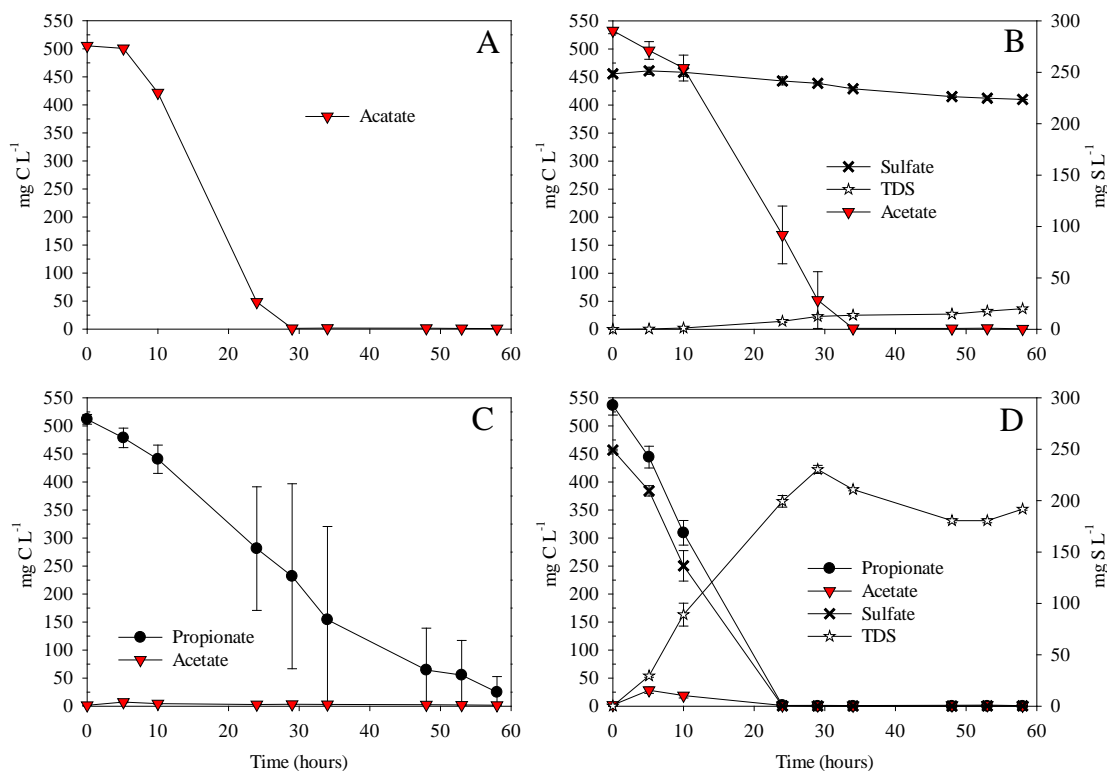


**Figure 5.3.** Activity tests of inoculum sludge of the UASB reactor feeding acetate (A, B) and propionate (C, D). A and C, without sulfate; B and D with sulfate.

### 5.3.1.3 Activity tests using butyrate, isobutyrate and valerate as carbon source

Specific activity tests of inoculum sludge of the UASB reactor using butyrate, isobutyrate and valerate as the carbon source are shown in Figure 5.4. When butyrate was used as a carbon source, butyrate was consumed and isobutyrate was produced both in the absence and presence of sulfate (Figure 5.4A, 5.4B). When isobutyrate was used as a carbon source, isobutyrate was consumed and butyrate was produced in the absence and presence of sulfate (Figure 5.4C, 5.4D). Tholozan et al. (1988) investigated the reversible isomerization between butyrate and isobutyrate in a mesophilic anaerobic digester. <sup>13</sup>C-nuclear magnetic resonance and cell extracts experiments proved that the isomerization between butyrate and isobutyrate was catalyzed by a butyryl-CoA:isobutyryl-CoA mutase to migrate carboxyl group (Matthies and Schink, 1992). It was also found that butyrate-degrading sulfate reducers were able to isomerize between butyrate and isobutyrate (Oude Elferink et al., 1996), but small conversions were achieved.



When valerate was selected as a carbon source, valerate was consumed at around  $0.1 \text{ mg C g VSS}^{-1} \text{ h}^{-1}$  in the absence and presence of sulfate (Figure 5.4E, 5.4F). McCollom and Seewald (2003) described the metabolic pathways of valerate decomposition, which involved the formation of shorter carboxylic acids, such as acetate and propionate. In the process of microbial sulfate reduction, the conversion of valerate to acetate and propionate has also been reported (Fukui et al., 1997). However, no acetate and propionate accumulation was observed throughout the entire test period. This can be explained by the consumption/production rate of acetate and propionate. It can be seen from Table 5.2 that the consumption rates of acetate and propionate were  $4.7$  and  $2.0 \text{ mg C g VSS}^{-1} \text{ h}^{-1}$ , respectively. The consumption rate of valerate was only  $0.1 \text{ mg C g VSS}^{-1} \text{ h}^{-1}$ , which implies that the possible production of acetate or propionate from valerate degradation was rapidly consumed.

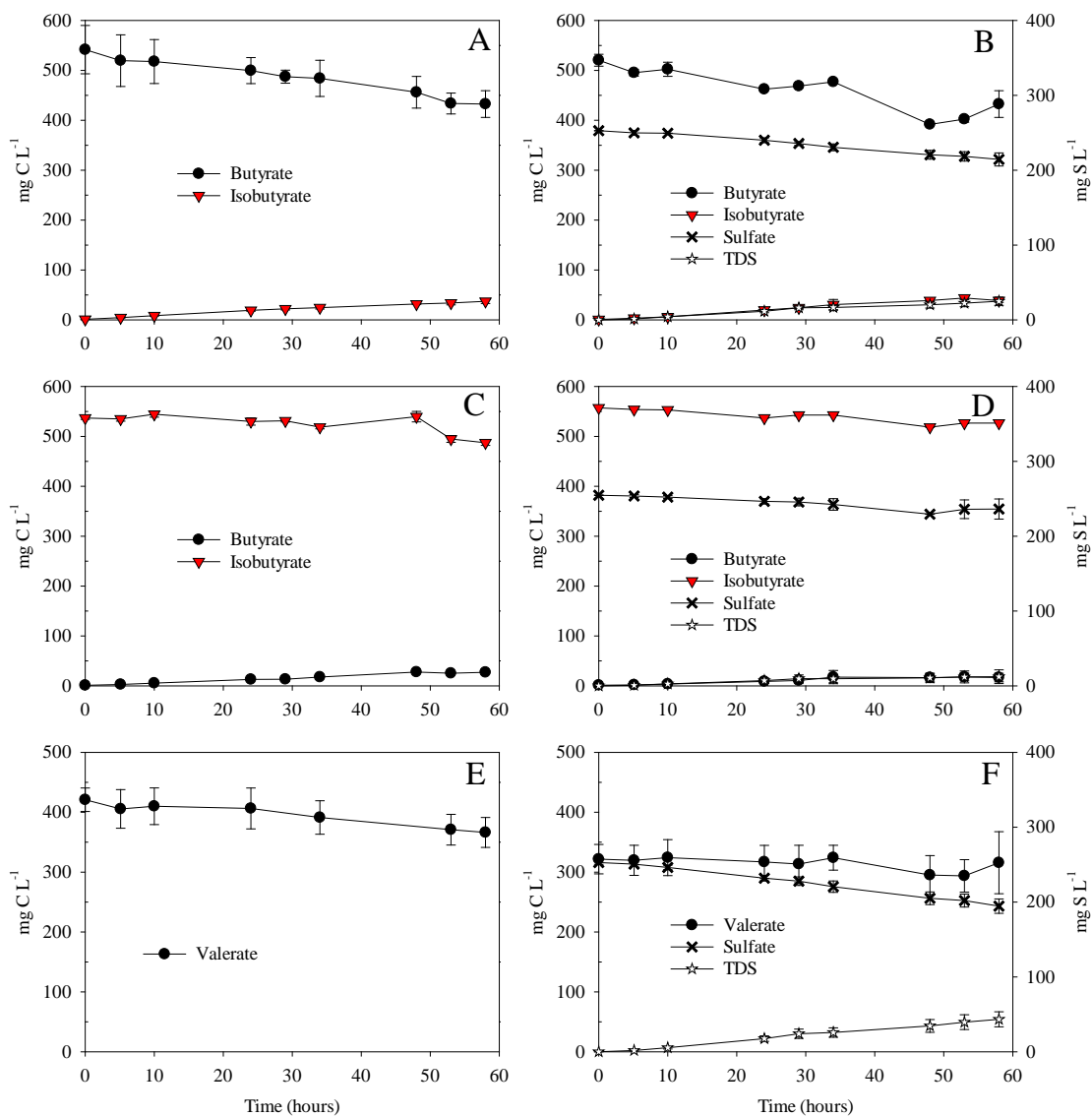


**Figure 5.4.** Activity tests of inoculum sludge of the UASB reactor feeding butyrate (A, B), isobutyrate (C, D) and valerate (E, F). A, C and E, without sulfate; B, D and F with sulfate.

Specific rates for tests fed with butyrate, isobutyrate and valerate are shown in Table 5.3. Through the activity tests of VFAs as carbon sources it is clear that, butyrate, isobutyrate and valerate might be used as electron donors to reduce sulfate. However, the sulfate reduction rates with these compounds were less than  $0.3 \text{ mg S g VSS}^{-1} \text{ h}^{-1}$ , while the rate up to  $2.1 \text{ mg S g VSS}^{-1} \text{ h}^{-1}$  were obtained when feeding propionate. Except for propionate, the sulfate reduction rate using valerate as a carbon source was the highest among other VFAs, reaching  $0.25 \text{ mg S g VSS}^{-1} \text{ h}^{-1}$ . This shows that propionate was mainly used as an electron donor to reduce sulfate in inoculum sludge, which also explains the

increase in sulfate reduction rate during glycerol fermentation when propionic acid accumulated. The further investigation of sludge activity tests targeted propionate and acetate instead of other VFAs.

**Table 5.3.** Specific rates were obtained from inoculum GS fed with butyrate, isobutyrate and valerate.

Carbon source	Sulfate	Time (hours)	Substrate consumption rate (mg C g VSS <sup>-1</sup> h <sup>-1</sup> )	Sulfate reduction rate (mg S g VSS <sup>-1</sup> h <sup>-1</sup> )
Butyrate	-	5-24	0.47 ± 0.11	
	+	0-58	0.72 ± 0.01	0.13 ± 0.03
Isobutyrate	-	0-24	0.14 ± 0.01	
	+	0-24	0.48 ± 0.11	0.08 ± 0.06
Valerate	-	0-24	0.12 ± 0.01	
	+	0-24	0.13 ± 0.01	0.25 ± 0.05

Note: - without sulfate; + with sulfate.

### 5.3.2 Specific activities through the UASB reactor heights

After 100 days of operation, the effluent of the UASB reactor began to accumulate acetate (see Figure 4.1). In order to understand the performance of the UASB sludge at different heights, specific activity tests of biomass withdrawn from the UASB (UASB1, UASB2 and UASB3) were performed on day 169 of operation. The experimental profiles to characterize the different activity of GS in the UASB reactor fed with glycerol as the carbon source are presented in Figure 5.5. As it can be observed, sulfate was reduced at rates of  $7.8 \pm 1.9$  mg S g VSS<sup>-1</sup> h<sup>-1</sup> with UASB1 biomass (Figure 5.5A),  $5.7 \pm 0.5$  mg S g VSS<sup>-1</sup> h<sup>-1</sup> with UASB2 biomass (Figure 5.5C) and  $5.6 \pm 1.8$  mg S g VSS<sup>-1</sup> h<sup>-1</sup> with UASB3 biomass (Figure 5.5E). Glycerol fermentation rate decreased significantly from  $15.7 \pm 0.8$  mg C g VSS<sup>-1</sup> h<sup>-1</sup> with UASB1 biomass to  $9.2 \pm 1.5$  mg C g VSS<sup>-1</sup> h<sup>-1</sup> with UASB2 biomass and  $8.4 \pm 1.8$  mg C g VSS<sup>-1</sup> h<sup>-1</sup> with UASB3 biomass. The degradation of glycerol produced intermediate metabolites such as VFAs. In comparison with UASB2 and UASB3 biomass, the glycerol fermentation rate was the highest with UASB1 biomass, indicating

---

that more VFAs were produced at UASB1 during the degradation of glycerol. The sulfate reduction rate was also the highest with UASB1 biomass. By comparing the accumulation of acetate in the sludge of different heights, it was found that UASB3 accumulated less acetate. When glycerol was terminated, the order of acetate consumption of sludge from different heights of the reactor was as follows: UASB1 ( $0.7 \text{ mg C g VSS}^{-1} \text{ h}^{-1}$ ) < UASB2 ( $1.4 \text{ mg C g VSS}^{-1} \text{ h}^{-1}$ ) < UASB3 ( $1.7 \text{ mg C g VSS}^{-1} \text{ h}^{-1}$ ). It was also found that the difference between the initial and final TOC concentrations were 253.1, 343.4 and 388.8  $\text{mg C L}^{-1}$  of sludge from UASB1, UASB2 and UASB3, respectively. This shows that compared with UASB1 and UASB2, the sludge from UASB3 had a stronger capacity to convert acetate to methane.

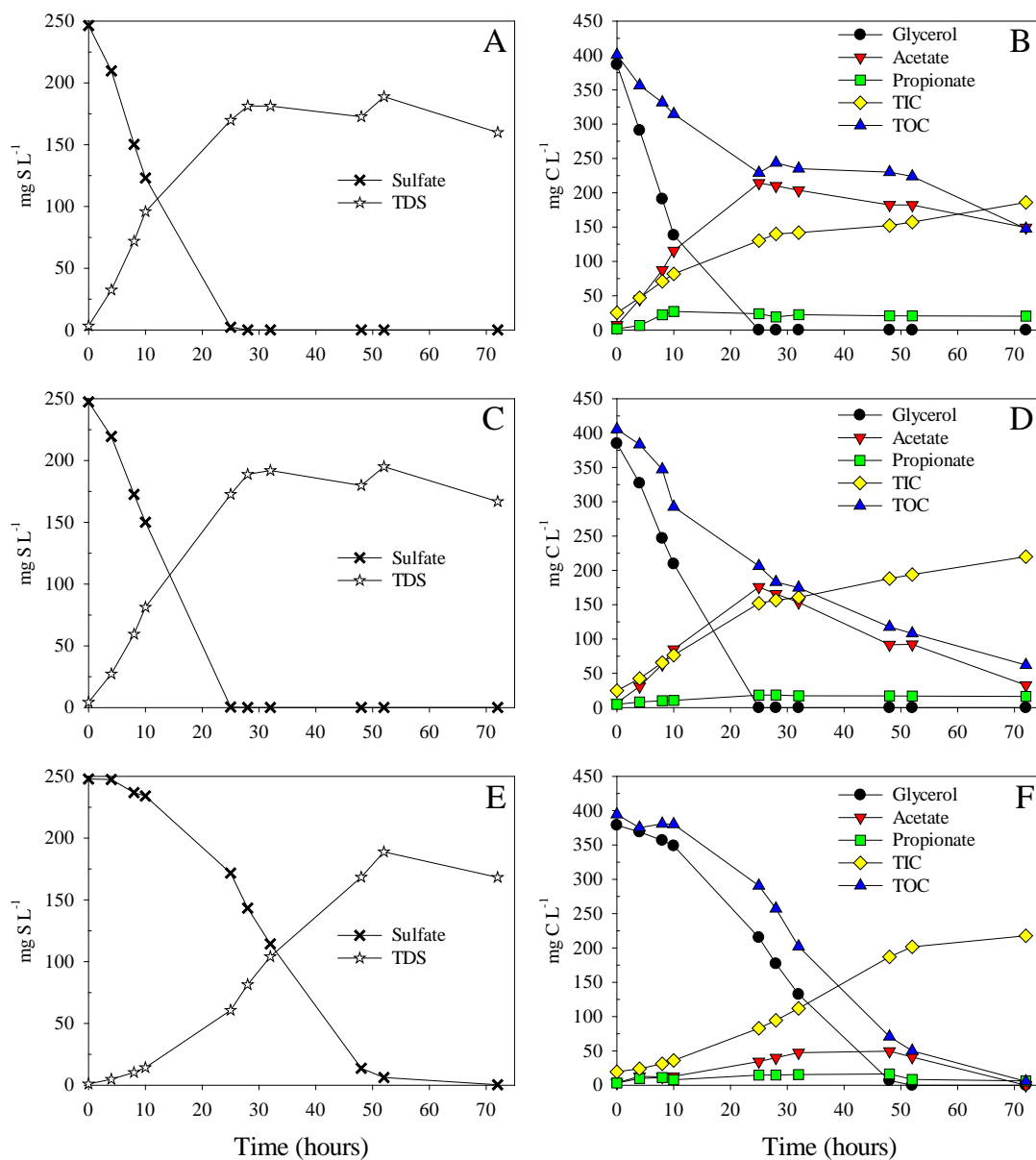


**Figure 5.5.** Activity tests of sludge from different heights of UASB reactor on day 169 feeding glycerol and sulfate. A, C and E show sulfur conversion of UASB1, UASB2 and UASB3, respectively; B, D and F show carbon species of UASB1, UASB2 and UASB3, respectively. TIC represents total inorganic carbon. TOC represents total organic carbon.

The consumption rate of glycerol with biomass from UASB1 was much higher than that taken from UASB2 and UASB3, which might be caused by the long-term exposure to glycerol of the bottom sludge that leads to the adaptability of the microbial population.

Microbial communities of stratification were analyzed on day 173. As shown in Figure 5.6, the relative abundances of *Dysgonomonas* of sludge from UASB1, UASB2 and

UASB3 were 4.3%, 2.7% and 1.6%, respectively. The relative abundances of *Enterococcus* of sludge from UASB1, UASB2 and UASB3 were 4.3%, 5.4% and 1.3%, respectively. The relative abundances of *Klebsiella* of sludge from UASB1, UASB2 and UASB3 were 2.9%, 0.5% and 5.2%, respectively. The relative abundances of *Propionispora* decreased along with the increasing height of the UASB reactor, 2.9% from UASB1 sludge, 2.1% from UASB2 sludge and 0.9% from UASB3 sludge. A wide range of microorganisms have been observed for glycerol fermentation, including *Dysgonomonas* (Moscoviz et al., 2018), *Enterococcus* (Doi, 2015), *Klebsiella* (Cheng et al., 2007), *Propionibacterium* (Himmi et al., 2000) and *Propionispora* (Abou-Zeid et al., 2004). *Dysgonomonas* and *Klebsiella* were able to convert glycerol to 1,3-propanediol (Cheng et al., 2007; Moscoviz et al., 2018). *Enterococcus* can convert crude glycerol to L-lactate at a high conversion efficiency (Doi, 2015). *Propionibacterium* and *Propionispora* convert crude glycerol to propionate and acetate (Abou-Zeid et al., 2004; Biebl et al., 2000; Himmi et al., 2000). The sum of relative abundances of these fermentative microorganisms decreased from 14.4% in UASB1 to 9% in UASB3.

The *Methanosaetai*, methanogenic archaea typically found in anaerobic digestion, increased their relative abundance from 1.2% in UASB1 to 4.1% in UASB3, which explains the highest acetate consumption on top of the UASB reactor. *Desulfovibrio* was the most abundant genus found in the reactor, accounted for 42.8% at UASB1, 49.8% at UASB2 and 19.5% at UASB3, respectively. The dominant microbial communities of SRB of sludge from different heights of UASB reactor indicated that SRB outcompeted methanogens on day 173. Moreover, the same sulfate reduction rate observed in UASB2 and UASB3 indicated that 19.5% of *Desulfovibrio* did not limit the sulfate reduction rate.

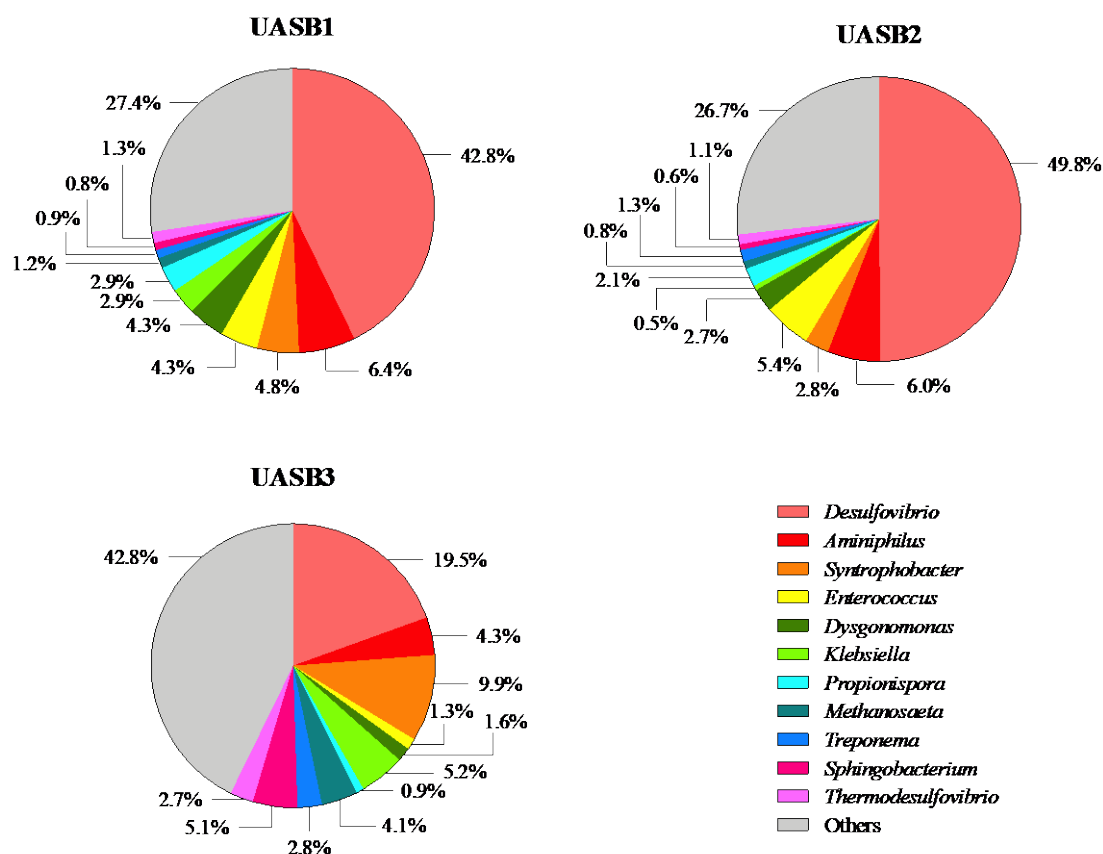


**Figure 5.6.** Microbial diversity of sludge taken from UASB1, UASB2 and UASB3 on day 173 (data adapted from Fernández Palacios, 2020).

After 198 days operation of the UASB reactor, it can be seen that acetate at the effluent exceeded  $200 \text{ mg C L}^{-1}$  (see Figure 4.1). In order to analyze the stratification of reactor at this time and compare it with the reactor operating for 169 days, the specific activities were tested on day 198 of operation. Figure 5.7 shows the experimental profiles in glycerol-fed batch tests as initial carbon source in presence of sulfate, where the sludge was taken from different heights of the UASB reactor (UASB1, 2 and 3) on day 198. It can be observed that sulfate was reduced at rates of  $8.4 \pm 2.4 \text{ mg S g VSS}^{-1} \text{ h}^{-1}$  with UASB1 biomass (Figure 5.7A),  $5.9 \pm 0.5 \text{ mg S g VSS}^{-1} \text{ h}^{-1}$  with UASB2 biomass (Figure 5.7C) and  $4.8 \pm 1.9 \text{ mg S g VSS}^{-1} \text{ h}^{-1}$  with UASB3 biomass (Figure 5.7E). The glycerol fermentation rate on day 198 by the GS taken from UASB1 ( $20.1 \pm 1.8 \text{ mg C g VSS}^{-1} \text{ h}^{-1}$ ) was significantly higher than that from UASB2 ( $9.2 \pm 0.8 \text{ mg C g VSS}^{-1} \text{ h}^{-1}$ ) and from UASB3 ( $9.6 \pm 2.2 \text{ mg C g VSS}^{-1} \text{ h}^{-1}$ ). In terms of acetate, tests show that acetate accumulated and remained constant after

glycerol degradation on all batch tests with biomass taken from UASB1, UASB2 and UASB3.

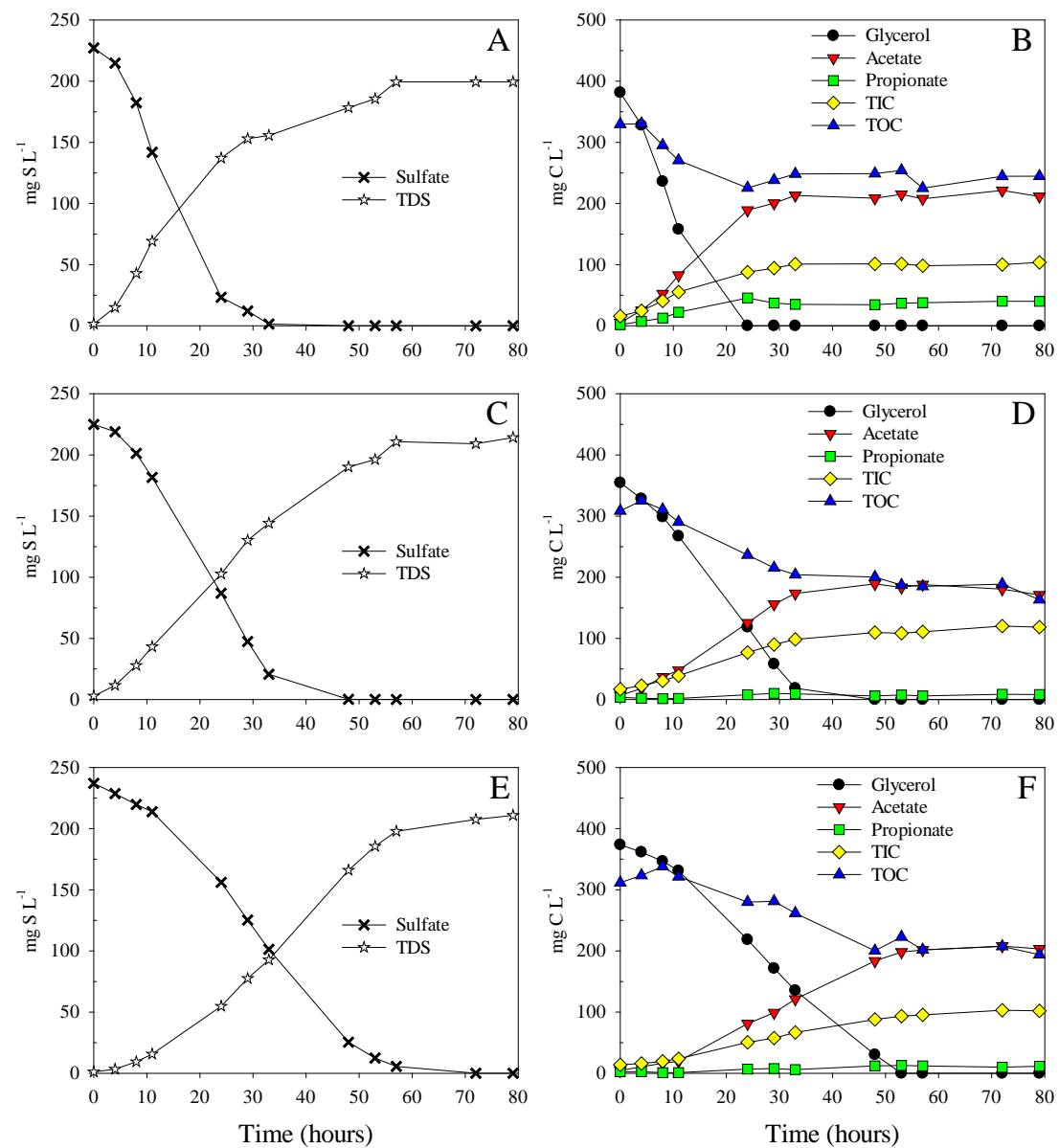


**Figure 5.7.** Activity tests of sludge from different heights of UASB reactor on day 198 feeding glycerol and sulfate. A, C and E show sulfur conversion of UASB1, UASB2 and UASB3, respectively; B, D and F show carbon species of UASB1, UASB2 and UASB3, respectively. TIC represents total inorganic carbon. TOC represents total organic carbon.

The comparison of the specific rates of inoculated sludge and the sludge from the different heights of UASB operating on days 169 and 198 is shown in Table 5.4. The specific consumption rate of glycerol of the inoculum sludge was the lowest. After the



microbial acclimation, the glycerol consumption rate of sludge in the reactor was significantly increased, especially in the bottom sludge (UASB1). Similar results were presented in the sulfate reduction rate. In the stratification analysis of section 4.3.2 in Chapter 4, the degradation of glycerol and sulfate reduction were mainly completed in the sludge of UASB1. In addition to the high concentration of the bottom sludge, the specific rate of the bottom sludge was highest with high biological activity of fermentation and sulfate reduction process.

**Table 5.4.** Specific rates of the inoculum sludge and sludge from UASB1, UASB2 and UASB3 on days 169 and 198 using glycerol as the carbon source.

Sample time	Sample	Time (hours)	Glycerol consumption rate (mg C h <sup>-1</sup> g VSS <sup>-1</sup> )	Sulfate reduction rate (mg S h <sup>-1</sup> g VSS <sup>-1</sup> )
0	Inoculum	10-72	4.7 ± 1.8	1.1 ± 0.7
169	UASB1	0-10	15.7 ± 0.8	7.8 ± 1.9
	UASB2	0-10	9.2 ± 1.5	5.7 ± 0.5
	UASB3	10-48	8.4 ± 1.8	5.6 ± 1.8
198	UASB1	4-11	20.1 ± 1.8	8.4 ± 2.4
	UASB2	8-33	9.2 ± 0.8	5.9 ± 0.5
	UASB3	8-53	9.6 ± 2.2	4.8 ± 1.9

Figure 5.8 shows the carbon compounds profile in the activity test using glycerol as the carbon source in the absence and presence of sulfate on day 198. In absence of sulfate, there was a gap between TOC and the sum of carbon (sum of glycerol and VFAs) at different heights of the reactor (Figure 5.8A, 5.8C and 5.8E). This indicates that glycerol was fermented to other intermediates different from VFAs that were not monitored. Previous studies mentioned that during anaerobic digestion, glycerol can be converted into ethanol, 1,3-propanediol, 1,2-propanediol, ethanol and 2,3-butanediol (Biebl et al., 1998; Clomburg and Gonzalez, 2013). Other products of glycerol fermentation contributed to the difference between TOC and sum of carbon in absence of sulfate. In the presence of sulfate, there was no difference between TOC and sum of carbon (Figure 5.8B, 5.8D and 5.8F),

indicating that other products of glycerol fermentation were used for sulfate reduction. It also shows that the consumption rate of intermediate products used by sulfate reduction was higher than the rate of glycerol degradation. Studies have reported that SRB were capable to degrade ethanol to acetate during the process of sulfate reduction (Wu et al., 2018). Therefore, in the subsequent investigation of the glycerol degradation (Chapter 6), other intermediate products such as ethanol and 1,3-propanediol were also monitored.

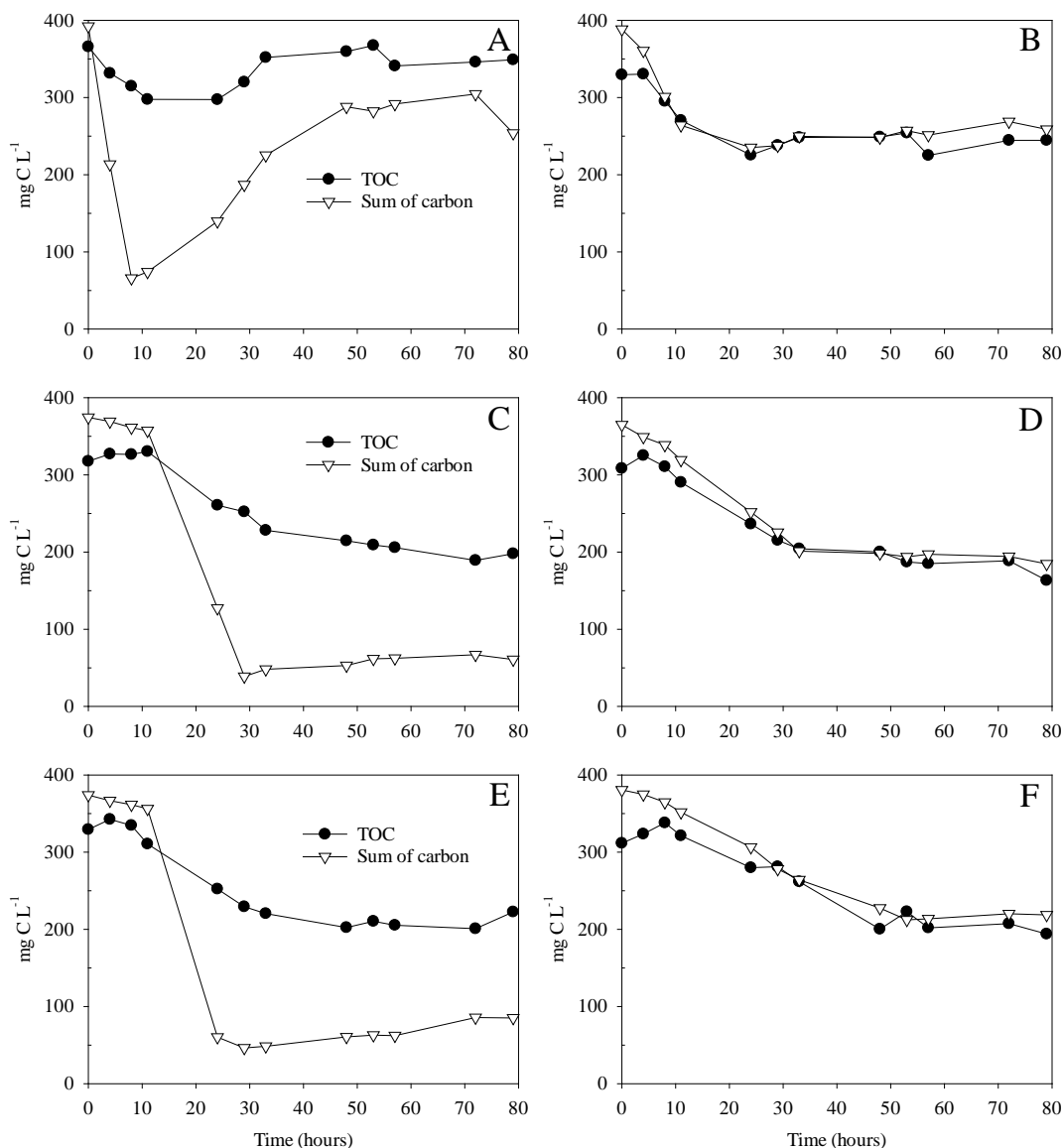


**Figure 5.8.** Activity tests of sludge from different heights of UASB reactor on day 198 using glycerol as the carbon source without sulfate (A, C and E) and with sulfate (B, D and F). A and B represent the sludge taken from UASB1; C and D represent the sludge taken from UASB2; E and F represent the sludge taken from UASB3. TOC represents total organic carbon. “Sum of carbon” represents sum of organic carbon, including glycerol and VFAs.

Microbial communities of biomass samples taken from different heights of the UASB were analyzed on day 230 (Figure 5.9). Due to flotation, sludge was extracted from UASB1, UASB4, UASB6, respectively. The relative abundances of *Methanosaeta* were only 0.1% at UASB1, 0.2% at UASB4 and 0.3% at UASB6. *Desulfovibrio* was still the most abundant genus found in different heights of the UASB reactor and did not show significant differences between the different sampling ports, 40.7% at UASB1, 36.2% at UASB4 and 36.1% at UASB6. *Propionispora* was the next genus with higher abundance, 13.9% at UASB1, 7.9% at UASB4 and 5.4% at UASB6. This indicated that SRB and fermentative microorganisms outcompeted methanogens on day 230. Microbial communities analyzed on day 230 may not be representative of the microbial populations found in day 198. However, the higher glycerol consumption rate on day 198 may be explained by the increase in fermentative microorganisms than on day 169.

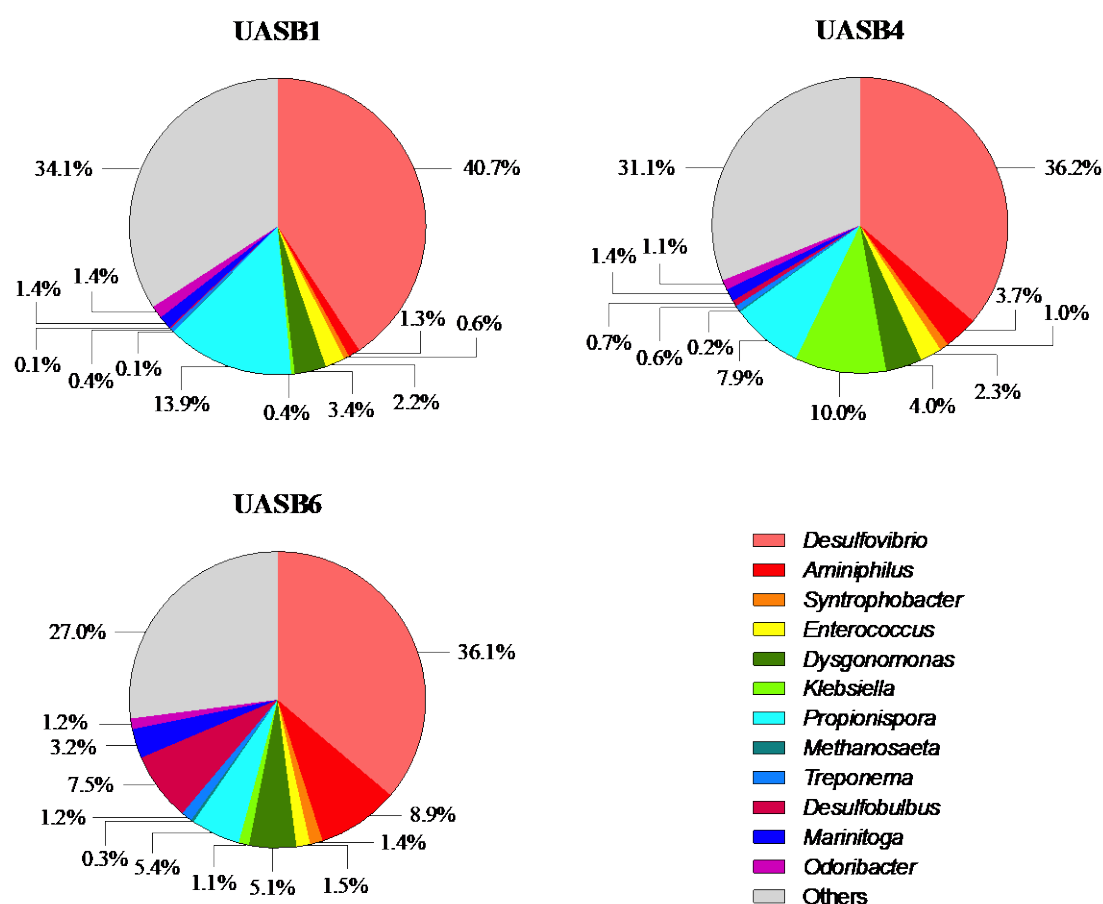


**Figure 5.9.** Microbial diversity of sludge at UASB1, UASB4 and UASB6 on day 230 (data adapted from Fernández Palacios, 2020).

Community shifts played a key role in the UASB performance for methane production. The relative abundance (%) of the detected methanogens in the inoculum sludge was 10.8%, including *Methanosaeta*, *Methanosarcina*, *Methanomicrobia* and *Methanobacteria*. *Methanosaeta*, with a relative abundance of 7.5%, was the most abundant group in the inoculum. Through microbial diversity dynamics analysis, methanogenic archaea first lost their competitiveness at the bottom of the sludge (UASB1 and UASB2) on day 173, because their relative abundances of *Methanosaeta* dropped to 1.2% in UASB1 and 0.8% in UASB2. And the relative abundance of *Methanosaeta* in UASB3 remained 4.1%. Other methanogens were not identified on day 173 at different heights of the reactor. On day 230, the relative abundances of *Methanosaeta* were around 0.2% in the UASB reactor. The microbial population confirmed that methanogenic archaea were almost washed out from the UASB reactor after 230 days of operation, which explained the acetate accumulation in the activity tests on day 198.

In the batch test fed with acetic acid as sole carbon source, acetoclastic methanogens in the inoculum sludge mainly converted acetate into methane for degradation (Figure 5.3). Since the rate of methane production was higher than the rate of acetate accumulation in the inoculum sludge, when glycerol was used as carbon source, there was almost no acetate accumulation (Figure 5.2). The high production of methane was due to the abundance of methanogens in the inoculum sludge.

In the test with biomass from day 169, comparing UASB1 and UASB2, the accumulation of acetate in the sludge from UASB3 was the minimum, indicating that the sludge from UASB3 produced more methane than UASB1 and UASB2, which was consistent with the microbial diversity results.

In the test with biomass from day 198, the accumulation of acetate in the sludge from UASB1, UASB2 and UASB3 was same and no acetate consumption was observed, indicating methanogens were washed out from the system. The washout of methanogens was confirmed by microbial diversity analysis on day 230.

Through activity tests and microbial diversity analysis, the relative abundances of methanogens had a negative correlation with acetate accumulation. The methanogens lose their competitiveness at the bottom of the sludge first (UASB1 and UASB2), and the methanogens were washed out of the reactor after 230 days of operation.

### **5.3.3 Specific activities of granular sludge and slime-like substances**

#### **5.3.3.1 Granular sludge (GS) and slime-covered granular sludge (SCGS)**

In order to study the SLS that accumulated in the reactor (as described in Chapter 4), characteristics of GS and SLS were investigated by activity batch tests to assess the influence of SLS on the mechanism of sulfate reduction. According to the above discussion, electron donors used in sulfate reduction were intermediate products of glycerol degradation, including acetate and propionate. Despite the fact that other carbon compounds produced as intermediates of glycerol fermentation were probably playing a role in sulfate reduction, they were not identified at the time of the study and only acetate and propionate were used as the electron donors in this batch test. Figure 5.10 shows the experimental profiles using acetate as carbon source, where the sludge collected from UASB1 on day 315 was divided into GS and SCGS. There was no change in acetate and sulfate in batch tests performed with GS and SCGS, which further confirmed that after 315 days of reactor operation, acetoclastic methanogens and acetotrophic SRB were suppressed.

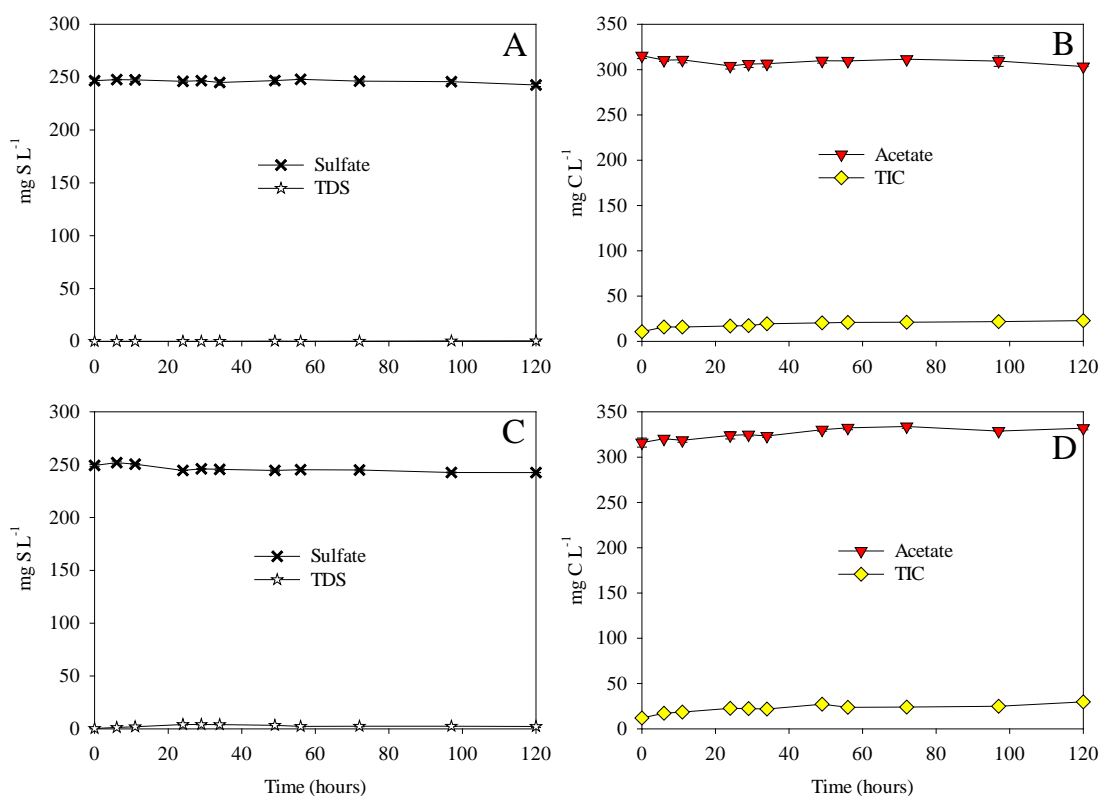


**Figure 5.10.** Activity tests of sludge obtained from UASB1 on day 315 feeding acetate and sulfate. A and B show sulfur species and carbon species using GS. C and D show sulfur species and carbon species using SCGS.

Figure 5.11 shows the time course of sulfate reduction measured with GS and SCGS using propionate as carbon source. GS and SCGS both reduced sulfate to sulfide, while acetate and inorganic carbon were produced. The specific rates of propionate consumption and sulfate reduction of GS and SCGS are shown in Table 5.5. The propionate consumption rate and sulfate reduction rate of GS were 1.68 and 1.66 times higher than those of SCGS.

When propionate was used as carbon source to reduce sulfate, SRB converted propionate to acetate and inorganic carbon. The mechanism of sulfate reduction with propionate observed herein is consistent with previous studies (Liamleam and Annachhatre, 2007; Muyzer and Stams, 2008). Since the same products were observed in the activity test performed with GS and SCGS using propionate to reduce sulfate as shown in Figure 5.11,

it can be concluded that SLS did not change the mechanism of sulfate reduction. However, the specific sulfate reduction rate (Table 5.5) was higher in the case of GS than in that of SCGS, indicating that the SLS may offer some mass transfer limitation of the substrates, resulting in a decrease of the specific sulfate reduction rate.

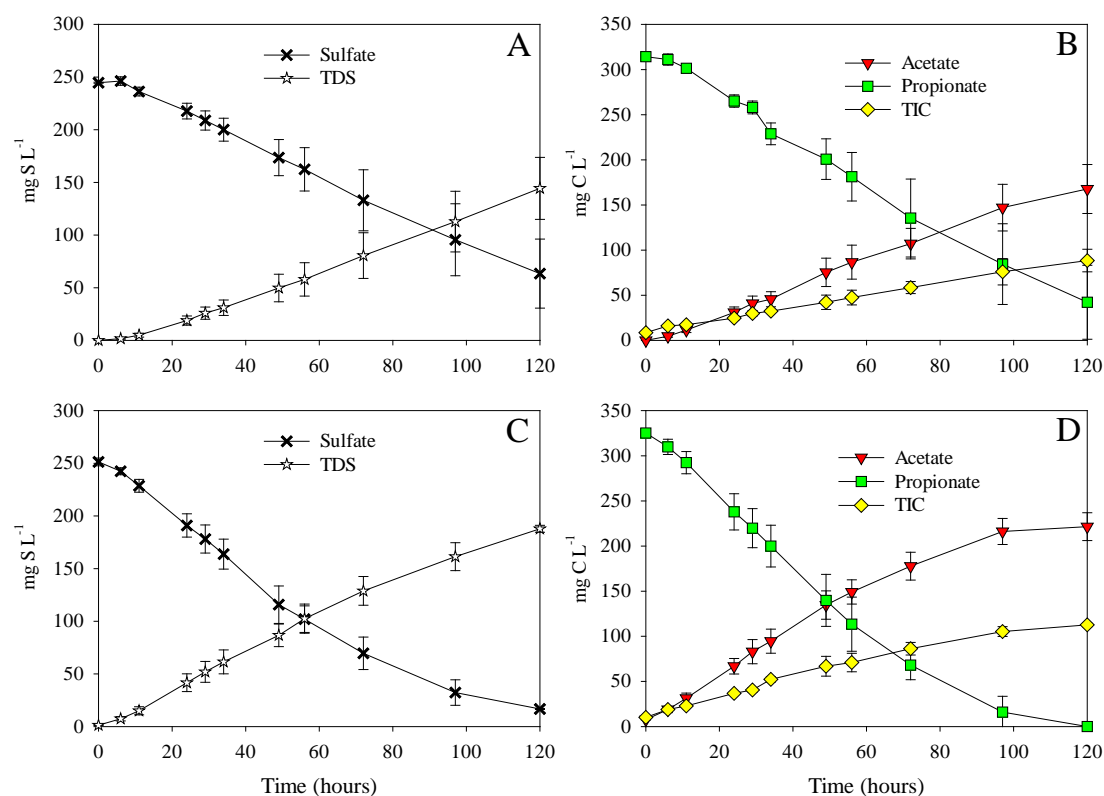


**Figure 5.11.** Activity tests of sludge obtained from UASB1 on day 315 feeding propionate and sulfate. A and B show sulfur species and carbon species using GS while C and D correspond to the SCGS batch test.

**Table 5.5.** Specific rates of the sludge collected from UASB1 on day 315 using propionate as the carbon source.

Sample	Time (hours)	Propionate consumption rate (mg C h <sup>-1</sup> g VSS <sup>-1</sup> )	Sulfate reduction rate (mg S h <sup>-1</sup> g VSS <sup>-1</sup> )
GS	6-120	6.9 ± 1.3	4.8 ± 0.6
SCGS	6-97	4.1 ± 0.8	2.9 ± 0.7

### 5.3.3.2 Activity tests with granular sludge or slime-like substances

In order to analyze the difference between GS and SLS and assess the influence of SLS on the process of glycerol fermentation, sludge from the UASB reactor on day 431 was manipulated (washed with sulfate-free MM, as described in section 5.2.1) to obtain GS and SLS for further batch tests.

Based on the C imbalance found in the batch tests of the experiments in Figure 5.8, other C compounds were monitored. Glycerol fermentation has been shown to produce also ethanol, n-butanol, 1,3-propanediol, 2,3-butanediol, formate (Viana et al., 2012). Consequently, these compounds were also monitored in the activity test reported herein.

Figure 5.12 shows the specific activity test using glycerol as the carbon source. GS reduced sulfate throughout the cultivation period (Figure 5.12A), while SLS started to reduce sulfate after 24 h (Figure 5.12C). This indicates that the SLS is able to reduce sulfate after an adaptation period. Glycerol was fermented both by GS and SLS, while ethanol, 1,3-propanediol, formate, acetate and propionate accumulated. In the experiment with GS, after glycerol had been degraded completely, ethanol, 1,3-propanediol, formate and propionate were consumed from 24 h to 72 h (Figure 5.12B), accompanied by sulfate reduction (Figure 5.12A). Acetate and inorganic carbon were accumulated throughout the test (Figure 5.12B). However, in the experiment with SLS, ethanol and formate were degraded after 24 h (Figure 5.12D) and 1,3-propanediol was consumed after 48 h. From Figure 5.12B and 5.12D, it can be seen that, again, sulfate reduction was not related to glycerol fermentation. Sulfate was reduced accompanied by the degradation of formate, ethanol and 1,3-propanediol. This confirmed that the carbon sources used for sulfate reduction were intermediate products of glycerol degradation, such as formate, ethanol and 1,3-propanediol. Due to the complexity of this results, the mechanism of sulfate reduction using glycerol as the carbon source will be further discussed in Chapter 6.



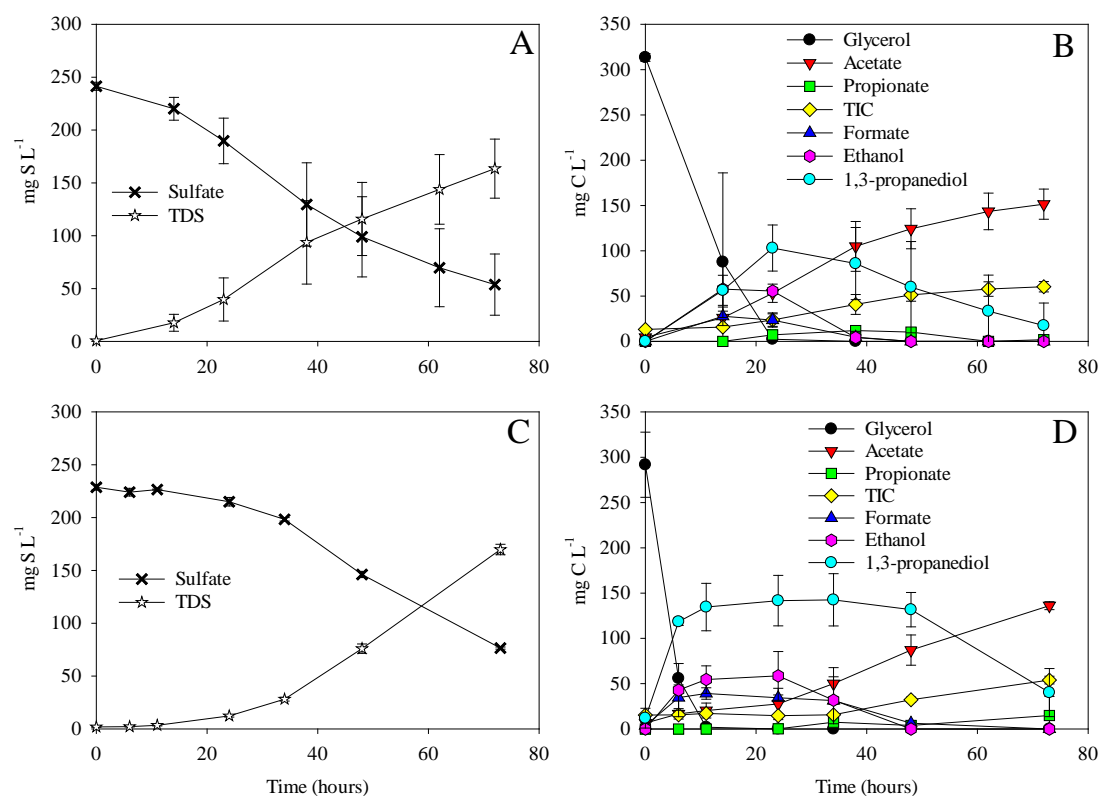


**Figure 5.12.** Activity tests of sludge obtained from UASB6 on day 431 feeding glycerol and sulfate. A and B show sulfur species and carbon species using GS. C and D used SLS.

Table 5.6 shows the specific rates calculated for glycerol consumption and sulfate reduction using GS and SLS where biomass was taken on day 431. During the degradation of glycerol, the glycerol consumption rate of SLS was 2.1 times that of GS. Without considering the adaptation period of SLS for sulfate reduction, the sulfate reduction rate of GS was 1.2 times higher than that of SLS when the carbon source required for sulfate reduction was sufficient.

**Table 5.6.** Specific rates of the sludge collected from UASB6 on day 431.

Carbon source	Sample	Time (hours)	Glycerol consumption rate (mg C h <sup>-1</sup> g VSS <sup>-1</sup> )	Sulfate reduction rate (mg S h <sup>-1</sup> g VSS <sup>-1</sup> )
Glycerol	GS	0-23	33.1 ± 12.2	6.3 ± 3.4
		23-62	0	9.1 ± 1.7
	SLS	0-11	70.1 ± 8.0	0.5 ± 0.5
		24-73	0	7.3 ± 2.7

In the activity tests performed with GS and SLS with glycerol as the carbon source to reduce sulfate, both GS and SLS fermented glycerol into formate, acetate, propionate, ethanol, 1,3-propanediol and inorganic carbon. In addition, the intermediate products of glycerol were consumed with sulfate reduction observed. This indicates that SLS is also capable of fermenting glycerol and reducing sulfate. When comparing the specific rates of glycerol fermentation between GS and SLS, SLS was more efficient in degrading glycerol than GS. The specific substrate utilization activity of GS and flocculant sludge was compared in UASB reactors processing wastewater from food industries (Oleszkiewicz and Romanek, 1989). They found that the flocculant sludge formed during the operation of UASB reactor had a higher specific activity for the degradation of complex polymers than the GS in anaerobic processes, which is similar to the results of this work.

Filamentous and fluffy flocculant material were also produced in the UASB reactor under anaerobic conditions to treat sulfate (Vallero et al., 2003; Weijma et al., 2000). Valero et al. (2003) and Weijma et al. (2000) described the flotation caused by flocculant material but did not mention the biological activity of these materials. This work investigated the activity experiment of SLS. When comparing the specific rates of sulfate reduction between GS and SLS, SLS was found to be less efficient in reducing sulfate than GS. In addition, as can be seen in Figure 5.12D, even if there was sufficient carbon source to reduce sulfate, SLS still needed time to adapt and perform the sulfate reduction process, which may be caused by mass transfer limitation of sulfate. Compared with GS in the UASB reactor, GS covered by SLS may cause sulfate to be discharged from the UASB

reactor before entering the cell due to mass transfer limitation, which may lead to a decrease in the sulfate reduction efficiency. Therefore, it can be explained here that in addition to biomass washout from the UASB reactor, the reason for the reduced sulfate removal efficiency in the UASB reactor may also be that the SLS affected the mass transfer limitation of sulfate. But the degradation process of glycerol was not affected by SLS, and the slime even accelerated glycerol fermentation rate.

The difference of specific rates between GS and SLS may also cause by the bacteria community diversity. 16S rRNA sequencing was performed to identify the biodiversity of GS and SLS by sampling the reactor on day 538 from UASB6 (Figure 5.13). *Propionispora* and *Dysgonomonas* were the most abundant genus detected on day 538 in both samples. The relative abundance of genus *Propionispora* increased from 15.2% to 21.5% in GS and SS, respectively. Moreover, *Enterobacter*, *Klebsiella* and *Helicobacter* genera increased their relative abundances in SS and GS, from 2.2% to 8.2%; from 2.1% to 8.5% and lastly from 0.3% to 6.3%, respectively. *Propionispora* is a genus of anaerobes, typically degrading organic carbon compounds in acidogenesis not acetogenesis. *Enterobacter* and *Klebsiella*, facultative anaerobes, are able to produce hydrogen and acetate through the fermentation of organic substrates (Hung et al., 2011; Joubert and Britz, 1987). *Helicobacter* is considered to be a microaerophile, which are capable of oxidizing variety of organic acids, such as formate, lactate, succinate and pyruvate (Joubert and Britz, 1987). The genus of these fermentative microorganisms is consistent with the glycerol fermentation rates in SS and GS.

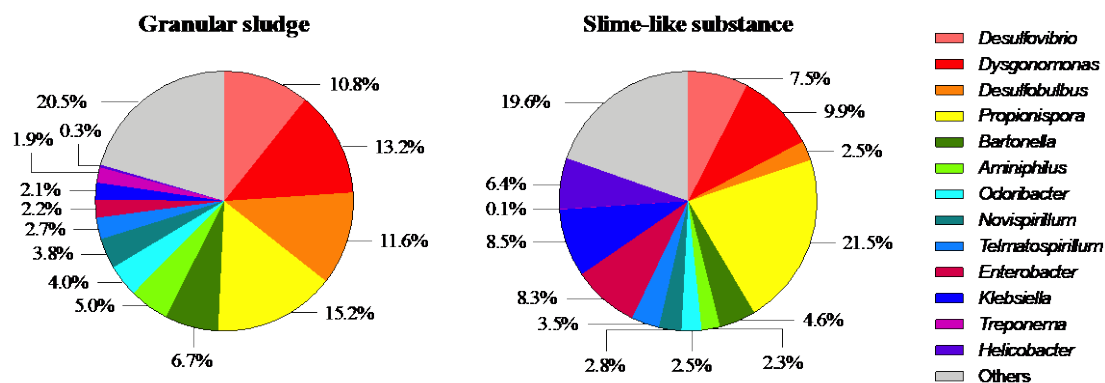


**Figure 5.13.** Microbial diversity of the most abundant genus detected in granular sludge and slime-like substance on day 538 (data adapted from Fernández Palacios, 2020).

*Desulfobulbus* decreased its relative abundances in the SLS compared to GS from 11.6% to 2.4% respectively, while *Desulfovibrio* decreased from 10.8% to 7.5%. *Desulfovibrio* is a genus of SRB, which oxidize organic carbon compounds (includes formate, lactate, ethanol, malate, pyruvate, succinate) to acetate for sulfate reduction (Odom and Peck, 1981; Qatibi et al., 1991c; Wu et al., 2018). *Desulfobulbus*, can oxidize pyruvate, propionate and ethanol to acetate (Bak and Pfennig, 1991; Bertolino et al., 2012; Muyzer and Stams, 2008; Zeng et al., 2019). The main sulfate reducers found were *Desulfobulbus* and *Desulfovibrio*, both of which are incomplete oxidizing SRB, which explains the accumulation of acetate in the batch activity tests. Compared to SS, higher relative abundances of *Desulfobulbus* and *Desulfovibrio* in GS are in agreement with the higher sulfate reduction rate found in GS.

Through batch activity tests of GS and SLS, GS played a more important role in sulfate reduction than SLS. The latter may affect the mass transfer limitation of sulfate, which might be one reason for the decrease of sulfate removal efficiency during the UASB operation. 16s rRNA gene analysis of the microbial communities revealed that compared to SS, GS contained more sulfate reducers (mainly *Desulfobulbus* and *Desulfovibrio*). In terms of fermentation process, glycerol fermentation was not affected by SS. Conversely, the fermentation rate of glycerol in SS was higher than that of GS. The analysis of microbial diversity revealed that high relative abundances of fermentative microorganisms

was identified in SS. This shows that the reason for the decrease of the glycerol removal efficiency in UASB reactor was not related to the degradation mechanism of glycerol by the SLS, but because the SLS triggered the reduction of biomass in the UASB reactor, as discussed in Chapter 4.

## 5.4 Conclusion

Inoculated sludge activity tests showed that glycerol can be used as a raw carbon source for sulfate reduction even though the products of glycerol degradation are the key electron donors used by sulfate-reducing bacteria to achieve the process of sulfate reduction. Compared with other VFAs, inoculated sludge using propionate had the fastest specific rate among the electron donors for sulfate reduction. Acetate was oxidized for methane production.

Stratification activity tests showed that UASB1 (bottom sludge) had a higher fermentation rate due to long-term exposure to glycerol, and the competition between methanogens and SRB led to bottom-up removal of methanogens. Methanogens mainly existed in UASB3 on day 173 and were washed out after 230 days of reactor operation. Compared to UASB2 and UASB3, more relatively abundant fermentative microorganisms were observed in UASB1. SRB did not show a significant difference in the stratification, and *Desulfovibrio* was the most abundant genus found in the UASB reactor. The higher sulfate reduction rate at the bottom was due to the faster fermentation rate that produced more electron donors for sulfate reduction.

The activity tests of GS, SLS and SCGS showed that SLS had fermenting and sulfate reducing capacity. The SLS required a longer adaptation period to reduce sulfate, which may be due to the mass transfer limitation of sulfate caused by SLS. Moreover, the SLS contained more fermentative microorganisms with higher fermenting rates, and higher relative abundances of the genus of SRB in GS was with higher sulfate reduction rate.

## Chapter 6

---

# Assessing main process mechanism and rates of sulfate reduction by granular biomass fed with glycerol under sulfidogenic conditions

**A modified version of this chapter has been published:**

Zhou, X., Fernández-Palacios, E., Dorado, A., Gamisans, X., Gabriel, D., 2022. Assessing main process mechanism and rates of sulfate reduction by granular biomass fed with glycerol under sulfidogenic conditions. *Chemosphere*, 131649. <https://doi.org/10.1016/J.CHEMOSPHERE.2021.131649>



Since the dispute described in the sulfate reduction pathway using glycerol as a carbon source in previous studies, the motivation of this chapter is to determine the main mechanisms and the process rates of glycerol fermentation under sulfidogenic conditions. In this case, this study was conducted with and without sulfate in activity tests using a range of electron donor including glycerol, ethanol, 1,3-propanediol, butanol, 2,3-butanediol and volatile fatty acids (VFAs).

## Abstract

Sulfate-reducing bioreactors for sulfide production are the initial stage of processes targeting elemental sulfur recovery from sulfate-rich effluents. In this chapter, the principal reactions involved in glycerol fermentation and sulfate reduction using glycerol and its fermentation products as electron donors were assessed together with their specific consumption/production rates. A battery of batch activity tests with and without sulfate were performed with glycerol and with each fermentation product using a non-methanogenic but sulfidogenic GS from an up-flow anaerobic sludge blanket (UASB) reactor operated under long-term while fed with crude glycerol. As a result, a mechanistic approach based on the experimental observations is proposed in this work. Glycerol was mainly fermented to 1,3-propanediol, ethanol, formate, propionate and acetate by fermentative bacteria. All organic intermediates were found to be further used by sulfate reducing bacteria (SRB) for sulfate reduction except for acetate. The most abundant genus detected under sulfidogenic conditions were *Propionispora* (15.2%), *Dysgonomonas* (13.2%), *Desulfobulbus* (11.6%) and *Desulfovibrio* (10.8%). The last two SRB accounted for 22.4% of the total amount of retrieved sequences, which were probably performing an incomplete oxidation of the carbon source in the sulfidogenic UASB reactor. As single substrates, specific sulfate reduction rates (SRRs) using low molecular weight (MW) carbon sources (formate and ethanol) were 39% higher than those using high-MW ones (propionate, 1,3-propanediol and butanol). However, SRRs in glycerol-fed tests showed that 1,3-propanediol played a major role in sulfate reduction in addition to formate and



Assessing main process mechanism and rates of sulfate reduction by granular biomass fed with glycerol under sulfidogenic conditions

---

ethanol.

## 6.1 Introduction

Sulfate is an anion widely present in natural environments. However, high concentration of sulfate can be toxic to aquatic life (Karjalainen et al., 2021). In aquatic environments, sulfate can be also reduced to hydrogen sulfide by sulfate-reducing bacteria (SRB) under anaerobic conditions generating further problems since hydrogen sulfide is poisonous and corrosive. Many industrial sites including pulp and paper and mining industries, tanneries, fermenting plants and thermal power plants generate flue gases or wastewaters containing large amounts of sulfur, mainly as sulfate, that require further treatment. As an alternative to costly physical-chemical technologies, environmentally friendly, biological processes arose recently, some considering the valorization of S-rich emissions into elemental sulfur (biosulfur) (Mora et al. 2020a), a value-added product currently obtained from the petrochemical industry. Since microbial communities able to reduce sulfate directly to biosulfur have not been described yet, one biological-based alternative relies on a two-stage process (Mora et al., 2020a). First, sulfate is reduced to sulfide in an up-flow anaerobic sludge blanket (UASB) bioreactor, and subsequently, sulfide is partially oxidized to elemental sulfur in a second bioreactor under microaerobic or anoxic conditions. The technical feasibility of biosulfur recovery in a two-stage bioscrubber has been demonstrated previously in the SONOVA process (Mora et al., 2020a) despite some operational problems in the long-term leading to biomass losses in the anaerobic stage (Fernández-Palacios et al., 2021). However, further fundamental analysis is warranted to reveal the underlying mechanisms in the UASB to develop a more robust, transferable technology to field applications.

UASB reactors are widely used in anaerobic digestion and have also been reported as an appropriate technology for sulfate reduction using different carbon sources, including methanol (Weijma and Stams, 2001), ethanol (Wu et al., 2018), sucrose (Weijma and Stams, 2001) and crude glycerol (Fernández-Palacios et al., 2019). As an alternative to other expensive electron donors, crude glycerol is a by-product mainly produced in the biodiesel

production industry with a high market potential. It was estimated that world glycerol production would reach 2.66 million tons in 2020 (Kumar et al., 2019). The composition of crude glycerol varies depending on the process, containing around 70% to 98% of glycerol plus some impurities including water, long-chain fatty acids, fatty acid methyl esters, salts, methanol, soap and ashes (Angeloni et al., 2016; Viana et al., 2012; Vivek et al., 2017).

Previous studies have reported that glycerol as electron donor can be directly oxidized to acetate and bicarbonate in the sulfate reduction process (Bertolino et al., 2014; Dinkel et al., 2010; Qatibi et al., 1991a). However, the TOC imbalance found in these works was suggested to be caused by other intermediate products. Several studies have shown that other products are produced when glycerol is used as electron donor to reduce sulfate. As examples, 3-hydroxypropionate (Qatibi et al., 1998) and butyrate (Bertolino et al., 2014) were produced in glycerol fermentation coupled to sulfate reduction. It was also found that glycerol was incompletely oxidized to acetate, lactate and 1,3-propanediol under low pH conditions (Santos et al., 2018). However, the mechanism of the sulfate reduction process, which is also culture dependent, is still unclear as most of literature have only shown the oxidized products of glycerol during this process.

The purpose of this work was to assess the main mechanism and the process rates of glycerol fermentation and sulfate reduction of a sulfidogenic granular sludge enriched in an UASB fed with crude glycerol under long-term operating conditions without methane production. To this aim, microbial activity was assessed in batch tests with a range of electron donors including glycerol, alcohols and volatile fatty acids (VFAs) with and without the presence of sulfate.

## **6.2 Materials and methods**

### **6.2.1 Batch activity tests**

In order to identify the main mechanisms of the granular sludge using glycerol as electron donor to reduce sulfate in the sulfidogenic UASB, granular sludge was taken from the UASB after 431, 549 and 578 days of operation, when no methane was produced. The

sludge withdrawn from the UASB on different days was tested with different carbon sources. Pure glycerol, ethanol, 1,3-propanediol, butanol and 2,3-butanediol were tested for the sludge collected on day 431. Formate was tested with the sludge collected on day 549, while acetate and propionate were tested with the sludge collected on day 578. Sludge samples were first rinsed with MM (without sulfate) and then transferred into 250 mL serum bottles, which were afterwards fed with 150 mL of MM that was used to feed the UASB. In all cases, a control group without sulfate and an experimental group were evaluated. The control group consisted of MM (without sulfate) supplied with different carbon sources only, while in the experimental group sulfate was added to the MM and the carbon source. The initial carbon concentration ranged from 318 to 372 mg C L<sup>-1</sup> in both the control and the experimental groups. The initial sulfate concentration of the experimental group was set to  $240 \pm 4$  mg S-SO<sub>4</sub><sup>2-</sup> L<sup>-1</sup>, and the TOC/S-SO<sub>4</sub><sup>2-</sup> ratio was  $1.4 \pm 0.1$  g C/g S-SO<sub>4</sub><sup>2-</sup>. After adding MM and the granular sludge, the pH was adjusted to 8 - 8.5 by adding either 2 M NaOH or 2 M HCl. The pH was not controlled during activity tests, but it was measured at the beginning and at the end of each test. The gas phase was exchanged with N<sub>2</sub> and bottles were instantly capped with rubber stoppers and aluminum caps. Bottles were cultivated in a shaker at a constant temperature of  $35 \pm 1^\circ$  C and a stirring rate of 150 rpm. The incubation time was between 96 h and 120 h depending on the test. Volatile suspended solids (VSS) in batch tests were obtained at the end of each experiment and ranged from 125 to 390 mg VSS L<sup>-1</sup>. All batch tests were carried out with two replicates.

### **6.2.2 Analytical methods**

The analysis of the liquid and gas phase is described in section 3.3 of Chapter 3.

### **6.2.3 Illumina sequencing analysis**

Identification of the microbial population was performed using Illumina platform, on day 538 of the long-term operation. Sequencing analysis method is introduced in Chapter 3 section 3.3.6.

#### **6.2.4 Stoichiometric calculation for the sulfate reducing process by glycerol**

From the batch tests, the contribution of each electron donor to sulfate reduction was calculated based on i) the specific net rates observed experimentally for each compound in each selected period, ii) the stoichiometric conversions, and iii) the mechanism of glycerol fermentation and sulfate reduction. As a result, a set of 11 reactions were established, while a total of 9 algebraic equations were solved. As an example, the observed glycerol consumption rate is equal to the sum of reactions  $r_1$  to  $r_4$  to form formate, acetate, propionate, ethanol and 1,3-propanediol while the observed rate for ethanol is that corresponding to its production from glycerol hydrolysis ( $r_4$ ) and its consumption to produce acetate linked to sulfate reduction ( $r_9$ ). The larger number of equations than measured variables allowed estimating the contribution of each electron donor to the overall SRR in each experimental period. Since hydrogen is the product of formate fermentation, the calculation of sulfate reduction by hydrogen is included in sulfate reduction by formate. During the period of glycerol degradation (10 to 33 h), the rate at which each substance was used for sulfate reduction cannot be calculated because there are more variables than algebraic equations established.

The fermentation and sulfidogenic reactions involved in anaerobic digestion is summarized in Table 6.1.

**Table 6.1.** Fermentation and sulfidogenic reactions involved in anaerobic digestion.

Stoichiometric equation	Eq.	Reference
<b>Fermentation reaction</b>		
$C_3H_8O_3(\text{glycerol}) + H_2O + 2NAD^+ \rightarrow C_2H_4O_2(\text{acetic acid}) + HCOOH + 2NADH + 2H^+$	6.1	Zeng et al., 1993
$C_3H_8O_3(\text{glycerol}) \rightarrow C_3H_6O_2(\text{propionic acid}) + H_2O$	6.2	Schauder and Schink, 1989
$C_3H_8O_3(\text{glycerol}) + NADH + H^+ \rightarrow C_3H_8O_2(1,3\text{-propanediol}) + NAD^+ + H_2O$	6.3	Sittijunda and Reungsang, 2017
$C_3H_8O_3(\text{glycerol}) + NAD^+ \rightarrow C_2H_6O(\text{ethanol}) + HCOOH + NADH + H^+$	6.4	Sittijunda and Reungsang, 2017
$HCOOH \rightarrow CO_2 + H_2$	6.5	Bijmans et al., 2008
<b>Sulfidogenic reaction</b>		
$4H_2 + SO_4^{2-} + H^+ \rightarrow HS^- + 4H_2O$	6.6	Muyzer and Stams, 2008
$4HCOO^- + SO_4^{2-} + H^+ \rightarrow HS^- + 4HCO_3^-$	6.7	Liamleam and Annachatre, 2007
$C_3H_5O_2^-(\text{propionate}) + 0.75SO_4^{2-} \rightarrow C_2H_3O_2^-(\text{acetate}) + HCO_3^- + 0.75HS^- + 0.25H^+$	6.8	Luis, 2018
$C_2H_6O(\text{ethanol}) + 0.5SO_4^{2-} \rightarrow 0.5HS^- + C_2H_3O_2^-(\text{acetate}) + H_2O + 0.5H^+$	6.9	Wu et al., 2018
$C_3H_8O_2(1,3\text{-propanediol}) + SO_4^{2-} \rightarrow C_2H_3O_2^-(\text{acetate}) + HS^- + HCO_3^- + H_2O + H^+$	6.10	Qatibi et al., 1991b
$C_3H_8O_2 + SO_4^{2-} + 3NADH + 3H^+ \rightarrow C_3H_5O_2^- + HS^- + 4H_2O + 3NAD^+$	6.11	In this work

According to all equations mentioned above, the stoichiometric formulas between substrates and products are shown as follows:

$$r_1' = \frac{2}{3}r_1, \text{ and } r_1'' = \frac{1}{3}r_1 \quad \text{Eq.6.12}$$

Where  $r_1$  is glycerol degradation rate based on Eq.6.1 (mg C-glycerol  $\text{h}^{-1}$  g VSS $^{-1}$ ),  $r_1'$  is the stoichiometric production rate estimated for acetate in Eq.6.1 (mg C-acetate  $\text{h}^{-1}$  g VSS $^{-1}$ ) and  $r_1''$  is the stoichiometric production rate estimated for formate in Eq.6.1 (mg C-formate  $\text{h}^{-1}$  g VSS $^{-1}$ ).

$$r_2' = r_2 \quad \text{Eq.6.13}$$

Where  $r_2$  is glycerol degradation rate based on Eq.6.2 (mg C-glycerol  $\text{h}^{-1}$  g VSS $^{-1}$ ), and  $r_2'$  is the stoichiometric production rate estimated for propionate in Eq.6.2 (mg C-propionate  $\text{h}^{-1}$  g VSS $^{-1}$ ).

$$r_3' = r_3 \quad \text{Eq.6.14}$$

Where  $r_3$  is glycerol degradation rate based on Eq.6.3 (mg C-glycerol  $\text{h}^{-1}$  g VSS $^{-1}$ ), and  $r_3'$  is the stoichiometric production rate estimated for 1,3-propanediol in Eq.6.3 (mg C-1,3-propanediol  $\text{h}^{-1}$  g VSS $^{-1}$ ).

$$r_4' = \frac{2}{3}r_4, \text{ and } r_4'' = \frac{1}{3}r_4 \quad \text{Eq.6.15}$$

Where  $r_4$  is glycerol degradation rate based on Eq.6.4 (mg C-glycerol  $\text{h}^{-1}$  g VSS $^{-1}$ ),  $r_4'$  is the stoichiometric production rate estimated for ethanol in Eq.6.4 (mg C-ethanol  $\text{h}^{-1}$  g VSS $^{-1}$ ), and  $r_4''$  is the stoichiometric production rate estimated for formate in Eq.6.4 (mg C-formate  $\text{h}^{-1}$  g VSS $^{-1}$ ).

$$r_5' = r_5, \text{ and } r_5'' = \frac{1}{6}r_5 \quad \text{Eq.6.16}$$

Where  $r_5$  is formate degradation rate based on Eq.6.5 (mg C-formate  $\text{h}^{-1}$  g VSS $^{-1}$ ),  $r_5'$  is the stoichiometric production rate estimated for IC in Eq.6.5 (mg C  $\text{h}^{-1}$  g VSS $^{-1}$ ), and  $r_5''$  is the stoichiometric production rate estimated for H $_2$  in Eq.6.5 (mg H $_2$   $\text{h}^{-1}$  g VSS $^{-1}$ ).

$$r_6' = 4r_6 \quad \text{Eq.6.17}$$

Where  $r_6$  is H $_2$  consumption rate based on Eq.6.6 (mg H $_2$   $\text{h}^{-1}$  g VSS $^{-1}$ ), and  $r_6'$  is the

stoichiometric consumption rate estimated for sulfate in Eq.6.6 (mg S-sulfate h<sup>-1</sup> g VSS<sup>-1</sup>).

$$r_7' = \frac{2}{3}r_7, \text{ and } r_7'' = r_7 \quad \text{Eq.6.18}$$

Where  $r_7$  is formate consumption rate based on Eq.6.7 (mg C-formate h<sup>-1</sup> g VSS<sup>-1</sup>),  $r_7'$  is the stoichiometric consumption rate estimated for sulfate in Eq.6.7 (mg S-sulfate h<sup>-1</sup> g VSS<sup>-1</sup>), and  $r_7''$  is the stoichiometric production rate estimated for IC in Eq.6.7 (mg C h<sup>-1</sup> g VSS<sup>-1</sup>).

$$r_8' = \frac{2}{3}r_8, r_8'' = \frac{2}{3}r_8, \text{ and } r_8''' = \frac{1}{3}r_8 \quad \text{Eq.6.19}$$

Where  $r_8$  is propionate consumption rate based on Eq.6.8 (mg C-propionate h<sup>-1</sup> g VSS<sup>-1</sup>),  $r_8'$  is the stoichiometric consumption rate estimated for sulfate in Eq.6.8 (mg S-SO<sub>4</sub><sup>2-</sup> h<sup>-1</sup> g VSS<sup>-1</sup>),  $r_8''$  is the stoichiometric production rate estimated for acetate in Eq.6.8 (mg C-acetate h<sup>-1</sup> g VSS<sup>-1</sup>), and  $r_8'''$  is the stoichiometric production rate estimated for IC in Eq.6.8 mg C h<sup>-1</sup> g VSS<sup>-1</sup>).

$$r_9' = \frac{2}{3}r_9, \text{ and } r_9'' = r_9 \quad \text{Eq.6.20}$$

Where  $r_9$  is ethanol consumption rate based on Eq.6.9 (mg C-ethanol h<sup>-1</sup> g VSS<sup>-1</sup>),  $r_9'$  is the stoichiometric consumption rate estimated for sulfate in Eq.6.9 (mg S- SO<sub>4</sub><sup>2-</sup> h<sup>-1</sup> g VSS<sup>-1</sup>), and  $r_9''$  is the stoichiometric production rate estimated for acetate in Eq.6.9 (mg C-acetate h<sup>-1</sup> g VSS<sup>-1</sup>).

$$r_{10}' = \frac{8}{9}r_{10}, r_{10}'' = \frac{2}{3}r_{10}, \text{ and } r_{10}''' = \frac{1}{3}r_{10} \quad \text{Eq.6.21}$$

Where  $r_{10}$  is 1,3-propanediol consumption rate based on Eq.6.10 (mg C-1,3-propanediol h<sup>-1</sup> g VSS<sup>-1</sup>),  $r_{10}'$  is the stoichiometric consumption rate estimated for sulfate in Eq.6.10 (mg S- SO<sub>4</sub><sup>2-</sup> h<sup>-1</sup> g VSS<sup>-1</sup>),  $r_{10}''$  is the stoichiometric production rate estimated for acetate in Eq.6.10 (mg C-acetate h<sup>-1</sup> g VSS<sup>-1</sup>), and  $r_{10}'''$  is the stoichiometric production rate estimated for IC in Eq.6.10 (mg C h<sup>-1</sup> g VSS<sup>-1</sup>).

$$r_{11}' = \frac{8}{9}r_{11}, \text{ and } r_{11}'' = r_{11} \quad \text{Eq.6.22}$$

Where  $r_{11}$  is 1,3-propanediol consumption rate based on Eq.6.11 (mg C-1,3-propanediol h<sup>-1</sup> g VSS<sup>-1</sup>),  $r_{11}'$  is the stoichiometric consumption rate estimated for sulfate in Eq.6.11 (mg S- SO<sub>4</sub><sup>2-</sup> h<sup>-1</sup> g VSS<sup>-1</sup>),  $r_{11}''$  is the stoichiometric production rate



estimated for propionate in Eq.6.11 mg C-propionate h<sup>-1</sup> g VSS<sup>-1</sup>).

According to the stoichiometric formulas mentioned above and the mechanism of glycerol fermentation and sulfate reduction, the algebraic equations were established as follows:

$$r_{\text{glycerol}} = r_1 + r_2 + r_3 + r_4 \quad \text{Eq.6.23}$$

$$r_{\text{acetate}} = r_1' + r_8'' + r_9'' + r_{10}'' = \frac{2}{3}r_1 + \frac{2}{3}r_8 + r_9 + \frac{2}{3}r_{10} \quad \text{Eq.6.24}$$

$$r_{\text{propionate}} = r_2' + r_{11}'' - r_8 = r_2 + r_{11} - r_8 \quad \text{Eq.6.25}$$

$$r_{\text{formate}} = r_1'' + r_4'' - r_5 - r_7 = \frac{1}{3}r_1 + \frac{1}{3}r_4 - r_5 - r_7 \quad \text{Eq.6.26}$$

$$r_{\text{1,3-Propanediol}} = r_3' - r_{10} - r_{11} = r_3 - r_{10} - r_{11} \quad \text{Eq.6.27}$$

$$r_{\text{ethanol}} = r_4' - r_9 = \frac{2}{3}r_4 - r_9 \quad \text{Eq.6.28}$$

$$r_{\text{CO}_2} = r_5' + r_7'' + r_8''' + r_{10}''' = r_5 + r_7 + \frac{1}{3}r_8 + \frac{1}{3}r_{10} \quad \text{Eq.6.29}$$

$$r_{\text{SO}_4^{2-}} = r_6' + r_7' + r_8' + r_9' + r_{10}' + r_{11}' = 4r_6 + \frac{2}{3}r_7 + \frac{2}{3}r_8 + \frac{2}{3}r_9 + \frac{8}{9}r_{10} + \frac{8}{9}r_{11} \quad \text{Eq.6.30}$$

$$r_{\text{H}_2} = r_5'' = \frac{1}{6}r_5 \quad \text{Eq.6.31}$$

Where the variables in the left side of the algebraic equations mean experimental rate for each compound conversion. For instance,  $r_{\text{glycerol}}$  is experimental consumption rate of glycerol and  $r_{\text{acetate}}$  is experimental production rate of acetate.

## 6.3 Results and discussion

### 6.3.1 Activity tests with glycerol as sole external carbon source

Long-term operation of the UASB reactor was performed under constant sulfate and organic loading rates for 639 days. The experimental results and discussion of the UASB performance and the evolution of the microbial diversity can be found in Chapter 4. In short, after operating the UASB reactor for 200 days, methane production decreased significantly concomitantly with VFAs production. At a TOC/S-SO<sub>4</sub><sup>2-</sup> ratio of  $1.49 \pm 0.31$ , the reactor had undergone a progressive washout of methanogens, including *Methanosaeta*, *Methanobacteria*, and *Methanomicrobiales*. SRB completely outcompeted methanogens after 230 days of operation, in which *Desulfobulbus* and *Desulfovibrio* were found the main sulfate-reducing genus. Through the treatment of sulfate-rich wastewater, the methanogenic sludge was shifted into sulfidogenic sludge. Activity tests resented herein were performed to study the sulfate reduction mechanism using glycerol as carbon source using sludge collected from the reactor when it was performing under sulfidogenic conditions. From day 200 to day 400, only VFAs were considered as the intermediate products of glycerol degradation, but a significant carbon imbalance was found during the process of glycerol fermentation. Therefore, other intermediate metabolites were considered in batch tests after day 400, such as ethanol and 1,3-propanediol.

#### 6.3.1.1 Glycerol fermentation process

Profiles for carbon and sulfur species using pure glycerol as the only carbon source externally added to the serum bottles with and without the presence of sulfate are shown in Figure 6.1. In the control group (Figure 6.1A and 6.1B), only glycerol was added with an initial granular sludge concentration of 230 mg VSS L<sup>-1</sup>. The 120 h culture in the control test was divided into three phases: a lag phase (0-10 h), a quick glycerol uptake phase (10-48 h), and a glycerol-free phase mediated by several intermediates (48-120 h). After the lag phase

(10 h), glycerol began to be consumed while ethanol, 1,3-propanediol, formate, acetate and propionate accumulated. Along this second period, glycerol was consumed at a rate of  $49.9 \pm 13.7 \text{ mg C g VSS}^{-1} \text{ h}^{-1}$  and ethanol, 1,3-propanediol, formate, acetate and propionate were accumulated at rates of  $2.1 \pm 2.9$ ,  $30.3 \pm 8.2$ ,  $1.6 \pm 2.4$ ,  $6.2 \pm 3.0$  and  $0.5 \pm 0.7 \text{ mg C g VSS}^{-1} \text{ h}^{-1}$ , respectively. At the end of the second phase (48 h), glycerol had already been completely converted to ethanol, 1,3-propanediol, formate, acetate, propionate and inorganic carbon, accounting for  $4.5 \pm 0\%$ ,  $57.5 \pm 0.6\%$ ,  $3.9 \pm 1.1\%$ ,  $12.2 \pm 2.7\%$ ,  $1.1 \pm 1.5\%$  and  $4.0 \pm 0.9\%$  of the initial glycerol content, respectively. During the last phase (48-120 h), 1,3-propanediol and inorganic carbon were maintained at  $195$  and  $23 \text{ mg C L}^{-1}$ , respectively. All formate ( $53.6 \text{ mg C L}^{-1}$ ) was completely consumed while butyrate increased from  $0$  to  $7.3 \text{ mg C L}^{-1}$  and propionate increased from  $3.5$  to  $17.6 \text{ mg C L}^{-1}$ . The pH decreased from  $8.4$  to  $7.2$  concomitantly with VFAs production.

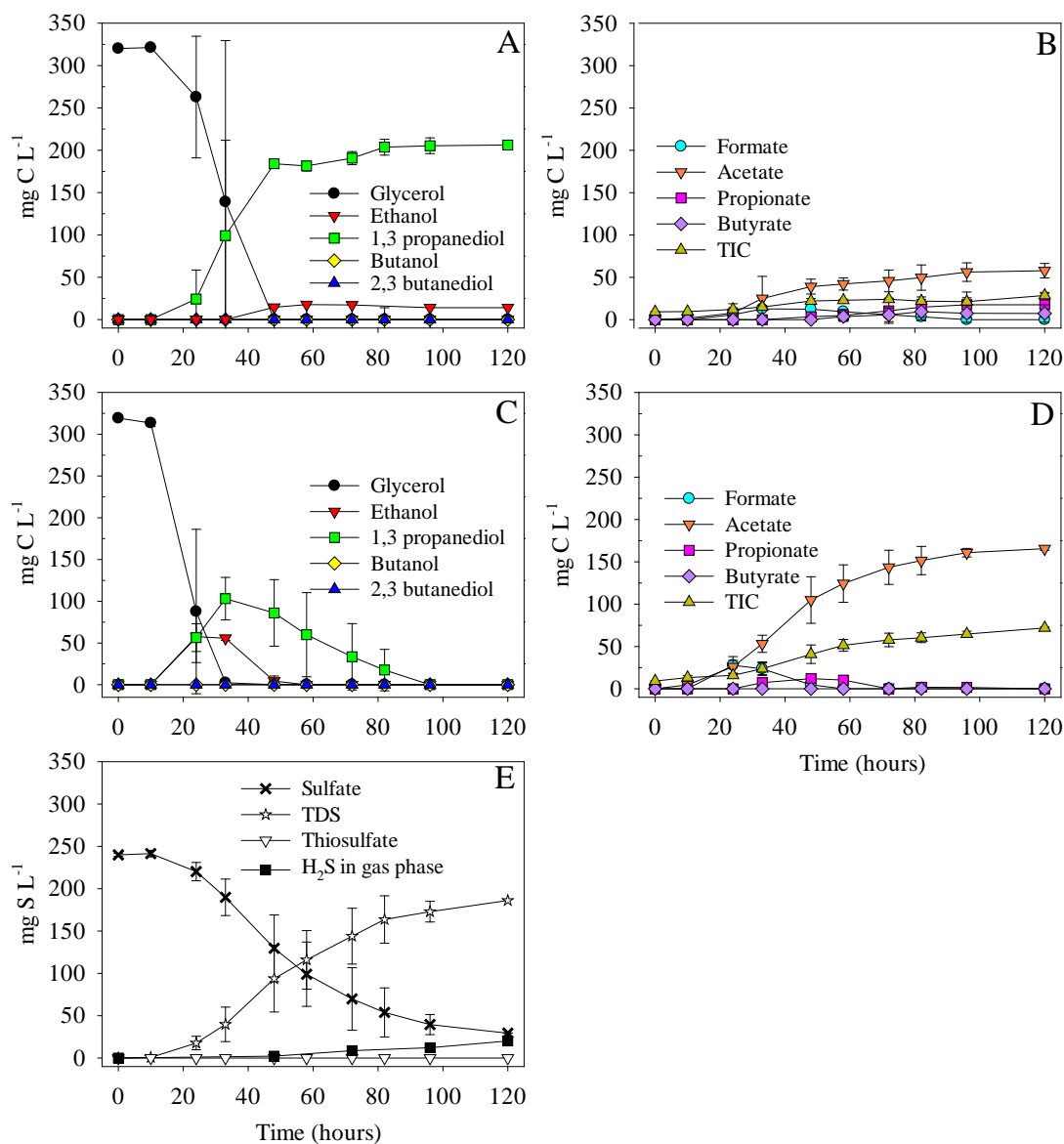


**Figure 6.1.** Anaerobic bioconversion of pure glycerol in serum bottles without sulfate (A, B) and with sulfate (C, D, E) showing the glycerol consumption and the concentration profiles for alcohols (A, C), volatile fatty acids and inorganic carbon (B, D) and sulfur species (E). Error bars represent standard deviations of duplicate tests. TIC represents total inorganic carbon.

Results obtained through Illumina sequencing analysis of the 16S rRNA with the sludge sample collected on day 538 from the UASB are presented in Figure 6.2. The most abundant genus detected were *Propionispora* (15.2%), *Dysgonomonas* (13.2%), *Desulfobulbus* (11.6%) and *Desulfovibrio* (10.8%). Bacteria from the genus *Dysgonomonas* are obligately anaerobic also known for their fermentative activity while

*Propionispora* is a genus of anaerobic fermentative bacteria that typically use glycerol, and other carbohydrates, fermenting them to produce propionic, acetic acid, CO<sub>2</sub> and H<sub>2</sub> (Abou-Zeid et al., 2004). Major fermentation products are usually butyric and acetic acid, while propionic, isovaleric, isobutyric and phenylacetic acids may also be produced (Sakamoto, 2014). Additionally, *Klebsiella* (2.1%) was also detected. The metabolism of *Klebsiella pneumoniae* with glycerol has also been described as follows: a) glycerol is converted to ethanol and formate (Jarvis et al., 1997); b) glycerol is degraded into acetate and formate (Zeng et al., 1993); c) lactate, acetate, ethanol and 1,3-propanediol are produced as end products (Cheng et al., 2007). According to the products of glycerol shown in Figure 6.1A and 6.1B and the metabolic pathways of glycerol mentioned above, the stoichiometry of the reactions involved in glycerol fermentation are shown in Table 6.1.

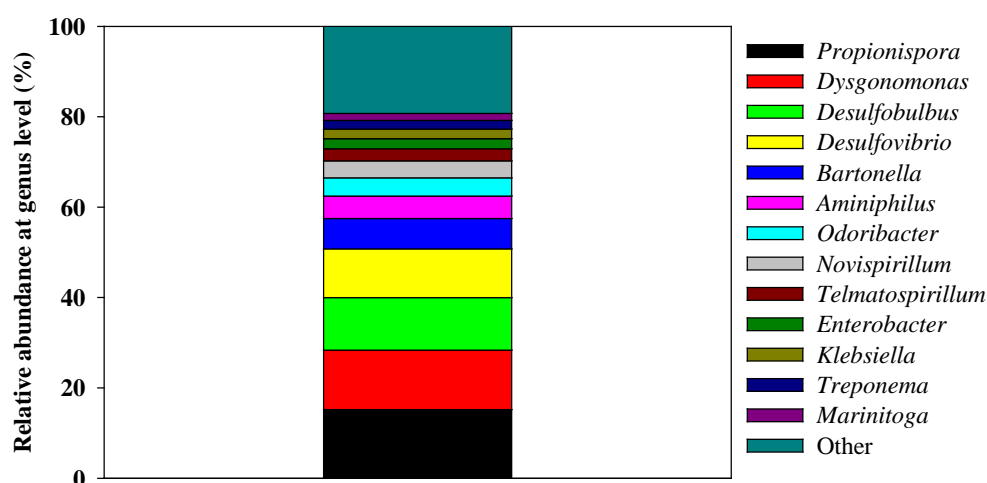


**Figure 6.2.** Relative abundances (%) at genus level of sample collected on day 538 of the UASB long-term operation.

### 6.3.1.2 Sulfate reduction in glycerol fed batch tests

The profiles obtained for the experimental group where glycerol and sulfate were added are shown in Figure 6.1C for alcohols, in Figure 6.1D for VFAs and in Figure 6.1E for sulfur species. The granular sludge concentration in the experimental bottles was 390 mg VSS L<sup>-1</sup>. The 120 h culture in the experimental test were also divided into three phases: the

lag phase (0-10 h), the glycerol fermentation phase (10-33 h) and a secondary carbon sources consumption/production phase (33-120 h). Similar to the control group, the granular sludge in the experimental group also experienced a 10 h lag phase with neither glycerol fermentation nor sulfate reduction. After the lag phase, the specific rates along the test with sulfate were assessed. In the second phase from 10 h to 33 h, glycerol was consumed at a rate of  $33.1 \pm 12.1 \text{ mg C g VSS}^{-1} \text{ h}^{-1}$ , while ethanol, 1,3-propanediol, formate, acetate and propionate accumulated at rates of  $5.0 \pm 7.9$ ,  $11.9 \pm 2.1$ ,  $2.0 \pm 4.5$ ,  $5.9 \pm 2.7$  and  $1.0 \pm 1.4 \text{ mg C g VSS}^{-1} \text{ h}^{-1}$ , respectively. Sulfate was reduced at a rate of  $6.3 \pm 3.4 \text{ mg S g VSS}^{-1} \text{ h}^{-1}$  along this phase. At the end of the second phase (33 h), glycerol was completely consumed while ethanol, 1,3-propanediol, formate, acetate, propionate and inorganic carbon accumulated, accounting for  $17.5 \pm 0.8\%$ ,  $32.3 \pm 8.0\%$ ,  $7.4 \pm 2.2\%$ ,  $16.7 \pm 3.2\%$ ,  $2.3 \pm 0.0\%$  and  $4.5 \pm 2.5\%$  of the initial glycerol content, respectively. In the third phase, when there was no glycerol, a net alcohols and VFAs consumption was observed, coupled to sulfate reduction and a significantly increasing accumulation of acetate and inorganic carbon. From 33 h to 96 h, the sulfate reduction rate (SRR) gradually decreased from  $10.4 \text{ mg S g VSS}^{-1} \text{ h}^{-1}$  (33-48 h) to  $2.6 \text{ mg S g VSS}^{-1} \text{ h}^{-1}$  (82-96 h). Ethanol, 1,3-propanediol, formate and propionate were completely consumed at a rate of  $8.9 \pm 0.6$ ,  $4.4 \pm 1.5$ ,  $1.9 \pm 1.2$  and  $1.2 \pm 1.0 \text{ mg C g VSS}^{-1} \text{ h}^{-1}$ , respectively. Almost no activity was observed after 96 h of test.

Bertolino et al. (2014) found that acetate and carbonate were the terminal products of glycerol oxidation under sulfidogenic conditions at a sulfate loading rate of  $4.7 \text{ kg m}^{-3} \text{ d}^{-1}$  but pointed out that some intermediate products in the degradation process of glycerol were not measured but probably consumed during sulfate reduction. In addition, the production of formate, ethanol and 1,3-propanediol have also been previously reported in the fermentation of glycerol (Jarvis et al., 1997; Katarzyna et al., 2011; Sittijunda and Reungsang, 2017). At the same time, these compounds could also act as intermediate products under sulfidogenic conditions. Ethanol, 1,3-propanediol, formate and propionate have been reported as suitable electron donors in biological sulfate reduction processes

applied in different bioreactors, such as UASB and expanded granular sludge bed reactors (De Smul and Verstraete, 1999; Qatibi et al., 1991b; Vallero et al., 2004a, 2004b; Wu et al., 2018). The stoichiometry of the reactions involved in sulfate reduction by non-methanogenic but sulfidogenic biomass is shown in Table 6.1. Results in Figure 1 confirmed that intermediate reduced organic carbon sources were used as electron donors in sulfate reduction processes. However, data was not sufficient to clearly identify which specific electron donors were used and their SRRs. As an example, when there was no glycerol fermentation, formate was consumed with and without the presence of sulfate (Figure 6.1B and Figure 6.1D). In the absence of sulfate, formate was consumed because of anaerobic fermentation. However, in the presence of sulfate, the consumption of formate cannot be interpreted as the direct attribution to anaerobic fermentation or its use as an electron donor by SRB. Consequently, separate experiments with individual organic compounds were required to confirm the metabolic pathway of sulfate reduction using ethanol, 1,3-propanediol, formate and propionate (see section 6.3.2).

The TOC removal (0 h to 120 h) in the absence and presence of sulfate were 5.7% and 19.0%, respectively, indicating that SRB played a major role in removing organics. The percentage of relative abundance of SRB on day 538 in the UASB could be considered as the sum of genus *Desulfobulbus* and *Desulfovibrio* accounting for a 22.4% of the total amount of sequences detected. Most bacteria that belong to the genus *Desulfobulbus* can oxidize propionate to acetate in the presence of sulfate and ferment pyruvate and lactate to a mixture of acetate and propionate (El Houari et al., 2017). This genus can also use lactate, pyruvate, ethanol or propanol as carbon sources and also as electron donors for anaerobic respiration oxidizing them incompletely to acetate. According to Rabus et al. (2013), *Desulfobulbus* and *Desulfovibrio* are not able to completely oxidize organic electron donors, therefore they perform an incomplete oxidation to acetate as end-product. *Desulfobulbus* and *Desulfovibrio* do not utilize acetate as electron donor even if some species of both genera are able to use H<sub>2</sub> as electron donor to reduce sulfate to sulfide (Rabus et al., 2013). *Desulfovibrio* spp. only carry out an incomplete oxidation of

substrates and they are able to excrete acetate as end-product (Rabus et al., 2013). This could indeed explain the accumulation of acetate in the experimental group indicating that SRB found in the UASB reactor performed an incomplete oxidization of the carbon sources used.

By comparing the consumption rate of glycerol during the glycerol fermentation phase in the control group (10-48 h) and the experimental group (10-33 h), it was found that the consumption rate of glycerol in the control group was  $29.4 \pm 8.1 \text{ mg C L}^{-1} \text{ h}^{-1}$ , similar to that in the experimental group ( $32.7 \pm 12.0 \text{ mg C L}^{-1} \text{ h}^{-1}$ ). This indicates that glycerol was not probably used by SRB for sulfate reduction but that glycerol was first fermented by granular sludge to produce secondary carbon substrates, and then SRB used these carbon sources to reduce sulfate. Therefore, it was necessary to explore the sulfate reduction mediated by other electron donors formed during glycerol fermentation in order to understand the mechanism of sulfate reduction by the granular sludge.

### 6.3.1.3 Mass balances

The carbon mass balance of the glycerol-added serum bottle experiment is presented in Figure 6.3A (without sulfate) and Figure 6.3B (with sulfate). The sum of carbon was calculated as the sum of volatile fatty acids and alcohols. In the absence of sulfate, the carbon imbalance was  $10.1 \pm 3.0\%$  between TOC and the sum of carbon species measured (Figure 6.3A) from 10 h to 120 h. This could be explained by the presence of some other organic carbon species not monitored as well as to biomass growth. Butyrate and propionate accumulation started only after glycerol depletion, which may be due to the accumulation of phosphoenolpyruvate during the fermentation of glycerol (Viana et al., 2012). Phosphoenolpyruvate was subsequently oxidized after 48 hours. Moreover, via a reductive pathway, glycerol not only produces 1,3-propanediol but also 3-hydroxypropionate as a metabolite of glycerol fermentation (Qatibi et al. 1998). Therefore, these possible intermediate metabolites of glycerol that were not measured may contribute to the 10.1% carbon imbalance. In the presence of sulfate, the carbon imbalance



between TOC and the sum of all the rest of carbon species was  $18.5 \pm 6.3\%$  (Figure 6.3B). Compared with the carbon imbalance without sulfate (10.1%), the increase in the imbalance was probably due to the formation of volatile organic sulfur compounds (VOSC). It has been reported that VOSC are produced in the anaerobic digestion of organic wastes (Papurello et al., 2012) as well as propylene glycol and glycerol (Trabue et al., 2007). Compounds such as methanethiol and dimethyl sulfide are formed by the degradation of sulfur-containing amino acids or sulfide methylation in anaerobic digestion (Lomans et al., 2002). As shown in Figure 6.1E, the concentration of  $H_2S$  in the gas phase measured at 120 h was  $20.1 \text{ mg S L}^{-1}$ . Compared with the TDS concentration measured in the liquid, the  $H_2S$  concentration in the gas phase accounted only for 6.6% of the total S fed. The sulfur mass balance was calculated by monitoring the sulfate, thiosulfate and TDS content in the liquid and the hydrogen sulfide content in the gas phase at the beginning and at the end of each test. On average, a 4.7% sulfur imbalance was observed between the S mass at 0 h and 120 h, which may be caused by the formation of organic sulfur compounds.

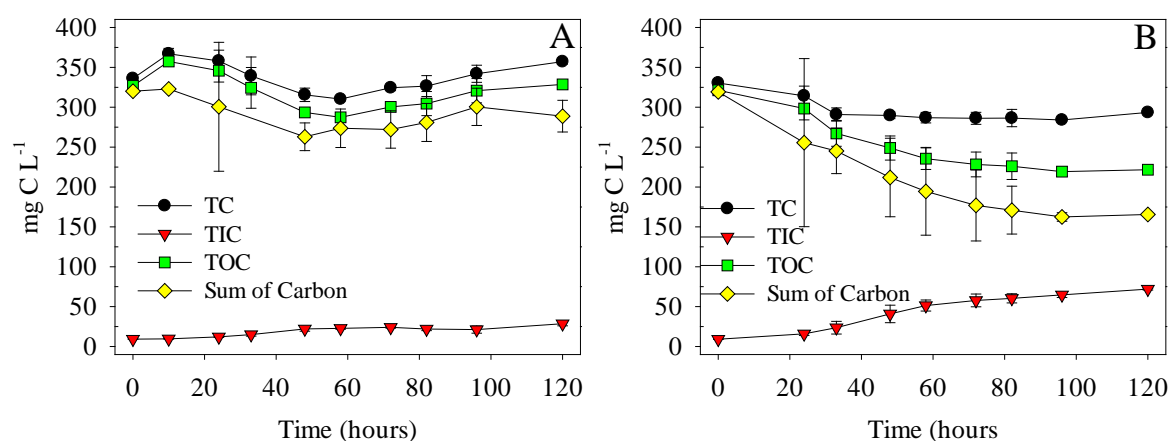


**Figure 6.3.** Carbon contents monitored in the batch test fed with glycerol only (A) and glycerol with sulfate (B). TOC, total organic carbon; TIC, total inorganic carbon; TC, total carbon; Sum of carbon represents the sum of volatile fatty acids and alcohols. Error bars represent standard deviations of duplicate tests.

### 6.3.2 Sulfate reduction with single organic compounds

During the sulfate reduction with glycerol, it was found that SRB metabolized simpler organic carbon intermediate products (Figure 6.1C and 6.1E). Combined with the description of the fermentation mechanism of glycerol described by Viana et al. (2012), the intermediate products observed in Figure 6.1, were used as individual carbon sources to further study the mechanism and rates of the sulfate reduction process.

When no sulfate was added, the carbon content remained constant when sludge was fed with propionate (Figure 6.4A), ethanol (Figure 6.4B), 1,3-propanediol (Figure 6.4C) and butanol (Figure 6.4E), respectively. This indicates that granular sludge was not capable of using those carbon sources without sulfate. However, in the test that used formate as the carbon source (Figure 6.4D), and after 40 hours of lag time, this compound was consumed at a rate of  $2.8 \pm 0.8 \text{ mg C g VSS}^{-1} \text{ h}^{-1}$  while inorganic carbon was accumulated at a rate of  $3.6 \pm 1.3 \text{ mg C g VSS}^{-1} \text{ h}^{-1}$ . Figure 6.5 shows the profiles of C and S species when single electron donors produced during glycerol fermentation were fed in batch tests to the UASB sludge. As can be observed, propionate (Figure 6.5A), ethanol (Figure 6.5B), 1,3-propanediol (Figure 6.5C), formate (Figure 6.5D) and butanol (Figure 6.5E) were consumed in the sulfate-added tests. Coupled to sulfate reduction, propionate was degraded to acetate and inorganic carbon according to Eq.6.8 (Table 6.1), ethanol was degraded to acetate according to Eq.6.9 (Table 6.1), formate was degraded to inorganic carbon, and butanol was oxidized to butyrate. When 1,3-propanediol was added, sulfate was reduced to sulfide and the consumption of 1,3-propanediol was accompanied by the accumulation of acetate, propionate and inorganic carbon (Figure 6.5C). Despite the VFA production, the buffering capacity of the mineral medium maintained the pH above 7.5.

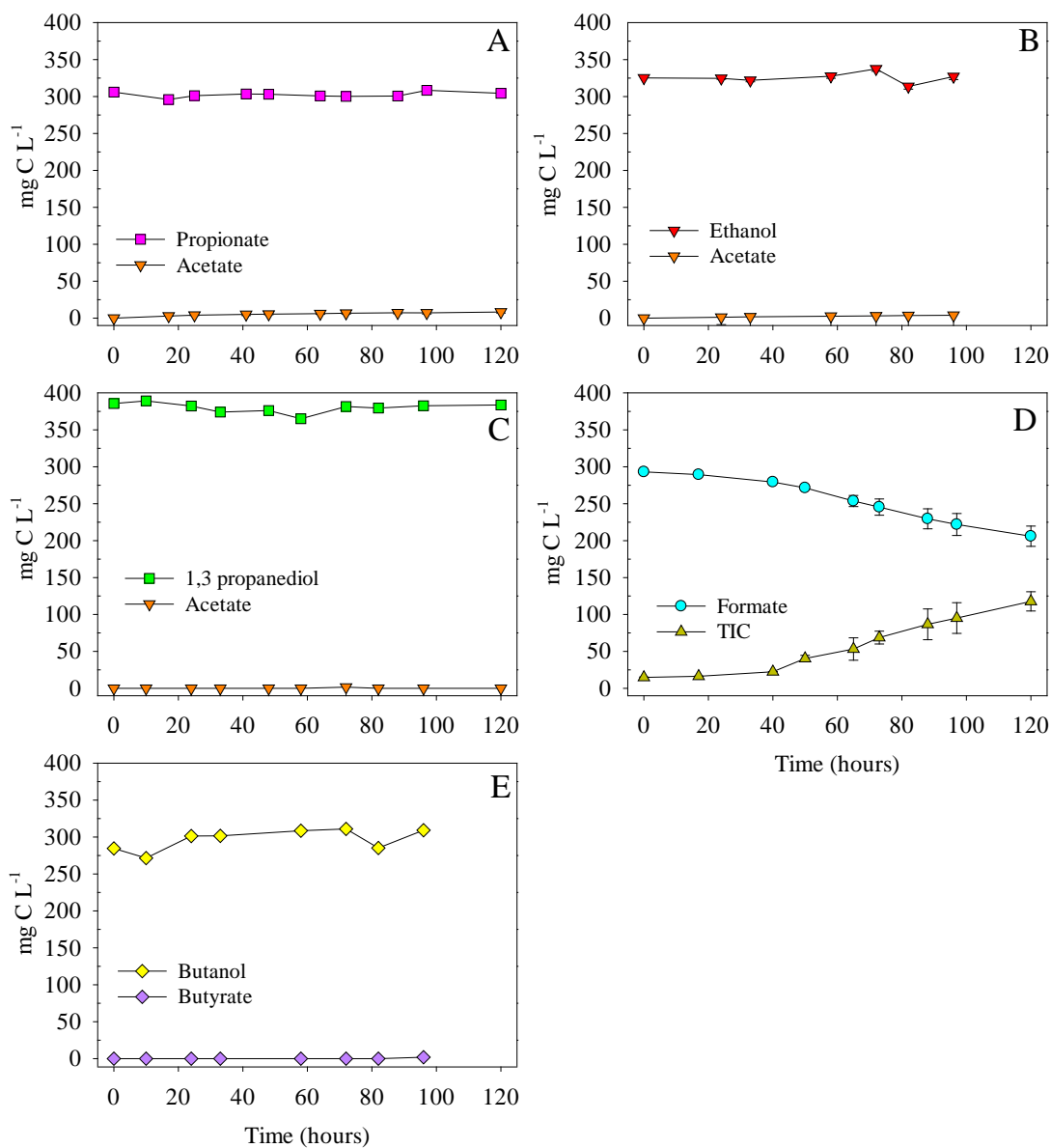


**Figure 6.4.** Carbon conversion observed in the control bottles fed with propionate (A), ethanol (B), 1,3-propanediol (C), formate (D) and butanol (E). Error bars represent standard deviations of duplicate tests. TIC represents total inorganic carbon.

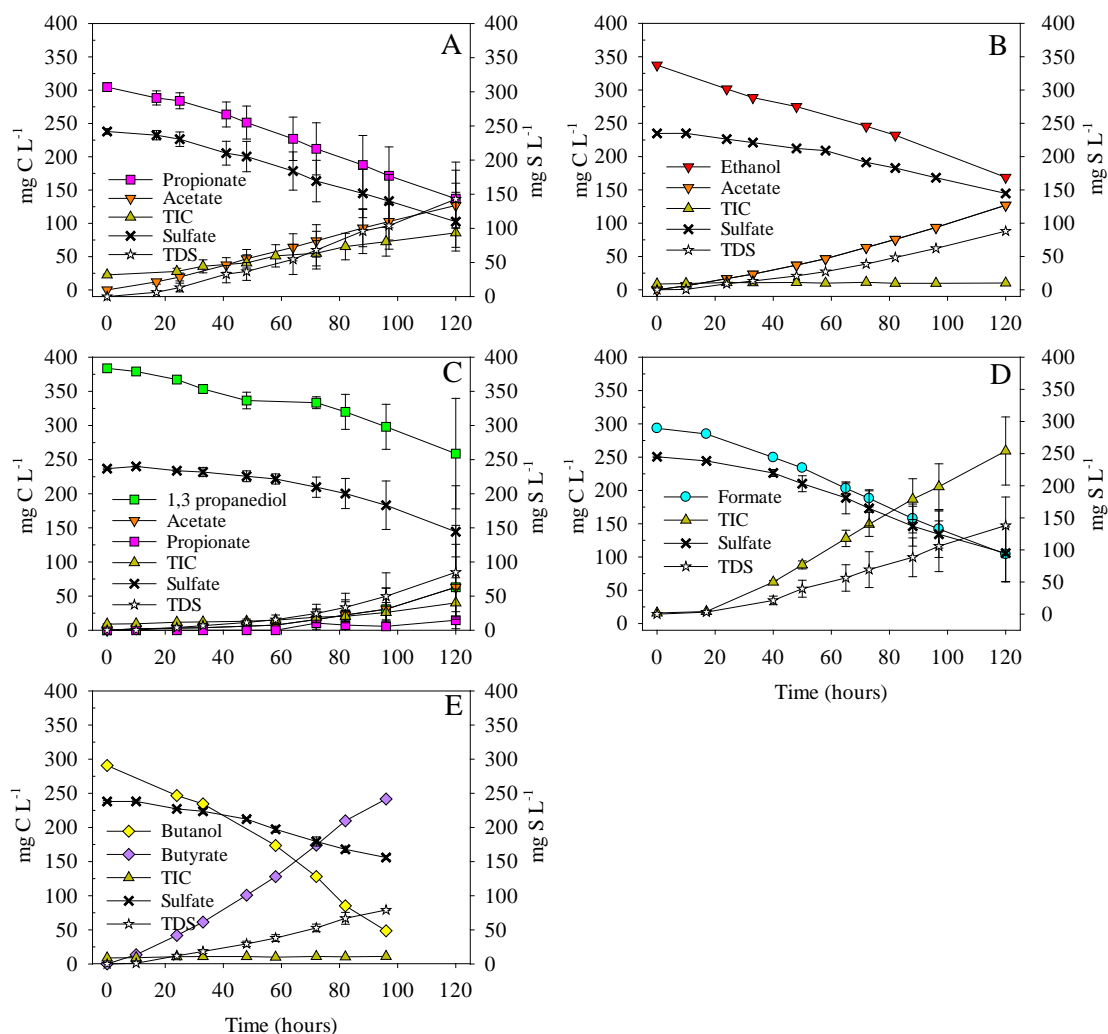


**Figure 6.5.** Carbon and sulfate conversions in the experimental bottles feeding sulfate with propionate (A), ethanol (B), 1,3-propanediol (C), formate (D) and butanol (E). Error bars represent standard deviations of duplicate tests. TIC represents total inorganic carbon.

### 6.3.2.1 Sulfate reduction with propionate

According to literature, there are two main pathways described for the sulfate reduction process using propionate as electron donor. One is acetogenesis, in which propionate is degraded into acetate and hydrogen by acetogens (Li et al., 2017), and then sulfate is reduced both by hydrogenotrophic and acetotrophic SRB (Muyzer and Stams, 2008). The other is the propionate oxidation pathway by propionate-degrading sulfate reducers, which directly uses propionate as an electron donor to reduce sulfate. The oxidation pathway includes partial oxidation of propionate to form acetate and bicarbonate and complete

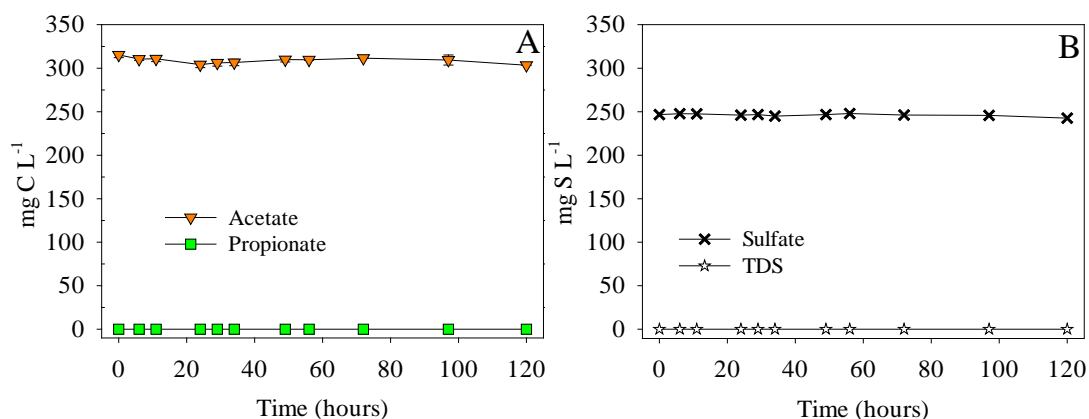
oxidation of propionate to bicarbonate (Luis, 2018). In the absence of sulfate, acetate and bicarbonate were not produced in this work, showing that there was no acetogenesis from propionate. However, propionate was incompletely oxidized to acetate in the presence of sulfate while acetate could not be further fermented to produce methane nor used to reduce sulfate, as shown in Figure 6.6. Although many studies have shown that acetate can be oxidized to CO<sub>2</sub> by SRB, including *Desulforhabdus amnigenus*, *Desulfobacca acetoxidans*, *Desulfarculus baarsii* and *Desulfatitalea* (Higashioka et al., 2013; Oude Elferink et al., 1998; Widdel and Pfennig, 1977), they were not present in this work as confirmed by 16S rRNA sequence analysis. In previous works in the same UASB reactor fed with crude glycerol as studied herein, it was reported that acetate accumulated in the long-term after increasing the sulfate loading rate or after a 24 h pH shock (Fernández-Palacios et al., 2019; Mora et al., 2020b), since methanogens were probably the only microorganisms that consumed acetate. After methanogens wash out, acetate cannot be further oxidized due to the lack of acetotrophic SRB. H<sub>2</sub>S inhibition could be another reason that lead to incompletely oxidizing SRB to dominate among SRB species. Maillacheruvu and Parkin (1996) reported that acetotrophic SRB and propionate fermenters were more sensitive to sulfide toxicity compared to hydrogenotrophic SRB and incomplete propionate-utilizing SRB. Thus, the mechanism of sulfate reduction using propionate was considered to be partial oxidation, represented by Eq.6.8. This was confirmed by comparing the stoichiometric rates and the experimental rates, as shown in Table 6.2.

Table 6.2 shows the maximum specific rate assessed from the experimental rates in Figure 6.5 and those estimated from the stoichiometry of each electron donor. Stoichiometry-based rates takes one of the experimental rate as reference, and this work is based on the consumption rate of the electron donor, defined as 'A'. A is substituted into the stoichiometric formula listed in Table 6.1, and therefore, the stoichiometric production rate of other substance in the formula can be obtained, which is set as 'B'. The other substance in the formula can also be calculated in Figure 6.5 to obtain the experimental rate, defined

as 'B'. By comparing the experimental rate 'B' and the stoichiometric rate 'B' of other substance, it can also be determined whether the experiment follows the mechanism listed in Table 6.1.

As an example, the mechanism of sulfate reduction using propionate as a carbon source, represented by Eq.6.8 in Table 6.1. The experimental consumption rate of propionate was  $4.4 \pm 0.5 \text{ mg C g VSS}^{-1} \text{ h}^{-1}$ . According to Eq.6.8, the stoichiometric relation between propionate and acetate is shown in Eq.6.19.

According to the equation mentioned above, the stoichiometric production rate of acetate was  $3.0 \pm 0.6 \text{ mg C g VSS}^{-1} \text{ h}^{-1}$ . By comparing the experimental production of acetate ( $3.0 \pm 0.2 \text{ mg C g VSS}^{-1} \text{ h}^{-1}$ ) with the stoichiometric production rate of acetate, it can be inferred that the pathway of oxidizing propionate in this work was according to Eq.6.8.



**Figure 6.6.** Anaerobic bioconversion in serum bottles fed with acetate and sulfate. (A) carbon species, (B) sulfur species. Error bars represent standard deviations of duplicate tests.

**Table 6.2.** Maximum specific rates of each electron donor during the sulfate reduction process.

<b>Carbon source</b>	<b>Time</b>	<b>Rate assessment</b>	<b>Consumption rate (mg C g VSS<sup>-1</sup> h<sup>-1</sup>)</b>	<b>Acetate production rate (mg C g VSS<sup>-1</sup> h<sup>-1</sup>)</b>	<b>Bicarbonate production rate (mg C g VSS<sup>-1</sup> h<sup>-1</sup>)</b>	<b>Butyrate production rate (mg C g VSS<sup>-1</sup> h<sup>-1</sup>)</b>	<b>Sulfate reduction rate (mg S g VSS<sup>-1</sup> h<sup>-1</sup>)</b>
Propionate	64-120	Experimental	4.4 ± 0.5	3.0 ± 0.2	1.5 ± 0.6	N.A.	3.7 ± 0.8
		Stoichiometric	4.4 ± 0.5	3.0 ± 0.6	1.5 ± 0.2	N.A.	3.0 ± 0.3
Ethanol	24-96	Experimental	9.3 ± 5.1	7.8 ± 1.8	N.A.	N.A.	5.8 ± 1.5
		Stoichiometric	9.3 ± 5.1	9.3 ± 5.1	N.A.	N.A.	6.2 ± 3.4
Butanol	24-120	Experimental	11.6 ± 4.4	N.A.	N.A.	12.2 ± 2.2	4.3 ± 1.6
		Stoichiometric	11.6 ± 4.4	N.A.	N.A.	11.6 ± 4.4	3.9 ± 1.5
1,3-propanediol	72-120	Experimental	4.7 ± 0.5	2.7 ± 1.3	1.1 ± 0.7	N.A.	3.9 ± 1.1
Formate	50-97	Experimental	6.9 ± 1.5	N.A.	7.9 ± 0.7	N.A.	5.2 ± 0.9

N.A. not applicable

### 6.3.2.2 Sulfate reduction with ethanol and 1,3-propanediol

In the control bottles fed with ethanol as carbon source, the ethanol concentration remained constant and no other products were produced (Figure 6.4B). However, in the presence of sulfate, sulfate was reduced to sulfide, while ethanol was converted to acetate (Figure 6.5B). When sulfidogenesis dominated in a long-term UASB treatment with sulfate-rich wastewater, SRB oxidized ethanol into acetate for sulfidogenesis, according to the Eq.6.9 (Wu et al., 2018). The experimental results of Figure 6.5B are well-explained through Eq.6.9, which was confirmed by the stoichiometric calculation in Table 6.2.

Similarly, results showed that 1,3-propanediol was not degraded to VFAs or inorganic carbon in the absence of sulfate (Figure 6.4C). However, in the presence of sulfate, 1,3-propanediol was oxidized to acetate, propionate and bicarbonate (Figure 6.5C). Qatibi et al. (1991b) reported that 1,3-propanediol was oxidized to acetate and bicarbonate according to Eq.6.10 during sulfate reduction (Table 6.1). They found that 3-hydroxypropionate, which was further oxidized to acetate, was the intermediate of the degradation of 1,3-propanediol by *Desulfovibrio alcoholovorans*. Interestingly, Liu and Liu (2016) reported that propionate was produced from 3-hydroxypropionate by *Metallosphaera sedula* through the autotrophic carbon dioxide assimilation cycle through 3-hydroxypropionyl-CoA synthesis, 3-hydroxypropionyl-CoA dehydration, acryloyl-CoA reduction and CoA hydrolysis (Figure 6.7). Then, 1,3-propanediol ( $C_3H_8O_2$ ) oxidation to propionate ( $C_3H_5O_2^-$ ) was lumped into Eq.6.11 in this work, as shown in Table 6.1.

Consequently, both Eq.6.10 and Eq.6.11 were used in the work herein to describe the mechanism for the oxidation of 1,3-propanediol coupled to the sulfate reduction following the pathway described in Figure 6.7. Since 3-hydroxypropionate was not monitored in this work, the process of 1,3-propanediol as an electron donor in reducing sulfate to acetate and propionate needs further investigation. This is discussed in chapter 7 to build a model based on the experimental data.



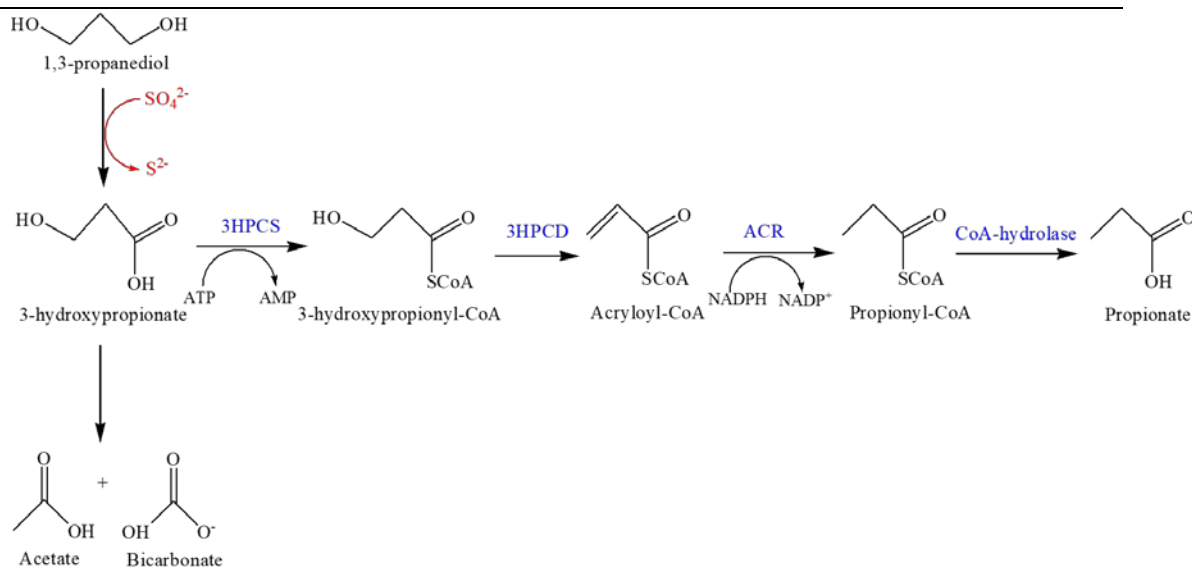


**Figure 6.7.** The metabolic pathway for the conversion of 1,3-propanediol into propionate, acetate and bicarbonate proposed in this work based on the mechanisms described in Qatibi et al. (1991b) (vertical pathway) and Liu and Liu (2016) (horizontal pathway). 3HPCS, 3-hydroxypropionyl-CoA synthetase; 3HPCD, 3-hydroxypropionyl-CoA dehydratase; ACR, acryloyl-CoA reductase.

### 6.3.2.3 Sulfate reduction with formate, butanol and 2,3-butanediol

Despite some extra inorganic carbon was produced based on the formate consumed, which was attributed to some remaining COD in the granules before the test, formate was oxidized to produce inorganic carbon in the absence of sulfate (Figure 6.4D). In addition, 2.6 mg L<sup>-1</sup> of H<sub>2</sub> were detected in the headspace of serum bottles at the end of the test. Thus, formate was converted into CO<sub>2</sub> and H<sub>2</sub> according to Eq.6.5 (Table 6.1). In the presence of sulfate, sulfate was reduced to TDS, while formate was oxidized to carbonate (Figure 6.5D). Similarly, 7.6 mg L<sup>-1</sup> of H<sub>2</sub> were also detected after cultivation. It has been reported that formate is rapidly oxidized into CO<sub>2</sub> and H<sub>2</sub>; then, hydrogen can be used as electron donor for further sulfate reduction by hydrogenotrophic SRB (Bijmans et al., 2008) according to Eq.6.6 (Table 6.1). It is worth mentioning that formate can also be used as electron donor to directly reduce sulfate by SRB (De Smul and Verstraete, 1999; Liamleam and Annachhatre, 2007). If all formate was oxidized and the H<sub>2</sub> produced was used for sulfate reduction only according to Eq.6.5 and Eq.6.6, respectively, the corresponding SRR calculated by the stoichiometric equations would be 3.8 ± 1.0 mg S g VSS<sup>-1</sup> h<sup>-1</sup>. Instead, the actual

experimental SRR was  $5.2 \pm 0.9 \text{ mg S g VSS}^{-1} \text{ h}^{-1}$ . Consequently, formate was converted into  $\text{CO}_2$  and  $\text{H}_2$  as well as used as electron donor for sulfate reduction (Eq.6.7). In addition, hydrogen was used by SRB as electron donor for sulfate reduction as represented by Eq.6.6.

Despite butanol was not found in the batch test with glycerol (Figure 6.1A and 6.1C), it has been reported as an electron donor for SRB to reduce sulfate. Particularly, *Desulfovibrio* spp. are capable to incompletely oxidize butanol to succinate coupled to sulfate reduction (Dowling et al., 1992). Sarti and Zaiat (2011) found that butanol was converted to acetic acid by incompletely oxidizing SRB in an anaerobic sequential batch reactor. Due to the significant presence of *Desulfovibrio*, it was decided to test butanol with the granular biomass from the UASB reactor. In the work herein, butanol was not degraded in the absence of sulfate (Figure 6.4E). When sulfate was added, all butanol was converted to butyrate while no acetate, other VFA nor alcohols were produced (Figure 6.5E). This observation has not been reported previously in literature and the specific strain of SRB that was able to oxidize butanol to butyrate needs to be further confirmed. Although sulfidogenic granular sludge can oxidize butanol to butyrate, no other organic compounds and inorganic carbon were produced during the oxidation of butanol to butyrate, which means that SRB could not further use butyrate formed to reduce sulfate. As observed in Figure 6.1C and 6.1D, glycerol was not converted into butanol or butyrate in the sulfate reduction process. Similarly, no VFAs were produced when only 2,3-butanediol was added (Figure 6.8A). Similar results were obtained adding sulfate (Figure 6.8B), thus indicating that there were no butanediol-degrading anaerobes in this work.

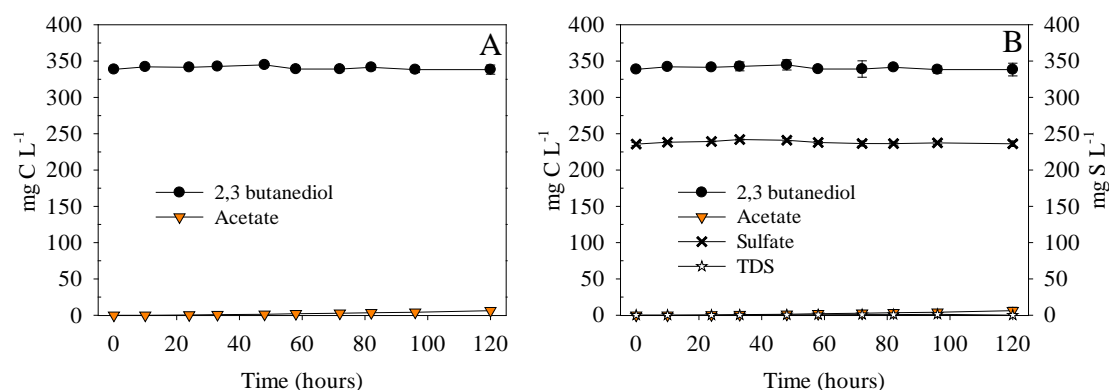


**Figure 6.8.** Anaerobic bioconversion of 2,3-butanediol in serum bottles without sulfate (A) and with sulfate (B). Error bars represent standard deviations of duplicate tests.

#### 6.3.2.4 The mechanism of biodegradation of glycerol and sulfate reduction

Based on the batch tests results, a mechanism for sulfate reduction using glycerol as electron donor was proposed in this work (Figure 6.9). From the sulfate reduction process performed by each single electron donor under non-methanogenic conditions, it was concluded that the granular sludge taken from the UASB operated under long-term sulfidogenic conditions while fed with crude glycerol was 1) able to ferment glycerol to acetate, formate, propionate, ethanol and 1,3-propanediol; 2) able to use H<sub>2</sub>, formate, propionate, ethanol and 1,3-propanediol for sulfate reduction; 3) able to oxidize formate to CO<sub>2</sub> and H<sub>2</sub>; and 4) there were no acetogens that used propionate, ethanol nor 1,3-propanediol directly. Despite other intermediates not considered in this mechanism play a role in the detailed metabolic pathways of the microbial cultures grown in the UASB, the approach proposed herein provides a simplified view of the granular sludge activity through the main VFA and alcohols involved in glycerol fermentation. Such an approach contributes to expand the knowledge of sulfate reducing bioreactors and clarifies the mechanism of sulfate reduction through intermediate products and their contribution to the sulfate reduction process.

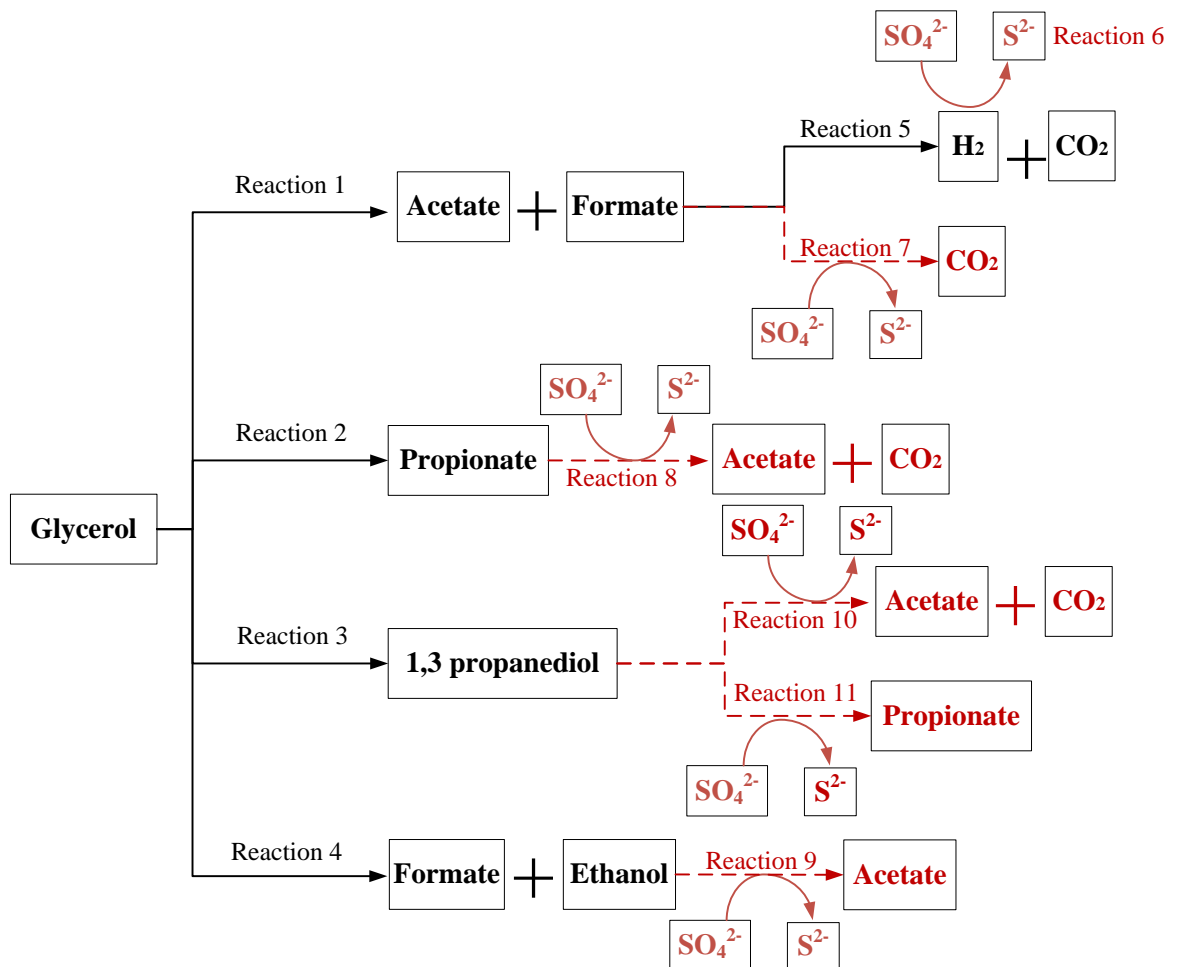


**Figure 6.9.** The main mechanism of biodegradation of glycerol and sulfate reduction without methane production. The repeated degradation and sulfate reduction pathways are not listed, such as propionate produced by reaction 11 and formate produced by reaction 4. Black reactions and continuous lines represent the fermentation process, while red reactions and discontinuous lines represent the sulfidogenic process.

### 6.3.3 Contribution of different electron donors to sulfate reduction

Table 6.3 shows the specific rates of different electron donors consumption and sulfate reduction in batch activity tests. Specific rates were obtained by dividing volumetric rates by VSS, while volumetric rates were calculated based on data from Figure 6.4 and Figure 6.5. In the present work, SRRs of tests performed with single electron donors were ranked as follows: ethanol > formate > butanol > 1,3-propanediol > propionate. The specific SRRs using ethanol and formate were 5.8 and 5.2 mg S g VSS<sup>-1</sup> h<sup>-1</sup>, respectively. Thus, the granular sludge cultivated under sulfidogenic anaerobic conditions of continuous feeding

with crude glycerol promoted formate-utilizing and ethanol-utilizing SRB species. SRB tend to use low molecular weight (MW) organic compounds in the cultivation of organic matrix mixtures (Neculita et al., 2007), which also has the benefit of improving sulfate reduction efficiency (Zhao et al., 2010). As can be observed from Table 6.3, the SRR obtained using formate and ethanol (compounds containing two carbons or less) was 39% higher than that obtained with compounds containing three carbons or more on average (propionate, 1,3-propanediol and butanol), which is in agreement with Neculita et al. (2007). Vallero et al. (2004a) reported a SRR of 3.2 mg S g VSS<sup>-1</sup> h<sup>-1</sup> in a methanogenic sludge fed with formate while Wu et al. (2018) reported a SRR of 22.1 mg S g VSS<sup>-1</sup> h<sup>-1</sup> using ethanol as sole carbon source, the later reported in a sulfidogenic dominant stage. The difference of SRRs between our work and previous studies was related to the development of microbial populations acclimated to a specific carbon source providing thus a larger affinity for such low-MW electron donors.

**Table 6.3.** Specific rates obtained from the sulfidogenic anaerobic digestion in batch activity tests.

Electron donors	Initial carbon		T(°C)	Initial pH	Final pH	Specific substrate	Specific sulfate	Reference
	concentration (mg C g L <sup>-1</sup> )	TOC/S-SO <sub>4</sub> <sup>2-</sup>				consumption rate (mg C g VSS <sup>-1</sup> h <sup>-1</sup> )	reduction rate (mg S g VSS <sup>-1</sup> h <sup>-1</sup> )	
Formate	1500	0.37	65	7.8	N.A.	92.8 ± 6.5	3.2 ± 0.6 <sup>a</sup>	Vallero et al., 2004a
Ethanol	750	0.27	35	N.A.	N.A.	N.A.	22.1 <sup>b</sup>	Wu et al., 2018
Formate	372	1.52	35	7.9	7.8	6.9 ± 1.5	5.2 ± 0.9 <sup>c</sup>	This study
Propionate	342	1.41	35	7.9	7.5	4.4 ± 0.5	3.7 ± 0.8 <sup>c</sup>	This study
Ethanol	318	1.35	35	8.4	7.6	9.3 ± 5.1	5.8 ± 1.5 <sup>c</sup>	This study
1,3-propanediol	339	1.43	35	8.4	7.8	4.7 ± 0.5	3.9 ± 1.1 <sup>c</sup>	This study
Butanol	334	1.40	35	8.4	7.5	11.6 ± 4.4	4.3 ± 1.6 <sup>c</sup>	This study

Note: N.A. not applicable.

<sup>a</sup> The specific rate was calculated by taking out the granular sludge from the UASB after 55 days of operation.

<sup>b</sup> The specific rate was calculated by taking out the granular sludge from the UASB after 330 days of operation.

<sup>c</sup> The specific rate was calculated by taking out the granular sludge from the UASB after 431 days of operation.

Table 6.4 shows the contribution of each electron donor to the overall SRR from the batch tests in which pure glycerol and sulfate were fed. The calculation process is shown in 6.2.5. From 33 h to 96 h, sulfate was mainly reduced using ethanol and 1,3-propanediol as electron donors. The overall contribution of these two compounds to the total sulfate reduction along the test with glycerol plus sulfate accounted for 78.6%. However, within 33 to 48 hours, SRB mainly used ethanol to reduce sulfate rather than formate or 1,3-propanediol since the concentration of ethanol fermented through glycerol was 2.4 times that of formate after 33 hours (Figure 6.1C, 6.1D). After ethanol was consumed in the sulfate reduction process (48 h), 1,3-propanediol became the main electron donor for the reduction of sulfate. Once glycerol was completely degraded after 33 h (Figure 6.1C), the production of 1,3-propanediol was 4.4 times that of formate. According to Table 6.4, the specific SRR for formate was higher than that of 1,3-propanediol. However, formate was not a key contributor to the overall sulfate reduction, probably due to its low-production from glycerol fermentation. The predominance of ethanol and 1,3-propanediol as main electron donors for sulfate reduction is consistent with previous works in which glycerol fermentation in anaerobic digestion lead also to a major production of both compounds (Metsoviti et al., 2012; Rossi et al., 2012; Wu et al., 2011). However, it is worth mentioning that the contribution of the different electron donors depends on several factors such as physiological differences among microbial cultures, the type of fermentation, substrate concentration and possible inhibitions (Biebl et al., 1999). Wu et al. (2011) reported that an excess amount of glycerol may cause a metabolic product shift from ethanol to 1,3-propanediol. Therefore, conditions can be accommodated to create an environment that is more conducive to the growth of SRB, such as the production of simpler carbon sources that SRB would use preferentially over complex ones.

**Table 6.4.** Stoichiometric specific SRRs according to Eq.6.1 to Eq.6.11, proposed mechanism and percentage contribution of each electron donor to the observed SRR of granular sludge fed with pure glycerol.

Time (h)	Formate and H <sub>2</sub> mg S g VSS <sup>-1</sup> h <sup>-1</sup> (%)	Propionate mg S g VSS <sup>-1</sup> h <sup>-1</sup> (%)	1,3-propanediol mg S g VSS <sup>-1</sup> h <sup>-1</sup> (%)	Ethanol mg S g VSS <sup>-1</sup> h <sup>-1</sup> (%)	Observed SRR mg S g VSS <sup>-1</sup> h <sup>-1</sup> (%)
33-48	2.2 (20.9%)	0	2.6 (25.3%)	5.9 (57.0%)	10.4
48-72	0.4 ± 0.57 (6.0 ± 8.7%)	1.1 ± 2.2 (16.2 ± 33.2%)	5.2 ± 1.2 (77.7 ± 27.1%)	0	6.7 ± 1.8
72-96	0	0.1 ± 1.1 (3.3 ± 31.9%)	3.3 ± 0.5 (88.8 ± 20.5%)	0	3.7 ± 0.6

## 6.4 Conclusion

The research in this work permitted to establish a simplified mechanism of sulfate reduction by granular sludge from a long-term operated sulfidogenic UASB using glycerol as electron donor. It also provides the experimental rates and stoichiometric equations considering the contribution of the intermediate products produced by the fermentation of glycerol previous to the sulfate reduction step. Under non-methanogenic but sulfidogenic conditions, SRB did not directly used glycerol to reduce sulfate. Glycerol was firstly fermented by the granular sludge to form simpler intermediates such as H<sub>2</sub>, formate, propionate, ethanol, 1,3-propanediol, and then SRB reduced sulfate with such intermediate products. The sulfate reduction process mainly used 1,3-propanediol and ethanol as electron donors, which were produced through glycerol fermentation. Butanol was not an intermediate product of glycerol fermentation, but it was capable to be oxidized to butyrate in the presence of sulfate. SRB performing an incomplete oxidation of the electron donors dominated in the granular sludge from the sulfidogenic UASB reactor. SRB preferred to use simple intermediate products containing less than 2 carbons as electron donors, except in the case of acetate that was not found to be used for sulfate reduction. *Desulfobulbus* and *Desulfovibrio* were found as the main sulfate reducing genus, accounting for 22.4% of the



Assessing main process mechanism and rates of sulfate reduction by granular biomass fed with glycerol under sulfidogenic conditions

---

total amount of sequences detected under sulfidogenic conditions.

## Chapter 7

---

# Modeling sulfate reduction and glycerol fermentation under sulfidogenic conditions

**Part of this chapter is in preparation for publication in:**

Zhou, X., Dorado, A., Gamisans, X., Gabriel, D. Modeling sulfate reduction and glycerol fermentation under sulfidogenic conditions.



*As described in Chapter 6, the mechanism of sulfate reduction using glycerol as the carbon source contained many intermediate products from alcohols to VFAs. The goal in this chapter was to setup a mechanistic model of the glycerol fermentation coupled to sulfate reduction occurring under sulfidogenic conditions. Since the mechanism proposed in Chapter 6 was not clearly elucidated, this chapter also evaluated three different alternatives for the mechanisms occurring to verify the most appropriate alternative of degradation pathways of glycerol and sulfate reduction. The modelling effort also included a sensitivity analysis to identify the most sensitive parameters of the model as well as the use of the Fisher Information Matrix to assess the uncertainty of the parameters calibrated. The calculated parameters of the model can be used in the future to simulate the performance of the reactor and to study the population dynamics competition between SRB and methanogens in the reactor.*

## **Abstract**

Glycerol can be converted to ethanol, 1,3-propanediol, formate, acetate, propionate and inorganic carbon under anaerobic conditions through oxidative and reductive pathways in the absence and presence of sulfate. In this chapter, a structured mathematical model was set up to describe sulfate reduction and glycerol fermentation with multi-intermediates in batch activity tests under a constant TOC/S ratio of  $1.4 \pm 0.1 \text{ g C g}^{-1} \text{ S}$ . Three mechanisms were proposed and verified through modeling. Mechanism I was referred to the metabolic pathway proposed in Chapter 6. Mechanism II considered the 1,3-propanediol degradation through 3-hydroxypropionate (3HP) coupled to sulfate reduction. Mechanism III added the degradation pathway of glycerol fermentation to 3HP. The model established based on Mechanism III predicted better results compared with Mechanism I and II. Mechanism III showed that the main pathway of glycerol fermentation was the oxidative pathway to produce ethanol, and the reductive pathway to produce 1,3-propanediol, accounted for 37.9% and 45.8%, respectively. Finally, 3HP

might be an intermediate product in the fermentation process of glycerol and the degradation of 1,3-propanediol with sulfate reduction. 3HP was mainly further oxidized to acetate. Student's t-test showed that there was no significant difference between the model and experimental data in Mechanism III.

## Nomenclature

$k_{m,j}$	Maximum specific substrate uptake rate of process j, mg C mg VSS <sup>-1</sup> h <sup>-1</sup> , or mg H <sub>2</sub> mg VSS <sup>-1</sup> h <sup>-1</sup>
$k_{s,i}$	Half saturation coefficient of component i, mg C L <sup>-1</sup> , or mg S L <sup>-1</sup>
$S_i$	Concentration of substrate component i, mg C L <sup>-1</sup> , or mg S L <sup>-1</sup>
$X_k$	Concentration of microbial trophic group k, mg VSS L <sup>-1</sup>
$R_j$	Rate of process j, mg C L <sup>-1</sup> h <sup>-1</sup> , or mg S L <sup>-1</sup> h <sup>-1</sup>
$v_{i,j}$	Biochemical rate coefficient for component i in process j
ASRB	Autotrophic sulfate reducing bacteria
HSRB	Heterotrophic sulfate reducing bacteria
Gly	Glycerol
For	Formate
Ace	Acetate
Pro	Propionate
Eth	Ethanol
13PDO	1,3-propanediol
3HP	3-hydroxypropionate

## 7.1 Introduction

Sulfate-rich wastewaters are originated from anthropogenic activities such as pulp and paper mills, food processing industries, composite tanneries, metal and coal mining (Alemu et al., 2016; Johnson and Sánchez-Andrea, 2019; Lens et al., 1998). The biotechnology of enriching and enhancing sulfate-reducing bacteria (SRB) could be a strategy for industrial and municipal sulfate-rich wastewater treatment applications (Hao et al., 2014). In anaerobic digestion processes, sulfate can be reduced to sulfide by SRB with various electron donors, and sulfide can be partially oxidized to elemental sulfur and recovered for valorization of waste effluents.

Glycerol, a by-product of the biodiesel industry, is an organic waste that can be valorized by the fermentation process to produce biogas, and it is also considered to be an electron donor for sulfate reduction (Mora et al., 2020a). Many studies have applied mathematical modeling to describe the bioconversion of glycerol. Mathematical models were set up to describe the pathways and kinetics of anaerobic fermentation of glycerol in batch and continuous cultures in terms of metabolic rates, enzyme-catalytic kinetics or yields, considering the consumption or production rates of glycerol, CO<sub>2</sub>, H<sub>2</sub>, formic acid, acetic acid, lactic acid, succinic acid, ethanol, 1,3-propanediol and 2,3-butanediol (Beschkov et al., 2012; Sun et al., 2008; Wang et al., 2012; Zeng et al., 1996). In addition to the products described above, the bioconversion of glycerol can also produce poly(3-hydroxybutyrate). The polymer concentration was evaluated and predicted by a mathematical model proposed by Das and Grover (2018). Moreover, Wang et al. (2009) proposed an improved model to describe a multistage simulation of cell growth and glycerol fermentation in batch cultures for prediction in the lag, exponential and stationary phases. In addition to the application of modeling in the batch experiment described above, model analysis of continuous bench-scale reactors was conducted using glycerol as organic load to describe methane production and microbial dynamics (Jensen et al., 2014).

Mathematical modeling has proven to be an important bioprocess engineering tool, which can be used to understand and evaluate the complexity of the sulfate reduction process in anaerobic digestion and facilitate process optimization (Batstone et al., 2006, 2015). Halkjaer Nielsen (1987) firstly discussed the sulfate kinetics in an anaerobic, sulfate-reducing biofilm reactor. A structured and comprehensive dynamic model was developed to evaluate methanogenesis and sulfate reduction in a CSTR by two groups of microorganisms, including methanogens and SRB (Gupta et al., 1994b). Later, an integrated mathematical model was developed to investigate the competition between SRB and methanogens in anaerobic reactors, in which SRB were divided into acetogenic SRB, acetotrophic SRB and hydrogenotrophic SRB (Kalyuzhnyi and Fedorovich, 1997, 1998). Fedorovich et al. (2003) first extended the Anaerobic Digestion Model No.1 (ADM1) with sulfate reduction processes, which separated SRB according to electron donors, including butyrate, propionate, acetate and H<sub>2</sub>. Afterwards, extension of the ADM1 model with sulfate reduction process was widely applied to sulfate-rich wastewater to simultaneously treat different types of organic compounds, such as cane-molasses vinasse (Barrera et al., 2015), glucose (Sun et al., 2021), lactate (Xu et al., 2017). These studies focused on the fermentation of organic compounds to produce volatile fatty acids (VFAs), but some organic compounds such as glycerol produce not only VFAs, but also ethanol or 1,3-propanediol. Ethanol was used as the organic substrate to investigate the competitive dynamics of anaerobes in anaerobic bioreactors (Chen et al., 2019; Sun et al., 2016). However, little information is available on 1,3-propanediol use as electron donors for sulfate reduction in model simulation.

Dinkel et al. (2010) developed a kinetic model to describe anaerobic degradation of glycerol with sulfate reduction by SRB, which mentioned that glycerol was directly fermented to acetate by acetogenic bacteria or SRB. However, in addition to acetate, other organic compounds (propionate, ethanol and 1,3-propanediol) were also produced in the process of glycerol dissimilation (Biebl et al., 1998; Cheng et al., 2007; González-Pajuelo et al., 2005; Saint-Amans et al., 1994; Wu et al., 2011; Yang et al., 2018). The model that



considered the direct degradation of glycerol to acetate cannot predict other intermediate metabolites. Therefore, a model describing sulfate reduction and glycerol fermentation with multi-intermediates is necessary.

The sulfate reduction using glycerol as the electron donor was investigated in Chapter 6, and its mechanism was first proposed, as shown in Figure 6.9. In the mechanism, glycerol was fermented to 1,3-propanediol, ethanol, formate, propionate and acetate. SRB reduced sulfate using formate, propionate, ethanol and 1,3-propanediol as electron donors, in which 1,3-propanediol was oxidized to acetate and propionate. However, there are still some doubts about the pathway of glycerol fermentation and 1,3-propanediol oxidation. 3-hydroxypropionate (3HP) can be a direct product of glycerol fermentation via a reductive pathway (Qatibi et al., 1998). When the 1,3-propanediol was the electron donor to reduce sulfate, 3HP was described as an intermediate product (Qatibi et al., 1991b). In order to further explore the mechanisms involved in the sulfidogenic UASB, the mechanism originally proposed in Chapter 6 for glycerol fermentation coupled to sulfate reduction was modified as shown in Figure 7.1. Three mechanisms were proposed herein to be simulated and verified through modeling. Mechanism I refers to the metabolism pathway proposed in Chapter 6 (Figure 7.1A). Corresponding reactions are shown from Eq.7.1 to Eq.7.11. As 3HP may be an intermediate product of 1,3-propanediol degradation in presence of sulfate (Qatibi et al., 1991a, 1991b), Mechanism II modifies the possible pathway of 1,3-propanediol degradation with sulfate reduction (Figure 7.1B), and the reactions are described from Eq.7.13 to Eq.7.15. Since 3HP was also an intermediate of glycerol fermentation (Qatibi et al., 1998), Mechanism III considers the pathway of glycerol fermentation to directly produce 3HP (Figure 7.1C), of which reaction is presented as Eq.7.12.

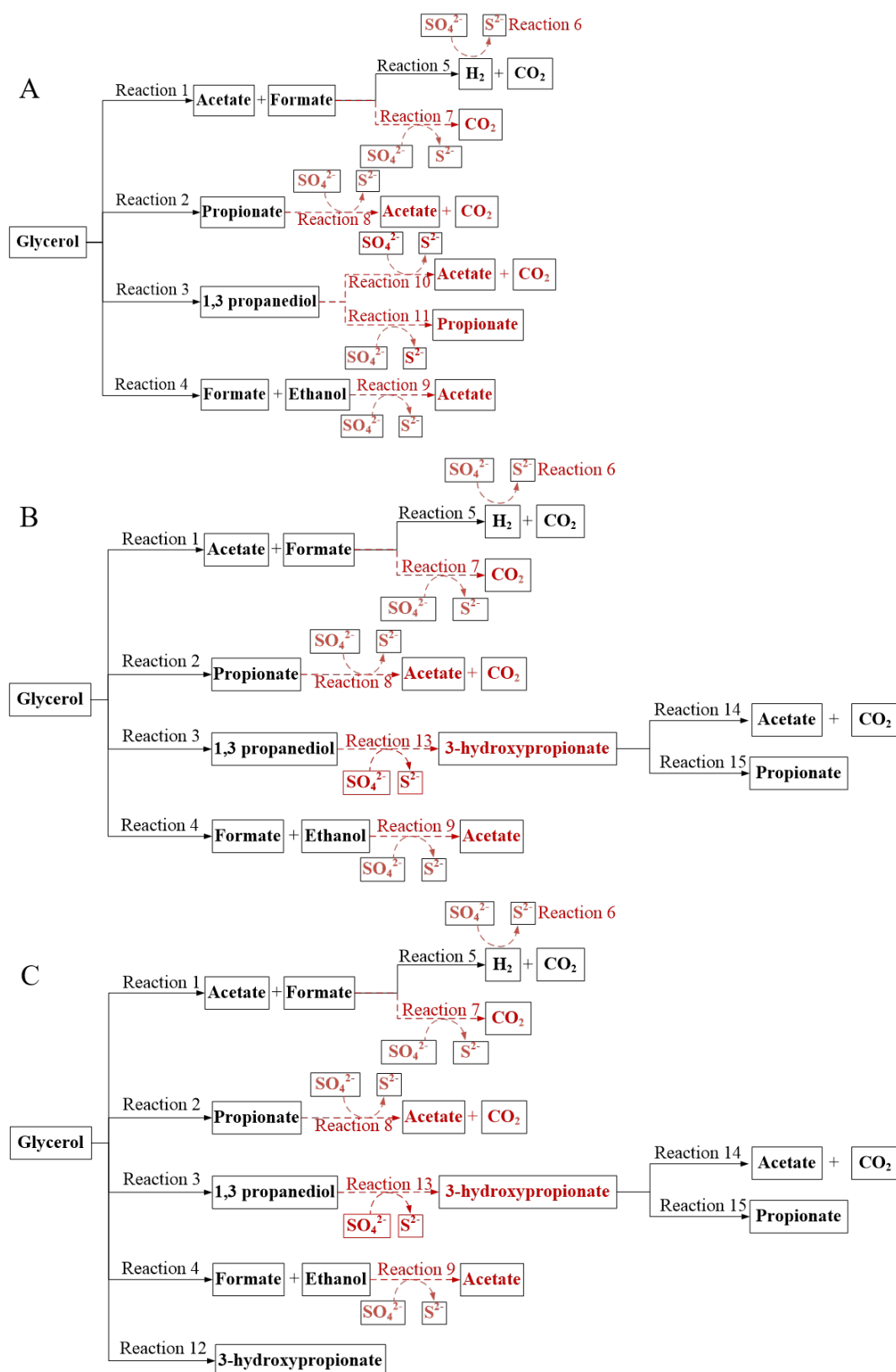
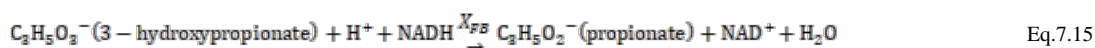
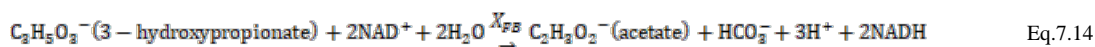
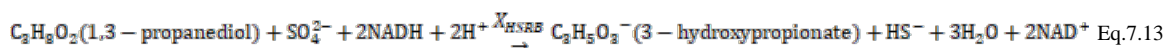
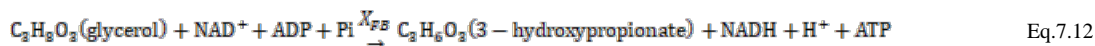
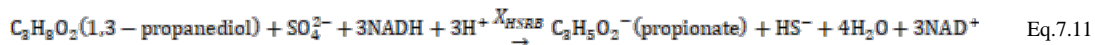
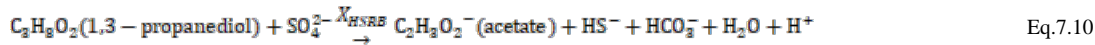
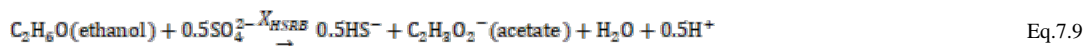
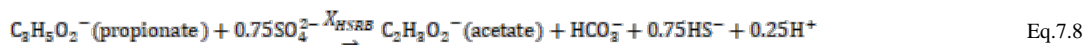
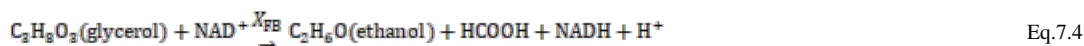
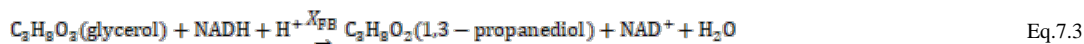
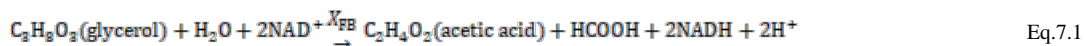


**Figure 7.1.** The potential mechanism of biodegradation of glycerol and sulfate reduction without methane production in Mechanism I (A), Mechanism II (B) and Mechanism III (C). Black and continuous lines represent the fermentation process, while red and discontinuous lines represent the sulfidogenic process.

The fermentation process and sulfate reduction of three mechanisms considered herein are summarized as follows:



Based on the three proposed mechanisms, a mathematical model was developed to investigate the process of sulfate reduction and the pathway of glycerol degradation in anaerobic digestion, and to evaluate the kinetic parameters for the degradation of different electron donors.

## 7.2 Materials and methods

### 7.2.1 Experimental data

To investigate the mechanism of sulfate reduction process using glycerol as the electron donor, the batch activity tests performed and described in Chapter 6 were modelled in Chapter 7. The experimental observations of Chapter 6 were used for model calibration and validation. Activity tests of single organic compounds (including propionate, ethanol, 1,3-propanediol and formate) in section 6.3.2 of Chapter 6 were used for sulfate reduction parameters calibration. Activity tests in absence and presence of sulfate with glycerol as a carbon source in section 6.3.1 of Chapter 6 were used for glycerol fermentation parameters calibration and sulfate reduction parameters validation.

### 7.2.2 Model development

Based on experimental observations discussed in Chapter 6, glycerol was not used as a direct electron donor by SRB, but glycerol was firstly fermented to produce simpler intermediates and then SRB reduced sulfate with these intermediate products. According to experimental observations in Chapter 6, butanol, butyrate and acetate were not considered as electron donors for SRB in the glycerol fermentation process under sulfidogenic conditions, while ethanol, propionate and 1,3-propanediol were considered as electron donors for the incomplete oxidation pathway. Formate and hydrogen were also considered as electron donors for sulfate reduction process. Kinetics were based on the following assumptions:

1. The fermentation and sulfate reduction process were carried out by three types of microorganisms:  $X_{FB}$ , Fermentative bacteria;  $X_{HSRB}$ , Heterotrophic sulfate reducing bacteria;  $X_{ASRB}$ , Autotrophic sulfate reducing bacteria. Each reaction is carried out by its specific microbial group ( $X_{FB}$ ,  $X_{ASRB}$  and  $X_{HSRB}$ ), as described from Eq.7.1 to Eq.7.15. The biomass fractions of the three types of microorganisms (77.6% of  $X_{FB}$ , 13.6% of  $X_{ASRB}$ , 8.8% of  $X_{HSRB}$ ) were set up based on microbial population identification, analyzed in Chapter 6 (Figure 6.2).

Genus *Desulfobulbus* and *Desulfovibrio*, accounting for 22.4%, were SRB detected in the sludge, where the distribution of autotrophic sulfate reducing bacteria (ASRB) (13.6%) and heterotrophic sulfate reducing bacteria (HSRB) (8.8%) were estimated as recommended (Kalyuzhnyi and Fedorovich, 1998).

2. The substrate consumption rates followed a Monod-type kinetic equation. Previous studies considered a dual-substrate Monod-type kinetic for  $X_{ASRB}$  and  $X_{HSRB}$  which includes electron donors (organic carbon compounds or  $H_2$ ) and the electron acceptor (sulfate) (Chen et al., 2019; Fedorovich et al., 2003) as given in the following equation:

$$R_j = k_{m,j} * \frac{S_i}{k_{s,i} + S_i} * \frac{S_{SO_4^{2-}}}{k_{SO_4^{2-},i} + S_{SO_4^{2-}}} * X_k \quad \text{Eq.7.16}$$

Where  $R_j$  is the kinetic rate of process  $j$ ,  $mg\ C\ L^{-1}\ h^{-1}$ , or  $mg\ S\ L^{-1}\ h^{-1}$ ;  $k_{m,j}$  is the maximum specific uptake rate of process  $j$ ,  $mg\ C\ mg\ VSS^{-1}\ h^{-1}$ , or  $mg\ H_2\ mg\ VSS^{-1}\ h^{-1}$ ;  $S_i$  is the concentration of substrate component  $i$ ,  $mg\ C\ L^{-1}$ , or  $mg\ H_2\ L^{-1}$ ;  $k_{s,i}$  is half saturation coefficient for the uptake of substrate component  $i$ ,  $mg\ C\ L^{-1}$ , or  $mg\ H_2\ L^{-1}$ ;  $S_i$  is the concentration of electron donor “ $i$ ”,  $mg\ C\ L^{-1}$ , or  $mg\ H_2\ L^{-1}$ ;  $k_{SO_4^{2-},i}$  is half saturation coefficient for the uptake of sulfate,  $mg\ S\ L^{-1}$ ;  $S_{SO_4^{2-}}$  is the concentration of sulfate,  $mg\ S\ L^{-1}$ ;  $X_k$  is the concentration of microbial trophic group  $k$ ,  $mg\ VSS\ L^{-1}$ .

The half saturation coefficient of sulfate for  $X_{ASRB}$  and  $X_{HSRB}$  was  $3.2\ mg\ S\ L^{-1}$  and  $6.7\ mg\ S\ L^{-1}$ , respectively, according to Fedorovich et al. (2003). In this work, the sulfate concentration in all the experiments for modeling in Chapter 6 were higher than  $30\ mg\ S\ L^{-1}$  at the end of the experiment, far higher than the half saturation coefficient for sulfate. Under carbon limiting conditions, kinetic equations were considered only dependant on organic electron donors for  $X_{FB}$ ,  $X_{ASRB}$ ,  $X_{HSRB}$  in this work:

$$P_j = k_{m,j}' * \frac{S_i}{k_{s,i} + S_i} * X_k \quad \text{Eq.7.17}$$

3. The effect of pH on the growth rates was not included, since  $K_2HPO_4$  was used in

this work as pH buffer in all the experiments for modeling. The pH ranged between 7.2 and 8.4 during the cultivation. Sulfidogenic activity can be carried out in a wide pH range (5.0-10.0), and the optimal pH has been reported in the range of pH 7.0-8.5 (Gutierrez et al., 2009; Visser et al., 1996).

4. The inhibition effects of products (such as H<sub>2</sub>S), substrates in the degradation process were also considered in previous models (Kaur et al., 2013; Zeng et al., 1994). Kalyuzhnyi and Fedorovich (1998) described 50% inhibitory concentration of free H<sub>2</sub>S for FB, ASRB and HSRB were 518, 268, 517 mg S-H<sub>2</sub>S L<sup>-1</sup>, respectively. Free H<sub>2</sub>S detected in the experiments of Chapter 6 ranged from 0 to 76 mg S-H<sub>2</sub>S L<sup>-1</sup>. Thus, free H<sub>2</sub>S inhibition in this work was not considered. The maximum tolerance concentrations for *Clostridium butyricum* and *Klebsiella pneumoniae* are 0.35 g L<sup>-1</sup> for undissociated acetic acid, 10.1 g L<sup>-1</sup> for total butyric acid, 16.6 g L<sup>-1</sup> for ethanol, 71.4 g L<sup>-1</sup> for 1,3-propanediol and 187.6 g L<sup>-1</sup> for glycerol, respectively (Zeng et al., 1994). These values are far beyond the concentration used in this work, so the inhibitory effect of substrate was also not considered.

According to biochemical processes mentioned before and the 14 components monitored in the experiments, the biochemical rate coefficients ( $v_{i,j}$ ) and kinetic rate equations ( $R_j$ ) are listed in Table 7.1 in a complete format.

**Table 7.1.** Biochemical rate coefficients ( $v_{i,j}$ ) and kinetic rate equations ( $R_j$ ) matrix.

Component →	i	1	2	3	4	5	6	7	8	9	10	11	12	13	14	Rate ( $R_j$ , mg C L <sup>-1</sup> h <sup>-1</sup> )
j	Process ↓	$S_{gly}$	$S_{for}$	$S_{H_2}$	$S_{pro}$	$S_{ace}$	$S_{eth}$	$S_{1,3PDO}$	$S_{IC}$	$S_{sulfate}$	$S_{sulfide}$	$S_{3HP}$	$X_{FB}$	$X_{ASRB}$	$X_{HSRB}$	
1	Uptake of glycerol by FB	-1	1/3			2/3							$Y_{FB}$			$k_{m,gly1} * \frac{S_{gly}}{k_{s,gly} + S_{gly}} * X_{FB}$
2	Uptake of glycerol by FB	-1			1								$Y_{FB}$			$k_{m,gly2} * \frac{S_{gly}}{k_{s,gly} + S_{gly}} * X_{FB}$
3	Uptake of glycerol by FB	-1						1					$Y_{FB}$			$k_{m,gly3} * \frac{S_{gly}}{k_{s,gly} + S_{gly}} * X_{FB}$
4	Uptake of glycerol by FB	-1	1/3			2/3							$Y_{FB}$			$k_{m,gly4} * \frac{S_{gly}}{k_{s,gly} + S_{gly}} * X_{FB}$
5	Uptake of formate by FB		-1	1/6					1				$Y_{FB}$			$k_{m,for,FB} * \frac{S_{for}}{k_{s,for,FB} + S_{for}} * X_{FB}$
6	Uptake of H <sub>2</sub> by ASRB			-1						-4	4			$Y_{ASRB}$		$k_{m,H_2} * \frac{S_{H_2}}{k_{s,H_2,ASRB} + S_{H_2}} * X_{ASRB}$
7	Uptake of formate by HSRB			-1					1	-2/3	2/3				$Y_{HSRB}$	$k_{m,for,HSRB} * \frac{S_{for}}{k_{s,for,HSRB} + S_{for}} * X_{HSRB}$
8	Uptake of propionate by HSRB					-1/2/3			1/3	-2/3	2/3				$Y_{HSRB}$	$k_{m,pro} * \frac{S_{pro}}{k_{s,pro,HSRB} + S_{pro}} * X_{HSRB}$
9	Uptake of ethanol by HSRB					1	-1			-2/3	2/3				$Y_{HSRB}$	$k_{m,eth} * \frac{S_{eth}}{k_{s,eth,HSRB} + S_{eth}} * X_{HSRB}$
10	Uptake of 1,3-propanediol by HSRB (produce acetate)					2/3		-1	1/3	-8/9	8/9				$Y_{HSRB}$	$k_{m,1,3PDO1} * \frac{S_{1,3PDO}}{k_{s,1,3PDO1,HSRB} + S_{1,3PDO}} * X_{HSRB}$
11	Uptake of 1,3-propanediol by HSRB (produce propionate)				1			-1		-8/9	8/9				$Y_{HSRB}$	$k_{m,1,3PDO2} * \frac{S_{1,3PDO}}{k_{s,1,3PDO2,HSRB} + S_{1,3PDO}} * X_{HSRB}$

12	Uptake of glycerol by FB	-1										1	$Y_{FB}$			$k_{m, glyS} * \frac{S_{gly}}{k_{s, gly} + S_{gly}} * X_{FB}$	
13	Uptake of 1,3-propanediol by HSRB (produce 3HP)							-1		-8/9	8/9	1		$Y_{HSRB}$		$k_{m, 13PDO2} * \frac{S_{13PDO}}{k_{s, 13PDO2, HSRB} + S_{13PDO}} * X_{HSRB}$	
<b>Component →</b>		<b>i</b>	<b>1</b>	<b>2</b>	<b>3</b>	<b>4</b>	<b>5</b>	<b>6</b>	<b>7</b>	<b>8</b>	<b>9</b>	<b>10</b>	<b>11</b>	<b>12</b>	<b>13</b>	<b>14</b>	<b>Rate (<math>\rho_j</math>, mg C L<sup>-1</sup> h<sup>-1</sup>)</b>
<b>j</b>	<b>Process ↓</b>	$S_{gly}$	$S_{for}$	$S_{H_2}$	$S_{pro}$	$S_{ace}$	$S_{eth}$	$S_{13PDO}$	$S_{IC}$	$S_{sulfate}$	$S_{sulfide}$	$S_{3HP}$	$X_{FB}$	$X_{ASRB}$	$X_{HSRB}$		
14	Uptake of 3HP by FB (produce acetate)					2/3				1/3			-1			$Y_{HSRB}$	$k_{m, 3HP1} * \frac{S_{3HP}}{k_{s, 3HP, FB1} + S_{3HP}} * X_{FB}$
15	Uptake of 3HP by FB (produce propionate)				1								-1			$Y_{HSRB}$	$k_{m, 3HP2} * \frac{S_{3HP}}{k_{s, 3HP, FB2} + S_{3HP}} * X_{FB}$
			Glycerol (mg C L <sup>-1</sup> )	Formate (mg C L <sup>-1</sup> )	H <sub>2</sub> (mg H <sub>2</sub> L <sup>-1</sup> )	Propionate (mg C L <sup>-1</sup> )	Acetate (mg C L <sup>-1</sup> )	Ethanol (mg C L <sup>-1</sup> )	1,3-propanediol (mg C L <sup>-1</sup> )	IC (mg C L <sup>-1</sup> )	Sulfate (mg S L <sup>-1</sup> )	Sulfide (mg S L <sup>-1</sup> )	3-hydroxypropionate (mg C L <sup>-1</sup> )	FB (mg VSS L <sup>-1</sup> )	ASRB (mg VSS L <sup>-1</sup> )	HSRB (mg VSS L <sup>-1</sup> )	



### 7.2.3 Model calibration and validation

The procedure carried out for the estimation of model parameters and determination of the mechanisms linked to glycerol fermentation coupled to sulfate reduction is illustrated in Figure 7.2. The procedure involves five steps as follows.

In Step 1, kinetic parameters were set up, including half saturation coefficient ( $k_s$ ) and biomass yields ( $Y$ ). Model parameters (biomass yield, half saturation coefficient) are referred and listed in Table 7.2. Among them, half saturation coefficient for 1,3-propanediol ( $k_{s,13PDO}$ ) by HSRB was not found in previous studies. In this work, the initial value of  $k_{s,13PDO}$  was selected as  $45 \text{ mg C L}^{-1}$  based on that reported for ethanol (Gonzalez-Silva et al., 2009) as both ethanol and 1,3-propanediol belong to primary alcohols and can be degraded by HSRB (Kalyuzhnyi and Fedorovich, 1998).

**Table 7.2.** Initial inputs of stoichiometric and kinetic parameters used in the model.

Parameter	Name	Value	Unit	Reference
$Y_{FB}$	Yield of FB	0.132	$\text{g VSS g C}^{-1}$	Barrera et al., 2015
$Y_{HSRB}$	Yield of HSRB	0.077	$\text{g VSS g C}^{-1}$	Barrera et al., 2015
$Y_{ASRB}$	Yield of ASRB	0.288	$\text{g VSS g H}_2^{-1}$	Barrera et al., 2015
<b>Fermentation process</b>				
$k_{s,for,FB}$	Half saturation coefficient for the uptake of formate by FB	0.03	$\text{mg C L}^{-1}$	Dornseiffer et al., 1995
$k_{s,gly}$	Half saturation coefficient for the uptake of glycerol by FB	1.96	$\text{mg C L}^{-1}$	Zeng et al., 1994
<b>Sulfate reduction process</b>				
$k_{s,pro}$	Half saturation coefficient for the uptake of propionate by HSRB	79	$\text{mg C L}^{-1}$	Kalyuzhnyi and Fedorovich, 1998
$k_{s,for,HSRB}$	Half saturation coefficient for the uptake of formate by HSRB	53	$\text{mg C L}^{-1}$	Kalyuzhnyi and Fedorovich, 1998
$k_{s,eth}$	Half saturation coefficient for the uptake of ethanol by HSRB	45	$\text{mg C L}^{-1}$	Gonzalez-Silva et al., 2009
$k_{s,13PDO}$	Half saturation coefficient for the uptake of 1,3-propanediol by HSRB	45	$\text{mg C L}^{-1}$	In this work
$k_{s,H_2}$	Half saturation coefficient for the uptake of $\text{H}_2$ by ASRB	0.00625	$\text{mg H}_2 \text{ L}^{-1}$	Kalyuzhnyi and Fedorovich, 1998

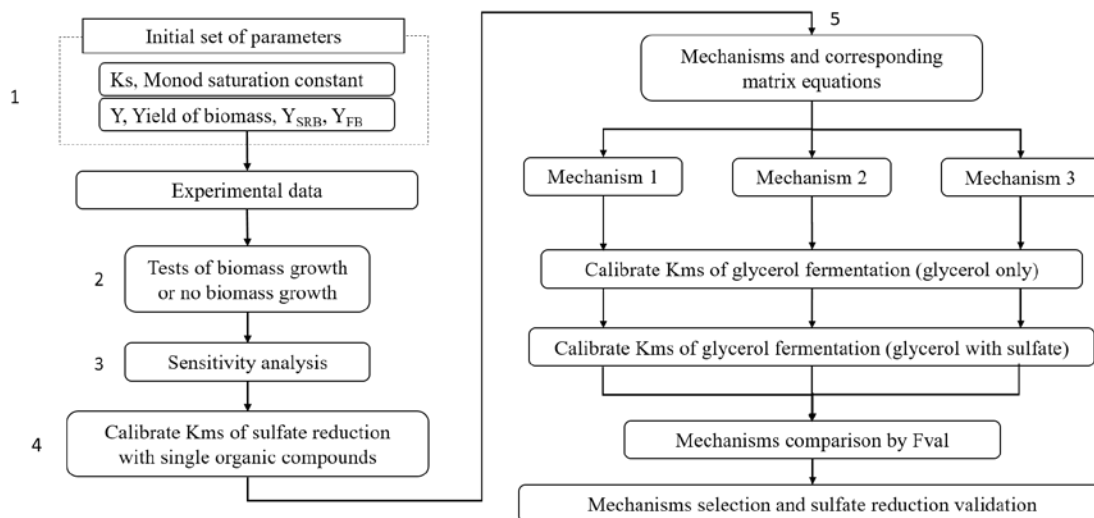


**Figure 7.2.** Generalized procedure for parameters estimation, calibration and mechanisms selection for sulfate reduction in this work.

In Step 2, the model was tested to verify if biomass growth was significant in the batch activity tests and, thus, a variable biomass concentration should be included in the model. Two-tailed Student's t-test was also used to statistically evaluate the significant difference between experimental data and results obtained from model fitting. P value < 0.05 was considered to be statistically significant.

In Step 3, a sensitivity analysis was performed to identify the most sensitive kinetic parameters in these biochemical processes. Sensitivity analysis can prioritize and analyze the impact of model parameters on process variables, thereby providing effective information for model calculation. Sensitivity functions were described by Dochain and Vanrolleghem (2001) to determine the significance of kinetic parameters, which used the finite difference approximation. Sensitivity functions have been applied in previous studies, which is based on the change of measurable process variables under the disturbance of model parameters caused by a perturbation value  $\delta$  (Barrera et al., 2015; Chen et al., 2019). The perturbation  $\delta$  of each parameter was chosen and the sensitivity of output caused by the perturbation of parameters is calculated as follows:

$$\Gamma_{i,j} = \frac{\partial y_j / y_j}{\partial \theta_i / \theta_i} = \frac{(y_j(\theta_i + \delta \cdot \theta_i) - y_j(\theta_i)) / y_j(\theta_i)}{(\delta \cdot \theta_i) / \theta_i} \quad \text{Eq.7.18}$$

Where  $\Gamma_{i,j}$  is the dimensionless sensitivity value of output  $y_j$  with respect to the kinetic

parameters  $\theta_i$  (such as  $k_{m,j}$ ,  $k_s$ );  $\theta_i + \delta \cdot \theta_i$  is the perturbation parameter value. The sensitivity values for each parameter were calculated as  $\sum \Gamma_{i,j}$  (show as % in respect to the total  $\sum \sum \Gamma_{i,j}$ ) and arranged in descending order.

In Step 4, the maximum specific uptake rates ( $k_{m,j}$ ) for sulfate reduction were calibrated from activity tests with single organic compounds, including formate, propionate, ethanol and 1,3-propanediol (data from section 6.3.2). The stoichiometry corresponding to propionate and ethanol are Eq.7.8 ( $k_{m,pro}$ ) and Eq.7.9 ( $k_{m,eth}$ ), respectively. The stoichiometry corresponding to formate include Eq.7.5 ( $k_{m,for,FB}$ ), Eq.7.6 ( $k_{m,H_2}$ ) and Eq.7.7 ( $k_{m,for,HSRB}$ ). When 1,3-propanediol is used as an electron donor, the sulfate reduction stoichiometry corresponds to Eq.7.10 ( $k_{m,13PDO1}$ ) and Eq.7.11 ( $k_{m,13PDO2}$ ) in Mechanism I, and corresponds to Eq.7.13 ( $k_{m,13PDO3}$ ), Eq.7.14 ( $k_{m,3hp1}$ ) and Eq.7.15 ( $k_{m,3hp2}$ ) in Mechanisms II and III.

In Step 5, the maximum specific uptake rates ( $k_{m,j}$ ) for glycerol fermentation were calibrated from activity tests with glycerol as the carbon source (data from section 6.3.1). Equations Eq.7.1 ( $k_{m,gly1}$ ), Eq.7.2 ( $k_{m,gly2}$ ), Eq.7.3 ( $k_{m,gly3}$ ), Eq.7.4 ( $k_{m,gly4}$ ) provide the stoichiometry related to the fermentation pathway of glycerol in Mechanism I and II. Mechanism III included the fermentation of glycerol to produce 3HP, corresponding to Eq.7.12 ( $k_{m,gly5}$ ). In this case, calibration was performed for each one of the three proposed mechanisms. This step also determined the optimal mechanism of the glycerol degradation pathway (I, II or III) by comparing the objective function value (Fval) of each one of the three mechanisms as well as validated the kinetic rates of sulfate reduction processes calibrated in Step 4 using data from single substrate batch tests.

Fval is the minimum value of the objective function in each simulation. The smaller the value, the smaller the difference between the experiment and the model. Fminsearch function, a MATLAB algorithm based on a multidimensional unconstrained nonlinear minimization (Nelder-Mead), was used to minimize the error between model and

experimental data and find out  $F_{val}$  that lead to optimum model parameters, as given in Eq.7.19.

$$F_{val} = \sum_{i=1}^N |C_E - C_M| \quad \text{Eq.7.19}$$

$C_E$  is the concentration of experimental data, which includes all sulfate reduction experiments with glycerol, formate, propionate, ethanol and 1,3-propanediol as the carbon source, and fermentation experiments with glycerol as the carbon source;  $C_M$  is the concentration predicted by the model; and  $N$  is the total number of data sets, including organic carbon compounds and sulfate in all the experiments for model fitting. The set of the differential equations was solved by ode45 function (based on Runge-Kutta method with a variable time step) in MATLAB. All simulations and calibrations were implemented in MATLAB 2015a.

Consequently, the optimal mechanism obtained through the above steps was analyzed by two-tailed Student's t-test between the experimental data and the modeling results.

#### 7.2.4 Confidence interval determination by Fisher Information Matrix

In order to evaluate the calibrated parameters and the quality of the estimation, the confidence intervals of estimated kinetic parameters were calculated based on the Fisher Information Matrix (FIM) method (Dochain and Vanrolleghem, 2001; Guisasola et al., 2006). The FIM method is calculated as the inverse of the covariance matrix of the measurement noise, with a relationship that higher FIM value and lower standard errors estimated. Since the FIM method takes into account the output sensitivity functions and the measurement errors, it well estimated the quantity and quality of experimental data. The FIM method has been widely applied to evaluate the reliability of estimated parameters in modeling of biofiltration on gas treatment (Dorado et al., 2008), aerobic biological sulfide oxidation (Mora et al., 2016), and sulfate-rich wastewater treatment (Barrera et al., 2015).

## **7.3 Results and discussion**

### **7.3.1 Parameters estimation and sensitivity analysis**

Microbial biomass growth was estimated in 120 h batch tests performed with glycerol as reported in section 6.3.1.1. Figure 7.3 shows the experimental data and the modelled profiles both considering the influence of biomass growth or no-biomass growth for the three proposed mechanisms. In mechanism I (Figure 7.3A and 7.3B), Student's t-test showed that there was no significant difference between the experimental data and the model predictions whether the biomass growth was considered or not. Same results were observed in mechanism II (Figure 7.3C and 7.3D). In mechanism III, when biomass growth was considered, there was a significant difference between the experimental data and model prediction of ethanol (Figure 7.3E), but overall there was not a significant difference when biomass yield was not considered (Figure 7.3F). Therefore, biomass growth was not considered to model the batch tests in this work.

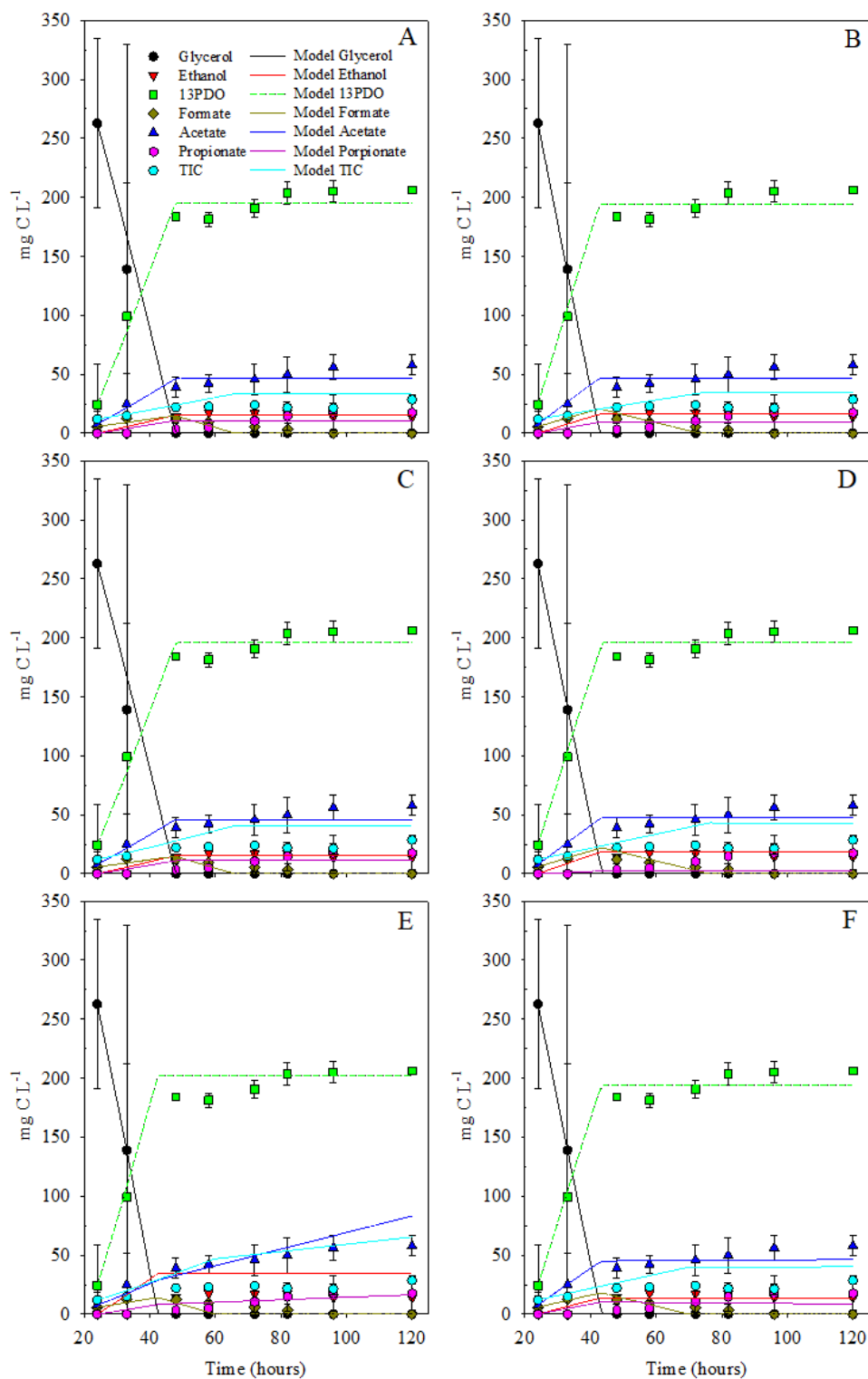


**Figure 7.3.** Experimental and simulated profiles of glycerol fermentation in Mechanism I (A, B), Mechanism II (C, D) and Mechanism III (E, F). A, C and E considered biomass yield; B, D and F considered no biomass yield. Data points illustrate the experimental data. Smooth curves represent model predictions.

In order to identify the most sensitive kinetic parameters, a sensitivity analysis was performed for the three mechanisms proposed and the experimental data from activity tests with glycerol as electron donor and sulfate as electron acceptor (data from Figure 6.1C, 6.1D and 6.1E). Output variables selected to assess the sensitivity were the concentrations of sulfate, TDS, propionate, acetate, formate, H<sub>2</sub>, TIC, 1-3PD, ethanol, 3HP and glycerol along the batch activity test. The parameters of the sensitivity analysis included all half saturation coefficients and maximum specific uptake rates involved in the three proposed mechanisms. The perturbation factor ( $\delta$ ), which is defined as the percentage change of a model parameter with respect to a reference value of that parameter, was set to  $\pm 10\%$ .

Simulations carried out allowed ranking the model parameters in descending order of sensitivity. Table 7.3 shows that the maximum specific uptake rates had a higher impact on process variables than half saturation coefficients in general.

**Table 7.3.** Model sensitive parameters arranged in descending order from the first to the last in Mechanism I, II and III (the perturbation factor was set as  $\pm 10\%$ ).

		Parameters					
Mechanism I ( $\delta = 10\%$ )	$k_{m,gly4}$	$k_{s,eth}$	$k_{m,gly3}$	$k_{m,eth}$	$k_{m,for,FB}$	$k_{m,H2}$	$k_{m,13PDO1}$
	$k_{m,gly1}$	$k_{m,13PDO2}$	$k_{m,pro}$	$k_{s,pro}$	$k_{m,gly2}$	$k_{s,13PDO}$	$k_{m,for,HSRB}$
	$k_{s,for,HSRB}$	$k_{s,H2}$	$k_{s,gly}$	$k_{s,for,FB}$			
Mechanism I ( $\delta = -10\%$ )	$k_{m,eth}$	$k_{m,gly3}$	$k_{m,gly4}$	$k_{m,for,FB}$	$k_{m,H2}$	$k_{m,13PDO1}$	$k_{s,eth}$
	$k_{m,gly1}$	$k_{m,13PDO2}$	$k_{m,pro}$	$k_{s,pro}$	$k_{m,gly2}$	$k_{s,13PDO}$	$k_{m,for,HSRB}$
	$k_{s,for,HSRB}$	$k_{s,H2}$	$k_{s,gly}$	$k_{s,for,FB}$			
Mechanism II ( $\delta = 10\%$ )	$k_{m,gly3}$	$k_{m,gly4}$	$k_{s,eth}$	$k_{m,13PDO3}$	$k_{m,eth}$	$k_{m,for,FB}$	$k_{m,H2}$
	$k_{s,3HP,FB1}$	$k_{m,gly1}$	$k_{m,3HP1}$	$k_{s,pro}$	$k_{m,for,HSRB}$	$k_{m,3HP2}$	$k_{m,pro}$
	$k_{s,for,HSRB}$	$k_{m,gly2}$	$k_{s,13PDO}$	$k_{s,3HP,FB2}$	$k_{s,for,FB}$	$k_{s,gly}$	$k_{s,H2}$
Mechanism II ( $\delta = -10\%$ )	$k_{m,eth}$	$k_{m,13PDO3}$	$k_{m,gly3}$	$k_{m,gly4}$	$k_{m,for,FB}$	$k_{m,H2}$	$k_{s,eth}$
	$k_{m,gly1}$	$k_{m,3HP1}$	$k_{s,3HP,FB1}$	$k_{m,pro}$	$k_{m,for,HSRB}$	$k_{s,pro}$	$k_{m,3HP2}$
	$k_{s,for,HSRB}$	$k_{m,gly2}$	$k_{s,13PDO}$	$k_{s,3HP,FB2}$	$k_{s,for,FB}$	$k_{s,gly}$	$k_{s,H2}$
Mechanism III ( $\delta = 10\%$ )	$k_{s,eth}$	$k_{m,gly3}$	$k_{m,gly4}$	$k_{m,13PDO3}$	$k_{m,eth}$	$k_{m,gly5}$	$k_{s,3HP,FB1}$
	$k_{m,for,FB}$	$k_{m,H2}$	$k_{m,gly1}$	$k_{s,for,HSRB}$	$k_{s,for,FB}$	$k_{m,for,HSRB}$	$k_{m,3HP1}$
	$k_{s,pro}$	$k_{m,pro}$	$k_{m,3HP2}$	$k_{m,gly2}$	$k_{s,H2}$	$k_{s,gly}$	$k_{s,13PDO}$
	$k_{s,3HP,FB2}$						
Mechanism III ( $\delta = -10\%$ )	$k_{m,H2}$	$k_{m,for,FB}$	$k_{m,gly3}$	$k_{m,eth}$	$k_{m,13PDO3}$	$k_{m,gly5}$	$k_{s,for,FB}$
	$k_{m,gly4}$	$k_{s,3HP,FB1}$	$k_{s,eth}$	$k_{m,3HP2}$	$k_{s,H2}$	$k_{s,for,HSRB}$	$k_{s,gly}$
	$k_{m,gly2}$	$k_{s,13PDO}$	$k_{s,pro}$	$k_{m,for,HSRB}$	$k_{m,pro}$	$k_{m,3HP1}$	$k_{m,gly1}$
	$k_{s,3HP,FB2}$						

The sensitivity values ( $\sum \Gamma_{ij} / \sum \sum \Gamma_{ij}$ , %) for the four most sensitive parameters in each mechanism are shown in Figure 7.4, when the perturbation factor  $\delta$  was set to 10%. Figure 7.4 shows that  $k_{m,gly4}$ ,  $k_{m,gly3}$ ,  $k_{m,eth}$  and  $k_{s,eth}$  were the most sensitive parameters for mechanism I, which is related to reactions in Eq.7.3, Eq.7.4 and Eq.7.9. In Mechanism I, II and III,  $k_{m,gly3}$ ,  $k_{m,gly4}$ ,  $k_{s,eth}$  and  $k_{m,13PDO3}$  were the most sensitive parameters, which is related to reactions Eq.7.3, Eq.7.4, Eq.7.9 and Eq.7.13. Figure 7.4 also shows the sensitive model parameters for each process variable. The process variable  $S_{eth}$  was highly sensitive to parameters  $k_{m,eth}$  and  $k_{s,eth}$ . Parameters  $k_{m,gly3}$  and  $k_{m,gly4}$  simultaneously affected the process variable  $S_{eth}$  and  $S_{13PDO}$ , while  $k_{m,13PDO3}$  mainly affected the process variable  $S_{3HP}$  and  $S_{13PDO}$  at the same time.



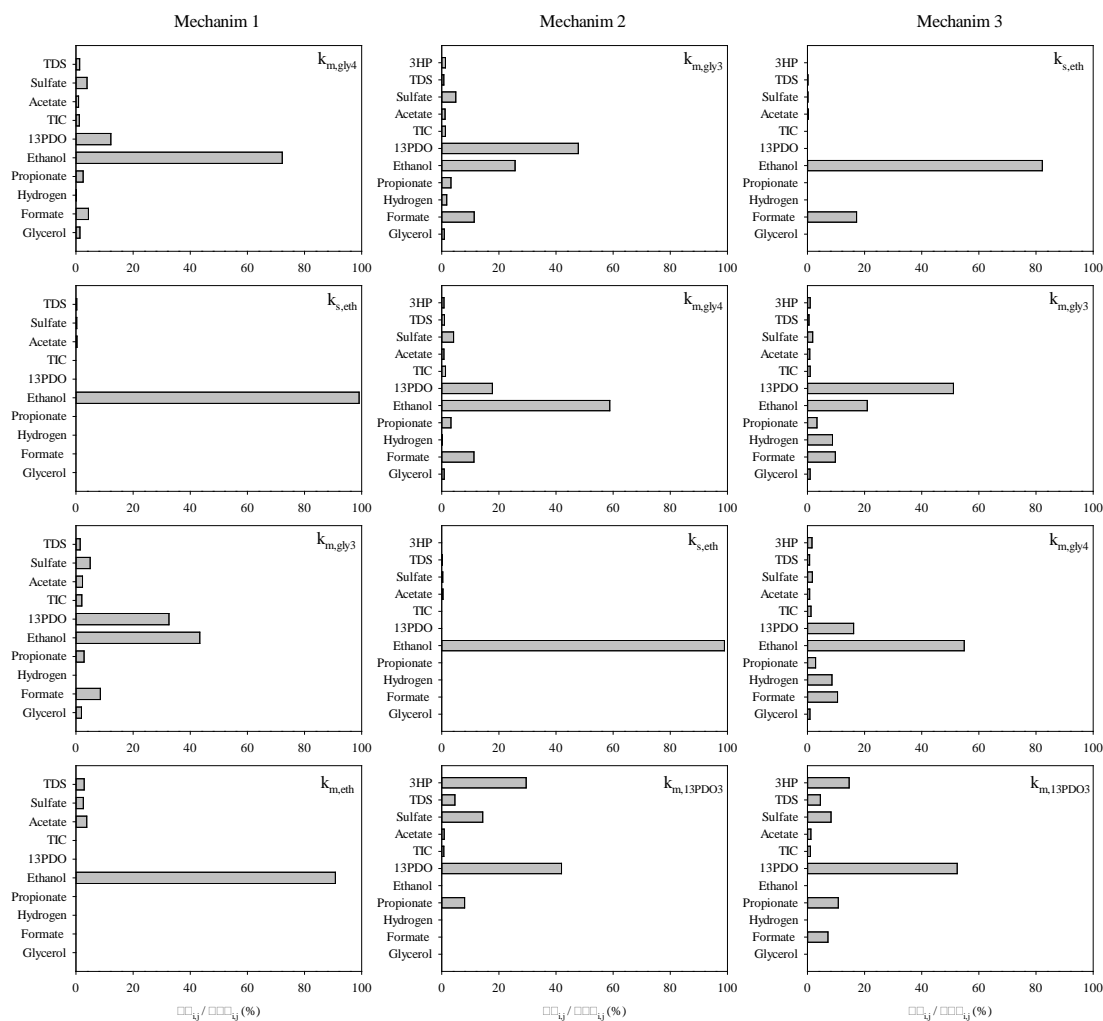


**Figure 7.4.** Most sensitive model parameters arranged in descending order from top to bottom for each one of the three mechanisms (the perturbation factor  $\delta$  was set as 10%).

When the perturbation factor  $\delta$  was set as -10%, the sensitivity values for the four most sensitive parameters in each mechanism are shown in Figure 7.5. The most sensitive parameters were the maximum specific uptake rates in the three mechanisms, including  $k_{m, gly3}$ ,  $k_{m, gly4}$ ,  $k_{m, eth}$ ,  $k_{m, for, FB}$ ,  $k_{m, 13PDO3}$  and  $k_{m, H2}$ . Therefore, all the substrates of the maximum specific uptake rates have been calibrated and half saturation coefficients mainly referred to previous studies.

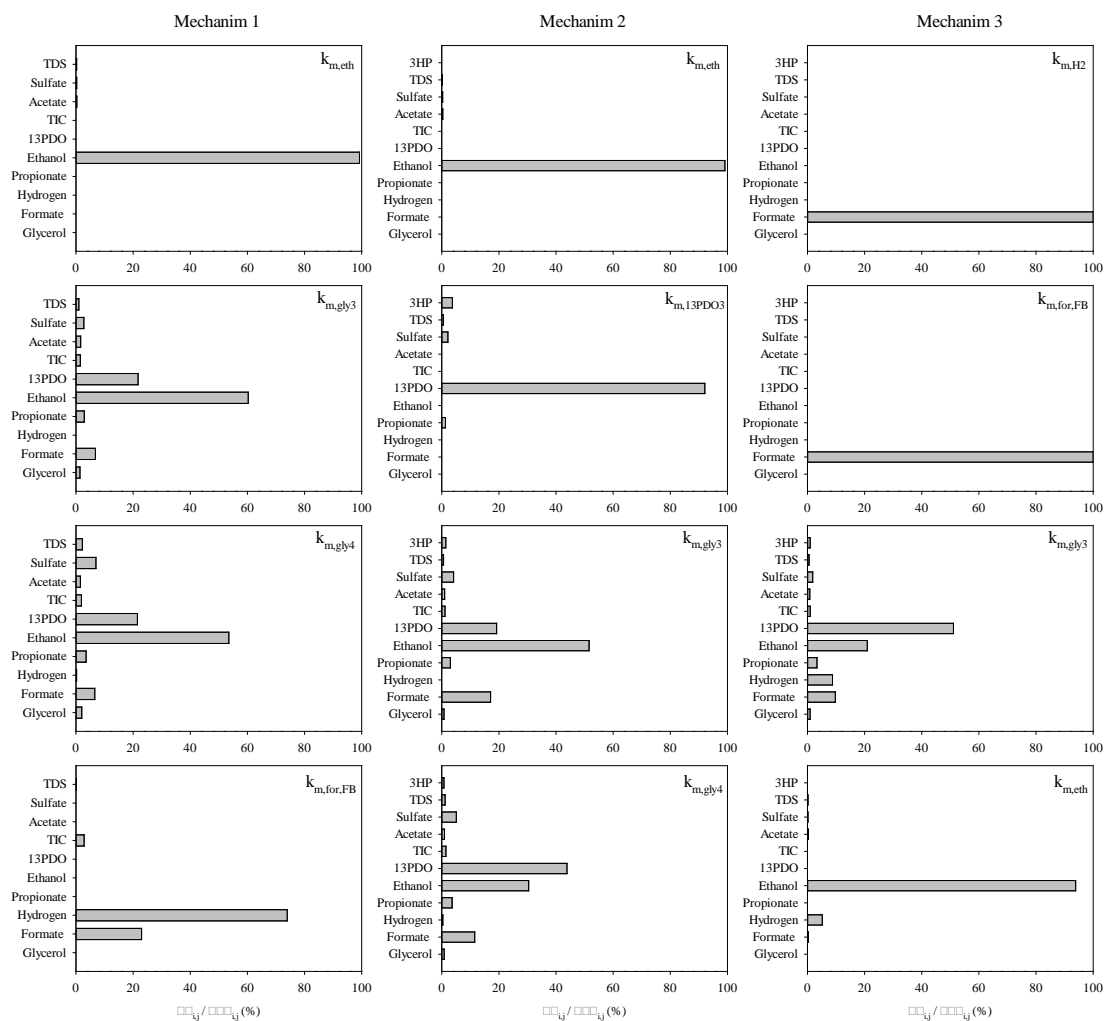


**Figure 7.5.** Most sensitive model parameters arranged in descending order from top to bottom for each one of the three mechanisms (the perturbation factor  $\delta$  was set as -10%).

Based on the sensitivity analysis results, the half saturation coefficient for the uptake of ethanol ( $k_{s,eth}$ ) is one of the most sensitive parameters in the sulfate reduction process with glycerol as electron donor. In this work,  $k_{s,eth}$  was initially taken from literature since no specific tests were carried out for its determination. Gonzalez-Silva et al. (2009) reported a  $k_{s,eth} = 45 \text{ mg C L}^{-1}$ . However, the lowest ethanol concentration detected during the experiment was  $4.3 \text{ mg C L}^{-1}$ , and the ethanol consumption rate was not limited. Thus, simulations with a  $k_{s,eth} = 45 \text{ mg C L}^{-1}$  (Figure 7.6A) and  $k_{s,eth} = 5 \text{ mg C L}^{-1}$  (Figure 7.6B) were compared. Figure 7.6A shows significant differences ( $P < 0.05$ ) between model predictions and experimental data for ethanol consumption after 24 h, whereas no significant differences in ethanol between model prediction and experimental data was

found in Figure 7.6B. Then,  $k_{s,eth}$  was set to  $5 \text{ mg C L}^{-1}$  in this work. Similarly,  $k_{s,13PDO}$  was initially set to  $45 \text{ mg C L}^{-1}$ , but the consumption of 1,3-propanediol in the model was slower than the experimental data (Figure 7.6A). Thus,  $k_{s,13PDO}$  was also set to  $5 \text{ mg C L}^{-1}$  to provide a better description of 1,3-propanediol consumption (Figure 7.6B). The half saturation coefficients for all other compounds were set as those provided in literature (Table 7.2). Further assessment of both  $k_{s,eth}$  and  $k_{s,13PDO}$  is warranted in future works.

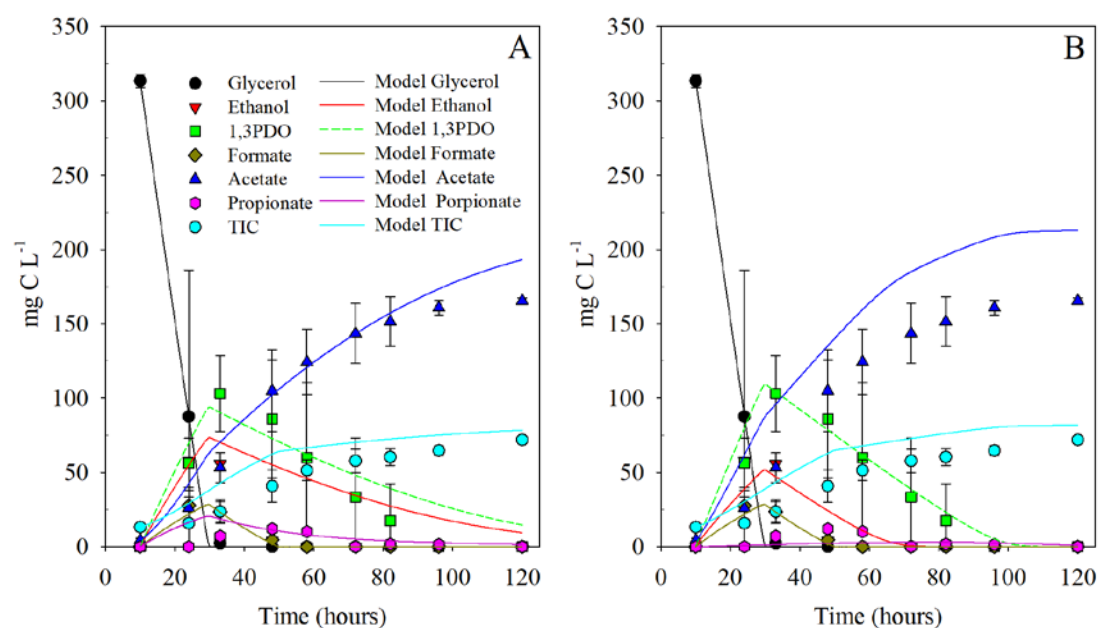


**Figure 7.6.** Experimental and simulated profiles of glycerol fermentation in Mechanism I. A)  $k_{s,eth}$  and  $k_{s,13PDO}$  were set to  $45 \text{ mg C L}^{-1}$ ; B)  $k_{s,eth}$  and  $k_{s,13PDO}$  were set to  $5 \text{ mg C L}^{-1}$ . Data points illustrate the experimental data. Smooth curves represent model predictions.

### 7.3.2 Model calibration of sulfate reduction process with single organic compounds

As described in Chapter 6, no methane was produced during the batch tests in which sulfate reduction was studied. Consequently, the model did not consider methanogenesis. Additionally, batch experiments showed that when acetate was used as carbon source, there was neither methane production nor sulfate reduction. Consequently, acetotrophic SRB were not included as model variable. Therefore, according to microbial communities analysis, this model considered FB, autotrophic SRB and heterotrophic SRB.

The mathematical model established in this work was first applied to batch activity tests with single organic compounds (data from Figure 6.5 of section 6.3.2). The pathways for sulfate reduction using propionate, ethanol and formate as electron donors are described in Eq.7.8, Eq.7.9 and Eq.7.7, respectively. The sulfate reduction process was the same among the three proposed mechanisms using these three electron donors.

The maximum specific uptake rates for single organic compounds ( $k_{m,j}$ ) involved in the sulfate reduction process using propionate, formate, ethanol and 1,3-propanediol as electron donors were estimated (Table 7.4). Predicted concentrations by the model of the abovementioned batch activity tests with the calibrated  $k_{m,j}$  are shown in Figure 7.7. According to Student's t-test, no significant differences were found between experimental data and model predictions for these activity tests. As can be observed in Table 7.4, there is a significant difference between the  $k_{m,j}$  of sulfate reduction calibrated in this chapter and the  $k_{m,j}$  in previous studies. The difference may be that the batch activity tests were performed in the sulfidogenic condition instead of methanogenic condition in this work, while the activity tests were conducted under the conditions of coexistence of methanogenesis and sulfidogenesis in previous studies.

**Table 7.4.** Maximum specific uptake rates of propionate, ethanol and formate calibrated in this work and found in literature.

Parameters	In this work	Reference
$k_{m,pro,HSRB}$ (mg C mg VSS <sup>-1</sup> h <sup>-1</sup> )	113.5 (± 0.9)	0.44 <sup>a</sup> , 0.24 <sup>b</sup>
$k_{m,eth,HSRB}$ (mg C mg VSS <sup>-1</sup> h <sup>-1</sup> )	51.1 (± 1.2)	0.003 <sup>c</sup>
$k_{m,H_2,ASRB}$ (mg H <sub>2</sub> mg VSS <sup>-1</sup> h <sup>-1</sup> )	3.3 (± 0.3)	0.46 <sup>a</sup> , 0.05 <sup>b</sup>
$k_{m,for,FB}$ (mg C mg VSS <sup>-1</sup> h <sup>-1</sup> )	3.8 (± 0.1)	0.56 <sup>d</sup>
$k_{m,for,HSRB}$ (mg C mg VSS <sup>-1</sup> h <sup>-1</sup> )	44.3 (± 1.3)	0.16 <sup>e</sup>

Note: Confidence level estimated through FIM is presented in parentheses.

<sup>a</sup> Barrera et al., 2015; <sup>b</sup> Fedorovich et al., 2003; <sup>c</sup> Gonzalez-Silva et al., 2009; <sup>d</sup> Vignolle et al., 2021;

<sup>e</sup> Bijmans et al., 2010

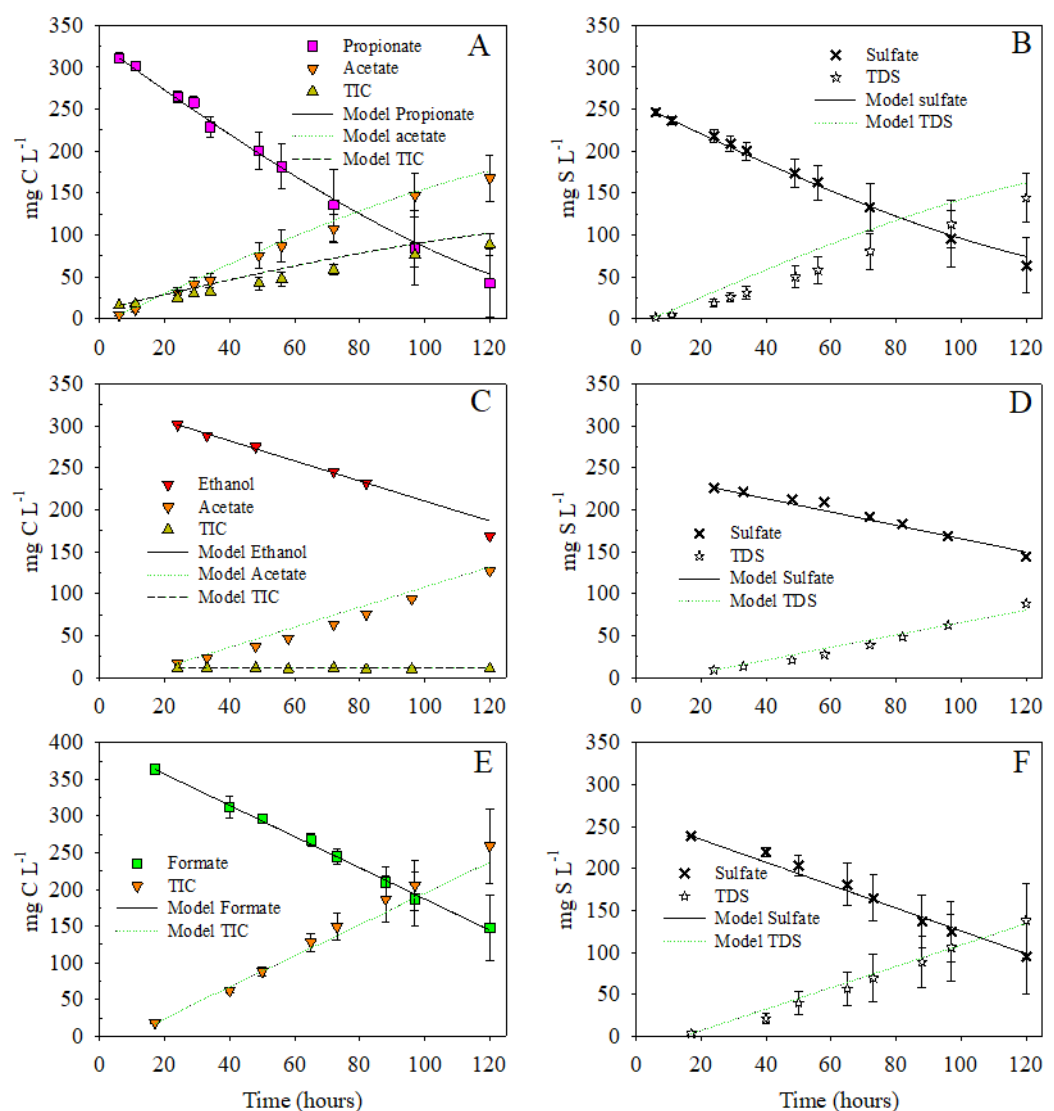


**Figure 7.7.** Experimental and model simulation of sulfate reduction using propionate (A and B), ethanol (C and D) and formate (E and F) as electron donors. A, C and E show the degradation process of organic carbon compounds; B, D and F show sulfate reduction process. Data points illustrate the experimental data. Smooth lines represent model predictions.

When 1,3-propanediol was used as carbon source to reduce sulfate and the production of 3HP was not considered, the degradation process of 1,3-propanediol can be described as Eq.7.10 and Eq.7.11 (Mechanism I). Its model fitting results are shown in Figure 7.8A and 7.8B. It is worth mentioning that 3HP was not monitored and it may be used as an intermediate product in the degradation process of glycerol and 1,3-propanediol (Qatibi et al., 1998, 1991c). When 3HP was considered as an intermediate product of

1,3-propanediol degradation, the process is followed by Eq.7.13, Eq.7.14 and Eq.7.15 (Mechanisms II and III). The degradation of 1,3-propanediol with sulfate reduction process were similar in Mechanism II and III, and the model fitting results are shown in Figure 7.8C and 7.8D. Through the Student's t-test, there was no significant difference between model and experimental data in these three mechanisms. Their corresponding maximum specific uptake rates obtained according to different degradation pathways are shown in Table 7.5. To the best of our knowledge, this is the first report that used 1,3-propanediol as an electron donor to calibrate its maximum specific uptake rate for sulfate reduction.

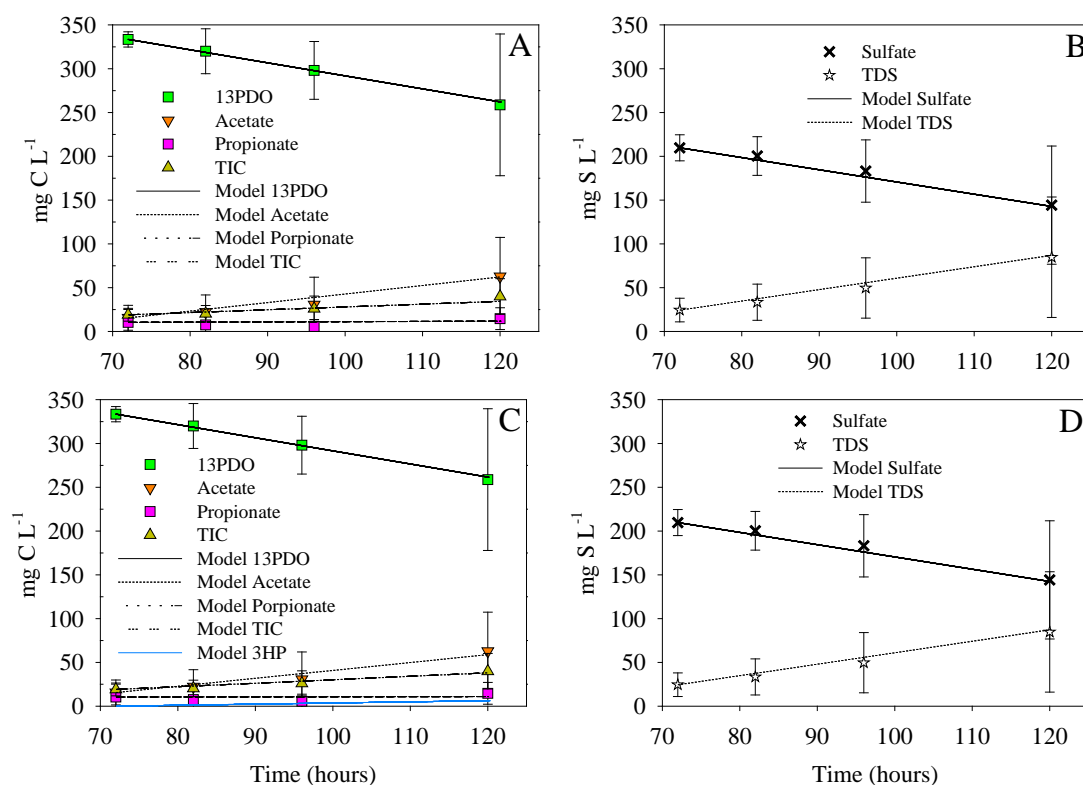


**Figure 7.8.** Sulfate reduction with 1,3-propanediol as the electron donor in Mechanism I (A, B) and Mechanism II (C, D). Data points illustrate the experimental data. Smooth lines represent model predictions.

**Table 7.5.** Maximum specific uptake rates of each single organic compounds in Mechanism I and II. Confidence level estimated through FIM is presented in parentheses.

Parameter	Mechanism I		Mechanism II		
	$k_{m,13PDO1}$	$k_{m,13PDO2}$	$k_{m,3HP1}$	$k_{m,3HP2}$	$k_{m,13PDO3}$
mg C mg VSS <sup>-1</sup> h <sup>-1</sup>	48.3 (± 1.9)	4.9 (± 0.4)	5.1 (± 0.2)	0.5 (± 0.0)	53.6 (± 4.7)

### 7.3.3 Model calibration with glycerol as carbon source

#### 7.3.3.1 Model calibration for glycerol fermentation and validation

In absence of sulfate, each  $k_{m,j}$  of glycerol fermentation processes based on Mechanism I were calibrated (data from section 6.3.1.1) through Eq.7.1 to Eq.7.4, as shown in Figure 7.9A. Through the Student's t-test, it is found that there was no significant difference between the model and experimental data of the glycerol degradation process. The maximum specific uptake rates of glycerol fermentation ( $k_{m,gly}$ ) in absence of sulfate are shown in Table 7.6. Estimated by the  $k_{m,gly}$ , the pathway through glycerol fermentation to 13PDO (Eq.7.3,  $k_{m,gly3}$ ) accounted for 65% of all pathways of glycerol degradation in Mechanism I, and 22% through glycerol fermentation to acetic acid and formic acid (Eq.7.1,  $k_{m,gly1}$ ).  $k_{m,j}$  of glycerol fermentation processes in Mechanism II and III were also calculated (Figures not shown). The glycerol degradation pathway of Mechanism II was the same as in Mechanism I. In Mechanism III, the pathway through glycerol fermentation to 13PDO (Eq.7.3,  $k_{m,gly3}$ ) and the pathway through glycerol fermentation to 3HP (Eq.7.12,  $k_{m,gly5}$ ) were the main degradation pathway of glycerol accounting for 65% and 23%.

The maximum specific uptake rates of glycerol fermentation processes and sulfate reduction using single organic compounds as electron donors estimated in sections 7.3.1 and 7.3.2, combined with the  $k_s$  listed in the literature and those adjusted in this work in section 7.3.1, were used for a validation attempt performed by simulating Mechanism I and the batch test in which glycerol and sulfate were added (experimental data from section 6.3.1.2). Model predictions are shown in Figure 7.9B and 7.9C. As can be

---

observed, the model prediction did not fit the experimental results. The production of 1,3-propanediol in the model was overestimated, while sulfate reduction was underestimated. Model predictions using Mechanism II and III (not shown) resulted exactly the same as the mechanism I. The reason was due to the contribution of other microbial communities on glycerol fermentation. Bryant et al. (1977) demonstrated that sulfate reducer genus *Desulfovibrio* fermented lactate or ethanol to acetate in anaerobic ecosystems containing little or no sulfate. *Desulfobulbus* species are also capable of fermenting lactate and ethanol to acetate and propionate (Muyzer and Stams, 2008). Plugge et al. (2011) described that some sulfate reducers can shift their metabolism from sulfidogenic in presence of sulfate to acetogenic, hydrogenogenic metabolism in the absence of sulfate. It can be concluded that sulfate reducers can be metabolically active in anaerobic digestion without sulfate, which may explain the overestimation of 1,3-propanediol production. Due to the different affinity of SRB for different organic compounds, the incorrect estimation of glycerol fermentation products resulted in underestimation of sulfate reduction rate. Thus, the recalibration of maximum specific rates of glycerol fermentation in the presence of sulfate was necessary.



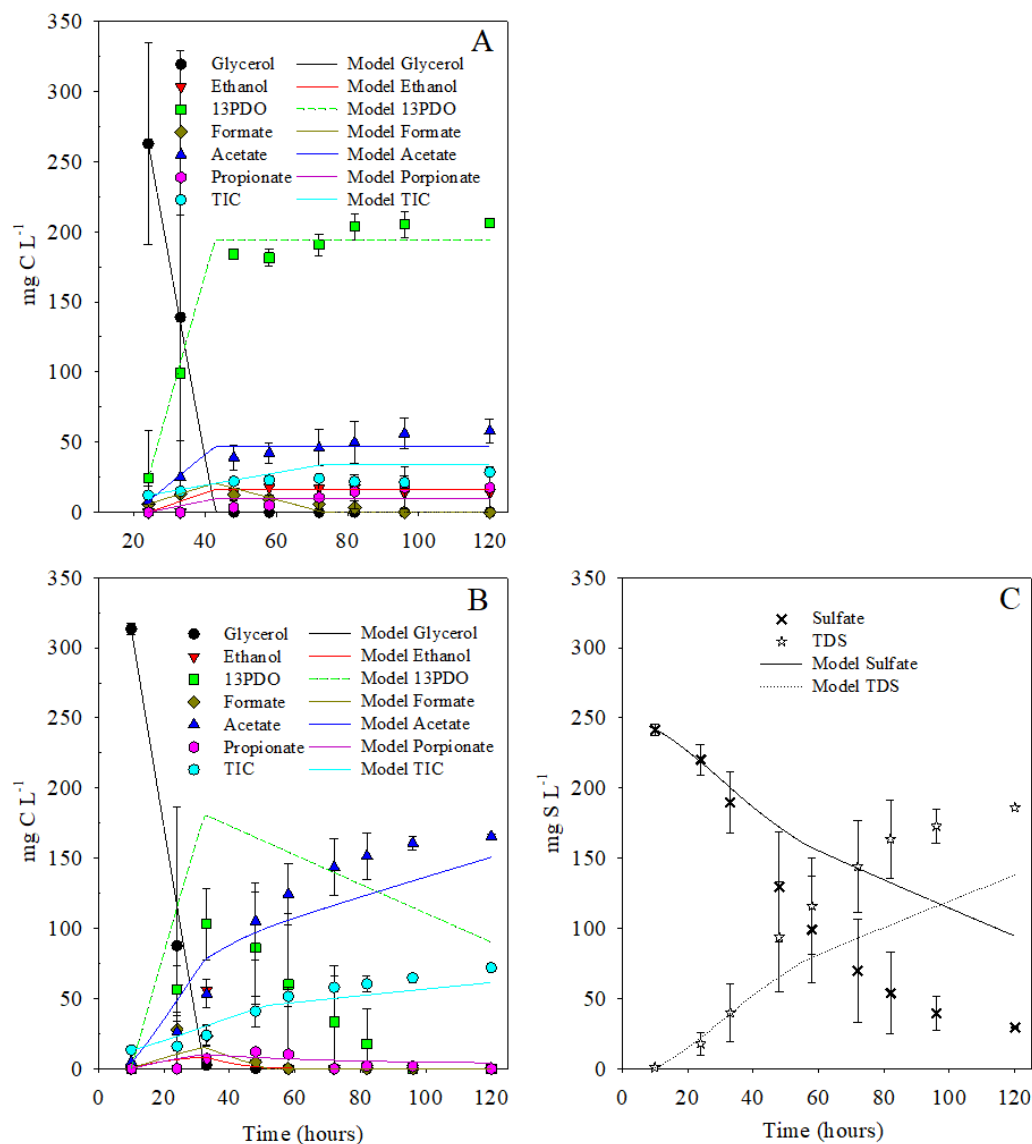


**Figure 7.9.** Model calibration of glycerol fermentation in absence of sulfate (A) and validation of glycerol fermentation in presence of sulfate (B, C). B shows glycerol fermentation processes and C shows sulfate reduction process. Data points illustrate the experimental data. Smooth lines represent model predictions.

**Table 7.6.** Monod maximum specific uptake rates of glycerol in three mechanisms.

	<b>Mechanism I</b>	<b>Mechanism II</b>	<b>Mechanism III</b>
$k_{m, gly1}$	17.8 ( $\pm 0.0$ )	17.6 ( $\pm 0.0$ )	2.1 ( $\pm 0.0$ )
$k_{m, gly2}$	2.9 ( $\pm 0.0$ )	0.7 ( $\pm 0.0$ )	1.8 ( $\pm 0.0$ )
$k_{m, gly3}$	51.6 ( $\pm 0.0$ )	50.1 ( $\pm 0.1$ )	50.2 ( $\pm 0.1$ )
$k_{m, gly4}$	7.4 ( $\pm 0.0$ )	8.3 ( $\pm 0.0$ )	5.9 ( $\pm 0.0$ )
$k_{m, gly5}$			17.4 ( $\pm 0.1$ )

Note: Confidence level estimated through FIM is presented in parentheses.

### 7.3.3.2 Model calibration for glycerol fermentation coupled to sulfate reduction

Maximum uptake rates of glycerol fermentation were recalibrated whereas the same  $k_{m,j}$  for sulfate reduction processes calibrated in the sulfate reduction process with single organic compounds (section 7.3.2, Table 7.5) were used. The three mechanisms (I, II and III) were simulated and compared through Student's t-test and Fval to also decide which mechanistic approach provided a better prediction of the experimental data. In the simultaneous presence of glycerol and sulfate, the predicted profiles for each model variable are shown in Figure 7.10. Figure 7.10A shows that the model prediction of acetate concentration was significantly higher than the experimental data in Mechanism I, while the sulfate reduction rate and the production rate of TDS in the model were both higher than the experimental data (Figure 7.10B). A significant difference ( $P < 0.05$ ) between the experimental data and the model prediction was obtained and a Fval of 243.7 was found in Mechanism I. Using Mechanism II (Figure 7.10C and 7.10D), the Fval was 166.7 that was lower than Fval in Mechanism I. Student's t-test showed that there was no significant difference in carbon compounds concentration between the model and the experimental data (Figure 7.10C). However, the model overestimated the sulfate reduction (Figure 7.10D). Using Mechanism III (Figure 7.10E and 7.10F), there was no significant difference between the model data and the experimental data in carbon (Figure 7.10E) and sulfur compounds (Figure 7.10F). The minimum error between model and experimental data was obtained in Mechanism III (Fval =148.3), which indicates that the mathematical model based on Mechanism III well-described the sulfate reduction process with glycerol as the electron donor, thus revealing that 3HP contribution as intermediate metabolite in the process of sulfate reduction during the glycerol fermentation and 1,3-propanediol degradation might be the main processes playing a role out of the 3 mechanisms compared herein. However, although the  $H_2S$  transferred from the liquid phase to the gas phase was considered in this model, the model predicted that the TDS in the liquid was still higher than the experimental data. This was attributed to the possible

production of organic sulfur compounds during the activity test (Mora et al., 2020b).

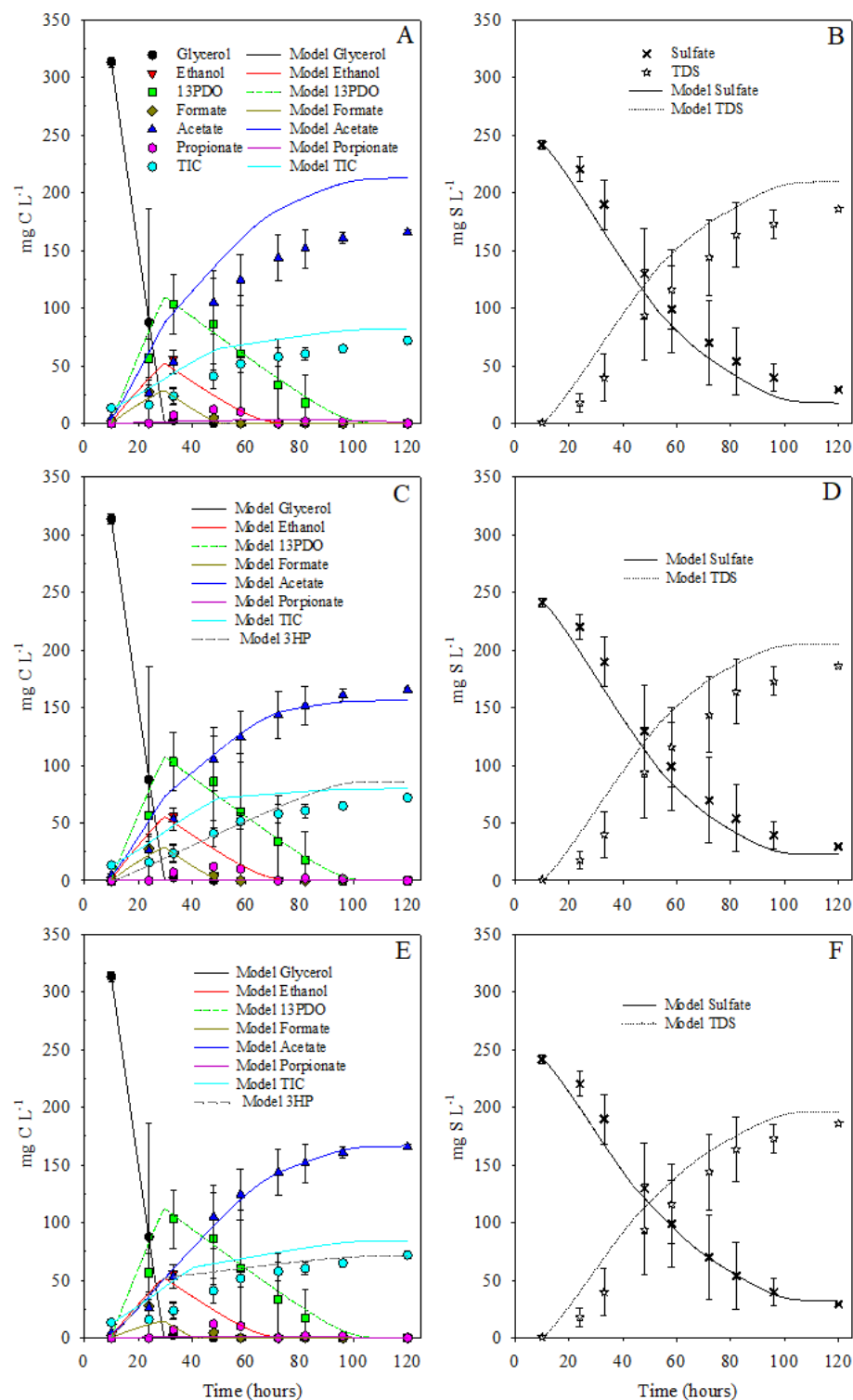


**Figure 7.10.** Experimental and simulated profiles of sulfate reduction process using glycerol as carbon source in Mechanism I (A, B), Mechanism II (C, D) and Mechanism III (E, F). Data points illustrate the experimental data. Smooth curves represent model predictions.

The mathematical model based on Mechanism III well-described the experimental data, and the sulfate reduction process was validated. In presence of sulfate, the calibrated maximum uptake rates of glycerol fermentation ( $k_{m, gly}$ ) and 3HP fermentation ( $k_{m, 3HP}$ ) of Mechanism III using glycerol as the electron donor are shown in Table 7.7. In Mechanism III, the pathway through glycerol fermentation to 1,3PDO (Eq.7.3,  $k_{m, gly3}$ ) and the pathway through glycerol fermentation to ethanol and formic acid (Eq.7.4,  $k_{m, gly4}$ ) were the main pathways of glycerol fermentation, accounting for 45.8% and 37.9%, respectively. This result agrees with previous studies (Rossi et al., 2012; Sittijunda and Reungsang, 2017), in which ethanol and 1,3-propanediol were found as the main products of glycerol fermentation.

The present work verified the degradation pathway of glycerol by the model simulation. 3HP was produced during the process of 1,3-propanediol degradation in presence of sulfate (Qatibi et al., 1991c), and it could be further converted mainly to acetate (Qatibi et al., 1991b). As shown in Table 7.7, the route through 3HP oxidized to acetate was the main route of 3HP degradation, accounting for up to 98.0%.

**Table 7.7.** Monod maximum specific uptake rates of glycerol and 3-hydroxypropionate in Mechanism III.

Parameter	$k_{m, gly1}$	$k_{m, gly2}$	$k_{m, gly3}$	$k_{m, gly4}$	$k_{m, gly5}$	$k_{m, 3HP1}$	$k_{m, 3HP2}$
mg C mg VSS <sup>-1</sup>	0.7	0.1	25.0	20.7	8.1	4.9	0.1
h <sup>-1</sup>	(± 0.1)	(± 0.1)	(± 0.1)	(± 0.1)	(± 0.1)	(± 0.0)	(± 0.0)

Note: Confidence level is presented in parentheses.

Previous kinetic models of anaerobic degradation of glycerol coupled to sulfate reduction proposed in the literature (Dinkel et al., 2010) were based on reactions in which glycerol was directly oxidized to acetate by fermentative bacteria and sulfate reducers. However, the present work showed that fermentation of glycerol contained a variety of intermediate products, including ethanol, 1,3-propanediol, propionate, acetate, carbonate,

etc. that must be added to the modelling approach. The model proposed in this work considered a set of intermediate metabolites of glycerol fermentation that can reproduce experimental results in a highly consistent manner. Based on the results of a sensitivity analysis, the maximum specific uptake rates involved in the degradation of glycerol and sulfate reduction were calculated, in which the parameter  $k_{m,j}$  of sulfate reduction were validated. The low confidence intervals in the parameter estimation indicated the reliability of the model. The kinetic parameters calibrated herein could be useful for the long-term operation in anaerobic reactors. Although the mathematical model based on Mechanism III was in agreement with the experimental data in this work, the model still needs to improve when it is considered in biological anaerobic reactors with a long-term operation, such as inhibition factors or the competition among microbial communities.

## 7.4 Conclusion

A mathematical model describing sulfate reduction and anaerobic glycerol fermentation through multiple pathways and multiple intermediate products with sulfate reduction process was established and discussed. The model described glycerol degradation through the reductive and oxidative pathways. The kinetic parameters of Monod maximum specific uptake rates of substrate were calibrated and then, the sulfate reduction process has been validated. The three proposed mechanisms were compared by fitting model to experimental data. It was found that the model established by Mechanism III was in higher agreement according to the objective function values. In this mechanism, apart from considering the products ethanol, 1,3-propanediol, formate, acetate, propionate and carbonate; 3HP was included as a metabolite in the fermentation of glycerol. Among them, the bioconversion of 1,3-propanediol and ethanol were the main pathway of glycerol fermentation, accounting for 45.8% and 37.9%, respectively. Moreover, it was determined that 3HP was an intermediate product of 1,3-propanediol degradation in the presence of sulfate.

# Chapter 8

---

## **General conclusions and future work**



## 8.1 General conclusions

In this thesis, the long-term operation of a UASB reactor was performed under a constant TOC/S-SO<sub>4</sub><sup>2-</sup> ratio of  $1.5 \pm 0.3$  g C g<sup>-1</sup> S and an OLR of  $7.3 \pm 1.6$  kg C m<sup>-3</sup> d<sup>-1</sup> for 639 days using crude glycerol as a carbon source.

Methanogenic granular sludge quickly adapted to the sulfidogenic conditions, and the sulfate removal efficiency exceeded 84% within 16 days. The reactor showed a sulfate removal capacity (SRC) of  $4.5 \pm 0.7$  kg S-SO<sub>4</sub><sup>2-</sup> m<sup>-3</sup> d<sup>-1</sup> in 280 days of operation and the SRC decreased to  $1.8 \pm 0.6$  kg S-SO<sub>4</sub><sup>2-</sup> m<sup>-3</sup> d<sup>-1</sup> from day 280 to day 639.

In terms of carbon species, a progressive VFAs accumulation (mainly acetate) coincided with a significant decrease of CH<sub>4</sub> production after operating the UASB reactor for 100 days, while the methanogenic activity was ceased after 200 days, resulting in a decline of TOC removal efficiency. Moreover, the glycerol removal efficiency exceeded 96% before 280 days, but it gradually decreased concomitantly with a decrease in the accumulation of acetate after 280 days.

After the methanogenesis activity ceased, degranulation of sludge was observed, and then, the sludge particles were gradually covered by SLS. The SLS led to the flotation of sludge, which resulted in the loss of a large amount of sludge. This ultimately led to the reduction of the sulfate removal efficiency of the UASB reactor and the failure of the operation. Activity tests showed that there was no difference between granular sludge and SLS in the mechanisms of glycerol fermentation and sulfate reduction. However, the SLS might affect the mass transfer of sulfate, thereby exacerbating the decline of sulfate removal efficiency in the UASB reactor.

The analysis of the stratification of the UASB reactor revealed that the glycerol fermentation and sulfate reduction processes were mainly achieved at the bottom part of the reactor because the sludge has a higher concentration in the bottom sludge bed. This indicates that the sludge in the UASB reactor can treat higher organic and sulfate loading rates. In addition, the specific glycerol fermentation rate of the sludge in UASB1 of the



reactor (lower section) was 1.7 times that of UASB2 (middle section), and 1.9 times that of UASB3 (upper section) on 169 days. On 198 day, the specific glycerol fermentation rate of sludge in UASB1 was 2.1 times that of UASB2 and UASB3. More relatively abundant fermentative microorganisms were observed in UASB1, compared to UASB2 and UASB3.

A mechanistic approach of glycerol fermentation and sulfate reduction was proposed in this work based on the specific net rates observed experimentally for each compound and the stoichiometric conversions. Glycerol was not used by SRB but was mainly fermented to 1,3-propanediol, ethanol, formate, propionate and acetate by fermentative microorganisms. All organic intermediates were found to be further used by sulfate reducing bacteria (SRB) for sulfate reduction except for acetate. The sulfate reduction process mainly used 1,3-propanediol and ethanol as electron donors in glycerol-fed tests.

A mathematical model describing sulfate reduction and anaerobic glycerol degradation through multiple pathways and multiple intermediate products was established and discussed. The model properly described glycerol degradation and its fermentation products through reductive and oxidative pathways. The maximum specific substrate uptake rates were calibrated. The model showed that 3-hydroxypropionate might be a key intermediate product in the fermentation process of glycerol and the degradation of 1,3-propanediol for sulfate reduction.

## **8.2 Future work**

This thesis investigated the long-term operation of a UASB reactor under constant conditions for biological sulfate reduction and focused on the metabolism of dissimilatory sulfate reduction using crude glycerol as an electron donor and carbon source. However, still several topics remain to be investigated in the future.

In the later stage of operation, a large amount of acetate accumulated in the UASB reactor, which reduced the utilization rate of organic carbon. The research should be further studied to benefit from acetate production. For example, it can set up another

anaerobic reactor after the effluent of the UASB reactor to use acetate for methane production, to use acetate for denitrifying nitrate from NO<sub>x</sub> or even produce biopolymers for bioplastics production by acetate-propionate accumulating microorganisms.

Appropriate shear forces and addition of trace metals added to the substrate could be a strategy to promote granulation that needs to be further evaluated. The change of shearing forces can be achieved by the effluent recycling system to adjust the up-flow velocity. Moreover, appropriate shear forces may also prevent the accumulation of SLS, but it is still necessary to study the possible washout of biomass through the recycling effluent system.

A structured mathematical model was set up to describe sulfate reduction and glycerol fermentation and the biokinetic parameters for the different substrates have been estimated in serum bottles. The model can reproduce experimental results in a highly consistent manner. However, this model still needs to improve when it is considered in biological anaerobic reactors with a long-term operation to reveal the competitive dynamics of microbial community and to evaluate the performance of the biological anaerobic reactors.



## **Chapter 9**

---

### **References**



- Abou-Zeid, D.M., Biebl, H., Spröer, C., Müller, R.J., 2004. *Propionispora hippei* sp. nov., a novel Gram-positive, spore-forming anaerobe that produces propionic acid. *Int. J. Syst. Evol. Microbiol.* 54, 951–954. <https://doi.org/10.1099/ijss.0.03054-0>
- Alemu, T., Lemma, E., Mekonnen, A., Leta, S., 2016. Performance of pilot scale anaerobic-SBR system integrated with constructed wetlands for the treatment of tannery wastewater. *Environ. Process.* 3, 815–827. <https://doi.org/10.1007/s40710-016-0171-1>
- Ambler, J.R., Logan, B.E., 2011. Evaluation of stainless steel cathodes and a bicarbonate buffer for hydrogen production in microbial electrolysis cells using a new method for measuring gas production. *Int. J. Hydrogen Energy.* 36, 160–166. <https://doi.org/10.1016/j.ijhydene.2010.09.044>
- Angelidaki, I., Ellegaard, L., Ahring, B.K., 1999. A Comprehensive model of anaerobic bioconversion of complex substrates to biogas. *Biotechnol Bioeng* 63, 363–372. [https://doi.org/10.1002/\(SICI\)1097-0290\(19990505\)63:3](https://doi.org/10.1002/(SICI)1097-0290(19990505)63:3)
- Angeloni, M., Remacha, P., Martínez, A., Ballester, J., 2016. Experimental investigation of the combustion of crude glycerol droplets. *Fuel.* 184, 889–895. <https://doi.org/10.1016/j.fuel.2016.06.045>
- APHA, 2012. Standard Methods for examination of water and wastewater. APHA, AWWA, WEF. 5, 185–186. [https://doi.org/10.5209/rev\\_ANHM.2012.v5.n2.40440](https://doi.org/10.5209/rev_ANHM.2012.v5.n2.40440)
- Baba, Y., Tada, C., Watanabe, R., Fukuda, Y., Chida, N., Nakai, Y., 2013. Anaerobic digestion of crude glycerol from biodiesel manufacturing using a large-scale pilot plant: Methane production and application of digested sludge as fertilizer. *Bioresour. Technol.* 140, 342–348. <https://doi.org/10.1016/j.biortech.2013.04.020>
- Baillod, C.R., Boyle, W.C., 1970. Mass transfer limitations in substrate removal. *J. Sanit. Eng. Div.* 96, 525–545. <https://doi.org/10.1061/jسدai.0001092>
- Bak, F., Pfennig, N., 1991. Sulfate-reducing bacteria in littoral sediment of Lake Constance. *FEMS Microbiol. Lett.* 85, 43-52. <https://doi.org/10.1111/j.1574-6968.1991.tb04696.x>
- Barrera, E.L., Spanjers, H., Solon, K., Amerlinck, Y., Nopens, I., Dewulf, J., 2015. Modeling the anaerobic digestion of cane-molasses vinasse: Extension of the Anaerobic Digestion Model

- No. 1 (ADM1) with sulfate reduction for a very high strength and sulfate rich wastewater. *Water Res.* 71, 42–54. <https://doi.org/10.1016/j.watres.2014.12.026>
- Barton, L.L., Fardeau, M.L., Fauque, G.D., 2014. Hydrogen sulfide: A toxic gas produced by dissimilatory sulfate and sulfur reduction and consumed by microbial oxidation. *Met. Ions Life Sci.* 237–277. <https://doi.org/10.1007/978-94-017-9269-1-10>
- Barton, L.L., Fauque, G.D., 2009. Chapter 2 Biochemistry, physiology and biotechnology of sulfate-reducing bacteria. *Adv. Appl. Microbiol.* 68, 41–98. [https://doi.org/10.1016/S0065-2164\(09\)01202-7](https://doi.org/10.1016/S0065-2164(09)01202-7)
- Barton, L.L., Hamilton, W.A., 2007. Sulphate-reducing bacteria: environmental and engineered systems. Cambridge University Press.
- Batstone, D.J., Keller, J., Angelidaki, I., Kalyuzhnyi, S. V., Pavlostathis, S.G., Rozzi, A., Sanders, W.T., Siegrist, H., Vavilin, V.A., 2002. The IWA Anaerobic Digestion Model No 1 (ADM1). *Water Sci. Technol.* 45, 65–73. <https://doi.org/10.2166/wst.2002.0292>
- Batstone, D.J., Keller, J., Steyer, J.P., 2006. A review of ADM1 extensions, applications, and analysis: 2002-2005. *Water Sci. Technol.* 54, 1–10. <https://doi.org/10.2166/wst.2006.520>
- Batstone, D.J., Puyol, D., Flores-Alsina, X., Rodríguez, J., 2015. Mathematical modelling of anaerobic digestion processes: applications and future needs. *Rev. Environ. Sci. Biotechnol.* 14, 595–613. <https://doi.org/10.1007/s11157-015-9376-4>
- Bertolino, S.M., Melgaço, L.A., Sá, R.G., Leão, V.A., 2014. Comparing lactate and glycerol as a single-electron donor for sulfate reduction in fluidized bed reactors. *Biodegradation.* 25, 719–733. <https://doi.org/10.1007/s10532-014-9694-1>
- Bertolino, S.M., Rodrigues, I.C.B., Guerra-Sá, R., Aquino, S.F., Leão, V.A., 2012. Implications of volatile fatty acid profile on the metabolic pathway during continuous sulfate reduction. *J. Environ. Manage.* 103, 15–23. <https://doi.org/10.1016/J.JENVMAN.2012.02.022>
- Beschkov, V., Sapundzhiev, T., Angelov, I., 2012. Modelling of biogas production from glycerol by anaerobic process in a baffled multi-stage digester. *Biotechnol. Biotechnol. Equip.* 26, 3244–3248. <https://doi.org/10.5504/bbeq.2012.0061>
- Biebl, H., Menzel, K., Zeng, A.P., Deckwer, W.D., 1999. Microbial production of 1,3-propanediol.

- Appl. Microbiol. Biotechnol. 52, 289–297. <https://doi.org/10.1007/s002530051523>
- Biebl, H., Schwab-Hanisch, H., Spröer, C., Lünsdorf, H., 2000. *Propionispora vibrioides*, nov. gen., nov. sp., a new gram-negative, spore-forming anaerobe that ferments sugar alcohols. Arch. Microbiol. 174, 239–247. <https://doi.org/10.1007/s002030000198>
- Biebl, H., Zeng, A.-P., Menzel, K., Deckwer, W.-D., 1998. Fermentation of glycerol to 1,3-propanediol and 2,3-butanediol by *Klebsiella pneumoniae*. Appl. Microbiol. Biotechnol. 50, 24–29. <https://doi.org/10.1007/s002530051251>
- Bijmans, M.F.M., Buisman, C.J.N., Meulepas, R.J.W., Lens, P.N.L., 2011. Sulfate reduction for inorganic waste and process water treatment, Compr. Biotechnol. 384-395. <https://doi.org/10.1016/B978-0-444-64046-8.00367-0>
- Bijmans, M.F.M., de Vries, E., Yang, C.H., Buisman, C.J.N., Lens, P.N.L., Dopson, M., 2010. Sulfate reduction at pH 4.0 for treatment of process and wastewaters. Biotechnol. Prog. 26, 1029–1037. <https://doi.org/10.1002/btpr.400>
- Bijmans, M.F.M., Peeters, T.W.T., Lens, P.N.L., Buisman, C.J.N., 2008. High rate sulfate reduction at pH 6 in a pH-auxostat submerged membrane bioreactor fed with formate. Water Res. 42, 2439–2448. <https://doi.org/10.1016/J.WATRES.2008.01.025>
- Blumensaat, F., Keller, J., 2005. Modelling of two-stage anaerobic digestion using the IWA Anaerobic Digestion Model No. 1 (ADM1). Water Res. 39, 171–183. <https://doi.org/10.1016/J.WATRES.2004.07.024>
- Bryant, M.P., Campbell, L.L., Reddy, C.A., Crabill, M.R., 1977. Growth of *desulfovibrio* in lactate or ethanol media low in sulfate in association with H<sub>2</sub> utilizing methanogenic bacteria. Appl. Environ. Microbiol. 33, 1162–1169. <https://doi.org/10.1128/aem.33.5.1162-1169.1977>
- Bryers, J.D., 1985. Structured modeling of the anaerobic digestion of biomass particulates. Biotechnol. Bioeng. 27, 638–649. <https://doi.org/10.1002/BIT.260270514>
- Buswell, A.M., Boruff, C.S., Wiesman, C.K., 1932. Anaerobic stabilization of milk waste. Ind. Eng. Chem. 24, 1423–1425.
- Cassarini, C., Rene, E.R., Bhattarai, S., Vogt, C., Musat, N., Lens, P.N.L., 2019. Anaerobic methane oxidation coupled to sulfate reduction in a biotrickling filter: Reactor performance



- and microbial community analysis. *Chemosphere*. 236, 124290. <https://doi.org/10.1016/J.CHEMOSPHERE.2019.07.021>
- Castro, H.F., Williams, N.H., Ogram, A., 2000. Phylogeny of sulfate-reducing bacteria. *FEMS Microbiol. Ecol.* 31, 1–9. <https://doi.org/10.1111/J.1574-6941.2000.TB00665.X>
- Chen, H., Ma, C., Yang, G.F., Wang, H.Z., Yu, Z.M., Jin, R.C., 2014. Flootation of flocculent and granular sludge in a high-loaded anammox reactor. *Bioresour. Technol.* 169, 409–415. <https://doi.org/10.1016/j.biortech.2014.06.063>
- Chen, H., Wu, J., Liu, B., Li, Y., Yasui, H., 2019. Competitive dynamics of anaerobes during long-term biological sulfate reduction process in a UASB reactor. *Bioresour. Technol.* 280, 173–182. <https://doi.org/10.1016/j.biortech.2019.02.023>
- Chen, J., Yan, S., Zhang, X., Tyagi, R.D., Surampalli, R.Y., Valéro, J.R., 2018. Chemical and biological conversion of crude glycerol derived from waste cooking oil to biodiesel. *Waste Manag.* 71, 164–175. <https://doi.org/10.1016/j.wasman.2017.10.044>
- Cheng, K.K., Zhang, J.A., Liu, D.H., Sun, Y., Liu, H.J., Yang, M. De, Xu, J.M., 2007. Pilot-scale production of 1,3-propanediol using *Klebsiella pneumoniae*. *Process Biochem.* 42, 740–744. <https://doi.org/10.1016/j.procbio.2007.01.001>
- Clomburg, J.M., Gonzalez, R., 2013. Anaerobic fermentation of glycerol: a platform for renewable fuels and chemicals. *Trends Biotechnol.* 31, 20–28. <https://doi.org/10.1016/j.tibtech.2012.10.006>
- Couvert, A., Charron, I., Laplanche, A., Renner, C., Patria, L., Requieme, B., 2006. Treatment of odorous sulphur compounds by chemical scrubbing with hydrogen peroxide—Application to a laboratory plant. *Chem. Eng. Sci.* 61, 7240–7248. <https://doi.org/10.1016/J.CES.2006.07.030>
- Dahiya, S., Anhäuser, A., Farrow, A., Thieriot, H., Kumar, A., Myllyvirta, L., 2020. Global SO<sub>2</sub> emission hotspot database. *Cent. Res. Energy Clean Air Greenpeace India* 48.
- Dar, S.A., Kleerebezem, R., Stams, A.J.M., Kuenen, J.G., Muyzer, G., 2008. Competition and coexistence of sulfate-reducing bacteria, acetogens and methanogens in a lab-scale anaerobic bioreactor as affected by changing substrate to sulfate ratio. *Appl. Microbiol. Biotechnol.* 78, 1045–1055. <https://doi.org/10.1007/s00253-008-1391-8>

- Das, M., Grover, A., 2018. Fermentation optimization and mathematical modeling of glycerol-based microbial poly(3-hydroxybutyrate) production. *Process Biochem.* 71, 1–11. <https://doi.org/10.1016/j.procbio.2018.05.017>
- Daud, M.K., Rizvi, H., Akram, M.F., Ali, S., Rizwan, M., Nafees, M., Jin, Z.S., 2018. Review of upflow anaerobic sludge blanket reactor technology: Effect of different parameters and developments for domestic wastewater treatment. *J. Chem.* 2018. <https://doi.org/10.1155/2018/1596319>
- De Smul, A., Verstraete, W., 1999. Retention of sulfate-reducing bacteria in expanded granular-sludge-blanket Reactors. *Water Environ. Res.* 71, 427–431. <https://doi.org/10.2175/106143097x122077>
- Deaver, J.A., Diviesti, K.I., Soni, M.N., Campbell, B.J., Finneran, K.T., Popat, S.C., 2020. Palmitic acid accumulation limits methane production in anaerobic co-digestion of fats, oils and grease with municipal wastewater sludge. *Chem. Eng. J.* 396, 125235. <https://doi.org/10.1016/j.cej.2020.125235>
- Demaman Oro, C.E., Bonato, M., Oliveira, J.V., Tres, M.V., Mignoni, M.L., Dallago, R.M., 2019. A new approach for salts removal from crude glycerin coming from industrial biodiesel production unit. *J. Environ. Chem. Eng.* 7, 102883. <https://doi.org/10.1016/j.jece.2019.102883>
- Dinkel, V.G., Frechen, F.B., Dinkel, A. V., Smirnov, Y.Y., Kalyuzhnyi, S. V., 2010. Kinetics of anaerobic biodegradation of glycerol by sulfate-reducing bacteria. *Appl. Biochem. Microbiol.* 46, 712–718. <https://doi.org/10.1134/s0003683810070069>
- Dochain, D., Vanrolleghem, P.A., 2001. *Dynamical modelling and estimation in wastewater treatment processes.* IWA Publishing.
- Doi, Y., 2015. L-lactate production from biodiesel-derived crude glycerol by metabolically engineered *Enterococcus faecalis*: Cytotoxic evaluation of biodiesel waste and development of a glycerol-inducible gene expression system. *Appl. Environ. Microbiol.* 81, 2082–2089. <https://doi.org/10.1128/AEM.03418-14>
- Donoso-Bravo, A., Mailier, J., Martin, C., Rodríguez, J., Aceves-Lara, C.A., Wouwer, A. Vande,

2011. Model selection, identification and validation in anaerobic digestion: A review. *Water Res.* 45, 5347–5364. <https://doi.org/10.1016/J.WATRES.2011.08.059>
- Dorado, A.D., Baquerizo, G., Maestre, J.P., Gamisans, X., Gabriel, D., Lafuente, J., 2008. Modeling of a bacterial and fungal biofilter applied to toluene abatement: Kinetic parameters estimation and model validation. *Chem. Eng. J.* 140, 52–61. <https://doi.org/10.1016/j.cej.2007.09.004>
- Dornseiffer, P., Meyer, B., Heinzle, E., 1995. Modeling of anaerobic formate kinetics in mixed biofilm culture using dynamic membrane mass spectrometric measurement. *Biotechnol. Bioeng.* 45, 219–228. <https://doi.org/10.1002/bit.260450306>
- Dowling, N.J.E., Brooks, S.A., Phelps, T.J., White, D.C., 1992. Effects of selection and fate of substrates supplied to anaerobic bacteria involved in the corrosion of pipe-line steel. *J. Ind. Microbiol.* 10, 207–215. <https://doi.org/10.1007/BF01569768>
- Drennan, D.M., Almstrand, R., Ladderud, J., Lee, I., Landkamer, L., Figueroa, L., Sharp, J.O., 2017. Spatial impacts of inorganic ligand availability and localized microbial community structure on mitigation of zinc laden mine water in sulfate-reducing bioreactors. *Water Res.* 115, 50–59. <https://doi.org/10.1016/J.WATRES.2017.02.037>
- Durme, G.P. Van, McNamara, B.F., McGinley, C.M., 1992. Bench-scale removal of odor and volatile organic compounds at a composting facility. *Water Environ. Res.* 64, 19–27. <https://doi.org/10.2175/WER.64.1.4>
- El Houari, A., Ranchou-Peyruse, M., Ranchou-Peyruse, A., Dakdaki, A., Guignard, M., Idouhammou, L., Bennisse, R., Bouterfass, R., Guyoneaud, R., Qatibi, A.I., 2017. *Desulfobulbus oligotrophicus* sp. Nov., a sulfate-reducing and propionate-oxidizing bacterium isolated from a municipal anaerobic sewage sludge digester. *Int. J. Syst. Evol. Microbiol.* 67, 275–281. <https://doi.org/10.1099/ijsem.0.001615>
- Fatolahi, Z., Arab, G., Razaviarani, V., 2020. Calibration of the Anaerobic Digestion Model No. 1 for anaerobic digestion of organic fraction of municipal solid waste under mesophilic condition. *Biomass and Bioenergy.* 139, 105661. <https://doi.org/10.1016/J.BIOMBIOE.2020.105661>

- Fedorovich, V., Lens, P., Kalyuzhnyi, S., 2003. Extension of anaerobic digestion model no. 1 with processes of sulfate reduction. *Appl. Biochem. and Biotechnol.* 109, 33–45. <https://doi.org/10.1385/ABAB:109:1-3:33>
- Fehmberger, C., Dos Santos, F.T., Aloisio, C.M., Hermes, E., Zenatti, D.C., Bautitz, I.R., 2020. Effectiveness of incorporation of crude glycerin as a source of labile carbon in the composting of poultry production residues. *J. Clean. Prod.* 251, 119739. <https://doi.org/10.1016/j.jclepro.2019.119739>
- Fernández-Palacios, E., Lafuente, J., Mora, M., Gabriel, D., 2019. Exploring the performance limits of a sulfidogenic UASB during the long-term use of crude glycerol as electron donor. *Sci. Total Environ.* 688, 1184–1192. <https://doi.org/10.1016/j.scitotenv.2019.06.371>
- Fernández-Palacios, E., Zhou, X., Mora, M., Gabriel, D., 2021. Microbial diversity dynamics in a Methanogenic-Sulfidogenic UASB reactor. *Int. J. Environ. Res. Public Health.* 18, 1305. <https://doi.org/10.3390/ijerph18031305>
- Fernández Palacios, E., 2020. Integrated assessment of long-term sulfidogenesis in UASB reactors using crude glycerol as carbon source. PhD thesis.
- Fike, D.A., Bradley, A.S., Leavitt, W.D., 2016. Geomicrobiology of sulfur. *Ehrlich's Geomicrobiol.* 3–8.
- Fukui, M., Suh, J., Yonezawa, Y., Urushigawa, Y., 1997. Major substrates for microbial sulfate reduction in the sediments of Ise Bay, Japan. *Ecol. Res.* 12, 201–209. <https://doi.org/10.1007/BF02523785>
- Gijs Kuenen, J., 1975. Colourless sulfur bacteria and their role in the sulfur cycle. *Plant Soil.* 43, 49–76. <https://doi.org/10.1007/BF01928476>
- González-Pajuelo, M., Meynial-Salles, I., Mendes, F., Andrade, J.C., Vasconcelos, I., Soucaille, P., 2005. Metabolic engineering of *Clostridium acetobutylicum* for the industrial production of 1,3-propanediol from glycerol. *Metab. Eng.* 7, 329–336. <https://doi.org/10.1016/j.ymben.2005.06.001>
- Gonzalez-Silva, B.M., Briones-Gallardo, R., Razo-Flores, E., Celis, L.B., 2009. Inhibition of sulfate reduction by iron, cadmium and sulfide in granular sludge. *J. Hazard. Mater.* 172,

- 400–407. <https://doi.org/10.1016/j.jhazmat.2009.07.022>
- Grein, F., Ramos, A.R., Venceslau, S.S., Pereira, I.A.C., 2013. Unifying concepts in anaerobic respiration: Insights from dissimilatory sulfur metabolism. *Biochim. Biophys. Acta - Bioenerg.* 1827, 145–160. <https://doi.org/10.1016/J.BBABIO.2012.09.001>
- Guisasola, A., Baeza, J.A., Carrera, J., Sin, G., Vanrolleghem, P.A., Lafuente, J., 2006. The influence of experimental data quality and quantity on parameter estimation accuracy. Andrews inhibition model as a case study. *Educ. Chem. Eng.* 1, 139–145. <https://doi.org/10.1205/ece06016>
- Guo, J., Kang, Y., 2018. Characterization of sulfate-reducing bacteria anaerobic granular sludge and granulometric analysis with grey relation. *Korean J. Chem. Eng.* 35, 1829–1835. <https://doi.org/10.1007/s11814-018-0092-y>
- Gupta, A., Flora, J.R.V., Gupta, M., Sayles, G.D., Suidan, M.T., 1994a. Methanogenesis and sulfate reduction in chemostats-I. Kinetic studies and experiments. *Water Res.* 28, 781–793. [https://doi.org/10.1016/0043-1354\(94\)90085-X](https://doi.org/10.1016/0043-1354(94)90085-X)
- Gupta, A., Flora, J.R.V., Sayles, G.D., Suidan, M.T., 1994b. Methanogenesis and sulfate reduction in chemostats-II. Model development and verification. *Water Res.* 28, 795–803. [https://doi.org/10.1016/0043-1354\(94\)90086-8](https://doi.org/10.1016/0043-1354(94)90086-8)
- Gutierrez, O., Park, D., Sharma, K.R., Yuan, Z., 2009. Effects of long-term pH elevation on the sulfate-reducing and methanogenic activities of anaerobic sewer biofilms. *Water Res.* 43, 2549–2557. <https://doi.org/10.1016/J.WATRES.2009.03.008>
- Halkjaer Nielsen, P., 1987. Biofilm dynamics and kinetics during high-rate sulfate reduction under anaerobic conditions. *Appl. Environ. Microbiol.* 53, 27–32. <https://doi.org/10.1128/aem.53.1.27-32.1987>
- Hao, T., Xiang, P., Mackey, H.R., Chi, K., Lu, H., Chui, H., van Loosdrecht, M.C.M., Chen, G.H., 2014. A review of biological sulfate conversions in wastewater treatment. *Water Res.* 65, 1–21. <https://doi.org/10.1016/j.watres.2014.06.043>
- Hill, D.T., Barth, C.L., 1977. A dynamic model for simulation of animal waste digestion. *J. Water Pollut. Control Fed.* 2129–2143.

- Himmi, E.H., Bories, A., Boussaid, A., Hassani, L., 2000. Propionic acid fermentation of glycerol and glucose by *Propionibacterium acidipropionici* and *Propionibacterium freudenreichii* ssp. *shermanii*. *Appl. Microbiol. Biotechnol.* 53, 435–440. <https://doi.org/10.1007/s002530051638>
- Hu, S., Luo, X., Wan, C., Li, Y., 2012. Characterization of Crude Glycerol from Biodiesel Plants. *J. Agric. Food Chem.* 60, 5915–5921. <https://doi.org/10.1021/jf3008629>
- Huang, J., Wen, Y., Ding, N., Xu, Y., Zhou, Q., 2012. Effect of sulfate on anaerobic reduction of nitrobenzene with acetate or propionate as an electron donor. *Water Res.* 46, 4361–4370. <https://doi.org/10.1016/j.watres.2012.05.037>
- Hulshoff Pol, L.W., De Castro Lopes, S.I., Lettinga, G., Lens, P.N.L., 2004. Anaerobic sludge granulation. *Water Res.* 38, 1376–1389. <https://doi.org/10.1016/j.watres.2003.12.002>
- Hung, C.H., Chang, Y.T., Chang, Y.J., 2011. Roles of microorganisms other than *Clostridium* and *Enterobacter* in anaerobic fermentative biohydrogen production systems - A review. *Bioresour. Technol.* 102, 8437–8444. <https://doi.org/10.1016/j.biortech.2011.02.084>
- J.W.H., S., Elferink, O., Visser, A., Hulshoff Pol, L.W., Stams, A.J.M., 1994. Sulfate reduction in methanogenic bioreactors. *FEMS Microbiol. Rev.* 15, 119–136. <https://doi.org/10.1111/j.1574-6976.1994.tb00130.x>
- Jarvis, G.N., Moore, E.R.B., Thiele, J.H., 1997. Formate and ethanol are the major products of glycerol fermentation produced by a *Klebsiella planticola* strain isolated from red deer. *J. Appl. Microbiol.* 83, 166–174. <https://doi.org/10.1046/j.1365-2672.1997.00217.x>
- Jeganathan, J., Nakhla, G., Bassi, A., 2006. Long-term performance of high-rate anaerobic reactors for the treatment of oily wastewater. *Environ. Sci. Technol.* 40, 6466–6472. <https://doi.org/10.1021/es061071m>
- Jeison, D., Chamy, R., 1999. Comparison of the behaviour of expanded granular sludge bed (EGSB) and upflow anaerobic sludge blanket (UASB) reactors in dilute and concentrated wastewater treatment. *Water Sci. Technol.* 40, 91–97. [https://doi.org/10.1016/S0273-1223\(99\)00613-7](https://doi.org/10.1016/S0273-1223(99)00613-7)
- Jensen, P.D., Astals, S., Lu, Y., Devadas, M., Batstone, D.J., 2014. Anaerobic codigestion of sewage sludge and glycerol, focusing on process kinetics, microbial dynamics and sludge dewaterability. *Water Res.* 67, 355–366. <https://doi.org/10.1016/j.watres.2014.09.024>

- Johnson, D.B., Sánchez-Andrea, I., 2019. Dissimilatory reduction of sulfate and zero-valent sulfur at low pH and its significance for bioremediation and metal recovery. *Adv. Microb. Physiol.* 75, 205–231. <https://doi.org/10.1016/bs.ampbs.2019.07.002>
- Joubert, W.A., Britz, T.J., 1987. Characterization of aerobic, facultative anaerobic, and anaerobic bacteria in an acidogenic phase reactor and their metabolite formation. *Microb. Ecol.* 13, 159–168. <https://doi.org/10.1007/BF02011251>
- Jung, Kim, Lee, 2019. Temperature effects on methanogenesis and sulfidogenesis during anaerobic digestion of sulfur-rich macroalgal biomass in sequencing batch reactors. *Microorganisms.* 7, 682. <https://doi.org/10.3390/microorganisms7120682>
- Kaksonen, A.H., Puhakka, J.A., 2007. Sulfate reduction based bioprocesses for the treatment of acid mine drainage and the recovery of metals. *Eng. Life Sci.* 7, 541-564. <https://doi.org/10.1002/elsc.200720216>
- Kalfas, H., Skiadas, I.V., Gavala, H.N., Stamatelatou, K., Lyberatos, G., 2006. Application of ADM1 for the simulation of anaerobic digestion of olive pulp under mesophilic and thermophilic conditions. *Water Sci. Technol.* 54, 149–156. <https://doi.org/10.2166/WST.2006.536>
- Kalyuzhnyi, S., Fedorovich, V., 1997. Integrated mathematical model of UASB reactor for competition between sulphate reduction and methanogenesis. *Water Sci. Technol.* 36, 201–208. [https://doi.org/10.1016/S0273-1223\(97\)00524-6](https://doi.org/10.1016/S0273-1223(97)00524-6)
- Kalyuzhnyi, S.V., Fedorovich, V.V., 1998. Mathematical modelling of competition between sulphate reduction and methanogenesis in anaerobic reactors. *Bioresour. Technol.* 65, 227–242. [https://doi.org/10.1016/S0960-8524\(98\)00019-4](https://doi.org/10.1016/S0960-8524(98)00019-4)
- Karjalainen, J., Mäkinen, M., Karjalainen, A.K., 2021. Sulfate toxicity to early life stages of European whitefish (*Coregonus lavaretus*) in soft freshwater. *Ecotoxicol. Environ. Saf.* 208, 111763. <https://doi.org/10.1016/j.ecoenv.2020.111763>
- Katarzyna, L., Katarzyna, C., Kamila, M., 2011. Biotechnological synthesis of 1,3-propanediol using *Clostridium* ssp. *African J. Biotechnol.* 10, 11093–11101. <https://doi.org/10.5897/AJB11.873>

- Kaur, G., Srivastava, A.K., Chand, S., 2013. Bioconversion of glycerol to 1,3-propanediol: A mathematical model-based nutrient feeding approach for high production using *Clostridium diolis*. *Bioresour. Technol.* 142, 82–87. <https://doi.org/10.1016/j.biortech.2013.05.040>
- Kellogg, W.W., Cadle, R.D., Allen, E.R., Lazrus, A.L., Martell, E.A., 1972. The sulfur cycle. *Science.* 175, 587–596. <https://doi.org/10.1126/SCIENCE.175.4022.587>
- Klotz, M.G., Bryant, D.A., Hanson, T.E., 2011. The microbial sulfur cycle. *Front. Microbiol.* 2, 241. <https://doi.org/10.3389/FMICB.2011.00241>
- Kobayashi, T., Xu, K.Q., Chiku, H., 2015. Release of extracellular polymeric substance and disintegration of anaerobic granular sludge under reduced sulfur compounds-rich conditions. *Energies* 8, 7968–7985. <https://doi.org/10.3390/en8087968>
- Koch, K., Lübken, M., Gehring, T., Wichern, M., Horn, H., 2010. Biogas from grass silage – Measurements and modeling with ADM1. *Bioresour. Technol.* 101, 8158–8165. <https://doi.org/10.1016/J.BIORTECH.2010.06.009>
- Komarnisky, L.A., Christopherson, R.J., Basu, T.K., 2003. Sulfur: its clinical and toxicologic aspects. *Nutrition.* 19, 54–61. [https://doi.org/10.1016/S0899-9007\(02\)00833-X](https://doi.org/10.1016/S0899-9007(02)00833-X)
- Kumar, L.R., Yellapu, S.K., Tyagi, R.D., Zhang, X., 2019. A review on variation in crude glycerol composition, bio-valorization of crude and purified glycerol as carbon source for lipid production. *Bioresour. Technol.* 293, 122155. <https://doi.org/10.1016/j.biortech.2019.122155>
- Lafita, C., Peña-Roja, J.M., Sempere, F., Waalkens, A., Gabaldón, C., 2012. Hydrogen sulfide and odor removal by field-scale biotrickling filters: Influence of seasonal variations of load and temperature. *J. Environ. Sci. Heal. - Part A Toxic/Hazardous Subst. Environ. Eng.* 47, 970–978. <https://doi.org/10.1080/10934529.2012.667302>
- Lauwers, J., Appels, L., Thompson, I.P., Degève, J., Van Impe, J.F., Dewil, R., 2013. Mathematical modelling of anaerobic digestion of biomass and waste: Power and limitations. *Prog. Energy Combust. Sci.* 39, 383–402. <https://doi.org/10.1016/J.PECS.2013.03.003>
- Leloup, J., Loy, A., Knab, N.J., Borowski, C., Wagner, M., Jørgensen, B.B., 2007. Diversity and abundance of sulfate-reducing microorganisms in the sulfate and methane zones of a marine sediment, Black Sea. *Environ. Microbiol.* 9, 131–142.



- <https://doi.org/10.1111/J.1462-2920.2006.01122.X>
- Lens, P., Vallero, M., Esposito, G., Zandvoort, M., 2002. Perspectives of sulfate reducing bioreactors in environmental biotechnology. *Rev. Environ. Sci. Biotechnol.* 1, 311-325. <https://doi.org/10.1023/A:1023207921156>
- Lens, P.N.L., Kuenen, J.G., 2001. The biological sulfur cycle: Novel opportunities for environmental biotechnology. *Water Sci Technol.* 44, 57–66. <https://doi.org/10.2166/wst.2001.0464>
- Lens, P.N.L., Visser, A., Janssen, A.J.H., Hulshoff Pol, L.W., Lettinga, G., 1998. Biotechnological treatment of sulfate-rich wastewaters. *Crit. Rev. Environ. Sci. Technol.* 28, 41-88. <https://doi.org/10.1080/10643389891254160>
- Li, X., Chen, S., Dong, B., Dai, X., 2020. New insight into the effect of thermal hydrolysis on high solid sludge anaerobic digestion: Conversion pathway of volatile sulphur compounds. *Chemosphere.* 244, 125466. <https://doi.org/10.1016/j.chemosphere.2019.125466>
- Li, Y., Sun, Y., Yang, G., Hu, K., Lv, P., Li, L., 2017. Vertical distribution of microbial community and metabolic pathway in a methanogenic propionate degradation bioreactor. *Bioresour. Technol.* 245, 1022–1029. <https://doi.org/10.1016/j.biortech.2017.09.028>
- Liamleam, W., Annachhatre, A.P., 2007. Electron donors for biological sulfate reduction. *Biotechnol. Adv.* 25, 452–463. <https://doi.org/10.1016/j.biotechadv.2007.05.002>
- Lide, D.R., 2004. *Handbook of chemistry and physics.* CRC Press 85. [https://doi.org/10.1016/0160-9327\(90\)90080-b](https://doi.org/10.1016/0160-9327(90)90080-b)
- Liu, Z., Liu, T., 2016. Production of acrylic acid and propionic acid by constructing a portion of the 3-hydroxypropionate/4-hydroxybutyrate cycle from *Metallosphaera sedula* in *Escherichia coli*. *J. Ind. Microbiol. Biotechnol.* 43, 1659–1670. <https://doi.org/10.1007/s10295-016-1843-6>
- Lomans, B.P., Van der Drift, C., Pol, A., Op den Camp, H.J.M., 2002. Microbial cycling of volatile organic sulfur compounds. *Cell. Mol. Life Sci.* 59, 575-588. <https://doi.org/10.1007/s00018-002-8450-6>
- Lopes, S.I.C., Sulistyawati, I., Capela, M.I., Lens, P.N.L., 2007a. Low pH (6, 5 and 4) sulfate

- reduction during the acidification of sucrose under thermophilic (55 °C) conditions. *Process Biochem.* 42, 580–591. <https://doi.org/10.1016/J.PROCBIO.2006.11.004>
- Lopes, S.I.C., Wang, X., Capela, M.I., Lens, P.N.L., 2007b. Effect of COD/SO<sub>4</sub><sup>2-</sup> ratio and sulfide on thermophilic (55 °C) sulfate reduction during the acidification of sucrose at pH 6. *Water Res.* 41, 2379–2392. <https://doi.org/10.1016/j.watres.2007.02.023>
- Lu, X., Zhen, G., Chen, M., Kubota, K., Li, Y.Y., 2015a. Biocatalysis conversion of methanol to methane in an upflow anaerobic sludge blanket (UASB) reactor: Long-term performance and inherent deficiencies. *Bioresour. Technol.* 198, 691–700. <https://doi.org/10.1016/j.biortech.2015.09.073>
- Lu, X., Zhen, G., Estrada, A.L., Chen, M., Ni, J., Hojo, T., Kubota, K., Li, Y.Y., 2015b. Operation performance and granule characterization of upflow anaerobic sludge blanket (UASB) reactor treating wastewater with starch as the sole carbon source. *Bioresour. Technol.* 180, 264–273. <https://doi.org/10.1016/j.biortech.2015.01.010>
- Luis, C.R.A., 2018. Optimization of the electron donor supply to sulphate reducing bioreactors treating inorganic wastewater, CRC Press. <https://doi.org/10.1017/CBO9781107415324.004>
- Lyberatos, G., Skiadas, I. V, 1999. Modelling of anaerobic digestion—a review. *Glob. Nest Int J.* 1, 63–76.
- Madigan, M.T., Martinko, J.M., 1997. Brock biology of microorganisms. Upper Saddle River, NJ: Prentice hall.
- Mahmoud, N., Zeeman, G., Gijzen, H., Lettinga, G., 2004. Anaerobic sewage treatment in a one-stage UASB reactor and a combined UASB-Digester system. *Water Res.* 38, 2348–2358. <https://doi.org/10.1016/j.watres.2004.01.041>
- Maillacheruvu, K.Y., Parkin, G.F., 1996. Kinetics of growth, substrate utilization and sulfide toxicity for propionate, acetate, and hydrogen utilizers in anaerobic systems. *Water Environ. Res.* 68, 1099–1106. <https://doi.org/10.2175/106143096x128126>
- Manchala, K.R., Sun, Y., Zhang, D., Wang, Z.W., 2017. Anaerobic digestion modelling. *Adv. Bioenergy.* 2, 69–141. <https://doi.org/10.1016/BS.AIBE.2017.01.001>
- Mangayil, R., Karp, M., Santala, V., 2012. Bioconversion of crude glycerol from biodiesel

- production to hydrogen. *Int. J. Hydrogen Energy*. 37, 12198–12204.  
<https://doi.org/10.1016/j.ijhydene.2012.06.010>
- Mansfield, L.A., Melnyk, P.B., Richardson, G.C., 1992. Selection and full-scale use of a chelated iron absorbent for odor control. *Water Environ. Res.* 64, 120–127.  
<https://doi.org/10.2175/WER.64.2.4>
- Matthies, C., Schink, B., 1992. Reciprocal isomerization of butyrate and isobutyrate by the strictly anaerobic bacterium strain WoG13 and methanogenic isobutyrate degradation by a defined triculture. *Appl. Environ. Microbiol.* 58, 1435–1439.  
<https://doi.org/10.1128/aem.58.5.1435-1439.1992>
- McCarty, P.L., Mosey, F.E., 1991. Modelling of Anaerobic Digestion Processes (A Discussion of Concepts). *Water Sci. Technol.* 24, 17–33. <https://doi.org/10.2166/WST.1991.0216>
- McCollom, T.M., Seewald, J.S., 2003. Experimental study of the hydrothermal reactivity of organic acids and acid anions: II. Acetic acid, acetate, and valeric acid. *Geochim. Cosmochim. Acta.* 67, 3645–3664. [https://doi.org/10.1016/S0016-7037\(03\)00135-2](https://doi.org/10.1016/S0016-7037(03)00135-2)
- McSwain, B.S., Irvine, R.L., Hausner, M., Wilderer, P.A., 2005. Composition and distribution of extracellular polymeric substances in aerobic flocs and granular sludge. *Appl. Environ. Microbiol.* 71, 1051–1057. <https://doi.org/10.1128/AEM.71.2.1051-1057.2005>
- Metsoviti, M., Paramithiotis, S., Drosinos, E.H., Galiotou-Panayotou, M., Nychas, G.J.E., Zeng, A.P., Papanikolaou, S., 2012. Screening of bacterial strains capable of converting biodiesel-derived raw glycerol into 1,3-propanediol, 2,3-butanediol and ethanol. *Eng. Life Sci.* 12, 57–68. <https://doi.org/10.1002/elsc.201100058>
- Meyer, L., 1864. Chemische Untersuchung der Thermen zu Landeck in der Grafschaft Glatz. *J. für Prakt. Chemie.* 91, 1–15.
- Meyer, T., Edwards, E.A., 2014. Anaerobic digestion of pulp and paper mill wastewater and sludge. *Water Res.* 65, 321–349. <https://doi.org/10.1016/J.WATRES.2014.07.022>
- Mhemid, R.K.S., Akmirza, I., Shihab, M.S., Turker, M., Alp, K., 2019. Ethanethiol gas removal in an anoxic bio-scrubber. *J. Environ. Manage.* 233, 612–625.  
<https://doi.org/10.1016/j.jenvman.2018.12.017>

- Mizuno, O., Li, Y.Y., Noike, T., 1994. Effects of sulfate concentration and sludge retention time on the interaction between methane production and sulfate reduction for butyrate. *Water Sci. Technol.* 30, 45.
- Molino, A., Nanna, F., Ding, Y., Bikson, B., Braccio, G., 2013. Biomethane production by anaerobic digestion of organic waste. *Fuel*. 103, 1003–1009. <https://doi.org/10.1016/J.FUEL.2012.07.070>
- Mora, M., Fernández-Palacios, E., Guimerà, X., Lafuente, J., Gamisans, X., Gabriel, D., 2020a. Feasibility of S-rich streams valorization through a two-step biosulfur production process. *Chemosphere*. 253, 126734. <https://doi.org/10.1016/j.chemosphere.2020.126734>
- Mora, M., Lafuente, J., Gabriel, D., 2020b. Influence of crude glycerol load and pH shocks on the granulation and microbial diversity of a sulfidogenic Upflow Anaerobic Sludge Blanket reactor. *Process Saf. Environ. Prot.* 133, 159–168. <https://doi.org/10.1016/j.psep.2019.11.005>
- Mora, M., Lafuente, J., Gabriel, D., 2018. Screening of biological sulfate reduction conditions for sulfidogenesis promotion using a methanogenic granular sludge. *Chemosphere*. 210, 557–566. <https://doi.org/10.1016/j.chemosphere.2018.07.025>
- Mora, M., López, L.R., Lafuente, J., Pérez, J., Kleerebezem, R., van Loosdrecht, M.C.M., Gamisans, X., Gabriel, D., 2016. Respirometric characterization of aerobic sulfide, thiosulfate and elemental sulfur oxidation by S-oxidizing biomass. *Water Res.* 89, 282–292. <https://doi.org/10.1016/j.watres.2015.11.061>
- Moscoviz, R., Trably, E., Bernet, N., 2018. Electro-fermentation triggering population selection in mixed-culture glycerol fermentation. *Microb. Biotechnol.* 11, 74–83. <https://doi.org/10.1111/1751-7915.12747>
- Mosey, F.E., 1983. Mathematical modelling of the anaerobic digestion process: Regulatory mechanisms for the formation of short-chain volatile acids from glucose. *Water Sci. Technol.* 15, 209–232. <https://doi.org/10.2166/WST.1983.0168>
- Muelas, A., Remacha, P., Pina, A., Barroso, J., Sobrino, A., Aranda, D., Bayarri, N., Estévez, C., Ballester, J., 2020. Combustion of crude glycerol and its blends with acetals. *Exp. Therm. Fluid Sci.* 114, 110076. <https://doi.org/10.1016/j.expthermflusci.2020.110076>

- Muyzer, G., Stams, A.J.M., 2008. The ecology and biotechnology of sulphate-reducing bacteria. *Nat. Rev. Microbiol.* 6, 441–454. <https://doi.org/10.1038/nrmicro1892>
- Nanqi, R., Hong, C., Shingyan, C., Yiu Fai, T., Sin, N., 2007. Effects of COD/SO<sub>4</sub><sup>2-</sup> ratios on an acidogenic sulfate-reducing reactor. *Ind. Eng. Chem. Res.* 46, 1661–1666. <https://doi.org/10.1021/IE060589W>
- Neculita, C.-M., Zagury, G.J., Bussière, B., 2007. Passive treatment of acid mine drainage in bioreactors using sulfate-reducing bacteria. *J. Environ. Qual.* 36, 1–16. <https://doi.org/10.2134/jeq2006.0066>
- Nomanbhay, S., Hussein, R., Ong, M.Y., 2018. Sustainability of biodiesel production in Malaysia by production of bio-oil from crude glycerol using microwave pyrolysis: A review. *Green Chem. Lett. Rev.* 11, 135–157. <https://doi.org/10.1080/17518253.2018.1444795>
- O’Flaherty, V., Mahony, T., O’Kennedy, R., Colleran, E., 1998. Effect of pH on growth kinetics and sulphide toxicity thresholds of a range of methanogenic, syntrophic and sulphate-reducing bacteria. *Process Biochem.* 33, 555–569. [https://doi.org/10.1016/S0032-9592\(98\)00018-1](https://doi.org/10.1016/S0032-9592(98)00018-1)
- Odom, J.M., Peck, H.D., 1981. Hydrogen cycling as a general mechanism for energy coupling in the sulfate-reducing bacteria, *Desulfovibrio* sp. *FEMS Microbiol. Lett.* 12, 47–50. <https://doi.org/10.1111/j.1574-6968.1981.tb07609.x>
- Oleszkiewicz, J.A., Romanek, A., 1989. Granulation in anaerobic sludge bed reactors treating food industry wastes. *Biol. Wastes* 27, 217–235. [https://doi.org/10.1016/0269-7483\(89\)90003-7](https://doi.org/10.1016/0269-7483(89)90003-7)
- Omil, F., Lens, P., Hulshoff Pol, L.W., Lettinga, G., 1997a. Characterization of biomass from a sulfidogenic, volatile fatty acid-degrading granular sludge reactor. *Enzyme Microb. Technol.* 20, 229–236. [https://doi.org/10.1016/S0141-0229\(96\)00119-6](https://doi.org/10.1016/S0141-0229(96)00119-6)
- Omil, F., Lens, P., Visser, A., Hulshoff Pol, L.W., Lettinga, G., 1998. Long-term competition between sulfate reducing and methanogenic bacteria in UASB reactors treating volatile fatty acids. *Biotechnol. Bioeng.* 57, 676–685. [https://doi.org/10.1002/\(SICI\)1097-0290\(19980320\)57:6<676::AID-BIT5>3.0.CO;2-I](https://doi.org/10.1002/(SICI)1097-0290(19980320)57:6<676::AID-BIT5>3.0.CO;2-I)
- Omil, F., Oude Elferink, S.J.W.H., Lens, P., Hulshoff Pol, L.W., Lettinga, G., 1997b. Effect of the inoculation with *Desulforhabdus amnigenus* and pH or O<sub>2</sub> shocks on the competition between

- sulphate reducing and methanogenic bacteria in an acetate fed UASB reactor. *Bioresour. Technol.* 60, 113–122. [https://doi.org/10.1016/S0960-8524\(97\)00014-X](https://doi.org/10.1016/S0960-8524(97)00014-X)
- Omri, I., Bouallagui, H., Aouidi, F., Godon, J.J., Hamdi, M., 2011. H<sub>2</sub>S gas biological removal efficiency and bacterial community diversity in biofilter treating wastewater odor. *Bioresour. Technol.* 102, 10202–10209. <https://doi.org/10.1016/j.biortech.2011.05.094>
- Oude Elferink, S.J.W.H., Lens, P.N.L., Dijkema, C., Stams, A.J.M., 1996. Isomerization of butyrate to isobutyrate by *Desulforhabdus amnigenus*. *FEMS Microbiol. Lett.* 142, 237–241. [https://doi.org/10.1016/0378-1097\(96\)00274-1](https://doi.org/10.1016/0378-1097(96)00274-1)
- Oude Elferink, S.J.W.H., Luppens, S.B.I., Marcelis, C.L.M., Stams, A.J.M., 1998. Kinetics of acetate oxidation by two sulfate reducers isolated from anaerobic granular sludge. *Appl. Environ. Microbiol.* 64, 2301–2303. <https://doi.org/10.1128/aem.64.6.2301-2303.1998>
- Ozekmekci, M., Salkic, G., Fellah, M.F., 2015. Use of zeolites for the removal of H<sub>2</sub>S: A mini-review. *Fuel Process. Technol.* 139, 49–60. <https://doi.org/10.1016/J.FUPROC.2015.08.015>
- Ozgun, H., Ersahin, M.E., Zhou, Z., Tao, Y., Spanjers, H., van Lier, J.B., 2019. Comparative evaluation of the sludge characteristics along the height of upflow anaerobic sludge blanket coupled ultrafiltration systems. *Biomass and Bioenergy.* 125, 114–122. <https://doi.org/10.1016/j.biombioe.2019.04.001>
- Papurello, D., Soukoulis, C., Schuhfried, E., Cappellin, L., Gasperi, F., Silvestri, S., Santarelli, M., Biasioli, F., 2012. Monitoring of volatile compound emissions during dry anaerobic digestion of the organic fraction of municipal solid waste by proton transfer reaction time-of-flight mass spectrometry. *Bioresour. Technol.* 126, 254–265. <https://doi.org/10.1016/j.biortech.2012.09.033>
- Plugge, C.M., Zhang, W., Scholten, J.C.M., Stams, A.J.M., 2011. Metabolic flexibility of sulfate-reducing bacteria. *Front. Microbiol.* 2, 81. <https://doi.org/10.3389/fmicb.2011.00081>
- Poggio, D., Walker, M., Nimmo, W., Ma, L., Pourkashanian, M., 2016. Modelling the anaerobic digestion of solid organic waste – Substrate characterisation method for ADM1 using a combined biochemical and kinetic parameter estimation approach. *Waste Manag.* 53, 40–54.

- <https://doi.org/10.1016/J.WASMAN.2016.04.024>
- Qatibi, A.I., Bennisse, R., Jana, M., Garcia, J.L., 1998. Anaerobic Degradation of Glycerol by *Desulfovibrio fructosovorans* and *D. carbinolicus* and Evidence for Glycerol-Dependent Utilization of 1,2-Propanediol. *Curr. Microbiol.* 36, 283–290. <https://doi.org/10.1007/s002849900311>
- Qatibi, A.I., Bories, A., Garcia, J.L., 1991a. Sulfate reduction and anaerobic glycerol degradation by a mixed microbial culture. *Curr. Microbiol.* 22, 47–52. <https://doi.org/10.1007/BF02106212>
- Qatibi, A.I., Cayol, J.L., Garcia, J.L., 1991b. Glycerol and propanediols degradation by *Desulfovibrio alcoholovorans* in pure culture in the presence of sulfate, or in syntrophic association with *Methanospirillum hungatei*. *FEMS Microbiol. Lett.* 85, 233–240. <https://doi.org/10.1111/j.1574-6968.1991.tb04729.x>
- Qatibi, A.I., Nivière, V., Garcia, J.L., 1991c. *Desulfovibrio alcoholovorans* sp. nov., a sulfate-reducing bacterium able to grow on glycerol, 1,2- and 1,3-propanediol. *Arch. Microbiol.* 155, 143–148. <https://doi.org/10.1007/BF00248608>
- Qian, Z., Tianwei, H., Mackey, H.R., van Loosdrecht, M.C.M., Guanghao, C., 2019. Recent advances in dissimilatory sulfate reduction: From metabolic study to application. *Water Res.* 150, 162–181. <https://doi.org/10.1016/J.WATRES.2018.11.018>
- Qiao, W., Takayanagi, K., Li, Q., Shofie, M., Gao, F., Dong, R., Li, Y.Y., 2016. Thermodynamically enhancing propionic acid degradation by using sulfate as an external electron acceptor in a thermophilic anaerobic membrane reactor. *Water Res.* 106, 320–329. <https://doi.org/10.1016/J.WATRES.2016.10.013>
- Qin, L., Tay, J.H., Liu, Y., 2004. Selection pressure is a driving force of aerobic granulation in sequencing batch reactors. *Process Biochem.* 39, 579–584. [https://doi.org/10.1016/S0032-9592\(03\)00125-0](https://doi.org/10.1016/S0032-9592(03)00125-0)
- Rabus, R., Hanses, T.A., Widdel, F., 2013. Dissimilatory sulfate- and sulfur- reducing prokaryotes. *The Prokaryotes.* 2, 309–404.
- Rabus, R., Strittmatter, A., 2007. Functional genomics of sulphate-reducing prokaryotes.

## Sulphate-reducing Bact.

- Ramírez, M., Fernández, M., Granada, C., Le Borgne, S., Gómez, J.M., Cantero, D., 2011. Biofiltration of reduced sulphur compounds and community analysis of sulphur-oxidizing bacteria. *Bioresour. Technol.* 102, 4047–4053. <https://doi.org/10.1016/j.biortech.2010.12.018>
- Reyes-Alvarado, L.C., Rene, E.R., Esposito, G., Lens, P.N.L., 2018. Bioprocesses for sulphate removal from wastewater. *Waste bioremediation*. Springer, Singapore. 35-60. [https://doi.org/10.1007/978-981-10-7413-4\\_3](https://doi.org/10.1007/978-981-10-7413-4_3)
- Rizvi, H., Ahmad, N., Abbas, F., Bukhari, I.H., Yasar, A., Ali, S., Yasmeen, T., Riaz, M., 2015. Start-up of UASB reactors treating municipal wastewater and effect of temperature/sludge age and hydraulic retention time (HRT) on its performance. *Arab. J. Chem.* 8, 780–786. <https://doi.org/10.1016/j.arabjc.2013.12.016>
- Rodriguez, R.P., Oliveira, G.H.D., Raimundi, I.M., Zaiat, M., 2012. Assessment of a UASB reactor for the removal of sulfate from acid mine water. *Int. Biodeterior. Biodegrad.* 74, 48–53. <https://doi.org/10.1016/j.ibiod.2012.07.012>
- Rossi, D.M., da Costa, J.B., de Souza, E.A., Peralba, M. do C.R., Ayub, M.A.Z., 2012. Bioconversion of residual glycerol from biodiesel synthesis into 1,3-propanediol and ethanol by isolated bacteria from environmental consortia. *Renew. Energy* 39, 223–227. <https://doi.org/10.1016/j.renene.2011.08.005>
- Saint-Amans, S., Perlot, P., Goma, G., Soucaille, P., 1994. High production of 1,3-propanediol from glycerol by *Clostridium butyricum* VPI 3266 in a simply controlled fed-batch system. *Biotechnol. Lett.* 16, 831–836. <https://doi.org/10.1007/BF00133962>
- Sakamoto, M., 2014. The Family Porphyromonadaceae. In: Rosenberg E., DeLong E.F., Lory S., Stackebrandt E., Thompson F. (eds) *The Prokaryotes*. Springer, Berlin, Heidelberg. [https://doi.org/10.1007/978-3-642-38954-2\\_132](https://doi.org/10.1007/978-3-642-38954-2_132)
- San-Valero, P., Peña-roja, J.M., Javier Álvarez-Hornos, F., Buitrón, G., Gabaldón, C., Quijano, G., 2019. Fully aerobic bioscrubber for the desulfurization of H<sub>2</sub>S-rich biogas. *Fuel*. 241, 884–891. <https://doi.org/10.1016/j.fuel.2018.12.098>
- Santos, A.L., Johnson, D.B., 2017. The effects of temperature and pH on the kinetics of an



- acidophilic sulfidogenic bioreactor and indigenous microbial communities. *Hydrometallurgy*. 168, 116–120. <https://doi.org/10.1016/J.HYDROMET.2016.07.018>
- Santos, S.C., Liebensteiner, M.G., van Gelder, A.H., Dimitrov, M.R., Almeida, P.F., Quintella, C.M., Stams, A.J.M.M., Sánchez-Andrea, I., 2018. Bacterial glycerol oxidation coupled to sulfate reduction at neutral and acidic pH. *J. Gen. Appl. Microbiol.* 64, 1–8. <https://doi.org/10.2323/jgam.2017.02.009>
- Saravanan, V., Sreekrishnan, T.R., 2006. Modelling anaerobic biofilm reactors—A review. *J. Environ. Manage.* 81, 1–18. <https://doi.org/10.1016/J.JENVMAN.2005.10.002>
- Sarti, A., Zaiat, M., 2011. Anaerobic treatment of sulfate-rich wastewater in an anaerobic sequential batch reactor (AnSBR) using butanol as the carbon source. *J. Environ. Manage.* 92, 1537–1541. <https://doi.org/10.1016/j.jenvman.2011.01.009>
- Sass, H., Berchtold, M., Branke, J., König, H., Cypionka, H., Babenzien, H.D., 1998. Psychrotolerant Sulfate-reducing Bacteria from an Oxidic Freshwater Sediment Description of *Desulfovibrio cuneatus* sp. nov. and *Desulfovibrio litoralis* sp. nov. *Syst. Appl. Microbiol.* 21, 212–219. [https://doi.org/10.1016/S0723-2020\(98\)80025-8](https://doi.org/10.1016/S0723-2020(98)80025-8)
- Schauder, R., Schink, B., 1989. *Anaerovibrio glycerini* sp. nov., an anaerobic bacterium fermenting glycerol to propionate, cell matter, and hydrogen. *Arch. Microbiol.* 152, 473–478. <https://doi.org/10.1007/BF00446932>
- Shang, Y., Johnson, B.R., Sieger, R., 2005. Application of the IWA Anaerobic Digestion Model (ADM1) for simulating full-scale anaerobic sewage sludge digestion. *Water Sci. Technol.* 52, 487–492. <https://doi.org/10.2166/WST.2005.0557>
- Shin, H.S., Oh, S.E., Bae, B.U., 1996. Competition between SRB and MPB according to temperature change in the anaerobic treatment of tannery wastes containing high sulfate. *Environ. Technol.* 17, 361–370. <https://doi.org/10.1080/09593331708616395>
- Sievert, S.M., Kiene, R.P., Heide N., S.V., 2007. The Sulfur Cycle. *Oceanography*. 20, 117–123.
- Silva, S.A., Salvador, A.F., Cavaleiro, A.J., Pereira, M.A., Stams, A.J.M., Alves, M.M., Sousa, D.Z., 2016. Toxicity of long chain fatty acids towards acetate conversion by *Methanosaeta concilii* and *Methanosarcina mazei*. *Microb. Biotechnol.* 9, 514–518.

<https://doi.org/10.1111/1751-7915.12365>

Siqueiros, E., Lamidi, R.O., Pathare, P.B., Wang, Y., Roskilly, A.P., 2019. Energy recovery from brewery waste: experimental and modelling perspectives. *Energy Procedia*. 161, 24–31.

<https://doi.org/10.1016/J.EGYPRO.2019.02.054>

Sittijunda, S., Reungsang, A., 2017. Fermentation of hydrogen, 1,3-propanediol and ethanol from glycerol as affected by organic loading rate using up-flow anaerobic sludge blanket (UASB) reactor. *Int. J. Hydrogen Energy*. 42, 27558–27569.

<https://doi.org/10.1016/j.ijhydene.2017.05.149>

Smet, E., Lens, P., Langenhove, H. Van, 1998. Treatment of waste gases contaminated with odorous sulfur compounds. *Environ. Sci. Technol.* 28, 89–117.

<https://doi.org/10.1080/10643389891254179>

Stams, A.J.M., Huisman, J., Encina, P.A.G., Muyzer, G., 2009. Citric acid wastewater as electron donor for biological sulfate reduction. *Appl. Microbiol. Biotechnol.* 83, 957–963.

<https://doi.org/10.1007/S00253-009-1995-7>

Sun, H., Yang, Z., Zhao, Q., Kurbonova, M., Zhang, R., Liu, G., Wang, W., 2021. Modification and extension of anaerobic digestion model No.1 (ADM1) for syngas biomethanation simulation: From lab-scale to pilot-scale. *Chem. Eng. J.* 403, 126177.

<https://doi.org/10.1016/j.cej.2020.126177>

Sun, J., Dai, X., Wang, Q., Pan, Y., Ni, B.J., 2016. Modelling methane production and sulfate reduction in anaerobic granular sludge reactor with ethanol as electron donor. *Sci. Rep.* 6, 1–11.

<https://doi.org/10.1038/srep35312>

Sun, Y.Q., Qi, W.T., Teng, H., Xiu, Z.L., Zeng, A.P., 2008. Mathematical modeling of glycerol fermentation by *Klebsiella pneumoniae*: Concerning enzyme-catalytic reductive pathway and transport of glycerol and 1,3-propanediol across cell membrane. *Biochem. Eng. J.* 38, 22–32.

<https://doi.org/10.1016/j.bej.2007.06.002>

Tholozan, J.L., Samain, E., Grivet, J.P., 1988. Isomerization between n-butyrate and isobutyrate in enrichment cultures. *FEMS Microbiol. Lett.* 53, 187–191.

[https://doi.org/10.1016/0378-1097\(88\)90441-7](https://doi.org/10.1016/0378-1097(88)90441-7)

- Turk, A., Sakalis, E., Lessuck, J., Karamitsos, H., Rago, O., 1989. Ammonia injection enhances capacity of activated carbon for hydrogen sulfide and methyl mercaptan. *Environ. Sci. Technol.* 23, 1242–1245.
- Vallero, M.V.G., Hulshoff Pol, L.W., Lettinga, G., Lens, P.N.L., 2003. Effect of NaCl on thermophilic (55°C) methanol degradation in sulfate reducing granular sludge reactors. *Water Res.* 37, 2269–2280. [https://doi.org/10.1016/S0043-1354\(03\)00024-1](https://doi.org/10.1016/S0043-1354(03)00024-1)
- Vallero, Marcus V.G., Camarero, E., Lettinga, G., Lens, P.N.L., 2004a. Thermophilic (55–65°C) and extreme thermophilic (70–80°C) sulfate reduction in methanol and formate-fed UASB reactors. *Biotechnol. Prog.* 20, 1382–1392. <https://doi.org/10.1021/bp034329a>
- Vallero, Marcus V. G., Sipma, J., Lettinga, G., Lens, P.N.L., 2004b. High-rate sulfate reduction at high salinity (up to 90 mS.cm<sup>-1</sup>) in mesophilic UASB reactors. *Biotechnol. Bioeng.* 86, 226–235. <https://doi.org/10.1002/bit.20040>
- Van Den Brand, T.P.H., Roest, K., Brdjanovic, D., Chen, G.H., Van Loosdrecht, M.C.M., 2014a. Temperature effect on acetate and propionate consumption by sulfate-reducing bacteria in saline wastewater. *Appl. Microbiol. Biotechnol.* 98, 4245–4255. <https://doi.org/10.1007/s00253-013-5482-9>
- Van Den Brand, T.P.H., Roest, K., Brdjanovic, D., Chen, G.H., van Loosdrecht, M.C.M.M., 2014b. Influence of acetate and propionate on sulphate-reducing bacteria activity. *J. Appl. Microbiol.* 117, 1839–1847. <https://doi.org/10.1111/jam.12661>
- Van Houten, R.T., Van Aelst, A.C., Lettinga, G., 1995. Aggregation of sulphate-reducing bacteria and homo-acetogenic bacteria in a lab-scale gas-lift reactor. *Water Sci. Technol.* 32, 85–90.
- Van Lier, J.B., Mahmoud, N., Zeeman, G., 2008. Anaerobic wastewater treatment. *Biol. wastewater Treat. Princ. Model. Des.* 415–456. [https://doi.org/10.2166/9781789060362\\_0701](https://doi.org/10.2166/9781789060362_0701)
- van Lier, J.B., van der Zee, F.P., Frijters, C.T.M.J., Ersahin, M.E., 2015. Celebrating 40 years anaerobic sludge bed reactors for industrial wastewater treatment. *Rev. Environ. Sci. Biotechnol.* 14, 681–702. <https://doi.org/10.1007/s11157-015-9375-5>
- Viana, M.B., Freitas, A. V., Leitão, R.C., Pinto, G.A.S., Santaella, S.T., 2012. Anaerobic digestion of crude glycerol: a review. *Environ. Technol. Rev.* 1, 81–92.

<https://doi.org/10.1080/09593330.2012.692723>

- Vignolle, Gabriel Alexander, Simon, C., Vignolle, Gabriel A, Derntl, C., Tomin, T., Novak, K., Mach, R.L., Birner-grünberger, R., Pflügl, S., 2021. A quantitative metabolic analysis reveals *Acetobacterium woodii* as a flexible and robust host for formate-based bioproduction. *Metab. Eng.* 68, 68–85. <https://doi.org/10.1016/j.ymben.2021.09.004>
- Visser, A., Gao, Y., Lettinga, G., 1993. Effects of short-term temperature increases on the mesophilic anaerobic breakdown of sulfate containing synthetic wastewater. *Water Res.* 27, 541–550. [https://doi.org/10.1016/0043-1354\(93\)90163-C](https://doi.org/10.1016/0043-1354(93)90163-C)
- Visser, A., Hulshoff Pol, L.W., Lettinga, G., 1996. Competition of methanogenic and sulfidogenic bacteria, *Water Sci. Technol.* 33, 99–110. [https://doi.org/10.1016/0273-1223\(96\)00324-1](https://doi.org/10.1016/0273-1223(96)00324-1)
- Vivek, N., Sindhu, R., Madhavan, A., Anju, A.J., Castro, E., Faraco, V., Pandey, A., Binod, P., 2017. Recent advances in the production of value added chemicals and lipids utilizing biodiesel industry generated crude glycerol as a substrate – Metabolic aspects, challenges and possibilities: An overview. *Bioresour. Technol.* 239, 507-517. <https://doi.org/10.1016/j.biortech.2017.05.056>
- Wang, A., Ren, N., Wang, X., Lee, D., 2008. Enhanced sulfate reduction with acidogenic sulfate-reducing bacteria. *J. Hazard. Mater.* 154, 1060–1065. <https://doi.org/10.1016/J.JHAZMAT.2007.11.022>
- Wang, J., Ye, J., Yin, H., Feng, E., Wang, L., 2012. Sensitivity analysis and identification of kinetic parameters in batch fermentation of glycerol. *J. Comput. Appl. Math.* 236, 2268–2276. <https://doi.org/10.1016/j.cam.2011.11.015>
- Wang, L., Ye, J., Feng, E., Xiu, Z., 2009. An improved model for multistage simulation of glycerol fermentation in batch culture and its parameter identification. *Nonlinear Anal. Hybrid Syst.* 3, 455–462. <https://doi.org/10.1016/j.nahs.2009.03.003>
- Weijma, J., Chi, T.M., Hulshoff Pol, L.W., Stams, A.J.M., Lettinga, G., 2003. The effect of sulphate on methanol conversion in mesophilic upflow anaerobic sludge bed reactors. *Process Biochem.* 38, 1259–1266. [https://doi.org/10.1016/S0032-9592\(03\)00002-5](https://doi.org/10.1016/S0032-9592(03)00002-5)
- Weijma, J., Gubbels, F., Hulshoff Pol, L.W., Stams, A.J.M., Lens, P., Lettinga, G., 2002.

- Competition for H<sub>2</sub> between sulfate reducers, methanogens and homoacetogens in a gas-lift reactor. *Water Sci. Technol.* 45, 75–80. <https://doi.org/10.2166/WST.2002.0294>
- Weijma, J., Stams, A.J.M., 2001. Methanol conversion in high-rate anaerobic reactors. *Water Sci. Technol.* 44, 7–14. <https://doi.org/10.2166/wst.2001.0452>
- Weijma, J., Stams, A.J.M., Hulshoff Pol, L.W., Lettinga, G., 2000. Thermophilic sulfate reduction and methanogenesis with methanol in a high rate anaerobic reactor. *Biotechnol. Bioeng.* 67, 354–363. [https://doi.org/10.1002/\(SICI\)1097-0290\(20000205\)67:3<354::AID-BIT12>3.0.CO;2-X](https://doi.org/10.1002/(SICI)1097-0290(20000205)67:3<354::AID-BIT12>3.0.CO;2-X)
- Westerholm, M., Isaksson, S., Karlsson Lindsjö, O., Schnürer, A., 2018. Microbial community adaptability to altered temperature conditions determines the potential for process optimisation in biogas production. *Appl. Energy* 226, 838–848. <https://doi.org/10.1016/j.apenergy.2018.06.045>
- Widdel, F., Pfennig, N., 1977. A new anaerobic, spring, acetate-oxidizing, sulfate-reducing bacterium, *Desulfotomaculum* (emend.) *acetoxidans*. *Arch. Microbiol.* 112, 119–122. <https://doi.org/10.1007/BF00446665>
- Wu, J., Afridi, Z.U.R., Cao, Z.P., Zhang, Z.L., Poncin, S., Li, H.Z., Zuo, J.E., Wang, K.J., 2016. Size effect of anaerobic granular sludge on biogas production: A micro scale study. *Bioresour. Technol.* 202, 165–171. <https://doi.org/10.1016/j.biortech.2015.12.006>
- Wu, J., Niu, Q., Li, L., Hu, Y., Mribet, C., Hojo, T., Li, Y.Y., 2018. A gradual change between methanogenesis and sulfidogenesis during a long-term UASB treatment of sulfate-rich chemical wastewater. *Sci. Total Environ.* 636, 168–176. <https://doi.org/10.1016/j.scitotenv.2018.04.172>
- Wu, K.J., Lin, Y.H., Lo, Y.C., Chen, C.Y., Chen, W.M., Chang, J.S., 2011. Converting glycerol into hydrogen, ethanol, and diols with a *Klebsiella* sp. HE1 strain via anaerobic fermentation. *J. Taiwan Inst. Chem. Eng.* 42, 20–25. <https://doi.org/10.1016/j.jtice.2010.04.005>
- Wu, S., Kuschik, P., Wiessner, A., Müller, J., Saad, R.A.B., Dong, R., 2013. Sulphur transformations in constructed wetlands for wastewater treatment: A review. *Ecol. Eng.* 52, 278–289. <https://doi.org/10.1016/J.ECOLENG.2012.11.003>

- Xu, X., Chen, C., Lee, D.J., Wang, A., Guo, W., Zhou, X., Guo, H., Yuan, Y., Ren, N., Chang, J.S., 2013. Sulfate-reduction, sulfide-oxidation and elemental sulfur bioreduction process: Modeling and experimental validation. *Bioresour. Technol.* 147, 202–211. <https://doi.org/10.1016/j.biortech.2013.07.113>
- Xu, X.J., Chen, C., Wang, A.J., Ni, B.J., Guo, W.Q., Yuan, Y., Huang, C., Zhou, X., Wu, D.H., Lee, D.J., Ren, N.Q., 2017. Mathematical modeling of simultaneous carbon-nitrogen-sulfur removal from industrial wastewater. *J. Hazard. Mater.* 321, 371–381. <https://doi.org/10.1016/j.jhazmat.2016.08.074>
- Xu, Y., Lu, Y., Zheng, L., Wang, Z., Dai, X., 2020. Perspective on enhancing the anaerobic digestion of waste activated sludge. *J. Hazard. Mater.* 389, 121847. <https://doi.org/10.1016/j.jhazmat.2019.121847>
- Yang, B., Liang, S., Liu, H., Liu, J., Cui, Z., Wen, J., 2018. Metabolic engineering of *Escherichia coli* for 1,3-propanediol biosynthesis from glycerol. *Bioresour. Technol.* 267, 599–607. <https://doi.org/10.1016/j.biortech.2018.07.082>
- Yao, X.Z., Chu, Y.X., Wang, C., Li, H.J., Kang, Y.R., He, R., 2019. Enhanced removal of methanethiol and its conversion products in the presence of methane in biofilters. *J. Clean. Prod.* 215, 75–83. <https://doi.org/10.1016/j.jclepro.2019.01.019>
- Zeng, A.P., Biebl, H., Schlieker, H., Deckwer, W.D., 1993. Pathway analysis of glycerol fermentation by *Klebsiella pneumoniae*: Regulation of reducing equivalent balance and product formation. *Enzyme Microb. Technol.* 15, 770–779. [https://doi.org/10.1016/0141-0229\(93\)90008-P](https://doi.org/10.1016/0141-0229(93)90008-P)
- Zeng, A.P., Ross, A., Biebl, H., Tag, C., Günzel, B., Deckwer, W., Gunzel, B., 1994. Multiple product inhibition and growth modeling of *Clostridium butyricum* and *Klebsiella pneumoniae* in glycerol fermentation. *Biotechnol. Bioeng.* 44, 902–911. <https://doi.org/10.1002/bit.260440806>
- Zeng, A.P., Menzel, K., Deckwer, W.D., 1996. Kinetic, dynamic, and pathway studies of glycerol metabolism by *Klebsiella pneumoniae* in anaerobic continuous culture: II. Analysis of metabolic rates and pathways under oscillation and steady-state conditions. *Biotechnol.*

- Bioeng. 52, 561–571.  
[https://doi.org/10.1002/\(SICI\)1097-0290\(19961205\)52:5<561::AID-BIT3>3.3.CO;2-F](https://doi.org/10.1002/(SICI)1097-0290(19961205)52:5<561::AID-BIT3>3.3.CO;2-F)
- Zeng, D., Yin, Q., Du, Q., Wu, G., 2019. System performance and microbial community in ethanol-fed anaerobic reactors acclimated with different organic carbon to sulfate ratios. *Bioresour. Technol.* 278, 34–42. <https://doi.org/10.1016/j.biortech.2019.01.047>
- Zhao, Y.-G., Wang, A.-J., Ren, N.-Q., 2010. Effect of carbon sources on sulfidogenic bacterial communities during the starting-up of acidogenic sulfate-reducing bioreactors. *Bioresour. Technol.* 101, 2952–2959. <https://doi.org/10.1016/j.biortech.2009.11.098>
- Zhou, G.M., Fang, H.H.P., 1998. Competition between methanogenesis and sulfidogenesis in anaerobic wastewater treatment. *Water Sci. Technol.* 38, 317–324. [https://doi.org/10.1016/S0273-1223\(98\)00707-0](https://doi.org/10.1016/S0273-1223(98)00707-0)
- Zhou, Q., Shi, Z.Y., Meng, D.C., Wu, Q., Chen, J.C., Chen, G.Q., 2011. Production of 3-hydroxypropionate homopolymer and poly(3-hydroxypropionate-co-4-hydroxybutyrate) copolymer by recombinant *Escherichia coli*. *Metab. Eng.* 13, 777–785. <https://doi.org/10.1016/j.ymben.2011.10.002>